

ABSTRACT

Title of Document: DIVERSIFIED REACTIONS OF ENOL DIAZOACETATE IN CHEMICAL CATALYSIS

Xichen Xu, Doctor of Philosophy, 2014

Directed By: Professor Michael P. Doyle, Department of Chemistry and Biochemistry

Silylated enol diazoacetates, prepared by the selective *O*-silylation of diazoacetoacetates in the presence of a mild base, are extremely valuable in synthesizing novel heterocyclic compounds. The incorporation of a silyl enol unit in the α -diazoacetate moiety creates a unique molecule that displays multifaceted reactivities under the catalysis of conceptually different catalytic systems.

Upon catalytic dinitrogen extrusion of silylated enol diazoacetate by dirhodium catalysis, the corresponding rhodium bound enol carbene intermediate resembles a metallo-1,3-dipolar species and undergoes a formal dearomatizing [3+3]-cycloaddition with isoquinolinium/pyridinium methylides that furnishes substituted quinolizidines. The development of the catalytic asymmetric variant of this cycloaddition reaction by catalysis with the previously unreported chiral dirhodium carboxylate catalyst–Rh₂(*S*-PTIL)₄ has allowed convenient access to highly enantioenriched quinolizidines. Coordination of the Lewis basic methylides to dirhodium(II) prompts the

rearrangement of the enol carbene that is bound to dirhodium to produce a donor–acceptor cyclopropene which undergoes a diastereoselective [3+2]-cycloaddition with isoquinolinium/pyridinium methylides. With the overall reaction outcome controlled by the amount of catalyst used, an increase in the mol % of catalyst loading suppresses the [3+2]-cycloaddition pathway.

In a reaction that proceeds under mild conditions with remarkable functional group tolerance, catalytically generated rhodium enol carbene intermediate reacts with nucleophilic silylated ketene imines and produced structurally diverse 3-amino-2-cyclopentenones bearing a quaternary carbon at the 4-position in high efficiency. The key step for the overall transformation emanates from the [3+2]-cycloaddition of silylated ketene imine and rhodium enol carbene with the nucleophilic silylated ketene imine attacking the vinylogous position of rhodium enol carbene.

Under Lewis acid catalysis, silylated enol diazoacetates participates in diastereoselective [3+2]-cycloaddition reactions with azomethine imines to produce highly functionalized β -methylene- β -silyloxy- β -amido- α -diazoacetates. Catalyst-directed selectivity of competitive 1,2-C \rightarrow C, -O \rightarrow C and -N \rightarrow C migrations from the β -methylene- β -silyloxy- β -amido- α -diazoacetates demonstrates that the differential selectivities rely on the control of the stereoelectronic property of the catalytically generated metal carbenes.

DIVERSIFIED REACTIONS OF ENOL DIAZOACETATE IN CHEMICAL
CATALYSIS

By

Xichen Xu

Dissertation submitted to the Faculty of the Graduate School of the
University of Maryland, College Park, in partial fulfillment
of the requirements for the degree of
Doctor of Philosophy
2014

Advisory Committee:
Professor Michael P. Doyle, Chair
Professor Andrei Vedernikov
Professor Herman O. Sintim
Professor Lyle Isaacs
Professor Yanjin Zhang

© Copyright by
Xichen Xu
2014

Dedication

This dissertation is dedicated to my parents, Chunshan Xu and Xiantao Tong for their
love and support.

Acknowledgements

After a 5-year study at the University of Maryland, I can nearly see the chequed flag waving at me. From my own perspective, this adventure in analogy is an endurance race and it is the support from many people that helps me finish this challenging race. Herein, I would like to express my deepest gratitude and most sincere appreciation to all the people who have helped me during my Ph.D career.

Most importantly, I would like to thank Dr. Michael P. Doyle for his guidance and mentorship over this five-year period. Looking back at the time that I have spent in Dr. Doyle' research group, I am truly confident to state that this challenging experience has reshaped my understanding about science. When I came to this country, I had great motivation but limited knowhow about making discoveries. While the first year was smooth and routine, my second year was especially challenging and tough however most memorable. Although few results have been delivered during this time frame, I personally believe that I have learned a lot from all the ideas that did not work. I am genuinely grateful for the support, encouragement and guidance from Dr. Doyle during that time. I also have plenty of chances of polishing my writing skills in Dr. Doyle's research group. Sometimes when I compare the first draft of my publications to its final form, I can see the enormous amount of efforts that Dr. Doyle devotes to teaching me how to write professionally from all the corrections and comments. The weekly group meetings that we have together provide me the chances of practicing my presentation skills and gradually grant me more confidence when presenting. These trainings will certainly have a long-lasting effect on my future career. Dr. Doyle's great passion on science will always motivate me.

I would like to thank Professor Anderi Vedernikov, Professor Herman O. Sintim and Professor Lyle Isaacs for serving on my Ph.D candidacy exam and Ph.D dissertation committee, and Professor Yanjin Zhang for serving as the Dean's representative. It is my great pleasure to have the opportunity to discuss my work with you.

For members of the Doyle group, I would like to give my special gratitude to Dr. Yu Qian who collaborated with me in the project of catalyst-directed 1,2-migration. I am also grateful to the help from other members of the Doyle group including Dr. Dmitry Shabashov, Dr. Lei Zhou, Dr. Deana Jaber, Dr. Ryan Burgin, Dr. Charles Shanahan, Dr. Maxim Ratnikov, Dr. Xiaochen Wang, Dr. Yu Qian, Dr. Yu Liu, Dr. Xinfang Xu, Phong Truong and all the new members.

Finally I would like to thank my parents, Chunshan Xu and Xiantao Tong for your support and love over the years.

Table of Contents

Dedication.....	ii
Acknowledgements.....	iii
Table of Contents.....	v
List of Figures.....	viii
List of Tables.....	ix
List of Schemes.....	x
List of Illustrations.....	xvii
Chapter 1: Competitive Enantioselective [3+3]-Cycloaddition and Diastereoselective [3+2]-Cycloaddition of Pyridinium/isoquinolium Ylides with Enol Diazoacetate	1
<i>I. Introduction</i>	1
1.1 General Information about Dirhodium(II) Carboxylates and Carboxamidates	1
1.2 General Information for Chiral Dirhodium(II) Carboxylates and Carboxamidate and Their Applications in Catalytic Asymmetric Transformations.....	3
1.3 General Information for Diazocompounds and Reactivity Profiles of vinyl diazoacetate.....	17
1.4 Donor/Acceptor Cyclopropene Generation from Enol Diazoacetate and Synthetic Application of the Donor/Acceptor Cyclopropene.....	20
1.5 Cyclopropene as Rhodium Vinylcarbene Precursor.....	22
1.6 Examples of [3+3]-Cycloaddition Reactions for Enol Diazoacetate.....	26
1.7 Chemistry of Heteroaromatic Ylides.....	28
1.8 Research Goal.....	31
<i>II. Results and Discussion</i>	33

2.1 Results.....	33
2.2 Discussions	41
<i>III. Conclusion</i>	54
<i>IV. Experimental Section</i>	54
4.1 General Information.....	54
4.2 Experimental Procedure.....	56
4.3 Characterization Data.....	64
<i>V. Reference</i>	74
Chapter 2: Catalytic [3+2]-Cycloaddition of Silylated Ketene Imine with Enol	
Diazoacetate.....	85
<i>I. Introduction</i>	85
1.1 General Information for Ketene Imines.....	85
1.2 Representative Examples for the Preparation of Ketene Imine and Their Chemical Properties	86
1.3 General Information and the Synthesis of Silylated Ketene Imines.....	87
1.4 Reactions Involving Nucleophilic SKIs.....	90
1.5 Reaction of Enol Diazoacetate with Silyl Enol Ether by Dirhodium Catalysis....	95
1.6 Research Proposal.....	101
<i>II. Results and Discussions</i>	102
2.1 Results.....	102
2.2 Discussions	108
<i>III. Conclusion</i>	109
<i>IV. Experimental Section</i>	110

4.1 General Information.....	110
4.2 Experimental Procedure.....	111
4.3 Characterization Data.....	112
<i>V. Reference</i>	118
Chapter 3: Catalyst Controlled Selective 1,2-Migrations from β -methylene- β - silyloxy- β -amido- α -diazoacetates	124
<i>I. Introduction</i>	124
1.1. General Information for α -Diazo Carbonyl compounds in Nucleophilic Addition Reactions.....	124
1.2 Ti(IV)-enol Diazoacetates in Nucleophilic Additions	126
1.3 Si-enol Diazoacetate in Nucleophilic Additions.....	128
1.4 Research Proposal.....	136
<i>II. Results and Discussion</i>	138
<i>III. Conclusion</i>	149
<i>IV. Experimental Section</i>	149
4.1 General Information.....	149
4.2 Experimental Procedure.....	150
4.3 Characterization Data.....	152
<i>V. Reference</i>	177

List of Figures

Figure 1.1 Structural Framework of Paddlewheel Dinuclear Complex- $\text{Rh}_2(\text{OAc})_4$	1
Figure 1.2 Representative Examples of Privileged Chiral Dirhodium(II) Catalyst.....	4
Figure 1.3 Dirhodium(II) Tetrakis(methyl 2-oxopyrrolidine-4(<i>R</i>)-carboxylate): (a) and (b) are Common Representations; (c) X-ray Structure of $\text{Rh}_2(\text{R-MEPY})_4$ Bisacetonitrile Complex.....	11
Figure 1.4 The Chiral Crown Conformation Adopted by $\text{Rh}_2(\text{S-PTTL})_4$	17
Figure 1.5 ORTEP View of Benzyl (<i>S</i>)-2-(<i>tert</i> -Butyldimethylsilyloxy)-4,4-dicyano-4,11b-dihydro-3H-pyrido-[2,1-a]isoquinoline-1-carboxylate (78b). Ellipsoids are Shown at 30% Probability. CCDC 946885 Contains Supplementary Crystallographic Data for 78b	40
Figure 1.6 UV-Vis Titration Curves and Equilibrium Constant K_1 for Complex Formation Between 70e and $\text{Rh}_2(\text{S-PTIL})_4$ in Toluene at Room Temperature. [$\text{Rh}_2(\text{S-PTIL})_4$] = $2.0 \times 10^{-3}\text{M}$; 0.17 equiv of 70e [Relative to $\text{Rh}_2(\text{S-PTIL})_4$] was Added in Each Increment. $K_1 = 545 \pm 14$	44
Figure 2.1 Structures for Ketene Imines	86
Figure 2.2 X-ray Crystal Structure of 69b and CCDC 965494 Contains the Supplementary Crystallographic data. Thermal Ellipsoids Set at 30% Probability .	108
Figure 3.1 X-Ray Single Crystal Structure for 59a	140

List of Tables

Table 1.1 Optimization of Reaction Conditions for Enantioselective Formal [3+3]-Cycloaddition of Isoquinolinium Dicyanomethylide 70a and Enol Diazoacetate 59a	35
Table 1.2 Solvent Screening for the Enantioselective Catalytic Formal [3+3]-Cycloaddition Reaction of Isoquinolinium Dicyanomethylide 70a and Enol Diazoacetate 59a	37
Table 1.3 Substrate Scope for Enantioselective Dearomatizing Formal [3+3]-Cycloaddition	38
Table 2.1 Optimization for the [3+2]-Cycloaddition Reaction	103
Table 2.2 Substrate Scope for the Formal [3+2]-Cycloaddition Reaction	105
Table 3.1 Lewis Acid Catalyst Screening for Formation of 59h from 58h	140
Table 3.2 Lewis Acid Catalyzed Diastereoselective [3+2]-Cycloaddition of Azomethine Imines 58 with Enol Diazoacetate 17	141
Table 3.3 Catalyst Screening with 59a for Selective 1,2-C→C, -O→C and -N→C Migrations	143
Table 3.4 Selective 1,2-C→C and -N→C migrations of 59 catalyzed by Rh ₂ (cap) ₄ and CuPF ₆	144
Table 3.5 Catalyst Screening with 59h for Selective 1,2-C→C, -O→C and -N→C Migrations	146
Table 3.6 Substrate Scope for Ligand-induced Divergent 1,2-C→C and -O→C Migrations	147

List of Schemes

Scheme 1.1 Transformations Involving Rhodium Carbene Intermediates (L = Carboxylate or Carboxamidate) from Catalytic Dinitrogen Extrusion of Diazocompounds.....	2
Scheme 1.2 Structural Representation and Potential Isomers of Dirhodium(II) Carboxamidates.....	3
Scheme 1.3 Dirhodium(II) Tetrakis[<i>N</i> -phenylsulfonylprolinate]-catalyzed Intramolecular Asymmetric C-H Insertion	6
Scheme 1.4 Rh ₂ (<i>S</i> -DOSP) ₄ -catalyzed Asymmetric C-H Insertion with Aryldiazoacetates and Styryldiazoacetates	7
Scheme 1.5 Preparation of Rh ₂ (<i>S</i> -PTAD) ₄ by Asymmetric C-H Insertion of Styryl Diazoacetate into a Tertiary C-H Bond of Adamantane.....	7
Scheme 1.6 Conformation of Amide Influences the Ligand Exchange Reaction.....	8
Scheme 1.7 Intramolecular Enantioselective Cyclopropanation Catalyzed by Rh ₂ (<i>5S</i> -MEPY) ₄	9
Scheme 1.8 Intramolecular Enantioselective C-H Insertion Catalyzed by Rh ₂ (<i>4S</i> -MPPIM) ₄	9
Scheme 1.9 Intramolecular Enantioselective Cyclopropanation of Phenyldiazoacetate Catalyzed by Rh ₂ (<i>4S</i> -MEAZ) ₄	9
Scheme 1.10 Hetero-Diels-Alder Reactions Catalyzed by Chiral Dirhodium Carboxamidates.....	11
Scheme 1.11 Hetero-Diels-Alder Reactions Catalyzed by Chiral Dirhodium Carboxylate with Rawal Diene	13

Scheme 1.12 (a) Formation of Chiral Cationic Dirhodium(II,III) Carboxamides by Oxidation of Nitrosonium Salts. (b) Enhanced Lewis Acidity and Stereocontrol with Chiral Cationic Dirhodium(II,III) Carboxamides in the Hetero-Diels-Alder Reaction	13
Scheme 1.13 Solvent Effect on Dirhodium(II,III) Carboxamide Catalyzed Asymmetric 1,3-Dipolar Cycloaddition Reactions.....	14
Scheme 1.14 Enhanced Reactivity and Selectivity by the Introduction of a Halogenated <i>N</i> -Phthaloyl Group	15
Scheme 1.15 Representative Examples for the Synthesis of Diazoacetate under Direct Diazo Transfer	18
Scheme 1.16 Intramolecular Cyclization of Styryldiazoacetates	18
Scheme 1.17 Classification of Substituted Metal Carbene Intermediates.....	19
Scheme 1.18 Diversified Reactivities of Vinyl Metal Carbenes	20
Scheme 1.19 Cyclopropene Generation by Catalytic Dinitrogen Extrusion and [4+2]-Cycloaddition Reaction of Cyclopentadiene and Donor/Acceptor Cyclopropenes....	21
Scheme 1.20 Diastereoselective Povarov Reaction of Donor/acceptor Cyclopropene and Substituted Imines.....	22
Scheme 1.21 Rhodium Vinylcarbene Formation from Cyclopropene by Rh ₂ (pfb) ₄ Catalysis.....	24
Scheme 1.22 Diastereoselective Construction of Carbocycles and Oxygen Heterocycles through Dirhodium-catalyzed Isomerization of Substituted Cyclopropenes.....	26

Scheme 1.23 Catalytic Asymmetric Synthesis of 3,6-Dihydro-1,2-oxazines by [3+3]-Cycloaddition of Enol Diazoacetate with Aryl Nitrones	27
Scheme 1.24 Construction of Tetrahydropyridazine by Cascade N-H Insertion and Intramolecular Mannich Addition.....	28
Scheme 1.25 Preparation of Pyridinium/Isoquinolium Dicyanomethylide from Tetracyanoethylene Oxide	29
Scheme 1.26 1,3-Dipolar Cycloaddition Reaction of Pyridinium/Isoquinolium Dicyanomethylide with Dimethyl Acetylenedicarboxylates	29
Scheme 1.27 [3+2]-Cycloaddition of Pyridinium Dicyanomethylide and Diphenylcyclopropanone	30
Scheme 1.28 Synthesis of Pyridinium/isoquinolium Dicarbomethoxymethylide under Dirhodium Catalysis	30
Scheme 1.29 In Situ Generation of an Isoquinolium Methylide and Its Subsequent [3+2]-Cycloaddition Reaction	31
Scheme 1.30 Reaction Pathways to Enantioselective Syntheses of Substituted Quinolizidines.....	32
Scheme 1.31 Formal Enantioselective [3+3]-Cycloaddition of Metallo-1,3-dipoles with Isoquinolinium/Pyridinium Methylides	33
Scheme 1.32 Formation of Both [3+3]- and [3+2]-Cycloaddition Products are Dependent on Metal Carbene Intermediate 81	43
Scheme 1.33 Lewis Bases Occupy Axial Coordination Sites on Dirhodium Complexes	45

Scheme 1.34 Stable Carbene on Dirhodium Undergoes Dissociation Prior to Reaction of Dirhodium with the Diazocarbonyl Compounds.....	46
Scheme 1.35 Reaction Pathway for the Formation of Cyclopropene 80	47
Scheme 1.36 Effect of Lewis Bases on Chemoselectivity	48
Scheme 1.37 Both [3+3]-Cycloaddition and [3+2]-Cycloaddition Product 78 and 79 Have Minimal Impact on Chemoselectivity	49
Scheme 1.38 Dependence of Product Distribution on Catalyst Loading with Cyclopropene 80a as the Metal Carbene Precursor.....	51
Scheme 1.39 Relationship Between the Cycloaddition Product Ratio (78:79) and the Dirhodium Catalyst.....	52
Scheme 1.40 Detailed General Mechanism for the Competing [3+3]- and [3+2]-Cycloaddition Reactions	53
Scheme 2.1 Ketene Imine Formation via Aza-Wittig Reaction.....	86
Scheme 2.2 Ketene Imine Generation via Hetero-Wolff Rearrangement of 1-Sulfonyl 1,2,3-Triazole.....	87
Scheme 2.3 Selective C-Silylation versus N-Silylation	88
Scheme 2.4 Synthesis of Silylated Ketene Imine from Simple Nitriles.....	88
Scheme 2.5 Preparation of TBS-substituted SKIs.....	89
Scheme 2.6 Structural Features for SKIs and Silyl Enol Ethers	89
Scheme 2.7 Nucleophilic Addition of SKIs to Aldehydes and Ketones	91
Scheme 2.8 Reactions of SKIs with Acid Chlorides	92
Scheme 2.9 Syntheses of Vinyl Nitriles from SKIs	92
Scheme 2.10 Conversion of Nitriles to Ketones through SKI Intermediates.....	93

Scheme 2.11 Cycloaddition Reaction of Vinyl SKIs with Propargylic Esters.....	93
Scheme 2.12 A Planar Chiral Pyridine Complex Catalyzes Asymmetric Addition of SKIs to Acid Anhydrides	94
Scheme 2.13 Chiral Sc(OTf) ₃ / <i>N</i> -Oxide Ligand Complex Promoted Aymmetric Mannich Addition of SKIs.....	95
Scheme 2.14 Catalytic Enantioselective Allylic C-H insertion/Cope Rearrangement of Methyl-Substituted Enol Diazoacetate with Silyl Enol Ether.....	96
Scheme 2.15 Alkynecarboxylate Formation through the Vinylogous Addition of Silyl Enol Ether over Carbene Addition to Unsubstituted Enol Diazoacetate	96
Scheme 2.16 (a) Enhanced Reactivity of <i>tert</i> -Butyl Enol Diazoacetate Compared to Methyl Enol Diazoacetate. (b) Tetrasubstituted Silyl Enol Ethers are Viable Substrates for Alkynecarboxylate Formation.....	97
Scheme 2.17 Proposed Mechanism for the Formation of Alkynecarboxylate.....	99
Scheme 2.18 Catalytic Asymmetric Synthesis of Alkynecarboxylate under the Catalysis by Rh ₂ (<i>S</i> -PTAD) ₄	99
Scheme 2.19 Chirality Transfer from Optical Active Silyl Enol Ether to Alkynecarboxylate by Catalysis of Rh ₂ (<i>esp</i>) ₂	100
Scheme 2.20 Catalytic Enantioselective Synthesis of Alkynecarboxylate by Using Acyclic (<i>Z</i>)-Silyl Enol Ether	100
Scheme 2.21 Catalytic Enantioselective Formal [3+2]-Cycloaddition Between Acyclic (<i>Z</i>)-Silyl Enol Ether and Enol Diazoacetate.....	101
Scheme 2.22 (a) SKIs as Nucleophiles. (b) Formal [3+2]-Cycloaddition of SKIs and Enol Diazoacetate	102

Scheme 2.23 The Proposed Mechanism for the [3+2]-Annulation Reaction.....	109
Scheme 3.1 The Resonance Structures for an α -Diazo Carbonyl Compound.....	124
Scheme 3.2 Construction of Complex α -Diazocarbonyl Compounds from α -Diazo Ketones or Esters	125
Scheme 3.3 Generation of Si- and Ti-enol Diazoacetate from α -Diazo- β -ketoesters	126
Scheme 3.4 Ti(O <i>i</i> -Pr) ₄ -catalyzed Addition of Ti-enol Diazoacetate to Ketones and Subsequent Intramolecular Allylic C-H Insertion	126
Scheme 3.5 Addition of Ti-enol Diazoacetate to Ketones and Subsequent Intramolecular OH-insertion or Lactone Formation.....	127
Scheme 3.6 Selectivity Reversal in Ti-promoted Addition of Ti-enol diazoacetate to α,β -Unsaturated Ketones.....	128
Scheme 3.7 Sc(OTf) ₃ -catalyzed Mukaiyama Aldol Addition of Si-enol Diazoacetate to Aldehydes and Imines.....	129
Scheme 3.8 Rh ₂ (OAc) ₄ -Catalyzed Intramolecular Oxonium Ylide Formation/1,2-Stevens Rearrangement.....	129
Scheme 3.9 Catalytic Asymmetric Mukaiyama Aldol Reactions for TMS-enol Diazoacetate	130
Scheme 3.10 Mukaiyama-Michael Addition of TBS-enol Diazoacetate to Cyclic and Acyclic enones	131
Scheme 3.11 Catalytic Asymmetric Mukaiyama-Michael Addition of TBS-enol Diazoacetate	132
Scheme 3.12 Synthesis of Enantioenriched 3-Phenyl Pentanedioic Acid Diesters..	132

Scheme 3.13 (a) Mukaiyama-Michael Addition of TBS-enol Diazoacetate to <i>trans</i> -4-methoxy-3-buten-2-one. (b) NaOH-Catalyzed Denitrogenative Cyclization of Highly Functionalized β -Keto- α -diazoesters to Produce Resorcinol. (c) NaOH-Catalyzed Rearrangement of Highly Functionalized β -Keto- α -diazoesters to Furnish 1,2-Diazepine	134
Scheme 3.14 Diastereoselective Mukaiyama Michael Addition of TBS-enol Diazoacetate to Pyranones, Dirhodium-catalyzed Oxonium Ylide Formation and 1,2-Stevens Rearrangement.....	135
Scheme 3.15 Mukaiyama-Mannich Addition of TBS-enol Diazoacetate with Diaryl Nitrones and the Following Catalytic Formal N-O Insertion Reaction	136
Scheme 3.16 Competitive OH-Insertion versus Formal N-O-Insertion.....	136
Scheme 3.17 Stereoelectronic Factors Influencing 1,2-Migration and the Strategy for the Synthesis of α -Diazoacetates Bearing β -Quaternary Carbons	138
Scheme 3.18 Directing Effect in Cu-catalyzed 1,2-N \rightarrow C Migration	148

List of Illustrations

Ar	aromatic
Bn	benzyl
t-Bu	<i>tert</i> -butyl
CAP	caprolactamate
DCM	dichloromethane
DCE	1,2-dichloroethane
DOSP	(<i>N</i> -dodecylbenzenesulfonyl)prolinate
dr	diastereomeric ratio
EDA	ethyl diazoacetate
ee	enantiomeric excess
Et	ethyl
Et ₃ N	triethylamine
EtOAc	ethyl acetate
equiv	equivalent
h	hour
Me	methyl
MEPY	pyrrolidine-4-carboxylic acid methyl ester
MenPy	pyrrolidine-4-carboxylic acid menthyl ester
ML _n	transition metal with ligands
MS	molecular sieves
NMR	nuclear magnetic resonance

NTTL	1,8-naphthaloyl-tert-leucinate
NTA	1,8-naphthaloylalaninate
OAc	acetate
Oct	octanoate
PTTL	phthaloyl-tert-leucinate
PTA	phthaloylalaninate
PTPA	phthaloylphenylalaninate
Ph	phenyl
<i>i</i> -Pr	<i>iso</i> -propyl
RT	room temperature
TBS	<i>tertiary</i> -butyldimethylsilyl
TFA	trifluoroacetic acid
THF	tetrahydrofuran
TMS	trimethylsilyl
TPA	triphenylacetate

Chapter 1: Competitive Enantioselective [3+3]-Cycloaddition and Diastereoselective [3+2]-Cycloaddition of Pyridinium/-Isoquinolinium Ylides with Enol Diazoacetate.

I. Introduction

1.1 General Information about Dirhodium(II) Carboxylates and Carboxamides

Dirhodium(II) carboxylates and carboxamides are catalysts noted for their ability to catalytically generate rhodium carbene intermediates with diazocompounds as well as for the diversity of their structural framework.¹⁻⁵ Dirhodium(II,II) tetraacetate - the first dirhodium compound to have been synthesized - possesses a paddlewheel structure with bridging ligands surrounding the dirhodium core and leaving two open coordination sites at the axial positions (**Figure 1.1**).⁶ Dirhodium(II) carboxylates and carboxamides share this fundamental structural motif, and they are capable of decomposing ethyl diazoacetate and generating rhodium carbene intermediate which undergoes subsequent group transfer reactions.^{7,8}

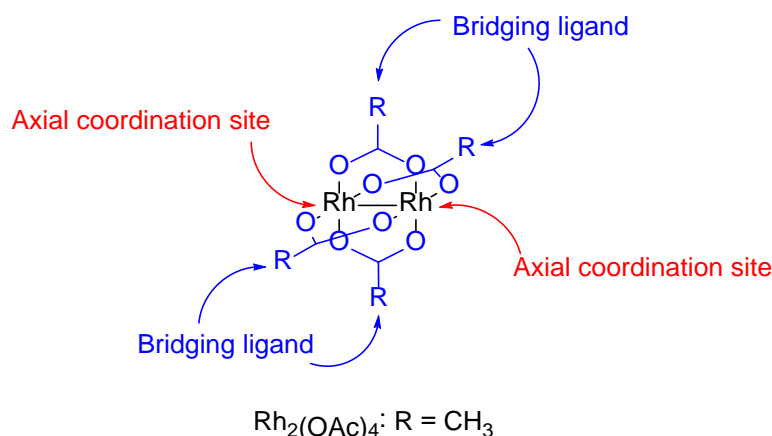
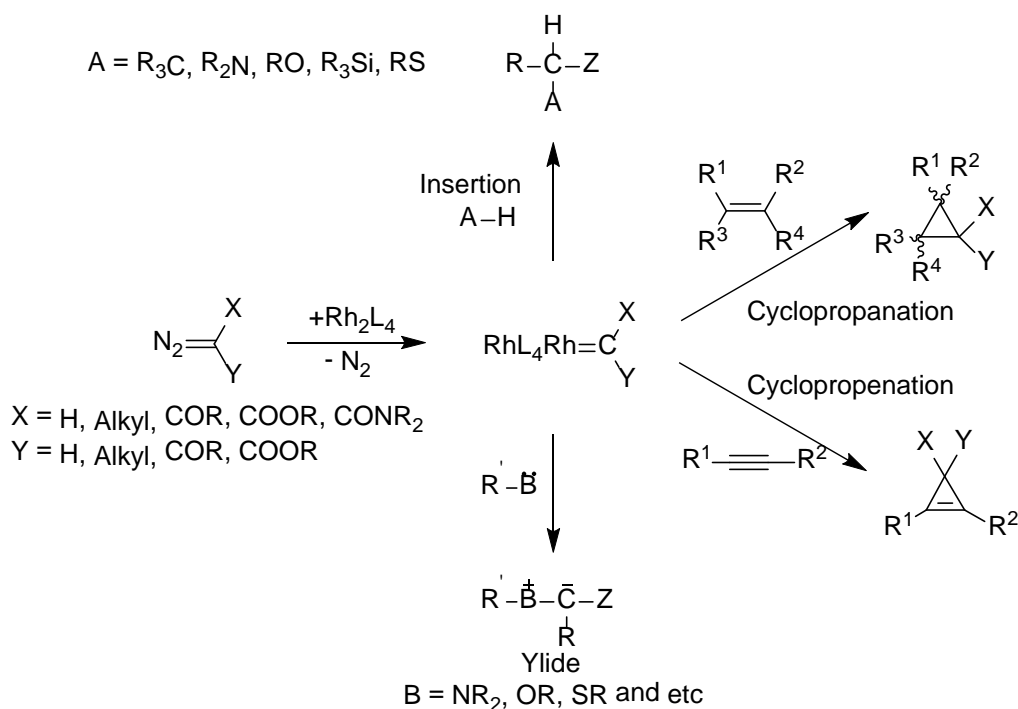


Figure 1.1 Structural Framework of Paddlewheel Dinuclear Complex- $\text{Rh}_2(\text{OAc})_4$.

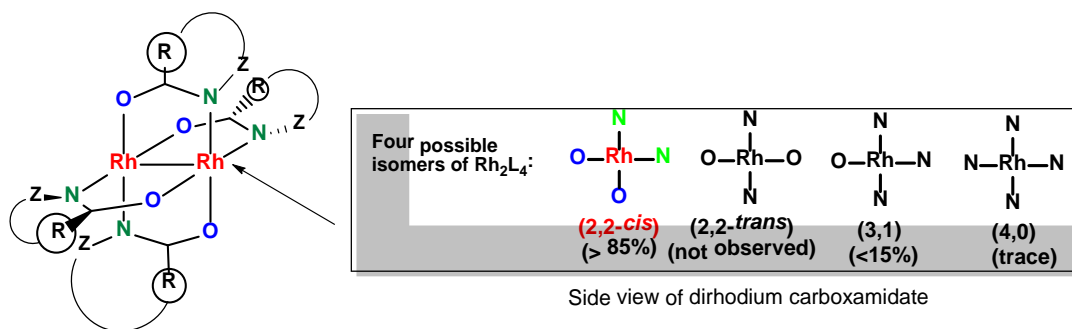
Subsequent developments in diazo chemistry, especially with α -diazocarbonyl compounds, have elevated dirhodium carboxylates and carboxamides to a superior position compared with other metal catalysts.⁹⁻¹¹ The catalytically generated rhodium carbene intermediate, which is highly electrophilic, can react with a variety of nucleophiles to furnish products ranging from C-H insertion, cyclopropanation, cyclopropanation and ylide formation (**Scheme 1.1**).^{4,7,8}



Scheme 1.1 Transformations Involving Rhodium Carbene Intermediates (L = Carboxylate or Carboxamide) from Catalytic Dinitrogen Extrusion of Diazocompounds.

Although sharing a common structural motif with dirhodium carboxylates, dirhodium carboxamides show more structural diversity.¹² Because of the unsymmetrical nature of bridging carboxamide ligands, four different isomers,

dependent upon the placement of nitrogens and oxygens on each rhodium, are viable: (2,2-*cis*), (2,2-*trans*), (3,1), and (4,0) (**Scheme 1.2**), but only the (2,2-*cis*)-isomer is formed in synthetically meaningful yields. A mechanistic study aiming at the understanding of the ligand exchange process suggests that the strong tendency for the formation of the (2,2-*cis*)-isomer is the result of a stepwise ligand replacement.¹³



Scheme 1.2 Structural Representation and Potential Isomers of Dirhodium(II) Carboxamidates.

1.2 General Information for Chiral Dirhodium(II) Carboxylates and Carboxamidate and Their Applications in Catalytic Asymmetric Transformations.

A dominant focus of chemical catalysis today is the enantioselective synthesis of chiral compounds, where one enantiomer of the two mirror-image forms is produced in a significantly larger quantity.¹⁴ One especially intriguing solution to this demand is the use of a chiral catalyst, which accelerates the reaction process and transfers its chirality to the reaction product(s). Among all the catalytic systems devised so far, a few stand out as exceptionally prominent for their high control of enantioselectivity on different reactions with broad substrate tolerance. This generality of the catalytic systems empowers synthetic practitioners, who increasingly initiate their synthetic

practices with well-established catalytic systems. Those catalytic systems that provide high enantiocontrol over a wide range of different reactions with broad substrate tolerance are referred as “privileged catalysts”.¹⁴ The development of chiral dirhodium carboxylates and carboxamidates has been one of the frontiers in asymmetric catalysis.^{2,4,12,15} Although various chiral carboxylate and carboxamidate ligands have been incorporated into the Rh₂⁴⁺ core,¹⁶⁻¹⁹ so far only those chiral dirhodium catalysts having chiral amino acid-derived ligands have displayed generally high enantiocontrol over different types of reactions;^{1-4,12,15,20,21} and they are privileged chiral dirhodium(II) catalysts. Three major types of privileged chiral dirhodium catalysts are presented in **Figure 1.2**.

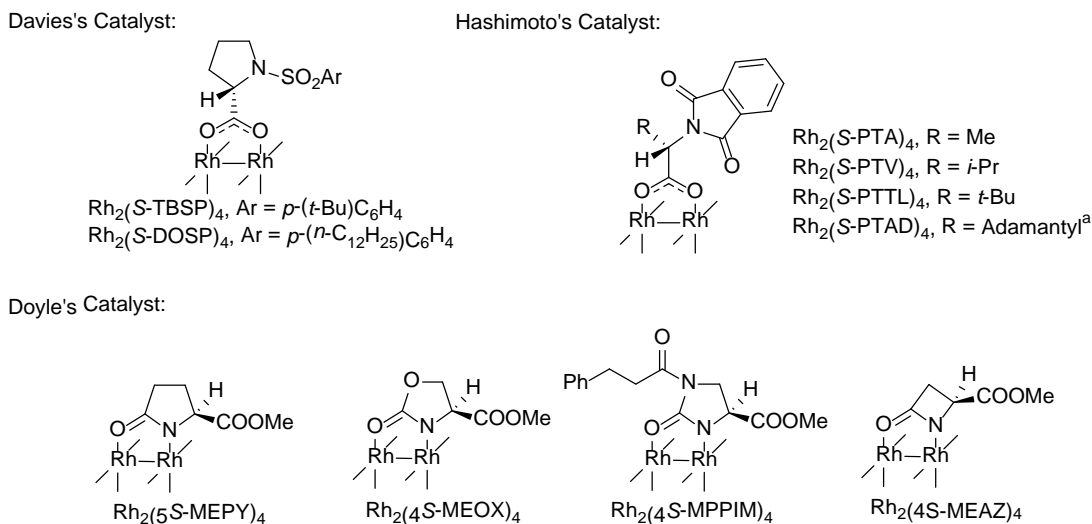
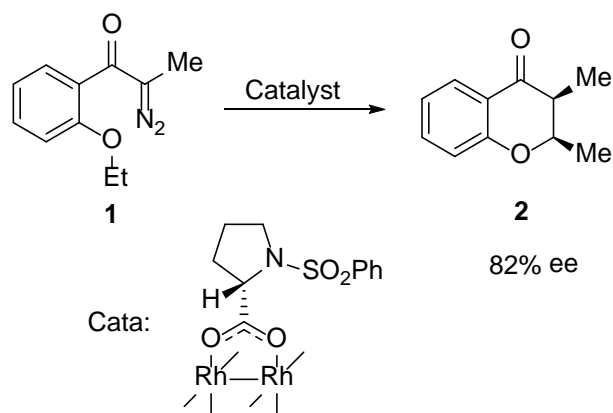


Figure 1.2 Representative examples of privileged chiral dirhodium(II) catalyst. ^aAlthough the synthesis of Rh₂(S-PTAD)₄ catalyst has been accomplished by Davies, it follows the same designing principle that Hashimoto first introduced.

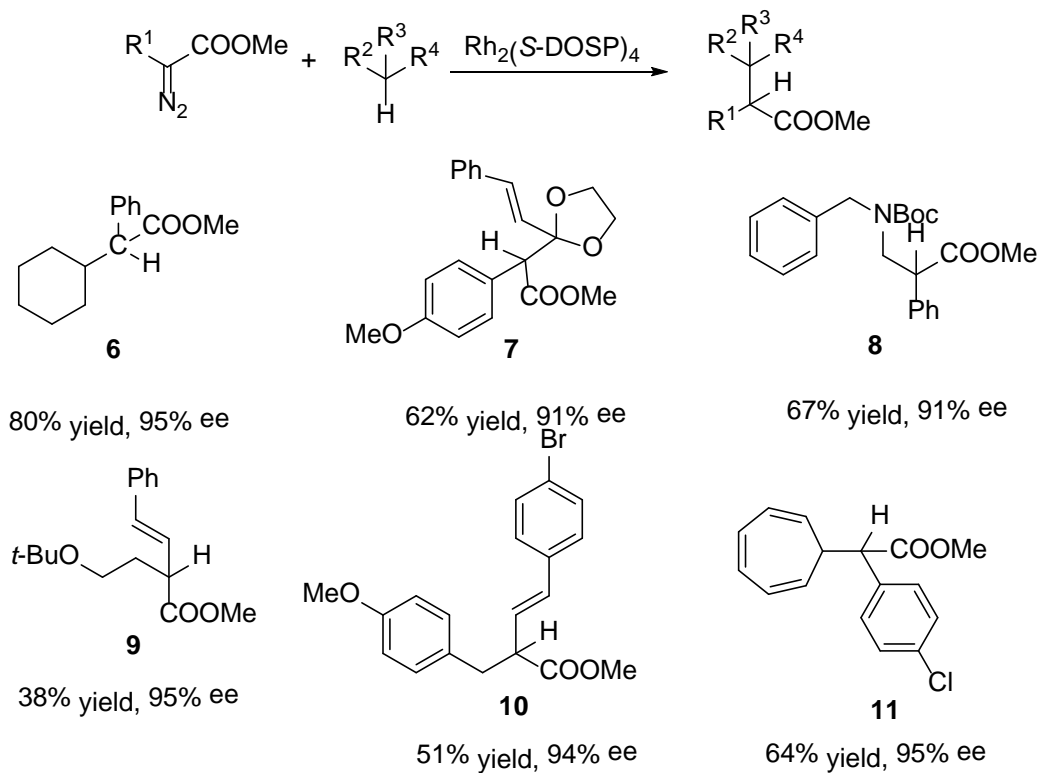
The dirhodium(II) tetrakis[*N*-phenylsulfonylproline] catalyst, which is initially developed by McKervery and coworkers,²⁰ exhibits good enantiocontrol in an

intramolecular C-H insertion reaction (**Scheme 1.3**). Further development of the catalyst by Davies leads to the discovery of $\text{Rh}_2(\text{DOSP})_4$,^{1,3,21,22} which has been demonstrated to display excellent stereoselectivity for asymmetric reactions involving styryldiazoacetates and aryldiazoacetates.^{23,24} Commercially available (*S*)- or (*R*)-prolines are used to synthesis the bridging ligand of $\text{Rh}_2(\text{DOSP})_4$. The presence of a long alkyl chain grants the catalyst excellent solubility in most organic solvents including *n*-pentane. As a result, this unique feature greatly expands the solvent compatibility of $\text{Rh}_2(\text{DOSP})_4$. Extensive studies have been performed targeting understanding of the exceptional stereocontrol achieved with uses of chiral dirhodium catalyst.^{23,25} The chiral proline ligands on dirhodium(II) can form a chiral environment that governs the alignment of the carbene and the trajectory of the incoming nucleophile. The concept of conformational flexibility for the carboxylate ligands was first introduced by Hashimoto and co-workers.²⁶ Later on, this explanation was used by Davies to rationalize the dramatic solvent effect associated with $\text{Rh}_2(\text{DOSP})_4$ catalytic system.¹ The orientation of the bridging ligands results in different conformers and each has its unique selectivity and reactivity. The solvent effect can be explained by the conformation change of the catalyst in different solvents. Although the flexible nature of dirhodium carboxylate catalyst invokes uncertainty of modeling as well as predictions of enantiocontrol, their applicability to a wider range of diazo compounds for highly stereoselective transformations is strengthened by their adaptive chiral environment.⁴

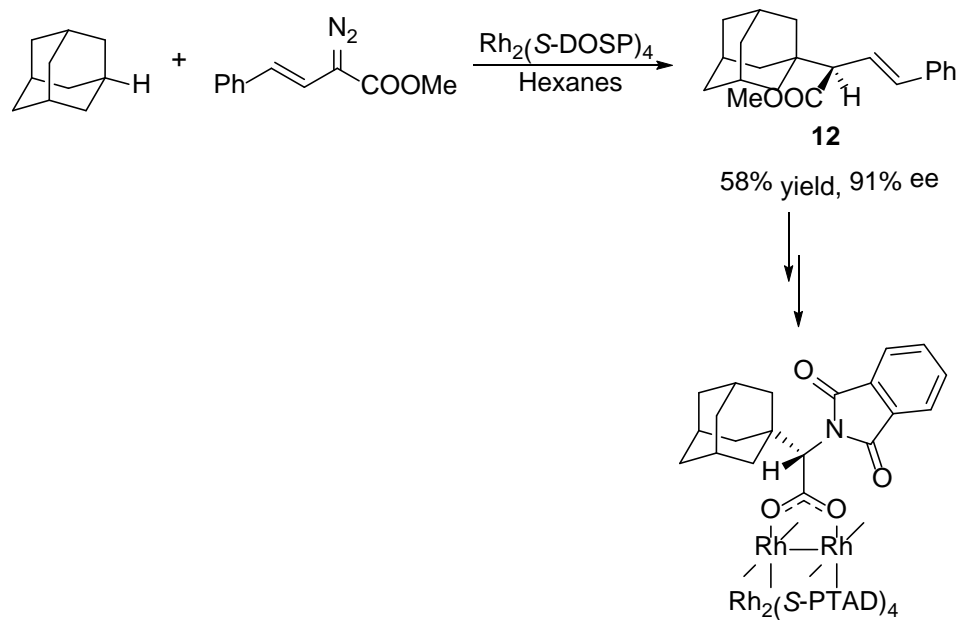


Scheme 1.3 Dirhodium(II) Tetrakis[*N*-phenylsulfonylprolinate]-catalyzed Intramolecular Asymmetric C-H Insertion.

The unmatched catalytic performance of $\text{Rh}_2(\text{DOSP})_4$ in asymmetric transformations involving donor/acceptor diazo compounds can be exemplified in the highly enantioselective C-H insertion reaction.¹ Selected examples of this type are shown in **Scheme 1.4**. The particularly challenging enantioselective C-H insertion into unactivated sp^3 -hybridized C-H bond can be rendered in high yield and excellent selectivity. Insertion reactions targeting activated C-H bonds such as an allylic or etheral C-H bond, during which there is stabilization of the build-up of partial positive charge in the transition state, shows high reactivity and enantioselectivity. An immediate application of this asymmetric C-H insertion methodology is the preparation of a chiral amino acid ligand that is not available from natural sources.²⁷ For instance, the reaction of adamantane with styryl diazoacetate under the catalysis of $\text{Rh}_2(\text{S-DOSP})_4$ results in the generation of a chiral ester in high optical purity, which, upon further elaboration, leads to the synthesis of $\text{Rh}_2(\text{S-PTAD})_4$ catalyst (**Scheme 1.5**). This same strategy has been implemented in the synthesis of other chiral dirhodium catalysts^{28,29} and chiral Co(II) porphyrin catalysts.³⁰

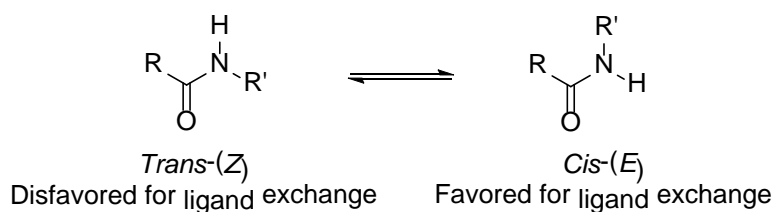


Scheme 1.4 $Rh_2(S-DOSP)_4$ -catalyzed Asymmetric C-H Insertion with Aryldiazoacetates and Styryldiazoacetates.



Scheme 1.5 Preparation of $Rh_2(S-PTAD)_4$ by Asymmetric C-H Insertion of Styryl Diazoacetate into a Tertiary C-H Bond of Adamantane.

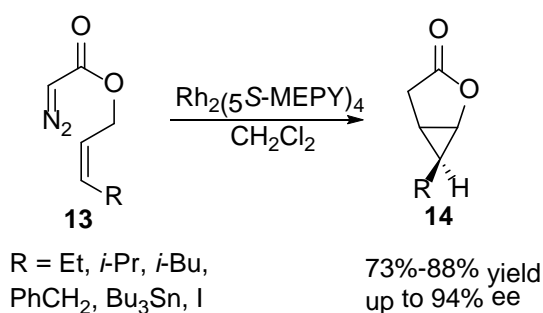
The establishment and understanding of chiral dirhodium carboxamidate catalytic systems is mainly through the efforts of Doyle and coworkers,^{2,4,8,12,15} who visualize that introduction of chiral carboxamidate ligands to the dirhodium core can be achieved by ligand exchange reactions in a high boiling-point solvent (chlorobenzene) with an acid scavenger (sodium carbonate) in a Soxhlet extractor.^{31,32} However, initial trials to screen a broad array of chiral carboxamides suggest that acyclic amides were not potent candidates because ligand substitution reactions demand the *cis-(E)*-amide conformation rather than the *trans-(Z)*-conformation (**Scheme 1.6**).³³



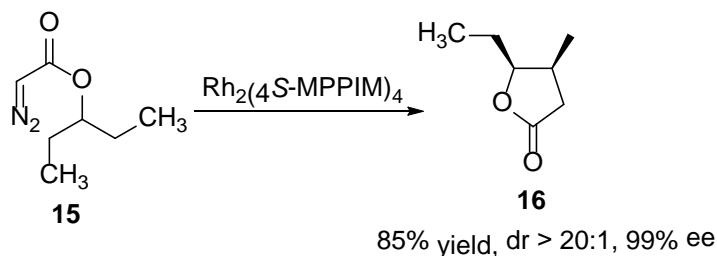
Scheme 1.6 Conformation of Amide Influences the Ligand Exchange Reaction.

Subsequent studies demonstrate that cyclic amides are generally applicable to ligand exchange under the condition stated above, and the structures are usually intended to represent only the (2,2-*cis*)-isomer (**Scheme 1.2**).³¹ The separation of the major (2,2-*cis*)-isomer from the minor (3,1)-isomer can be easily achieved by crystallization or using CN-bonded silica gel chromatography.³¹ Two rhodium atoms are connected by a Rh-Rh single bond, and the Lewis basic species such as acetonitrile occupies the axial coordination sites to form air-stable red crystalline solids.³² Following the first report of a chiral dirhodium carboxamidate catalyst - dirhodium(II) tetrakis[methyl 2-oxopyrrolidine-5(*S*)-carboxylate] $[\text{Rh}_2(5S\text{-MEPY})_4]$,⁷ four types of amino acid-derived ligand motifs have been developed and incorporated into the

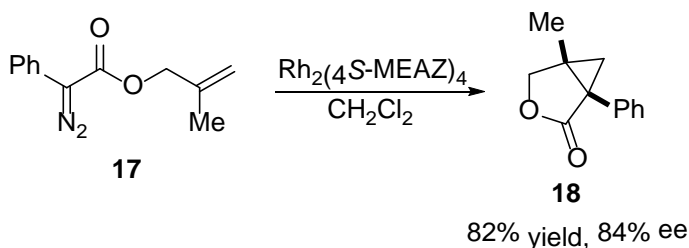
dirhodium core with the chirality of the ligand dictated by the carbon adjacent to the nitrogen.⁴ The ester attached to the chiral center on the pyrrolidinone ring is crucial for asymmetric induction in catalytic reactions. The more electron-rich carboxamidate ligand compared to carboxylate causes the reactivity of dirhodium carboxamidates to be generally lower but more selective towards rhodium carbene formation and subsequent reactions.² For instance, the $\text{Rh}_2(5\text{S-MEPY})_4$ catalyst is an effective catalyst for intramolecular cyclopropanation reactions (**Scheme 1.7**).¹⁵



Scheme 1.7 Intramolecular Enantioselective Cyclopropanation Catalyzed by $\text{Rh}_2(5\text{S-MEPY})_4$.



Scheme 1.8 Intramolecular Enantioselective C-H Insertion Catalyzed by $\text{Rh}_2(4\text{S-MPPIM})_4$.



Scheme 1.9 Intramolecular Enantioselective Cyclopropanation of Phenyl diazoacetate Catalyzed by $\text{Rh}_2(4\text{S-MEAZ})_4$.

The conformational bias exerted by the imidazolidinone ligand of $\text{Rh}_2(\text{MPPIM})_4$ imparts additional steric interaction with rhodium-bonded carbene and this catalyst offers superior enantiocontrol for intramolecular C-H insertion reaction (**Scheme 1.8**).³⁴ Incorporation of the strained four-membered azetidinone ligands into the dirhodium core elongates the Rh-Rh bond distance, and $\text{Rh}_2(\text{MEAZ})_4$ has significantly higher reactivity than $\text{Rh}_2(\text{MEPY})_4$ (**Scheme 1.9**).³⁵ Although the more reactive chiral dirhodium(II) carboxylates are useful for certain intramolecular reactions, they are most effective for intermolecular C-H insertion reactions of aryldiazoacetates and styryldiazoacetates.¹⁵ A computational study addressing ligand effect on the dirhodium system suggests that electron donation of the ligand to the rhodium atom is responsible for the differential selectivity and reactivity between dirhodium carboxylate and carboxamidate systems.¹⁹ The relatively rigid chiral environment of chiral dirhodium(II) carboxamidates is another distinctive feature of the dirhodium carboxylate system (**Figure 1.3**).³³ The ester functionality attached to the chiral center protrudes from the “walls” of the catalyst and creates an asymmetric environment and influences the alignment of the carbene. The approach of a nucleophile is impaired from the regions occupied by the carboxylate groups of the four ligands (**Figure 1.3c**). Unlike the $\text{Rh}_2(\text{DOSP})_4$ catalytic system, a strong solvent effect of the chiral dirhodium carboxamidate system in metal carbene catalysis has not been observed.

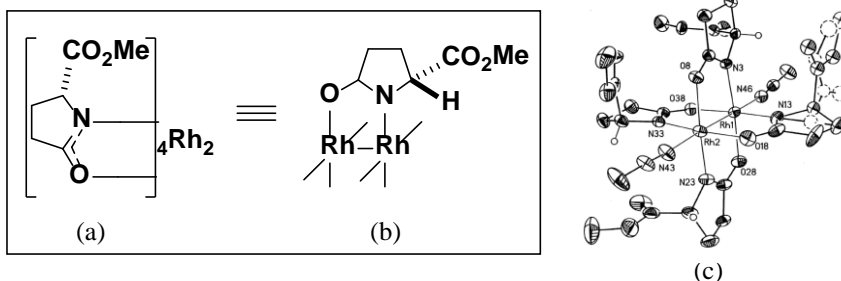
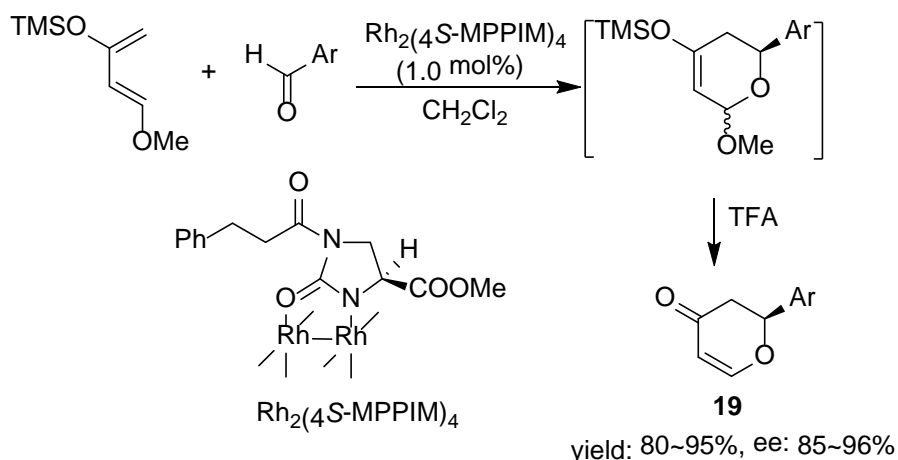


Figure 1.3 Dirhodium(II) Tetrakis(methyl 2-oxopyrrolidine-4(*R*)-carboxylate): (a) and (b) are Common Representations; (c) X-ray Structure of Rh₂(*R*-MEPY)₄ Bisacetonitrile Complex.

In an effort to expand catalytic applications of chiral dirhodium carboxamidates, a major breakthrough has been unveiled when chiral dirhodium(II,II) carboxamidates were found out to be capable of catalyzing the hetero-Diels-Alder reactions of 1-methoxy-3-trimethylsilyloxy-butadiene (“Danishefsky diene”) and aromatic aldehydes in excellent yields and good enantiomeric excesses (**Scheme 1.10**).³⁶ Further optimization of the reaction condition reveals that turnover numbers as high as 10,000 could be achieved with Rh₂(4*S*-MPPIM)₄ in greater than 90% yield and more than 95% ee.³⁷

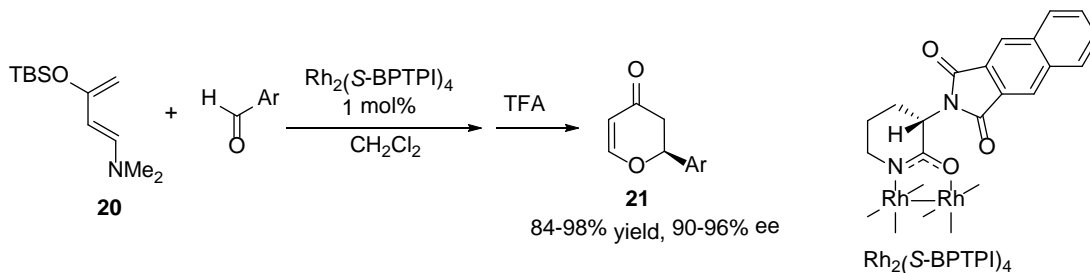


Scheme 1.10 Hetero-Diels-Alder Reactions Catalyzed by Chiral Dirhodium Carboxamidates.

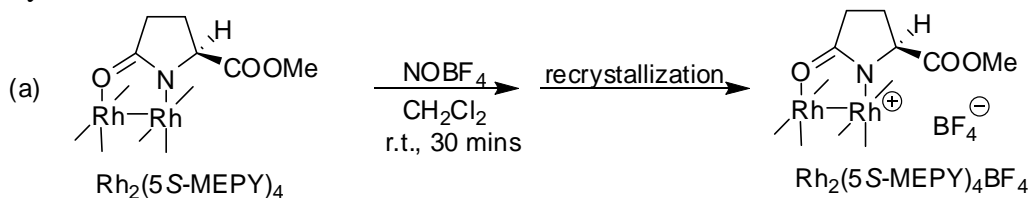
Although excellent results have been achieved in the hetero-Diels-Alder reaction with chiral dirhodium(II,II) carboxamidates as highly effective chiral Lewis catalysts, the scope of the reaction is limited to aromatic aldehydes bearing electron-withdrawing substituents on the aromatic ring.^{36,37} One feasible solution to the problem is to employ a more electron-rich diene as potential substrate, and this approach has been successfully implemented by Hashimoto in the $\text{Rh}_2(\text{S-BPTPI})_4$ -catalyzed the hetero-Diels-Alder reactions of various aldehydes with (*E*)-1-dimethylamino-3-*tert*-butyldimethylsiloxy-1,3-butadiene (“Rawal diene”) (**Scheme 1.11**).³⁸

An alternative solution is enhancement of the Lewis acidity of the catalyst through the formation of cationic dirhodium(II,III) carboxamidates from the corresponding dirhodium(II,II) carboxamidates in the presence of a stoichiometric amount of nitrosonium salts (**Scheme 1.12a**).³⁹ The chiral cationic dirhodium(II,III) carboxamidates exhibit enhanced Lewis acidity along with better stereocontrol (**Scheme 1.12b**). Encouraged by the remarkable performance of chiral dirhodium(II,III) carboxamidates in the catalytic enantioselective hetero-Diels-Alder reactions, a series of cationic dirhodium(II,III) carboxamidates have been employed in catalyzing the asymmetric 1,3-dipolar cycloaddition of α,β -unsaturated aldehydes with nitrones.³⁹ Despite the fact that excellent diastereoselectivity and enantiocontrol could be easily achieved, the regioselectivity issue remains unsolved. A recent study of solvent effects on dirhodium(II,III) carboxamidate catalytic system shows that halogenated solvents such as dichloromethane or chlorobenzene coordinate to the electrophilic rhodium center and deactivate the catalyst.⁴⁰ Reactions carried out in toluene display much faster reaction rates and enhanced regioselectivities compared to

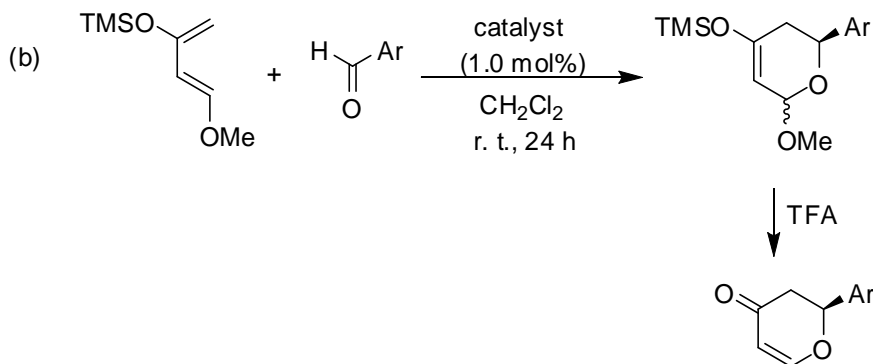
reactions performed in halogenated solvents (**Scheme 1.13**). Overall, the chiral dirhodium carboxamidate catalytic system has been demonstrated to be highly effective in both metal carbene and Lewis acid catalysis.



Scheme 1.11 Hetero-Diels-Alder Reactions Catalyzed by Chiral Dirhodium Carboxylate with Rawal Diene.

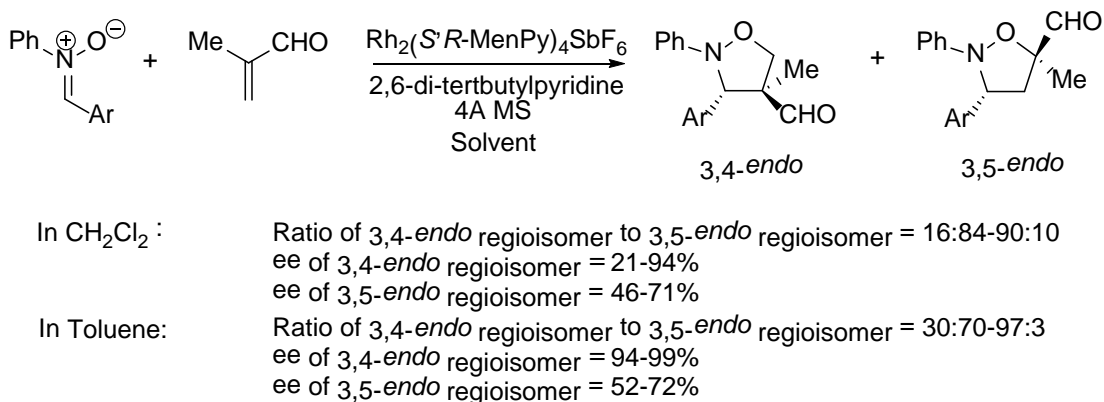


Note: NOSbF_6 can be used instead of NOBF_4 and then $\text{Rh}_2(5\text{S-MEPY})_4\text{SbF}_6$ will be formed.



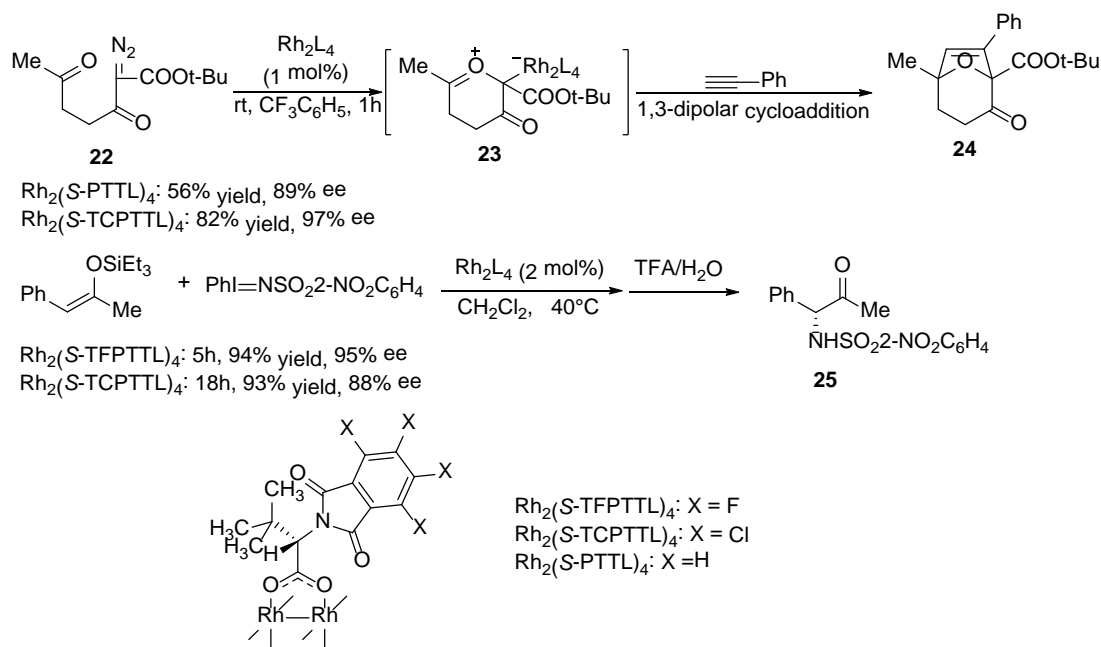
When Ar = *p*-nitro,
 With $\text{Rh}_2(5\text{S-MEPY})_4$, 53% conversion, 73% ee;
 With $\text{Rh}_2(5\text{S-MEPY})_4\text{BF}_4$, 94% conversion, 94% ee.

Scheme 1.12 (a) Formation of Chiral Cationic Dirhodium(II,III) Carboxamidates by Oxidation of Nitronium Salts. (b) Enhanced Lewis Acidity and Stereocontrol with Chiral Cationic Dirhodium(II,III) Carboxamidates in the Hetero-Diels-Alder Reaction.



Scheme 1.13 Solvent Effect on Dirhodium(II,III) Carboxamidate Catalyzed Asymmetric 1,3-Dipolar Cycloaddition Reactions.

Hashimoto and coworkers have developed a catalytic system that combines the high reactivity of the dirhodium prolinato system as well as the diversity of the chiral dirhodium carboxamidate system.^{26,38,41-53} The approach for the preparation of the ligand can be applicable to a variety of amino acids and the ligand exchange reaction with $\text{Rh}_2(\text{OAc})_4$ is facile and often high yielding. The resulting catalyst is compatible with normal silica gel chromatography, and the separation is generally easily. The combination of *N*-protecting group and the R group of the amino acid side chain (**Figure 1.2**) enables the generation of a matrix of chiral dirhodium catalysts, which maximizes the tuneability of the chiral environment surrounding the catalytically generated rhodium carbene center. More importantly, the substitution on *N*-phthaloyl group with halogens furnishes a more Lewis acidic dirhodium catalyst with dramatically enhanced catalytic reactivity and stereoselectivity in several transformations (**Scheme 1.14**).⁴⁹⁻⁵¹ The benefit for the introduction of halogen atoms on the *N*-phthaloyl group has been verified in the catalytic asymmetric intramolecular ylide formation/1,3-dipolar cycloaddition and the amination of silyl enol ethers.⁴⁹⁻⁵¹



Scheme 1.14 Enhanced Reactivity and Selectivity by the Introduction of a Halogenated *N*-Phthaloyl Group.

The wide applications of Hashimoto's catalysts in catalytic asymmetric transformations illustrate their effective enantiocontrol and high reactivity. The low catalyst loading often required demonstrates their robustness under the reaction conditions. Among all the Hashimoto' Rh(II)-carboxylate catalysts reported, those derived from *N*-phthaloyl-protected amino acids have emerged as exceptionally powerful catalyst for asymmetric synthesis. In this series, the *tert*-leucine-derived complex-dirhodium(II) tetrakis[*N*-phthaloyl-(*S*)-*tert*-leucinate] [$\text{Rh}_2(\text{S-PTTL})_4$], has displayed outstanding catalytic performances in asymmetric reactions, including intramolecular C-H insertion,⁵⁴⁻⁵⁶ tandem ylide formation/1,3-dipolar cycloaddition,^{50,57} amination,^{58,59} cascade ylide formation/2,3-sigmatropic rearrangement, cyclopropanation.⁶⁰ Although the crystal structure of dirhodium(II) tetrakis[*N*-phthaloyl-(*S*)-phenylalaninate],⁶⁰ $\text{Rh}_2(\text{S-PTPA})_4$, indicates that two phthalimido groups are oriented in parallel on each face of the dirhodium

tetracarboxylate, independent proposals from Fox^{61,62} and Charette^{63,64} for the origin of enantioselectivity in $\text{Rh}_2(\text{S-PTTL})_4$ -catalyzed asymmetric transformations suggest that a “chiral crown” conformation, where all four *N*-phthalimide groups are located on the same face of the catalyst in an $\alpha,\alpha,\alpha,\alpha$ -conformation, is ultimately the structure that affords high enantioselectivity. Crystallographic evidence for the chiral crown structure in bimetallic paddlewheel complexes has been established in subsequent studies,⁶¹ which includes work on $\text{Rh}_2(\text{S-NTTL})_4$ -catalyzed cyclopropanation⁶⁵, $\text{Rh}_2(\text{S-TBPTTL})_4$ -catalyzed cyclopropanation,⁴³ and $\text{Rh}_2(\text{S-NTTL})_4$ -catalyzed electrophilic aromatic substitution of indoles.⁶⁶ Inspection of transition state models involving chiral crown catalysts implies that non-covalent ligand-substrate interactions contribute to the induction of asymmetry.^{61,62,66} Examination of the X-ray structure of $\text{Rh}_2(\text{S-PTTL})_4$ crystals grown from ethyl acetate (**Figure 1.4**), reveals that two chiral cavities are located on the two faces of the dirhodium catalyst. All four *tert*-butyl groups are oriented on the same face of the catalyst with each C-(*t*-Bu) bond roughly parallel to the central Rh-Rh bond and this unique displacement forms a shallow chiral cavity (~11 Å in dimension). The alignment of the four phthalimido groups on the opposite face of the catalyst generates a wider cavity (~15 Å in dimension). This wide chiral cavity constitutes the reactive face and contributes the high level of asymmetric induction. Moreover, computational analyses further support that the chiral crown conformation has the lowest energy for all conformations that are tested. Consistent with this hypothesis, only the Rh atom on the wider chiral face is bound by solvent in the crystal structure.⁶¹

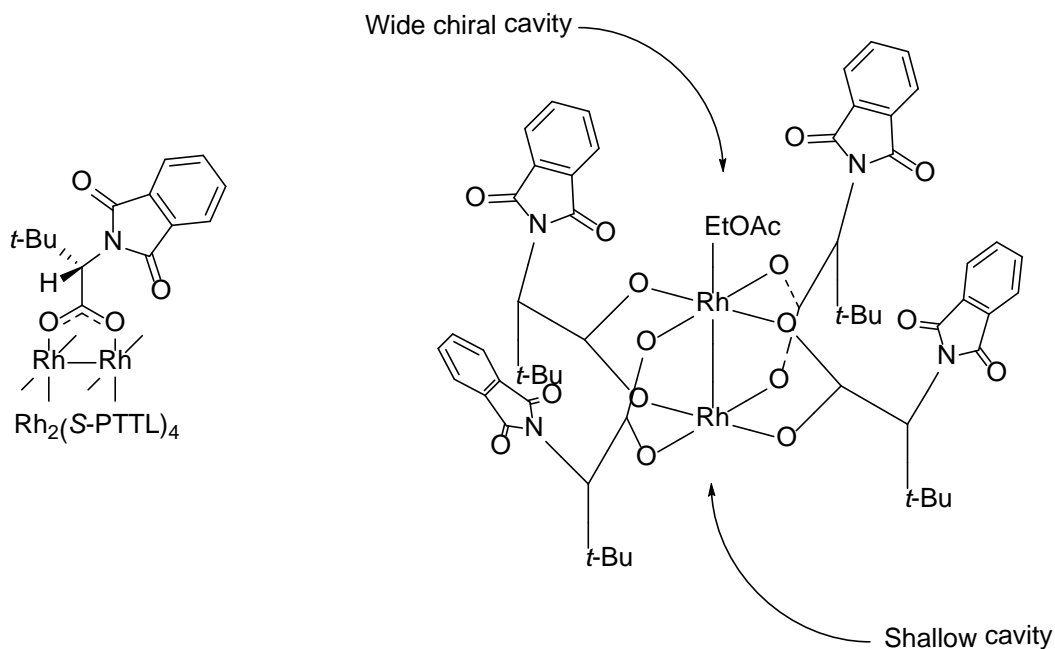
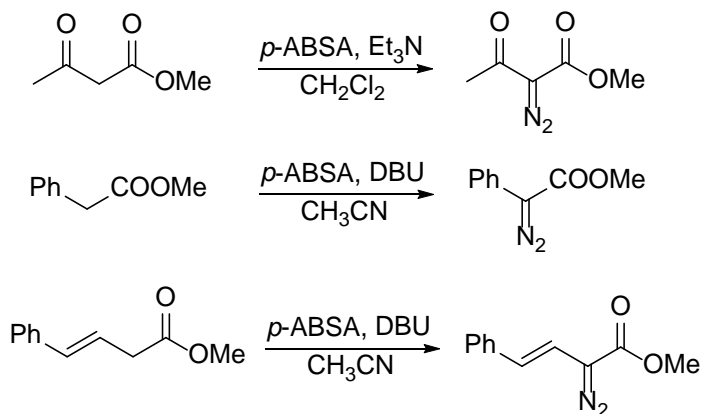


Figure 1.4 The Chiral Crown Conformation Adopted by $\text{Rh}_2(\text{S-PTTL})_4$.

1.3 General Information for Diazocompounds and Reactivity Profiles of Vinyl diazoacetate

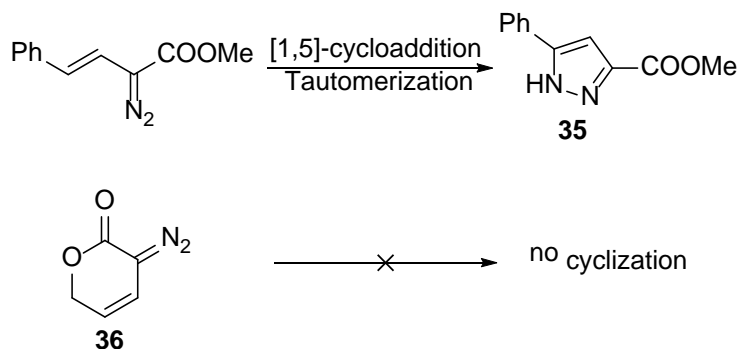
Ethyl diazoacetate can be synthesized by diazotization of glycine, and this reaction represents the first report on the preparation of an α -diazocarbonyl compound.⁶⁷ Introduced by Regitz and coworkers,⁶⁸ the diazo transfer technique, which invokes transferring a diazo group from a donor to an acceptor, is now a general and exceptionally useful method for the syntheses of various types of diazocarbonyl compounds. Sulfonyl azides are the most frequent donors, and a ketone or an ester is usually the acceptor. Deprotonation of a carbonyl compound by an appropriate base is required to achieve transfer of a diazo group to the α -methylene position. For those substrates, which bear two flanking carbonyl groups, the α -methylene protons are acidic enough to ensure smooth diazo transfer in the presence of a mild base.⁵ For

instance, the conversion of acetoacetate to diazoacetoacetate occurs smoothly in the presence of Et₃N at room temperature (**Scheme 1.15**). The synthesis of styryldiazoacetate and phenylacetate can also be accomplished by the standard diazo transfer method in the presence of DBU with appropriate precursors (**Scheme 1.15**).



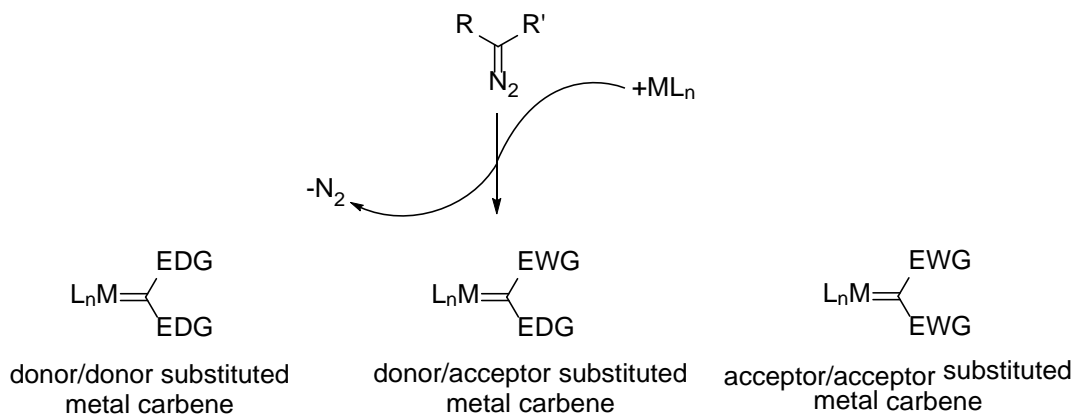
Scheme 1.15 Representative Examples for the Synthesis of Diazoacetate under Direct Diazo Transfer.

Although, diazocarbonyl compounds are in general stable and storable, most vinyldiazoacetates are unstable, undergoing a spontaneous [1,5]-cycloaddition to yield pyrazoles (**Scheme 1.16**), therefore they can only be stored only for a short time.⁵ Cyclic vinyldiazoacetate and enol diazoacetate in general do not participate in intraloecular [1,5]-cyclization and they are stable and storable for extended period of time.

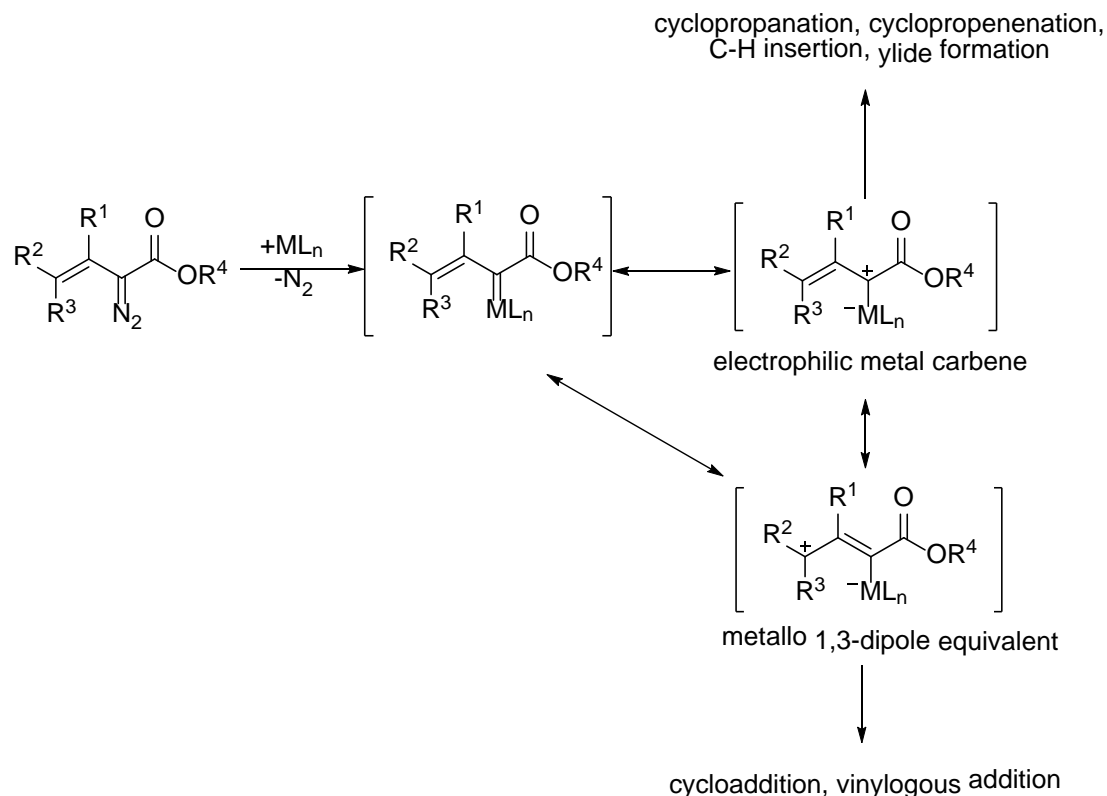


Scheme 1.16 Intramolecular Cyclization of Styryldiazoacetates.

Based on the electronic nature of the substituents bonded to the carbene center, the metal carbene intermediate can be broadly categorized into donor/donor, donor/acceptor, and acceptor/acceptor metal carbenes (**Scheme 1.17**).¹ Catalytic dedinitrogenation of vinyldiazoacetate leads to the formation of a donor/acceptor metal carbene that possesses unique reactivity due to the delocalization of the double bond π electrons (**Scheme 1.18**). The resulting vinyl metal carbene intermediate can undergo the typical reactions of an electrophilic metal carbene, namely cyclopropanation, cyclopropanation, C-H insertion and ylide rearrangement. More importantly, it resembles a metallo 1,3-dipole equivalent and participates in cycloaddition reactions or engages in addition reactions at the vinylogous position rather than at the carbene position.⁶⁹⁻⁷⁴ This unique reactivity profile is due to the extended conjugation of the double bond attached to the carbene center (**Scheme 1.18**).



Scheme 1.17 Classification of Substituted Metal Carbene Intermediates.



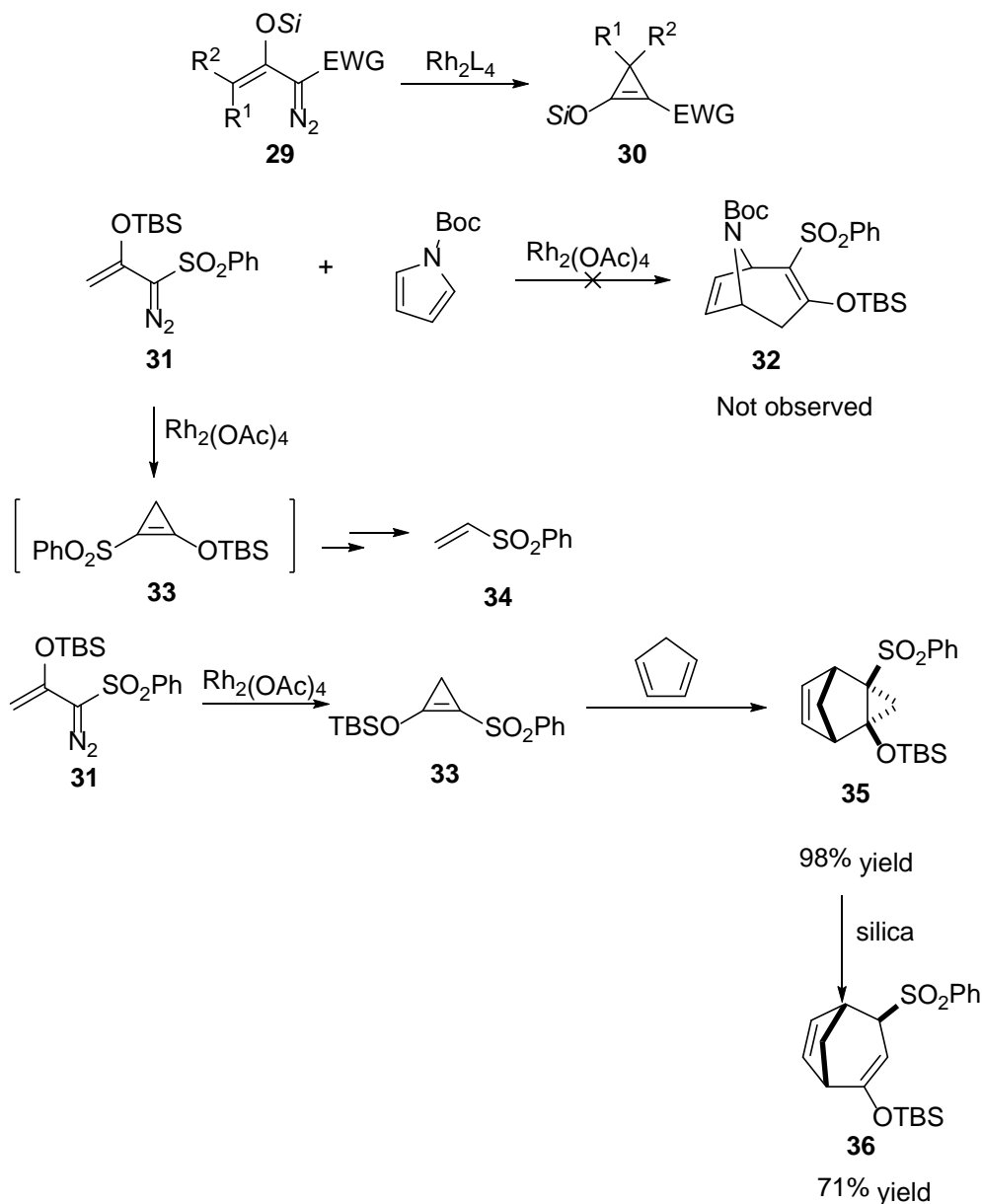
Scheme 1.18 Diversified Reactivities of Vinyl Metal Carbenes.

1.4 Donor/Acceptor Cyclopropene Generation from Enol Diazoacetate and Synthetic

Application of the Donor/Acceptor Cyclopropene

The generation of donor/acceptor cyclopropenes from enol diazoacetates has been reported by Davies and coworkers en route to the study of the cyclopropanation/Cope rearrangement reaction sequence between pyrroles and silylated enol diazosulfinate.⁷⁵ Upon reacting the enol diazosulfinate **31** with Boc-protected pyrrole, the anticipated [4+3]-cycloaddition product **32** is not observed. Instead vinylsulfone **34** is afforded in low reaction yield. A key intermediate proposed was the donor/acceptor cyclopropene **33** generated by the enol diazosulfinate (**Scheme 1.19**). The donor/acceptor cyclopropene could undergo [4+2]-cycloaddition reaction

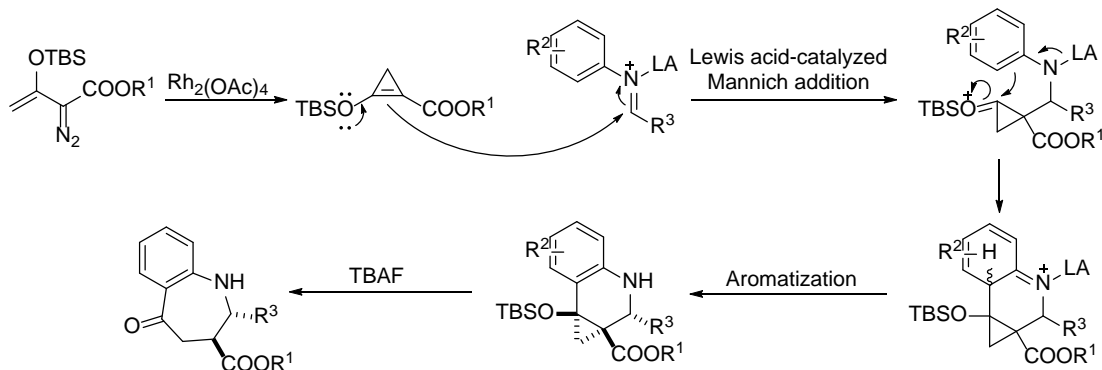
with cyclopentadiene to generate **35**, which further rearranges to afford the [3.2.1]-bicyclooctadiene **36** under weakly acidic condition.



Scheme 1.19 Cyclopropene Generation by Catalytic Dinitrogen Extrusion and [4+2]-Cycloaddition Reaction of Cyclopentadiene and Donor/Acceptor Cyclopropenes.

Since this preliminary report, the synthetic utility of the cyclopropene has been largely underappreciated until several recent efforts by Doyle and coworkers to unearth the great potential of these donor/acceptor cyclopropenes in organic synthesis.^{73,74,76} In

an elegant example the use of donor/acceptor cyclopropene as the alkene component in a diastereoselective Povarov reaction with imines underscores the high reactivity and selectivity associated with the donor/acceptor cyclopropenes (**Scheme 1.20**).⁷⁶



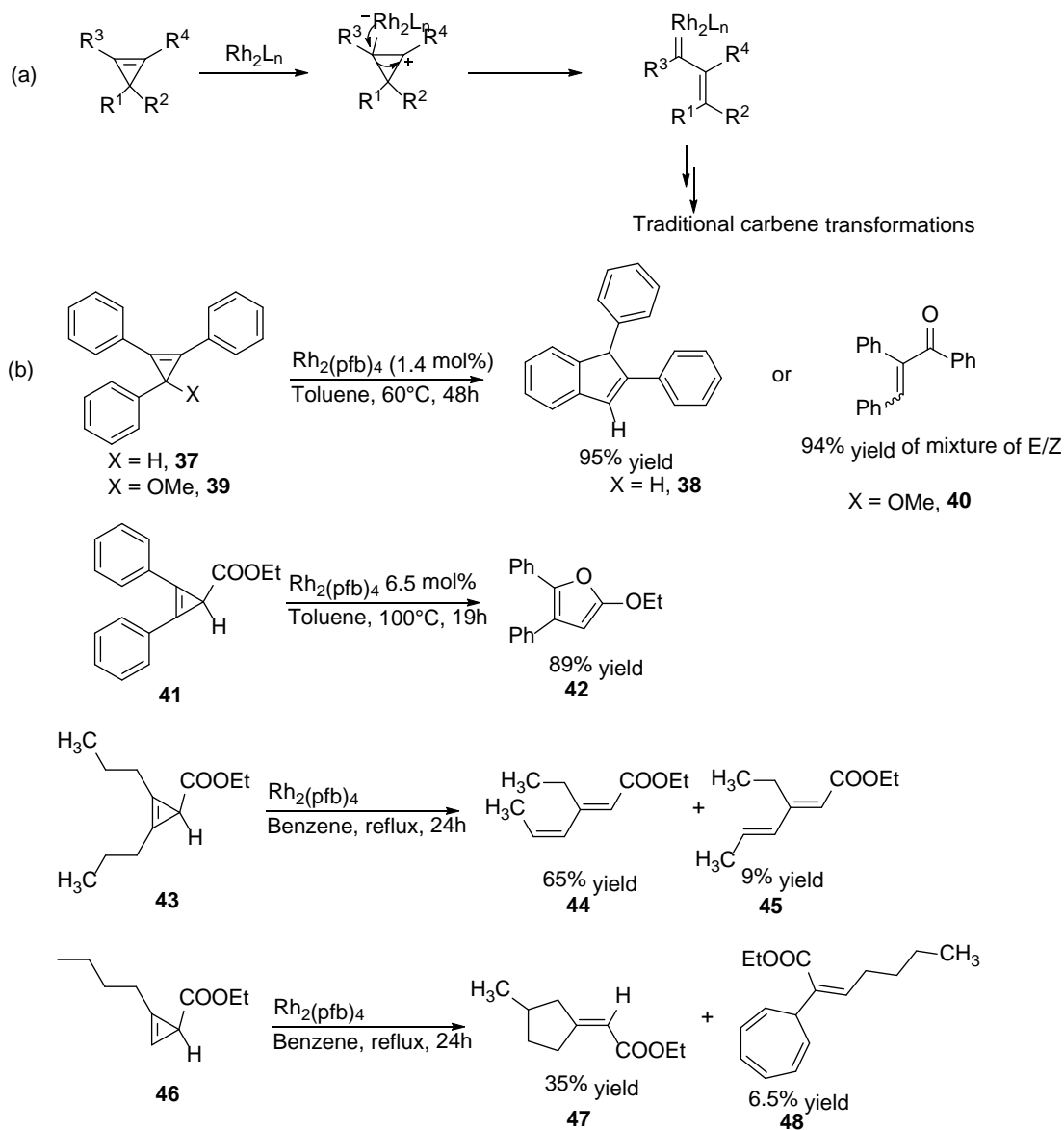
Scheme 1.20 Diastereoselective Povarov Reaction of Donor/acceptor Cyclopropene and Substituted Imines.

1.5 Cyclopropene as Rhodium Vinylcarbene Precursor

Dirhodium-catalyzed cyclopropanation reactions of alkynes with a catalytically generated rhodium carbene intermediate from diazo compounds have been intensively studied, and several chiral dirhodium catalytic systems have been employed to control the enantioselectivity of such transformations.⁸ By comparison to the well-known cyclopropanation reactions, the use of substituted cyclopropenes as carbene precursors has not been fully explored; and their applications in organic synthesis are still primitive.

Paul Müller has systematically examined the differential catalytic reactivity of $\text{Rh}_2(\text{pfb})_4$ with other transition metal complexes in the rearrangement of multisubstituted cyclopropenes (**Scheme 1.21**).⁹⁻¹¹ Although some degree of similarity has been discovered for $\text{Rh}_2(\text{pfb})_4$ and Cu complexes, the drastic differences in most cases have highlighted the uniqueness of dirhodium catalysts in these transformations,

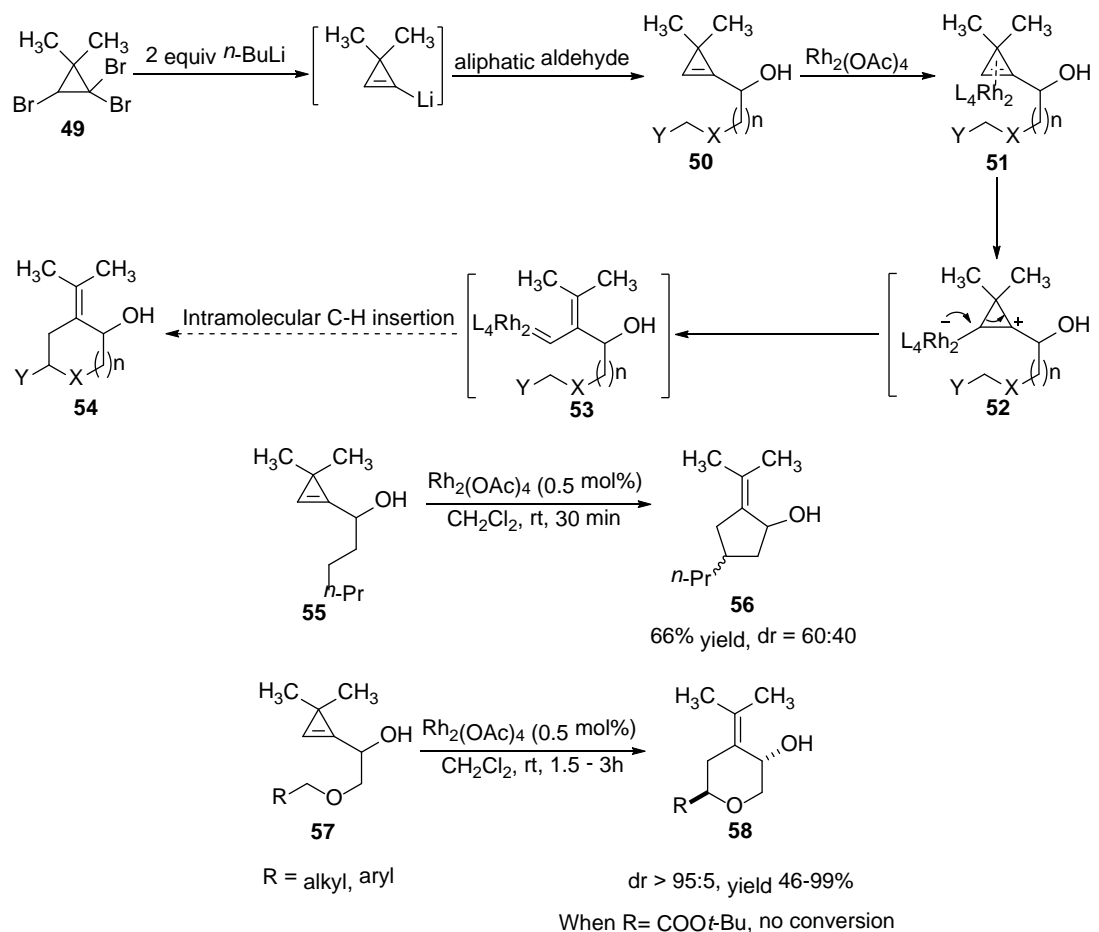
and their reaction outcomes are consistent with the formation of a rhodium vinylcarbene from substituted cyclopropenes. For instance, treatment of the triphenylcyclopropene **37** and **39** with a catalytic amount of $\text{Rh}_2(\text{pfb})_4$ results in the formation of 1,2-diphenylindene **38** or α,β -unsaturated ketone **40** depending on the substitution pattern on the cyclopropene ring. Heating the diphenylcyclopropenecarboxylate **41** under catalysis by $\text{Rh}_2(\text{pfb})_4$ in toluene presumably generates a vinylcarbene, which forms an oxonium ylide via intramolecular addition of the ester carbonyl that rearranges to the final furan product **42**. Rhodium vinylcarbene formation and subsequent 1,2-hydride migration have been observed when an alkyl-substituted cyclopropene **43** is employed. Interestingly, a small amount of cycloheptatriene product **48** is also isolated accompanied by the anticipated C-H insertion product **47**, which could be rationalized by the Büchner reaction of the vinylrhodium carbene intermediate.



Scheme 1.21 Rhodium Vinylcarbene Formation from Cyclopropene by $\text{Rh}_2(\text{pfb})_4$ Catalysis.

Janine Cossy has recognized the unique advantage of using cyclopropenes as rhodium vinylcarbene precursor to access to pure donor-type carbenes and has recently reported a very useful approach for the diastereoselective construction of multi-substituted carbocycles and oxygen heterocycles (**Scheme 1.22**).^{77,78} Dimethylcyclopropene **50** can be easily prepared by treating the tribromocyclopropane

49 with two equivalents of *n*-BuLi to afford the corresponding lithiated dimethylcyclopropene, which subsequently adds to an aliphatic aldehyde. The aliphatic chain attachment on the dimethylcyclopropene structure offers an opportunity to study the intramolecular C-H insertion reaction of the rhodium vinylcarbene generated from the dimethylcyclopropene. The dimethylcyclopropene **50** shows very high reactivity towards dirhodium-catalyzed vinylcarbene formation, and the reaction proceeds rapidly at room temperature in dichloromethane with only 0.5 mol% Rh₂(OAc)₄. While the reaction outcomes could be complicated by the formation of the two regioisomeric vinylcarbene intermediates, reaction seems to proceed exclusively towards the formation of the rhodium vinylcarbene **53**, which can be schematically understood by the initiation of dirhodium catalyst coordination to the less substituted cyclopropene carbon. The rhodium vinylcarbene **53** undergoes intramolecular 1,5-C-H insertion with moderate diastereoselectivity, and inserts into a sp³-hybridized ethereal C-H bond with excellent diastereocontrol. A deuterium labeling experiment suggests that the C-H insertion process of the rhodium vinylcarbene proceeds through a concerted stereospecific mechanism, and the observed high diastereoselectivity can be interpreted from a seven-membered cyclic boat conformation as the transition state with minimal 1,3-allylic strain.



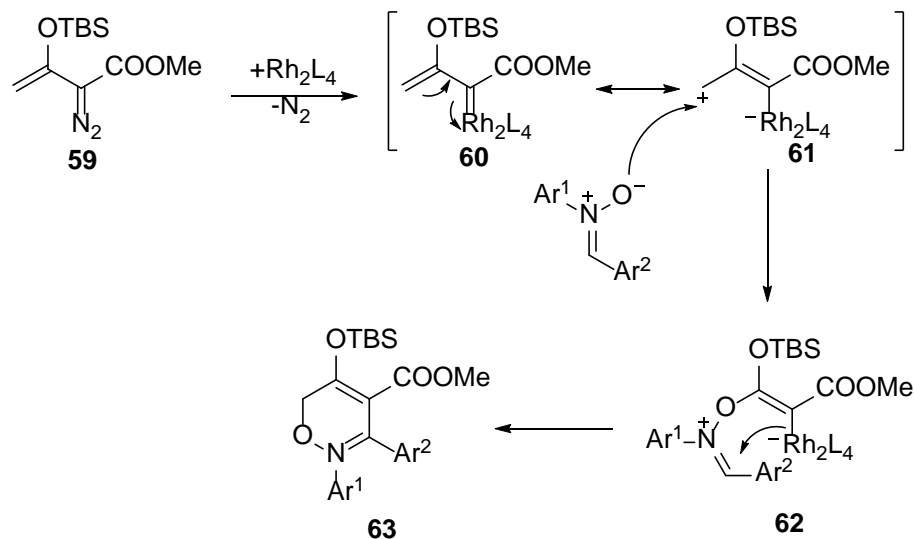
Scheme 1.22 Diastereoselective Construction of Carbocycles and Oxygen Heterocycles through Dirhodium-catalyzed Isomerization of Substituted Cyclopropenes.

The direct use of the donor/acceptor cyclopropenes as rhodium vinylcarbene precursors has not been studied.

1.6 Examples of [3+3]-Cycloaddition Reactions for Enol Diazoacetate.

The first example of [3+3]-cycloaddition for enol diazoacetates is reported by Doyle and coworkers.⁷⁹ Activation of enol diazoacetate is achieved by the catalytic formation of a rhodium bound enol carbene intermediate. Although two potential reaction sites are available for nucleophilic addition reactions, only the vinylogous position preferentially undergoes electrophilic addition to the nitrene oxygen and

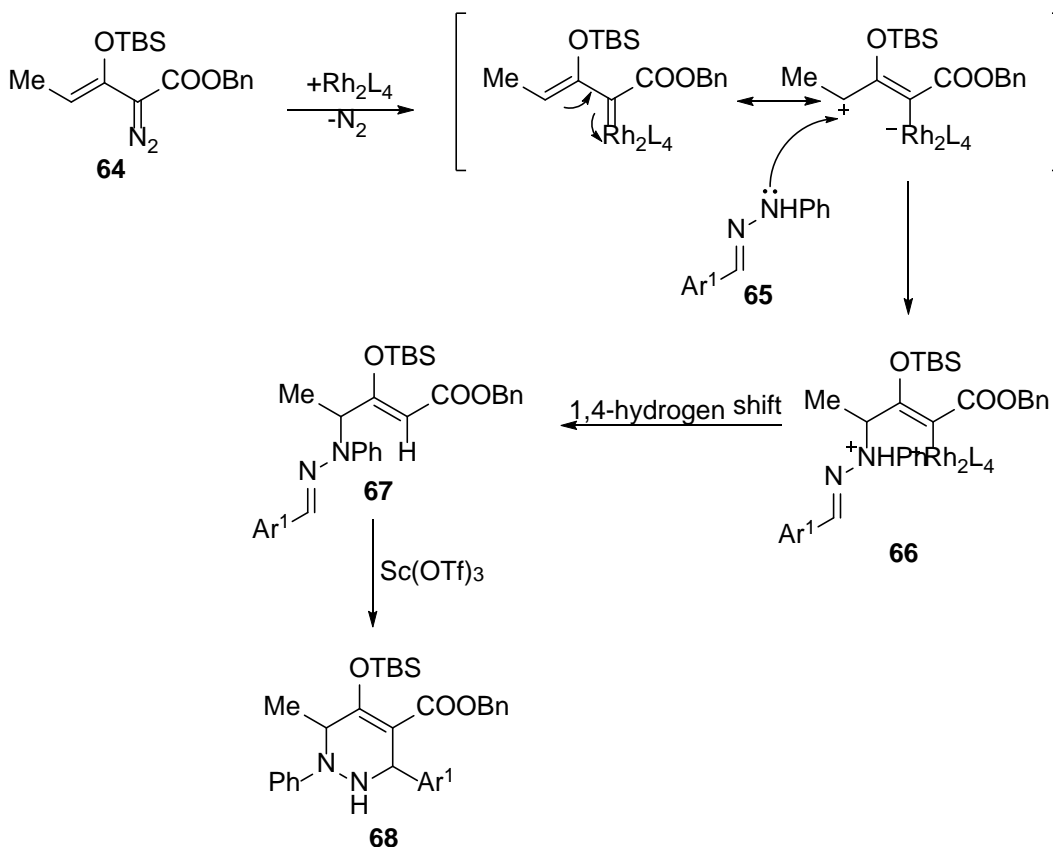
subsequent ring closure and concomitant release of dirhodium catalyst complete the catalytic cycle (**Scheme 1.23**). The reaction can be rendered highly enantioselective when Hashimoto's chiral dirhodium catalyst $\text{Rh}_2(\text{S-PTA})_4$ is used.



Scheme 1.23 Catalytic Asymmetric Synthesis of 3,6-Dihydro-1,2-oxazines by [3+3]-Cycloaddition of Enol Diazoacetate with Aryl Nitrones.

As an extension for the [3+3]-cycloaddition of nitrones and enol diazoacetate, a formal [3+3]-cycloaddition reaction of enol diazoacetate **64** and hydrozone **65** has also been accomplished.⁷⁰ The lone pair of nitrogen on hydrozone attacks the vinylogous electrophilic carbon followed by a 1,4-hydrogen transfer to furnish the imino enol product **67**, which under Lewis acid catalysis undergoes intramolecular Mukaiyama-Mannich addition to generate tetrahydropyridazine **68** (**Scheme 1.24**).

The unusual reactivity that enol diazoacetates display in the [3+3]-cycloaddition reactions presents a major impetus for the exploration of enol diazoacetate reacting with other 1,3-dipolar species.

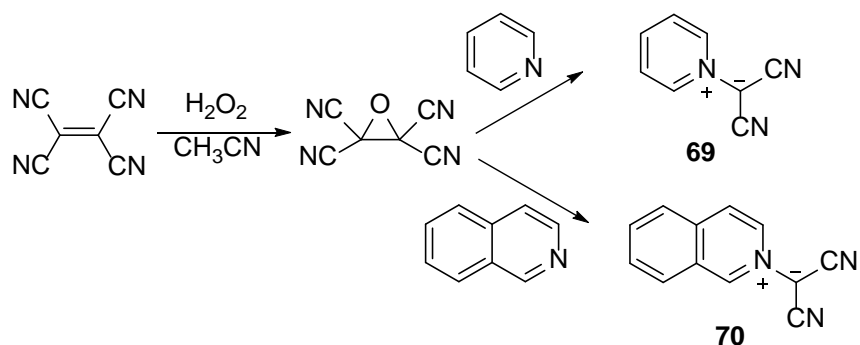


Scheme 1.24 Construction of Tetrahydropyridazine by Cascade N-H Insertion and Intramolecular Mannich Addition.

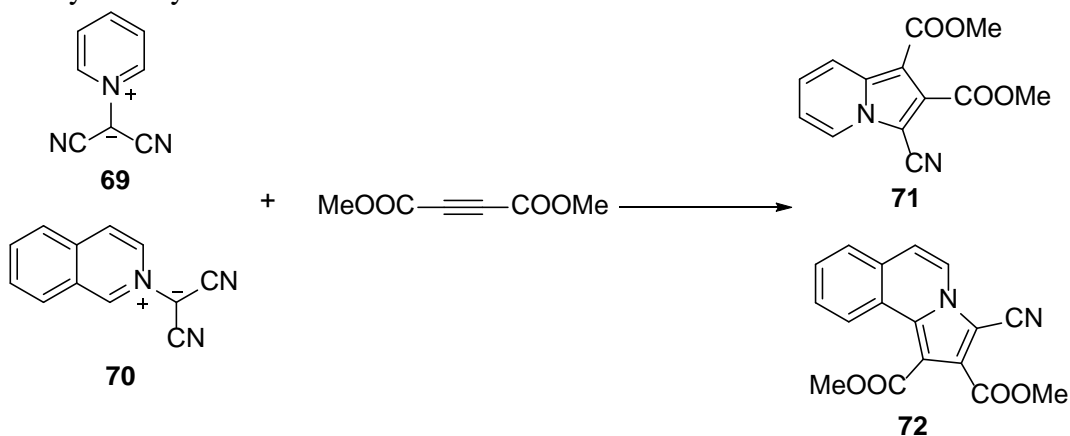
1.7 Chemistry of Heteroaromatic Ylides.

The pyridinium/isoquinolinium dicyanomethylides **69** and **70** have been discovered during the investigation of the reactivity of tetracyanoethylene oxide with different nucleophiles.⁸⁰ Condensation of tetracyanoethylene oxide with excess pyridine in THF at 0 °C forms a yellow precipitate which has a composition of 1:1 ratio pyridine and dicyanomethylide (**Scheme 1.25**). The related isoquinolinium dicyanomethylide **70** is prepared in a similar way. The pyridinium/isoquinolinium dicyanomethylides are immediately recognized as 1,3-dipoles, and they react smoothly with dimethyl acetylenedicarboxylates to produce the corresponding [3+2]-

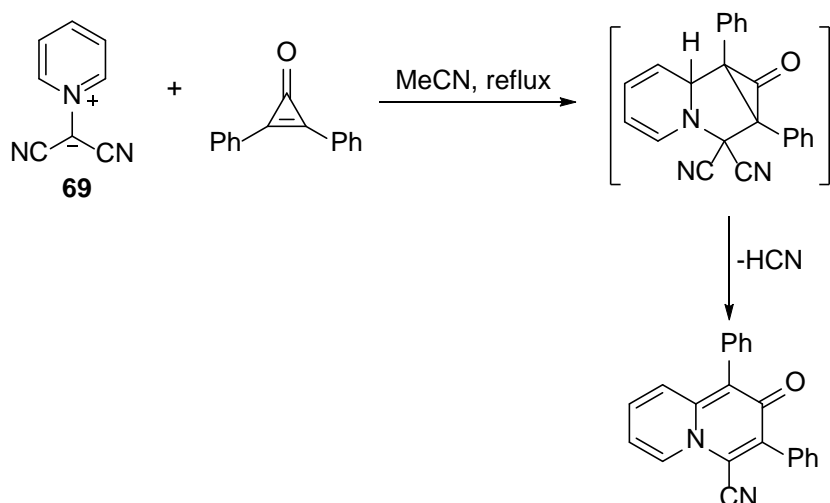
cycloaddition products, which upon loss of hydrogen cyanide affords indolizidine **71** and **72** in good yields (**Scheme 1.26**). Since this initial discovery, a few reports studying the cycloaddition reaction of pyridinium/isoquinolium methylides with different dienophiles have emerged.⁸¹⁻⁸³ In an interesting example, diphenylcyclopropenones engage in the [3+2]-cycloaddition with pyridinium dicyanomethylides (**Scheme 1.27**).⁸⁴ The resulting indolizidine undergoes ring expansion reaction to generate the quinolizidine product.



Scheme 1.25 Preparation of Pyridinium/Isoquinolium Dicyanomethylide from Tetracyanoethylene Oxide.

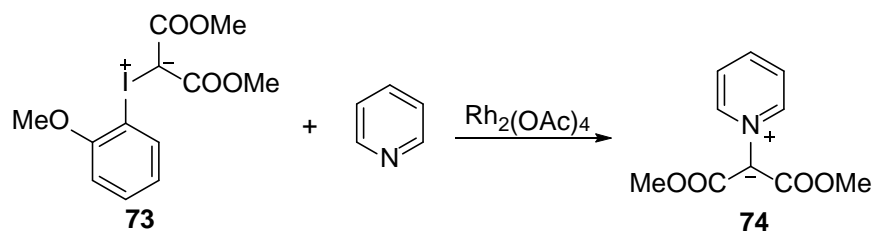


Scheme 1.26 1,3-Dipolar Cycloaddition Reaction of Pyridinium/Isoquinolium Dicyanomethylide with Dimethyl Acetylenedicarboxylates.

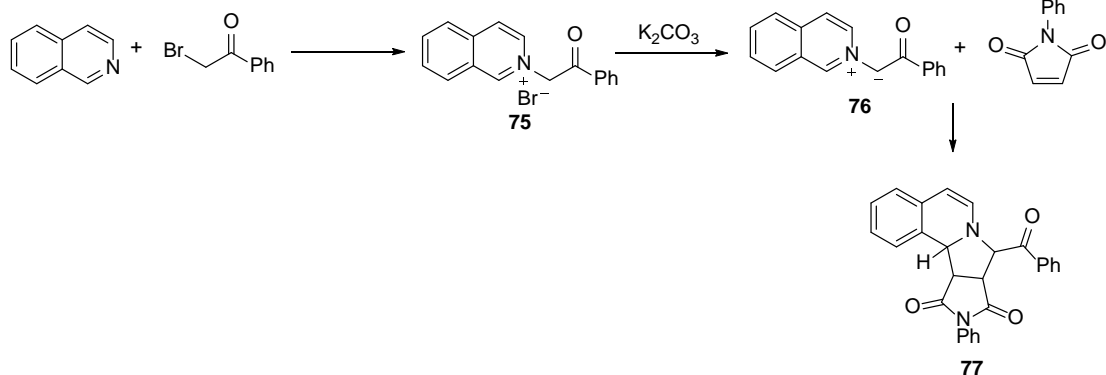


Scheme 1.27 [3+2]-Cycloaddition of Pyridinium Dicyanomethylide and Diphenylcyclopropanone.

Pyridinium/isoquinolinium dicarbomethoxymethylides are isolable and are stable solids.⁸⁵ They can be prepared as stable ylides from phenyliodonium ylides under dirhodium catalysis (**Scheme 1.28**). Although they have also been shown to undergo [3+2]-cycloaddition reaction with dienophiles, they are significantly less reactive than are the corresponding dicyanomethylides.⁸⁵ Ylides stabilized with only one electron-withdrawing group can only be generated in situ by the deprotonation of an isoquinolinium bromide precursor.⁸⁶ The methylide is highly reactive toward dipolar cycloaddition reactions (**Scheme 1.29**).



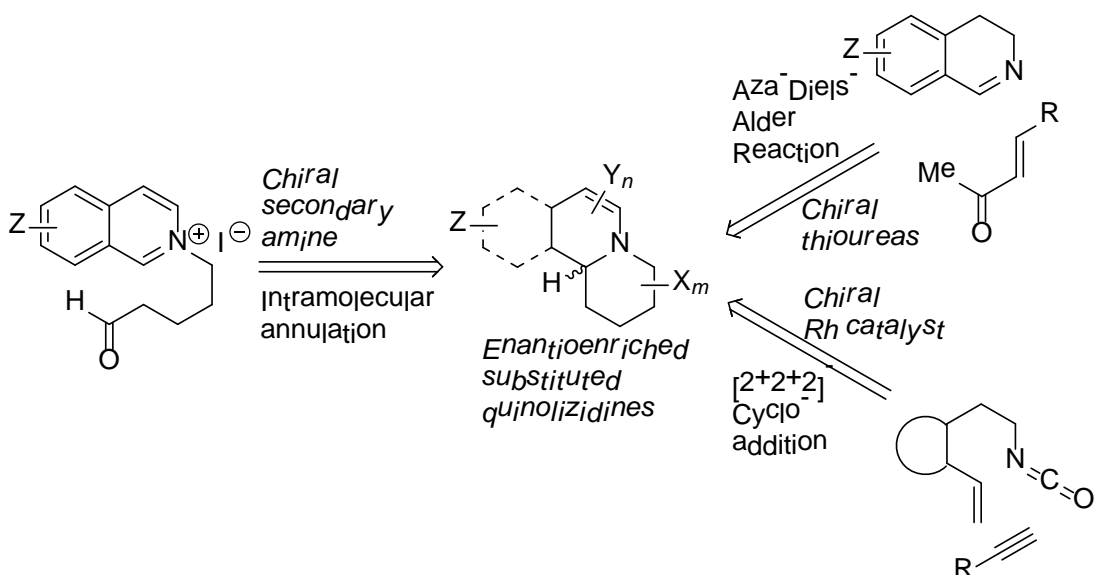
Scheme 1.28 Synthesis of Pyridinium/isoquinolinium Dicarbomethoxymethylide under Dirhodium Catalysis.



Scheme 1.29 In Situ Generation of an Isoquinolium Methylide and Its Subsequent [3+2]-Cycloaddition Reaction.

1.8 Research goal

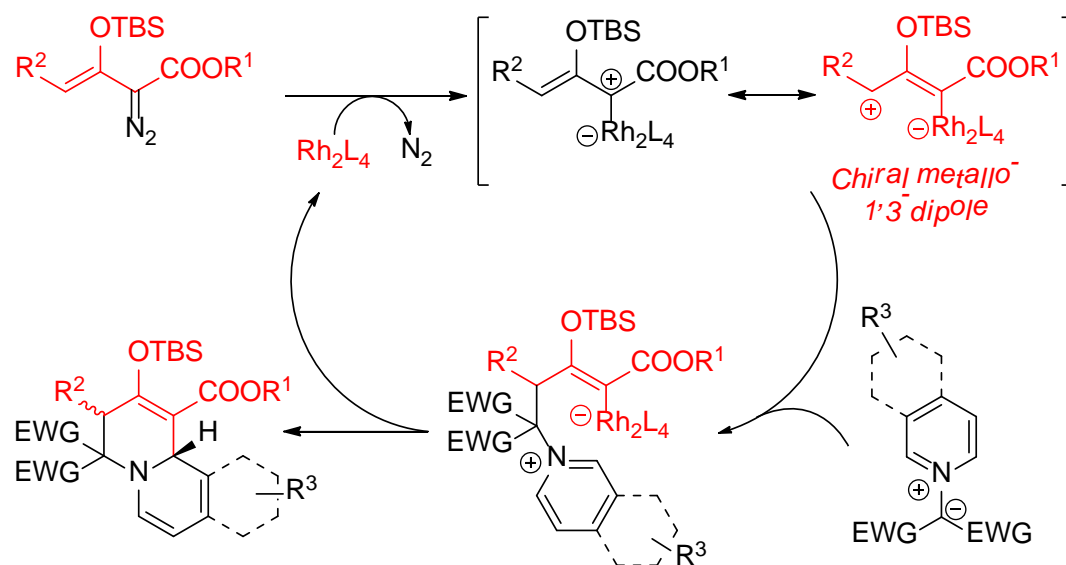
Quinolizidines are isolated from myriad sources in nature, and they display diverse biological activities.⁸⁷⁻⁹¹ Among nitrogen-containing heterocyclic compounds, substituted quinolizidine alkaloids are exceptionally prominent,⁸⁷ and some of them are lead compounds for the development of anticancer, anti-inflammatory, and cardiovascular drugs.⁸⁸⁻⁹¹ Despite longstanding biological and synthetic interest in quinolizidines, methodologies for the synthesis of these valuable compounds have been limited. Asymmetric approaches to these systems have relied on either using reactants from the chiral pool,⁸⁸⁻⁹¹ introducing chirality through the use of chiral auxiliaries,^{92,93} or catalytic enantioselective approaches.⁹⁴⁻⁹⁷ However, catalytic methods have been limited as well, and rhodium-catalyzed asymmetric [2+2+2]-cycloadditions of isocyanates,⁹⁴ catalytic asymmetric formal aza-hetero-Diels-Alder reactions^{95,96} and one report of an organocatalytic enantioselective dearomatization of *N*-alkyl isoquinolinium salts (**Scheme 1.30**)⁹⁷ constitute the only current examples.



Scheme 1.30 Reaction Pathways to Enantioselective Syntheses of Substituted Quinolizidines.

Although aromatic frameworks are capable of participating in reactions as electrophiles⁹⁸⁻¹⁰⁴ or nucleophiles,¹⁰⁵⁻¹⁰⁸ the development of catalytic asymmetric transformations directly engaging the aromatic π system has been achieved only recently.¹⁰⁹ Catalytically generated metal carbene intermediates⁷⁹ have been shown to react with aromatic and heteroaromatic rings and furnish products ranging from electrophilic aromatic substitution (Friedel-Crafts reaction),¹¹⁰ cyclopropanation and the subsequent Cope rearrangement (Büchner reaction),¹¹⁰ and stable ylide-forming reactions.¹¹¹ In these transformations, the electrophilic nature of metal carbenes dominates. Since the catalytically generated chiral dirhodium carbene intermediates from enoldiazoacetates can be visualized as chiral metallo-1,3-dipole equivalents with their vinylogous position electrophilic and their metal carbene center nucleophilic, the formal [3+3]-cycloaddition strategy could be extended to stable and readily available isoquinolinium/pyridinium methylides with asymmetry introduced in the ring-closing dearomatization stage (**Scheme 1.31**).¹¹² Successful development of the asymmetric

variant of this cycloaddition reaction would offer direct access to enantioenriched highly substituted quinolizidines that are amenable to further functionalization.^{113,114} Meanwhile, the donor/acceptor cyclopropene generated from enol diazoacetate could potentially undergo [3+2]-cycloaddition reaction with pyridinium/isoquinolinium methylides, which will be in direct competition with the [3+2]-cycloaddition if both reaction pathways have comparable reaction rates. The exploration of these two competing reactions will provide fundamental mechanistic insights into rhodium carbene and cyclopropene chemistry.



Scheme 1.31 Formal Enantioselective [3+3]-Cycloaddition of Metallo-1,3-dipoles with Isoquinolinium/Pyridinium Methylides

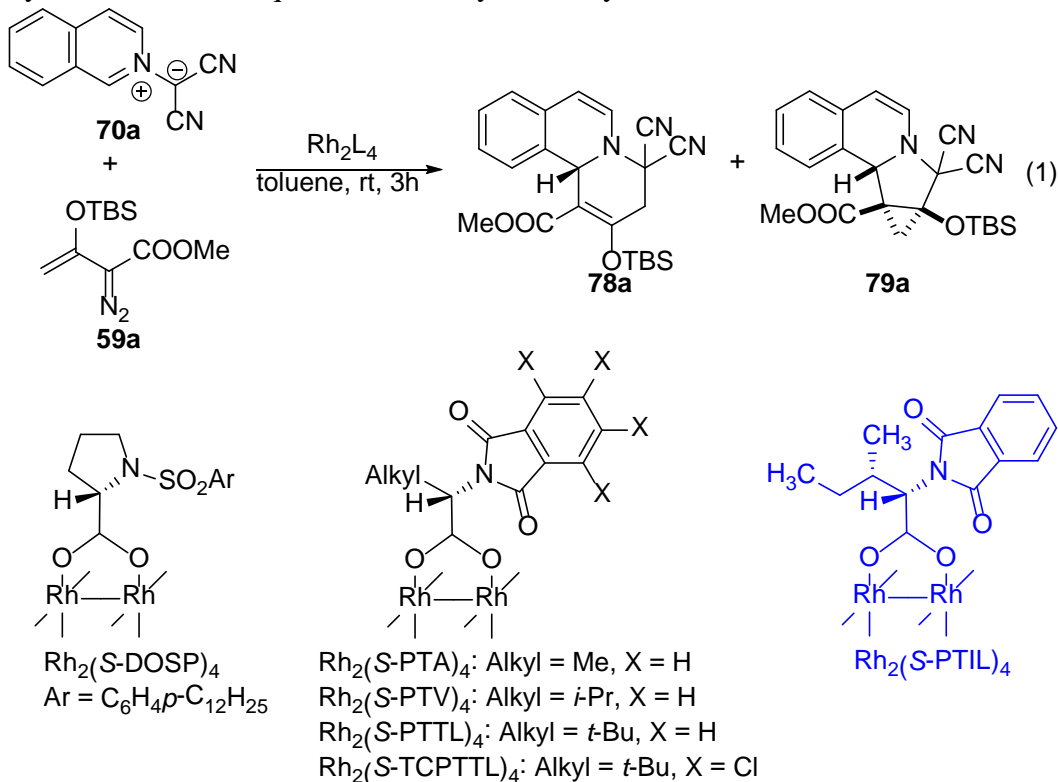
II. Results and Discussions

2.1 Results

Optimization of reaction conditions aimed at maximizing the efficiency and selectivities for [3+3]-cycloaddition was initiated between isoquinolinium dicyanomethylide **70a** and enol diazoacetate **59a**. Performed in toluene by slowly

adding a solution of enol diazoacetate **59a** to a mixture of partially soluble isoquinolinium dicyanomethylide **70a** and the dirhodium catalyst, reactions occurred at room temperature (**Table 1.1**). When conducting the title reaction (eq 1) with excess **59a** in the presence of 1.0 mol% Rh₂(Oct)₄, complete consumption of the dicyanomethylide **70a** was achieved after 3 h. Two products were obtained as a 2:1 mixture in high isolated yield, and their structures were determined by spectroscopic analysis to be those from the anticipated (**Scheme 1.31**) [3+3]-cycloaddition (**78a**) and an unexpected diastereoselective [3+2]-cycloaddition of **70a** with the donor-acceptor cyclopropene formed from **59a** by catalytic dinitrogen extrusion reaction (**79a**).^{75,115,116} Use of Rh₂(*S*-DOSP)₄^{1,3,23,24} as the catalyst formed **78a** and **79a** in a 1:4.2 product ratio (entry 2), but enantioselectivity for **78a** was very poor and for **79a** was not evident. Switching to Hashimoto's Rh₂(*S*-PTA)₄ catalyst¹¹⁷⁻¹¹⁹ resulted in a significant increase in enantioselectivity for the [3+3]-cycloaddition product **78a** (entry 3). The alkyl group of the Hashimoto's dirhodium catalysts impacted the enantiomeric excess for **78a** (entries 3-6), and optimal enantioselectivity for **78a** was achieved with previously unreported Rh₂(*S*-PTIL)₄ whose ligand incorporates an additional chiral center. Lowering the reaction temperature to 0°C slightly enhanced both the chemo- and enantioselectivity for **79a** but with low reaction yield (entry 7); and alternatively performing the reaction at 60°C provided only inferior selectivities (entry 8). Use of the more Lewis acidic Rh₂(*S*-TCPTTL)₄,^{44-46,50,51,54,56-58} however, reversed chemoselectivity with [3+2]-cycloaddition product **79a** as the sole reaction outcome (entry 9), and this reversal in chemoselectivity was mirrored in results from the use of Lewis acidic achiral Rh₂(tfa)₄ under otherwise identical conditions (entry 10).

Table 1.1 Optimization of Reaction Conditions for Enantioselective Formal [3+3]-Cycloaddition of Isoquinolinium Dicyanomethylide **70a** and Enol Diazoacetate **59a**.



entry ^a	catalyst (y mol%)	78a:79a ^{b,c}	yield (%) ^d	ee (%) of 78a ^e
1	Rh ₂ (Oct) ₄ (1.0 mol%)	2.0:1	85	—
2	Rh ₂ (S-DOSP) ₄ (1.0 mol%)	1:4.2	83	-20
3	Rh ₂ (S-PTA) ₄ (1.0 mol%)	3.7:1	81	49
4	Rh ₂ (S-PTV) ₄ (1.0 mol%)	1:1.7	79	90
5	Rh ₂ (S-PTTL) ₄ (1.0 mol%)	10:1	69	89
6	Rh ₂ (S-PTIL) ₄ (1.0 mol%)	1.6:1	83	93
7 ^f	Rh ₂ (S-PTIL) ₄ (1.0 mol%)	1.9:1	49	94
8 ^g	Rh ₂ (S-PTIL) ₄ (1.0 mol%)	1:2.1	70	90
9 ^h	Rh ₂ (S-TCPTTL) ₄ (1.0 mol%)	1:>20	49	nd
10 ^h	Rh ₂ (tfa) ₄ (1.0 mol%)	1:>20	71	—
11	Rh ₂ (S-PTIL) ₄ (0.5 mol%)	1:1.5	69	93
12	Rh ₂ (S-PTIL) ₄ (1.5 mol%)	4.3:1	82	93
13	Rh ₂ (S-PTIL) ₄ (2.0 mol%)	15:1	85	93
14	Rh ₂ (S-PTIL) ₄ (2.5 mol%)	>20:1	89	93
15	Rh ₂ (S-PTIL) ₄ (3.0 mol%)	>20:1	90	93

16 Rh₂(S-PTV)₄ (3.0 mol%) >20:1 88 90

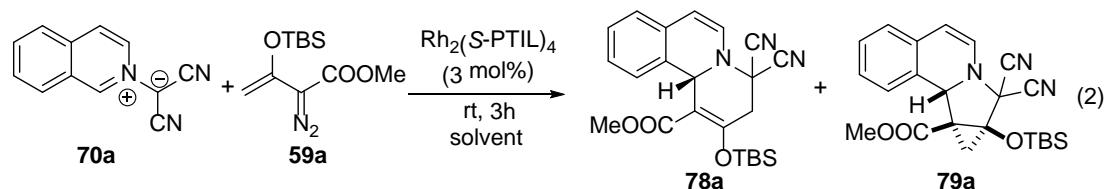
^aReactions were performed at room temperature with 0.1 mmol of **70a** (1.0 equiv). An excess of **59a** (1.8 equiv) in 1.0 mL toluene was added to the reaction mixture via syringe pump over 1 h with continued stirring for another 2 h. ^bRatios were determined by ¹H NMR analysis of reaction mixtures. Duplicate reactions show remarkable consistency in the **78a:79a** ratio. ^cThe stereochemistry of **79a** was determined by ¹H NOE experiments. ^dYields reported are combined isolated yields of **78a** and **79a**. ^eEnantiomeric excesses were determined by chiral HPLC analysis. ^fReaction performed at 0°C. ^gReaction performed at 60°C. ^hReaction was continued for 23 h after the completion of adding **59a**.

Surprisingly, catalyst loading has a pronounced effect on chemoselectivity (**78a:79a**). For instance, reactions catalyzed by 0.5 mol% (entry 11) and 1.0 mol% (entry 6) of Rh₂(S-PTIL)₄ at room temperature showed low selectivity for the formation of the [3+3]-cycloaddition product **78a**, and only a slight increase in the **78a:79a** ratio occurred when the temperature was lowered to 0°C. However, significant increases in the ratio were observed with incremental increases in mol % catalyst so that at 2.0 mol% catalyst the ratio was 15.4±0.4 (entry 13), and a further increase in catalyst loading to 2.5 then to 3.0 mol% led to the formation of **78a** as the sole reaction product [entries 14, 15 and 16 with Rh₂(S-PTV)₄]. The excellent enantiomeric excesses obtained for **78a** were not at all affected by catalyst loading, which suggested that the formation of **78a** and **79a** are independent. The [3+2]-cycloaddition product **79a** was only obtained as a racemate.

The reaction solvent strongly influenced both chemoselectivity and enantioselectivity. As is evident from the results reported in **Table 1.2**, reactions performed in chlorinated hydrocarbons (entries 1-4) gave significantly lower product control (**78a:79a**) and enantioselectivities for [3+3]-cycloaddition; aromatic solvents generally provided good chemoselectivities and high enantiocontrol (entries 5-7) except

when chlorobenzene was used as solvent (entry 4). Toluene stood out as the optimal choice (entry 8).

Table 1.2 Solvent Screening for the Enantioselective Catalytic Formal [3+3]-Cycloaddition Reaction of Isoquinolinium Dicyanomethylide **70a** and Enol Diazoacetate **59a**.



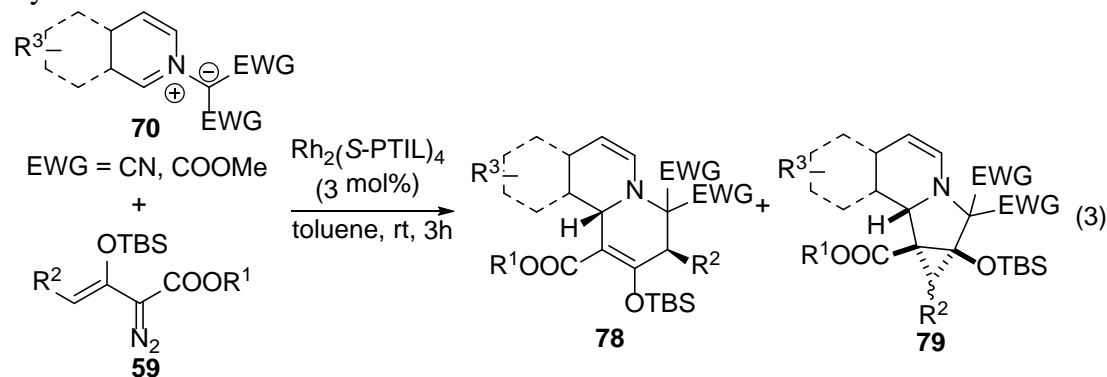
entry ^a	solvent	yield (%) ^b	78a:79a ^c	ee(%) of 78a ^d
1	CH ₂ Cl ₂	71	2.4:1	72
2	(CH ₂ Cl) ₂	59	4.8:1	80
3	CHCl ₃	65	1.2:1	88
4	PhCl	79	1.6:1	90
5	<i>o</i> -xylene	77	>20:1	91
6	<i>p</i> -xylene	80	>20:1	80
7	PhF	74	>20:1	90
8	toluene	90	>20:1	93

^aReactions were performed on 0.1 mmol of **59a** (1.0 equiv), and an excess of **70a** (1.8 equiv) in 1.0 mL solvent was added to the reaction mixture via syringe pump over 1 h, and then reaction was continued with stirring for 2 h. ^bRatios were determined by ¹H NMR analysis of reaction mixtures. ^cReported yields are combined isolated yields of **78a** and **79a**. ^dEnantiomeric excesses were determined by chiral HPLC analysis.

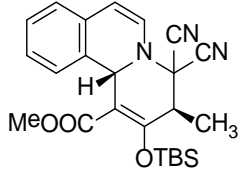
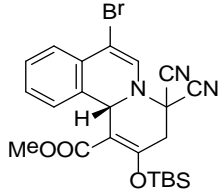
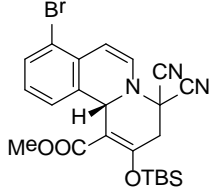
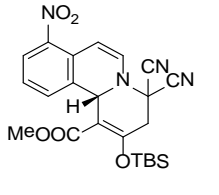
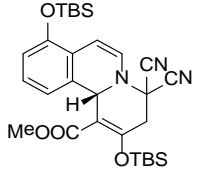
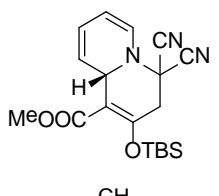
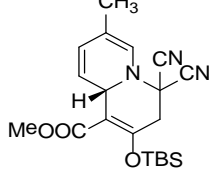
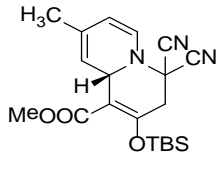
The substrate scope of the enantioselective [3+3]-cycloaddition reaction was examined using the optimal conditions obtained with **70a** and **59a** (Table 1.1 entry 15), and these results are presented in Table 1.3. Product yields and enantioselectivities appear to be independent of the ester substituent of enol diazoacetate **59a** (entries 1 and 2). The absolute configuration of **78b**, and others in this series by analogy, was unambiguously determined to be *S* through X-ray single crystal analysis (Figure 1.5). Enol diazoacetate **59c** with a methyl group instead of hydrogen attached at the vinylogous position underwent the [3+3]-cycloaddition reaction with complete

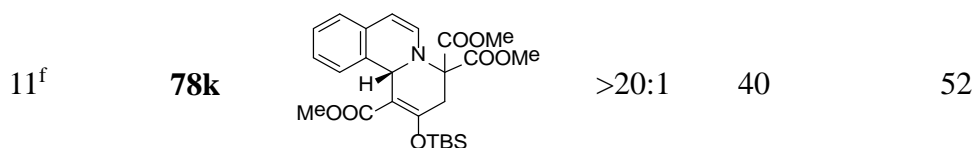
diastereocontrol (entry 3). Electronically disparate substituents on the isoquinolinium ring are well tolerated (entries 4-7); consistently high reaction yields and high enantiomeric excesses were achieved. Furthermore, the more challenging¹²⁰ pyridinium dicyanomethylides (entries 8-10) participated in the [3+3]-cycloaddition transformation providing high yields and high enantiomeric excesses of quinolizidines that were comparable to those from the isoquinolinium systems. Interestingly, only a single regioisomer was obtained for 3-picolinium dicyanomethylide **78i**, although there were two potential reaction sites (entry 9), and the product obtained was the one from addition to the less sterically encumbered 6-position rather than to the 2-position.

Table 1.3 Substrate Scope for Enantioselective Dearomatizing Formal [3+3]-Cycloaddition.



entry ^a		78:79 ^b	yield (%) ^c	ee (%) ^d
1	78a 	>20:1	90	93
2	78b 	>20:1	89	93

3 ^e	78c		>20:1	78	82
4	78d		>20:1	81	96
5	78e		>20:1	73	94
6	78f		>20:1	85	96
7	78g		1.7:1	63	95
8	78h		>20:1	85	87
9	78i		>20:1	88	86
10	78j		>20:1	76	74



^aReactions were performed with 0.1 mmol of **70** (1.0 equiv) and an excess of **59** (1.8 equiv) in 1.0 mL toluene was added to the reaction mixture over 1 h, and then reacted for another 2 h. ^bRatios were determined by ¹H NMR analyses of reaction mixtures. ^cYields reported are combined isolated yields of **78** and **79**. ^dEnantiomeric excesses were determined by HPLC analyses on a chiral stationary phase. ^eThe stereochemistry of **78c** was determined by ¹H NOE experiments. ^fReaction performed at 60 °C.

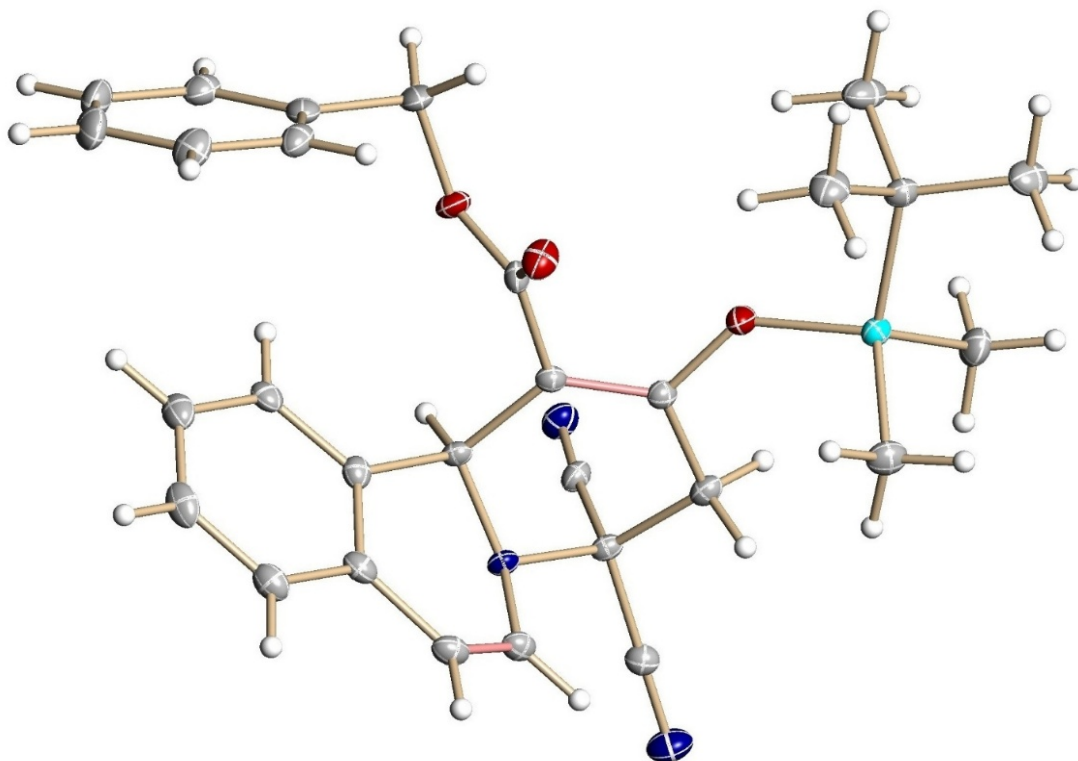


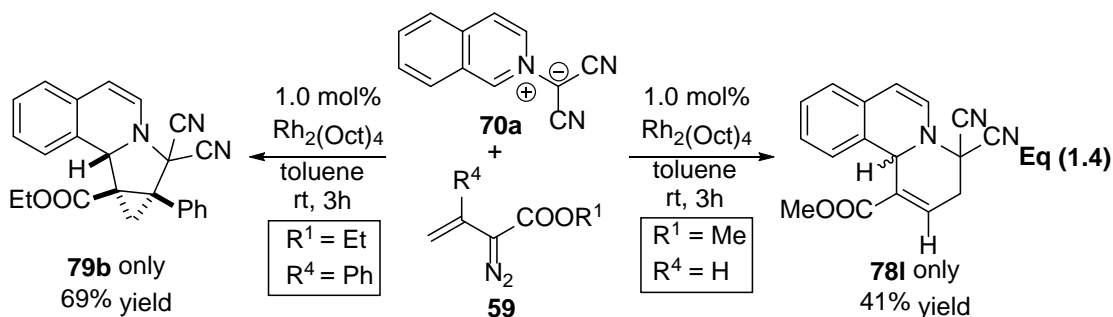
Figure 1.5 ORTEP View of Benzyl (*S*)-2-(*tert*-Butyldimethylsilyl)oxy-4,4-dicyano-4,11b-dihydro-3H-pyrido-[2,1-*a*]isoquinoline-1-carboxylate (**78b**). Ellipsoids are Shown at 30% Probability. CCDC 946885 Contains Supplementary Crystallographic Data for **78b**.

In contrast to the corresponding isoquinolinium dicyanomethylides (**70a**, EWG = CN), the dicarbomethoxy isoquinolinium methylide (**74b**, EWG = COOMe) was much less reactive towards dirhodium-catalyzed reaction with enol diazoacetate **59a**; reactions performed at room temperature reached only 30% completion in the normal

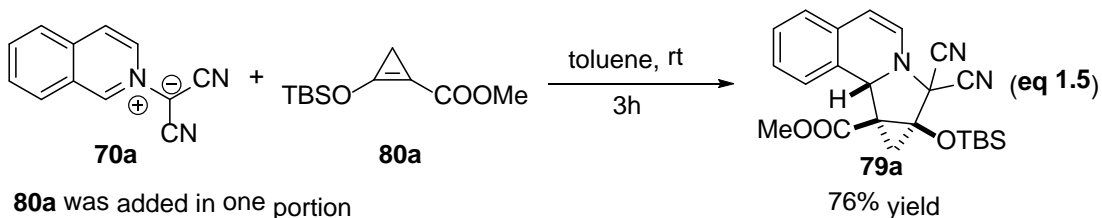
3 h reaction time. However, at 60°C over the same time period the reaction reached full consumption of **74b**, and **78k** was isolated in moderate yield although with significantly lower enantiomeric excess (**Table 1.3**, entry 11) than from reaction with the corresponding dicyanomethylide **70a**. Overall, the dearomatizing [3+3]-cycloaddition methodology represents a general approach for the catalytic asymmetric functionalization of the dicyanomethylides of isoquinoline and pyridine. Although the dicarbomethoxy isoquinolinium methylide **74b** was much less reactive than **70a**, other heterocyclic ylides^{86,121-125} may have enhanced reactivity and selectivity for these cycloaddition reactions.

2.2 Discussions

To probe the influence from alternate substituents (R^4) to the OTBS group on the vinyl group of **59**, combinations of vinyl diazoacetates **59** and methylide **70a** were subjected to $Rh_2(Oct)_4$ catalysis. Although such determinations have been conducted to compare product yields for individual transformations,¹²⁶ competitive reactions with **59** have not been reported. Whereas the reaction of **59a** ($R^4 = OTBS$) with **70a** gave a mixture of **78a** and **79a** (**Table 1.1** entry 1); with $R^4 = Ph$ the $Rh_2(Oct)_4$ -catalyzed reaction afforded only the [3+2]-cycloaddition product **79b** (**eq 1.4**) and vinyl diazoacetate **59d** ($R^4 = H$) gave exclusive formation of the [3+3]-cycloaddition product **78l**. Similar to reaction outcomes with varying catalyst and reaction solvent, the influence of the vinyl substituent R^4 is substantial in its effect on the reaction pathway.

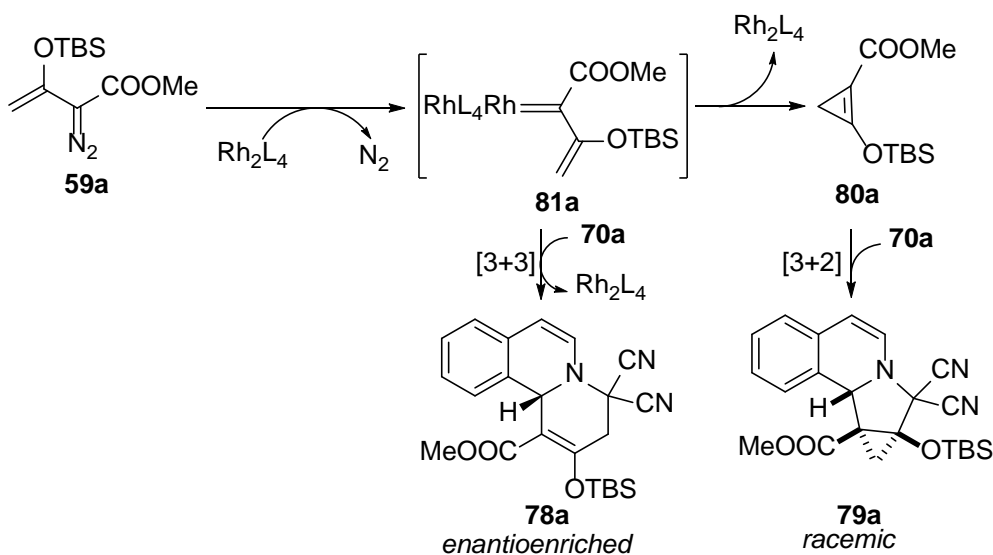


The results from these experiments show a gradation in reactivity of the intermediate metal carbene towards either intermolecular [3+3]-cycloaddition with methylide **70** to form **78** or isomerization to afford donor-acceptor cyclopropene **80**¹⁵ that is susceptible to [3+2]-cycloaddition with **70a**. Since only racemic product was obtained with the diverse array of chiral catalysts that was employed (**Table 1.1**), the diastereoselective [3+2]-cycloaddition of **80** and **70a** can be regarded to be a catalyst-free process. In sharp contrast, the high enantiocontrol in the [3+3]-cycloaddition process demonstrates its direct dependence on the dirhodium catalyst. In a separate experiment, treating the preformed and catalyst-free cyclopropene **80a** with isoquinolinium dicyanomethylide **70a** produced the [3+2]-cycloaddition product **79a** exclusively at room temperature (**Eq 1.5**).



However, the mechanistic explanation in which the metal carbene formed from dirhodium carboxylate and the enol diazoacetate either reacts with methylide **70** to produce the product from [3+3]-cycloaddition or dissociates the bound carbene with rearrangement in the form of the donor-acceptor cyclopropene **80** (**Scheme 32**) does

not explain the dramatic increase in the ratio of **78**:**79** with increasing mol % of catalyst loading (**Table 1.1**, entry 4,6, 11-16). The formation of both **78** and **79** have the same catalyst dependence in this scheme; both emanate from the metal carbene intermediate, and product formation for both involves reaction with methylide **70**. Thus dependence of catalyst on product distribution suggests a more complex role for dirhodium in these transformations, and perhaps one that involves its coordination with methylide Lewis bases.



Scheme 1.32 Formation of Both [3+3]- and [3+2]-Cycloaddition Products are Dependent on Metal Carbene Intermediate **81**.

The coordination of the dirhodium carboxylate with an isoquinolinium methylide was assessed in toluene at room temperature. Unlike most of the methylides used in this study, 5-(*tert*-butyldimethylsilyloxy)isoquinolinium dicyanomethylide **70e** displayed good solubility in most common organic solvents, and this feature enabled us to accurately determine the first coordination constant (K_1) of **70e** and $\text{Rh}_2(\text{S-PTIL})_4$. Coordination between $\text{Rh}_2(\text{S-PTIL})_4$ and dicyanomethylides **70e** was indicated by the

intense color change of $\text{Rh}_2(\text{S-PTIL})_4$ from light green to deep red when they were mixed. A plot of the spectrum of the $\text{Rh}_2(\text{S-PTIL})_4$ -containing solution as function of increasing amounts of methyllide **70e** with minimal change in volume (**Figure 1.6**) shows a clear isosbestic point at 684 nm. The equilibrium constant for association between $\text{Rh}_2(\text{S-PTIL})_4$ and dicyanomethylides **70e** was determined to be 545 ± 14 by the methodology that we have previously employed,¹²⁷ which is a binding affinity comparable to that of the same dirhodium compound and acetonitrile ($K_1 = 155 \pm 2$). Although coordination to rhodium through either the methanide carbon center of **70** or through one of its nitrile nitrogens is possible, association through the nitrile nitrogen offers the lesser steric resistance.

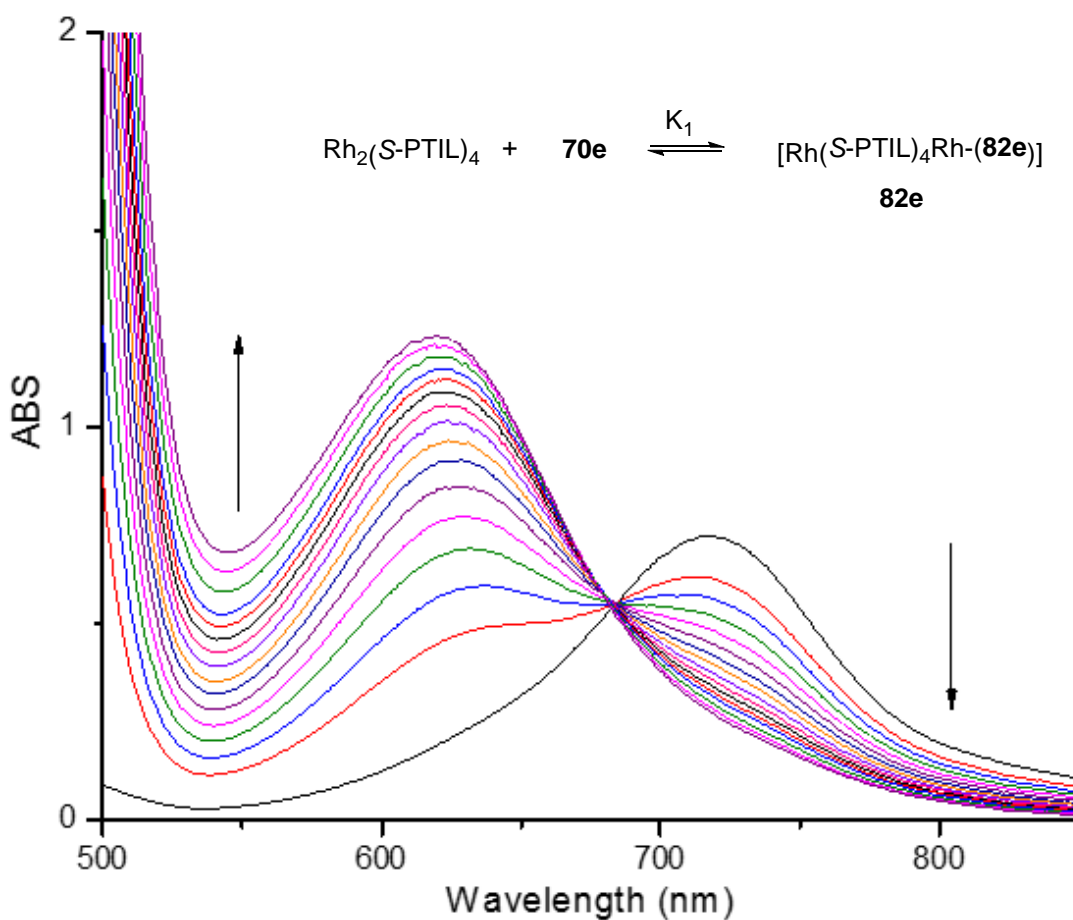
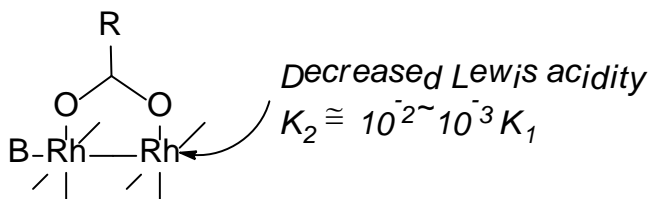
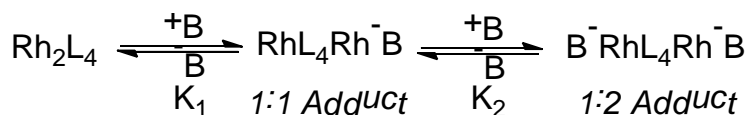


Figure 1.6 UV-Vis Titration Curves and Equilibrium Constant K_1 for Complex Formation Between **70e** and $\text{Rh}_2(\text{S-PTIL})_4$ in Toluene at Room Temperature. $[\text{Rh}_2(\text{S-PTIL})_4] = 2.0 \times 10^{-3} \text{ M}$; 0.17 equiv of **70e** [Relative to $\text{Rh}_2(\text{S-PTIL})_4$] was Added in Each Increment. $K_1 = 545 \pm 14$.

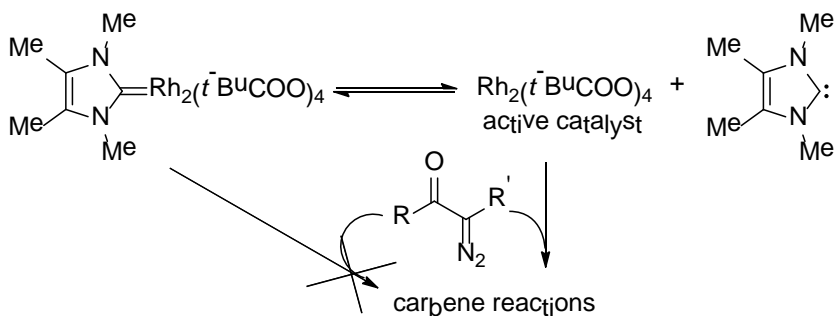
Pioneering work by Drago¹²⁸⁻¹³⁰ established that Lewis base coordination with Lewis acidic dirhodium carboxylates occurs at the axial positions to form 1:1 and 2:1 adducts with acetonitrile and with pyridine, and that the second coordination constant K_2 was at least two to three orders of magnitude lower than K_1 (**Scheme 1.33**). From this and a vast array of related investigations of the equilibrium processes of dirhodium carboxylates, the influence of one coordinated ligand on the association of a second ligand clearly established an inhibition for association;¹³¹⁻¹³⁵ but attempts to displace bound carbenes¹³⁶⁻¹³⁸ or demonstrate the influence of axial ligands on catalytic reactivity or selectivity^{139,140} have not been successful.



Scheme 1.33 Lewis Bases Occupy Axial Coordination Sites on Dirhodium Complexes.

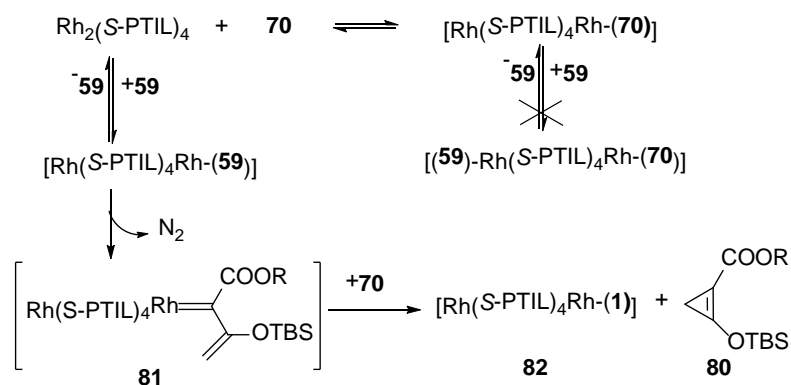
In a recent attempt to determine if a bound ligand could influence a catalytic reaction, Padwa and coworkers synthesized a stable dirhodium carbene complex between an Arduengo carbene and dirhodium pivalate,¹³⁹ but all endeavors to detect a

unique reactivity or selectivity in cycloaddition or insertion reactions from diazocarbonyl compounds for this complex were unsuccessful. Identical catalytic reactivities and selectivities were obtained with the parent dirhodium catalyst, and the authors concluded that the ligated dirhodium carbene complex underwent dissociation of carbene ligand to release the active dirhodium catalyst (**Scheme 1.34**) that then underwent the catalytic metal carbene reactions. In contrast to this S_N1-like role for an axial carbene ligand, could the dependence of catalyst on product distribution in reactions of **70** with **59** be influenced by **70** as an axial ligand?



Scheme 1.34 Stable Carbene on Dirhodium Undergoes Dissociation Prior to Reaction of Dirhodium with the Diazocarbonyl Compounds.

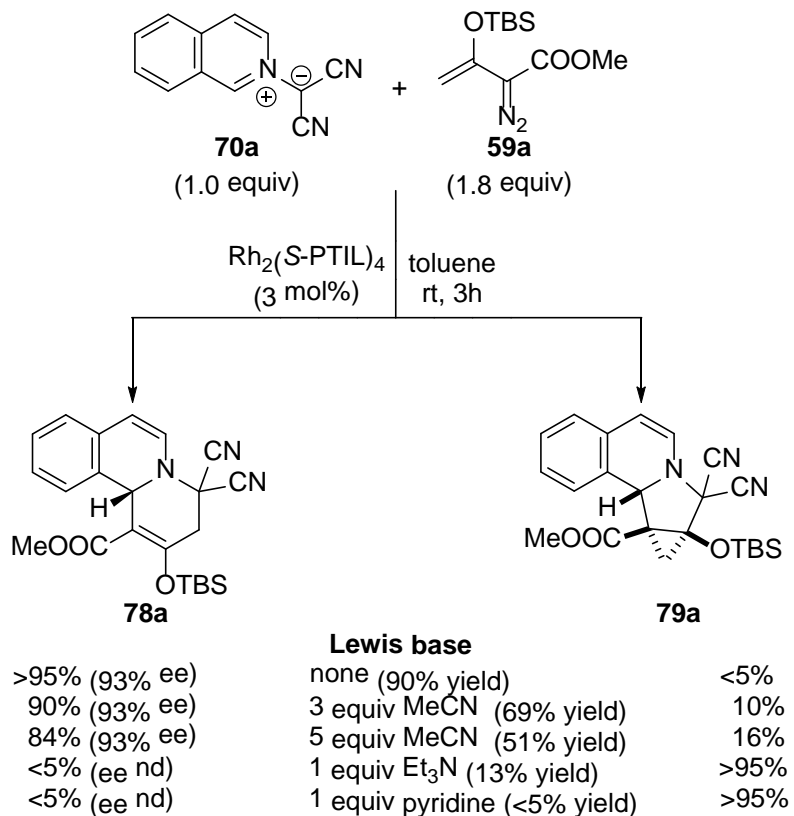
Recognizing that the catalyst in the reaction solution is in equilibrium with methylene **70**, addition of enol diazoacetate **59** could associate with the methylene-coordinated dirhodium catalyst or the catalyst that is free of **70**. The equilibrium constant for association between **70e** and Rh₂(S-PTIL)₄ gives evidence of a complex, which is highly unlikely to associate the weakly coordinating diazo compound **59**. Instead, coordination with the catalyst that is free of methylene is most likely, and with dinitrogen extrusion this complex forms the metal carbene intermediate (**Scheme 1.35**). However, previous reports of the catalytic formation of donor-acceptor cyclopropenes **80** from enol diazoacetate **59** did not discuss how this product was formed.



Scheme 1.35 Reaction Pathway for the Formation of Cyclopropene **80**.

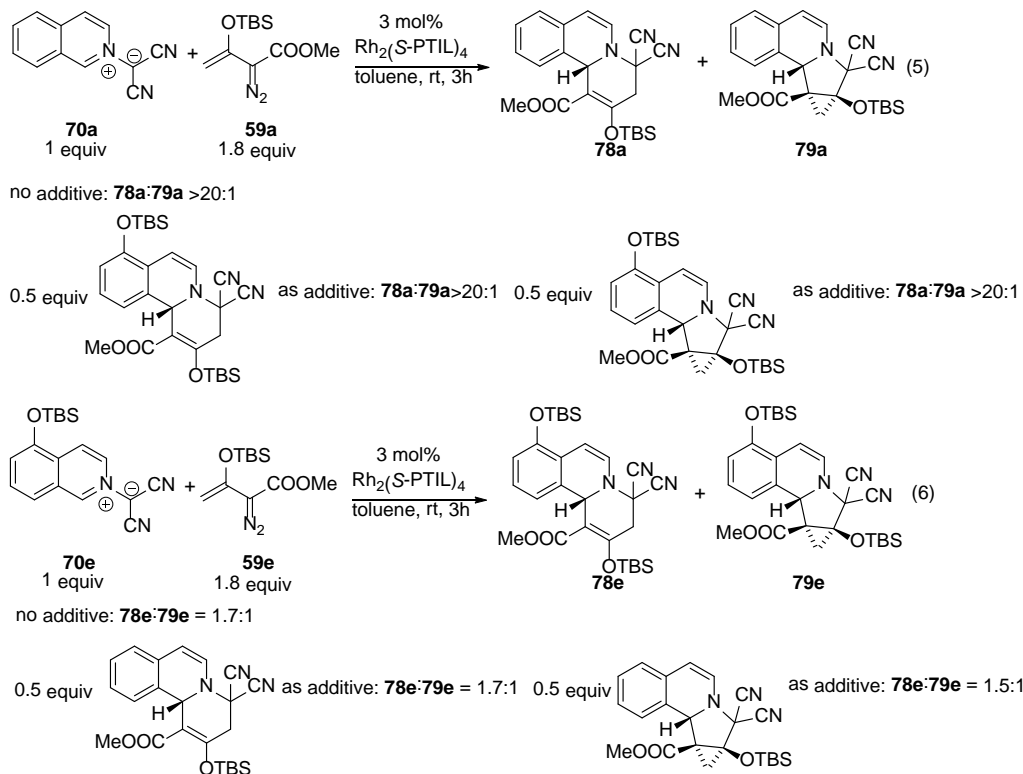
Two possible pathways exist for the displacement of the rhodium-bound carbene of **81** as cyclopropene **80**. One is the $\text{S}_{\text{N}}1$ -like pathway that was demonstrated for the dirhodium carbene complex between an Arduengo carbene and dirhodium pivalate (**Scheme 1.35**). However, in this case increasing the mol% of catalyst could not have influenced the ratio of [3+3]- to [3+2]-cycloaddition products, as has been explained (**Scheme 1.32**). However, if methylide **70** serves to induce formation of cyclopropene **80** in a through dirhodium $\text{S}_{\text{N}}2'$ -like displacement reaction, the effect of increased dirhodium catalyst concentration will be to increase the concentration of **81** and thereby increase the rate for formation of [3+3]-cycloaddition product **78** relative to that of [3+2]-cycloaddition product **79** whose formation occurs subsequent to the formation of **5**. There are several lines of evidence that support this interpretation: (1) If the Lewis basic methylide **70** does assist the generation of cyclopropene **80** with concomitant release of a Lewis acid-base complex (**Scheme 1.32**), this effect should be more pronounced in reactions catalyzed by more Lewis acidic dirhodium compounds (higher K_{eq} , lower concentration of ligand-free catalyst). As predicted, the [3+2]-cycloaddition pathway completely overrides the competing [3+3]-cycloaddition

reaction when $\text{Rh}_2(\text{S-TCPTTL})_4$ (Table 1.1, entry 9) or $\text{Rh}_2(\text{tfa})_4$ (Table 1.1, entry 10) is used. (2) External Lewis base additives decrease the catalyst concentration and increase the production of cyclopropene **80**, thereby decreasing chemoselectivity for [3+3]-cycloaddition obtained from the reaction catalyzed by 3 mol% $\text{Rh}_2(\text{S-PTIL})_4$ (Scheme 1.32). As anticipated, more of the [3+2]-cycloaddition product **79** is formed in reactions where CH_3CN or the more strongly coordinating Lewis base (Et_3N or pyridine) is present. That these additives do not influence the [3+3]-cycloaddition pathway is indicated by the observation that enantiomeric excesses of **78** are not influenced by the presence of CH_3CN . Use of the stronger σ -donors - Et_3N or pyridine - completely shuts down the [3+3]-cycloaddition pathway.



Scheme 1.36 Effect of Lewis Bases on Chemoselectivity.

Although the enantioselective [3+3]-cycloaddition and the diastereoselective [3+2]-cycloaddition reactions are linked through the intermediate rhodium carbene **81**, they are separated by the divergent outcomes from actions of methylide **70** on **81**. Lewis base additives do not participate in the enantioselective [3+3]-cycloaddition but they do induce rearrangement of rhodium carbene to generate cyclopropene **80**. Indeed, it is possible that the influence of at least some of the chlorinated solvents on reaction selectivity may arise from Lewis base displacement of cyclopropene **80** from the dirhodium carbene **81**.²⁸ However, when the bulky nitriles **78** or **79** were used as additives in the catalytic reactions, minimal impact on the product distribution was displayed (**Scheme 1.37**).

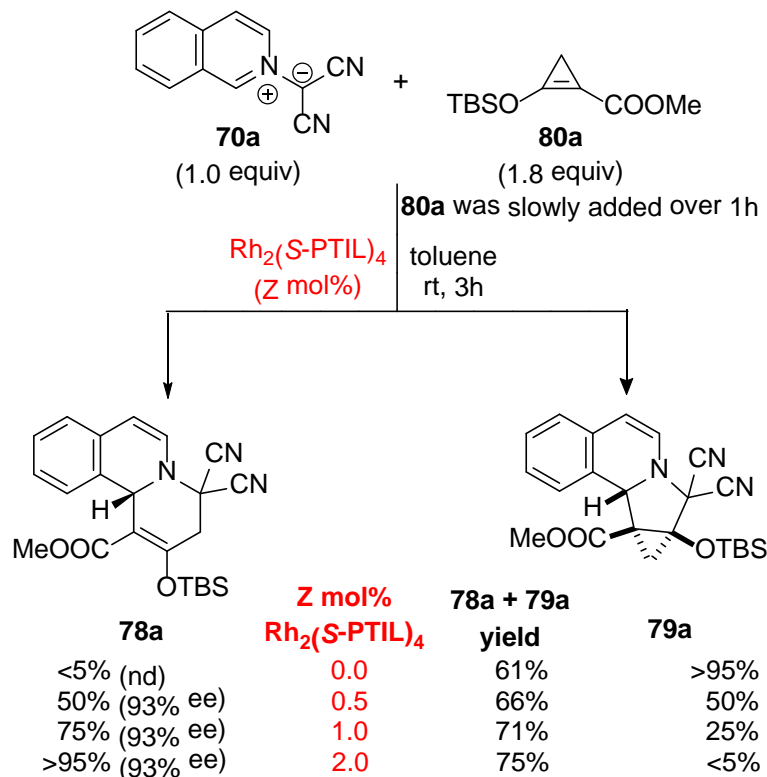


Scheme 1.37 Both [3+3]-Cycloaddition and [3+2]-Cycloaddition Product **78** and **79** Have Minimal Impact on Chemoselectivity.

Although the uncatalyzed reaction of methylene **70** with donor-acceptor cyclopropene **80a**, formed by catalytic dinitrogen extrusion from enol diazoacetate **59a**, underwent [3+2]-cycloaddition exclusively, and this process adequately accounts for the formation of **79**, the effect of increasing mol% catalyst on the relative yield of [3+3]-cycloaddition product **78** (Table 1.1) coupled with the Lewis base promoted cyclopropene formation (Schemes 1.33 and 1.34) suggested that the role of the cyclopropene intermediate is more complex than what has been portrayed. Could cyclopropene **80a** form metal carbene **81a** in what would be a reversal of the reaction that formed **80a**? Although there is no precedent for such an interchange, cyclopropenes are known to be stoichiometric precursors to metal carbenes in selected cases.¹⁴¹⁻¹⁴³ Only recently, however, have reports emerged of catalytic reactions of cyclopropenes in metal carbene transformations.^{9-11,144,145}

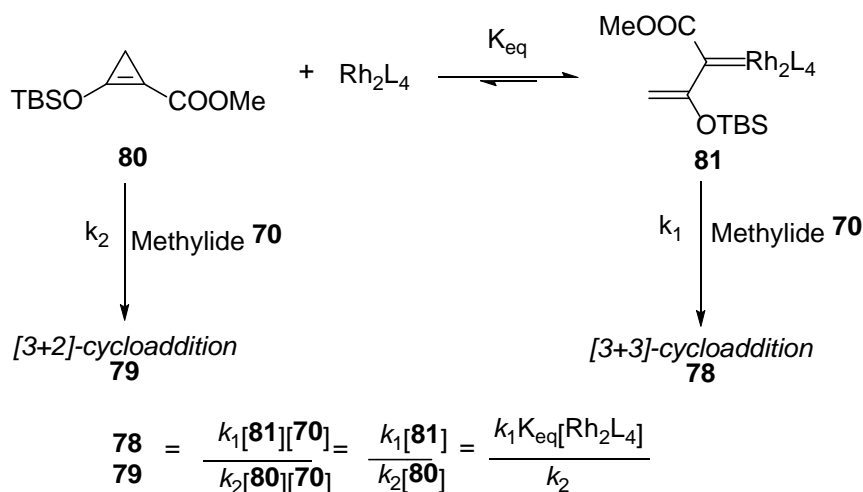
To test this hypothesis we replaced enoldiazoacetate **59a** in eq 1 with cyclopropene **80a**, generated with rhodium(II) acetate but separated from the catalyst, and performed reactions in the presence of variable mol% of $\text{Rh}_2(\text{S-PTIL})_4$ under otherwise identical conditions. As anticipated, high enantiocontrol for the formation of the [3+3]-cycloaddition product **78** was achieved; and this transformation and its enantioselectivity demonstrated the direct involvement of the chiral catalyst in the bond-forming steps. Chemoselectivities (**78:79**) directly correlated with the mol% of $\text{Rh}_2(\text{S-PTIL})_4$ used, and the enantioselective [3+3]-cycloaddition product **78** was obtained with greater than 95% selectivity when the catalyst loading was increased to 2 mol% (Scheme 1.38). Thus the outcomes of these reactions, including the

enantioselectivity of **78** and chemoselectivity for **78:79**, were identical, independent of the source of the carbene-forming reactant.



Scheme 1.38 Dependence of Product Distribution on Catalyst Loading with Cyclopropene **80a** as the Metal Carbene Precursor.

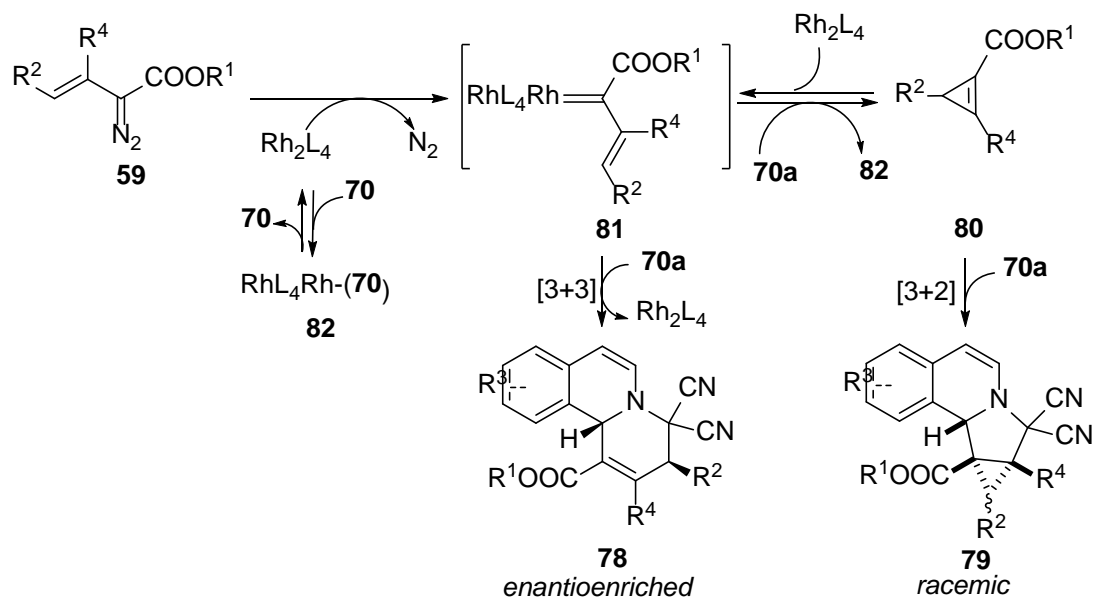
Considering the interconversion between the enol-TBS substituted chiral dirhodium carbene **81** and the donor-acceptor cyclopropene **80**, the relationship between the amount of catalyst and the ratio of products from [3+3]- and [3+2]-cycloaddition reactions now resembles the experimental observation (**Scheme 1.38**). If the interconversion between (**80** + Rh_2L_4) and **81** is rapid relative to cycloadditions, the ratio **78:79** is directly related to the concentration of catalyst (**Scheme 1.39**). However a plot of the ratio **78:79** versus mol% $\text{Rh}_2(\text{S-PTIL})_4$ suggests a more complex exponential relationship with the catalyst that awaits further mechanistic definition.



Scheme 1.39 Relationship Between the Cycloaddition Product Ratio (**78:79**) and the Dirhodium Catalyst.

Taking these findings into account, we now have a more complete rationale for the events that occur during the highly enantioselective dearomatizing [3+3]-cycloaddition reaction of enol diazoacetates and isoquinolinium or pyridinium methylides (**Scheme 1.40**). The central outcome is stereoselective cycloaddition that results from the vinylogous reaction of enol-TBS substituted chiral dirhodium carbene **81** with isoquinolinium or pyridinium methylides that is accompanied by ring closure to cycloaddition product **78** with displacement of the chiral catalyst. In competition with this process the enol-TBS-substituted dirhodium carbene **81** forms donor-acceptor cyclopropene **80** that is proposed to occur by a through-rhodium-rhodium bond displacement by a Lewis base that includes isoquinolinium or pyridinium methylides. The dirhodium catalyst is in equilibrium with reactant isoquinolinium or pyridinium methylides that has the effect of lowering the turnover rate for [3+3]-cycloaddition. The decreased amount of catalyst allows direct [3+2]-cycloaddition of the donor-acceptor cyclopropene with isoquinolinium or pyridinium methylides to form **79**. As with the isoquinolinium or pyridinium methylides that have multiple reaction pathways

for product formation, so also does cyclopropene **80** which undergoes either [3+2]-cycloaddition with **70** or forms dirhodium carbene **81**. The net result is that the catalyst has ultimate control on the reaction pathway and reaction stereoselectivity.



Scheme 1.40 Detailed General Mechanism for the Competing [3+3]- and [3+2]-Cycloaddition Reactions.

The new processes uncovered in this study – $\text{S}_{\text{N}}2'$ induced formation of donor-acceptor cyclopropene **80** and its equilibrium with the axial ligand-free dirhodium catalyst - are fundamental to understanding metal carbene reaction chemistry. The dirhodium carbene derived from enol diazoacetate **59** is uniquely capable of rearrangement to cyclopropene **80** with release of the dirhodium catalyst, and this reaction occurs in competition with vinylogous addition. Isoquinolinium and pyridinium methylides are relatively strong Lewis bases compared to acetonitrile which is a much stronger Lewis base than the reactant diazo compound, and their Lewis basicity prompts competing association with the dirhodium catalyst, vinylogous

addition to the enol-TBS substituted dirhodium carbene **81**, and displacement of cyclopropene **80** from the enol-TBS substituted dirhodium carbene **81**. The further implications of these processes are under investigation.

III. Conclusion

In summary, we have disclosed a highly enantioselective dearomatizing [3+3]-cycloaddition reaction. A [3+2]-cycloaddition of isoquinolinium or pyridinium methylides with the cyclopropene derived from rhodium carbene competes with the [3+3]-cycloaddition reaction but can be turned on or off with a higher mol% of catalyst or increasing amount of Lewis base. Investigations of these systems not only revealed a highly enantioselective dearomatizing formal [3+3]-cycloaddition transformation of isoquinolinium/pyridinium methylides with enol diazacetates catalyzed by chiral dirhodium carboxylates in up to 96% ee, but they provided evidence for competitive coordination-induced displacement of the dirhodium-bound enol-carbene as a donor-acceptor cyclopropene that either reforms the enol-carbene of dirhodium or undergoes [3+2]-cycloaddition to form densely functionalized indolizidines with complete regioselectivity and diastereoselectivity.

IV. Experimental section

4.1 General Information

Experiments involving moisture- and/or air-sensitive components were performed in flame-dried glassware under a nitrogen atmosphere using freshly distilled solvents. Solvents including toluene, *p*-xylene, *o*-xylene, chlorobenzene, fluorobenzene, CHCl₃, (CH₂Cl)₂, THF were dried over activated molecular sieves

under nitrogen atmosphere and distilled prior to use. Commercial reagents and chromatography solvents (hexanes and ethyl acetate) were used without further purification. Thin layer chromatography (TLC) was carried out using EM Science silica gel 60 F254 plates. Chromatograms were analyzed by UV lamp (254 nm) or by development using cerium ammonium molybdate (CAM). Liquid chromatography was performed using a forced flow (flash chromatography) of the indicated system on silica gel (230-400 mesh). Proton nuclear magnetic resonance spectra (^1H NMR) were recorded on a Bruker AMX 400 spectrophotometer (in CDCl_3 or $\text{DMSO-}d^6$ as solvent). Chemical shifts for ^1H NMR spectra are reported as δ in units of parts per million (ppm) downfield from SiMe_4 ($\delta = 0.00$) and relative to the signal of chloroform- d ($\delta = 7.26$, singlet) or $\text{DMSO-}d^6$ ($\delta = 2.50$, pentet). Multiplicities were given as: s (singlet); d (doublet); t (triplet); q (quartet); p (pentet); dd (doublet of doublets); ddd (doublet of doublet of doublets); dddd (doublet of doublet of doublet of doublets); dt (doublet of triplets); m (multiplet), and comp (composite). The number of protons (n) for a given resonance is indicated by $n\text{H}$. Coupling constants are reported as a J value in Hz. Carbon nuclear magnetic resonance spectra (^{13}C NMR) are reported in δ units of parts per million (ppm) downfield from SiMe_4 ($\delta = 0.0$) and relative to the central singlet from the signal of chloroform- d ($\delta = 77.0$, triplet) or $\text{DMSO-}d^6$ ($\delta = 39.5$, septet). High-resolution mass spectra (HRMS) were obtained on a JEOL AccuTOF-ESI mass spectrometer using CsI as the standard. Enantioselectivity was determined on an Agilent 1200 Series HPLC using a Daicel Chiralpak column. Optical rotation was measured using a JASCO P-1030 polarimeter equipped with a sodium vapor lamp at

589 nm; concentration is denoted as c and was calculated as grams per deciliters (g/100mL).

Isoquinolinium dicyanomethylides **70**,⁸⁰ pyridinium dicyanomethylides **69**⁸⁰ and isoquinolinium diester methylides **74**⁸⁹ were synthesized according to literature procedures. Enol diazoacetate **59a-c**^{146, 147} and vinyl diazoacetates **59d-e**²⁴⁰ were prepared by known methods. *N*-phthaloyl-(*S,S*)-*iso*-leucine was synthesized by literature method.¹¹⁸ Rh₂(*S*-DOSP)₄ was purchased from Strem Chemicals, Inc. Rh₂(*S*-PTA)₄, Rh₂(*S*-PTV)₄, Rh₂(*S*-PTTL)₄, Rh₂(*S*-TCPTTL)₄ and Rh₂(*S*-PTIL)₄ were prepared by established methods.^{41, 117, 118}

4.2 Experimental Procedures

Sample Procedure for the Preparation of Isoquinolinium/Pyridinium Dicyanomethylides. To a THF solution (2.0 mL) of 4-bromoisoquinoline (416 mg, 2.0 mmol) cooled to 0°C, tetracyanoethylene oxide (298 mg, 2.1 mmol) dissolved in 2.0 mL THF was added dropwise over 10 min. The reaction solution was stirred at 0 °C for 12 h during which time a yellow precipitate formed. After warming to room temperature, the reaction mixture was diluted with diethyl ether (10 mL), and the precipitate was filtered and washed with diethyl ether (5.0 mL). The resulting yellow solid was collected then dissolved in CH₂Cl₂. Celite (3.0 g) was added to the solution and then solvent was removed under reduced pressure. The solid residue was loaded onto a silica gel column (with CH₂Cl₂ and ethyl acetate as eluents) to isolate 4-bromoisoquinolinium dicyanomethylide **70b** (234 mg, 0.86 mmol, 43% yield).

Preparation of Dirhodium(II) Tetrakis[*N*-Phthaloyl-(*S,S*)-*iso*-leucinate] Bis(ethyl acetate) Adduct [Rh₂(*S*-PTIL)₄(EtOAc)₂]. To a flame-dried, 50-mL,

single-necked, round-bottomed flask equipped with a magnetic stirring bar, Rh₂(OAc)₄ (221 mg, 0.50 mmol), *N*-phthaloyl-(*S,S*)-*iso*-leucine (653 mg, 2.50 mmol) and chlorobenzene (25 mL) were added sequentially under a nitrogen pressure. The flask was fitted with a 10-mL Soxhlet extraction apparatus into which was placed a thimble containing 5 g of an oven-dried mixture of 2 parts sodium carbonate and 1 part of sand. The mixture was heated to reflux for 3 h and then cooled to room temperature. Solvent was removed under reduced pressure, and the residue was dissolved in ethyl acetate (30 mL). The resulting solution was washed with saturated aqueous NaHCO₃ (2×20 mL) and brine (20 mL) and then dried over anhydrous Na₂SO₄. Filtration and subsequent solvent removal under reduced pressure furnished a green solid that was purified by column chromatography on silica gel (hexanes/EtOAc). The resulting green solid was dissolved in 5 mL ethyl acetate and 50 mL hexanes was then added to the solution. Green solids that formed after standing overnight at room temperature were collected by filtration, washed with hexanes (2×5 mL) and dried under high vacuum (0.1 Torr) at room temperature for 3 h to provide dirhodium(II) tetrakis[*N*-phthaloyl-(*S,S*)-*iso*-leucinate] bis(ethyl acetate) adduct [Rh₂(*S*-PTIL)₄(EtOAc)₂] (590 mg, 0.42 mmol, 83% yield).

Sample Procedure for the Enantioselective [3+3]-Cycloaddition of Isoquinolinium/Pyridinium Methylides (70) and Enol Diazoacetate (59). To a 10-mL flame-dried Schlenk flask containing a magnetic stirring bar, [Rh₂(*S*-PTIL)₄(EtOAc)₂] (4.2 mg, 0.0030 mmol), isoquinolinium dicyanomethylide **70a** (20 mg, 0.10 mmol) and 1.0 mL of toluene were added sequentially under a nitrogen atmosphere. Then the flask was capped by a rubber septum and the resulting solution

was stirred at room temperature for 5 min before methyl 3-(*tert*-butyldimethylsilyl)oxy-2-diazobut-3-enoate **59a** (46 mg, 0.18 mmol) dissolved in 1.0 mL of toluene was added via syringe pump over 1 h. Stirring was continued at room temperature for 2 h after the completion of adding **59a**. Then the reaction solution was concentrated under reduced pressure and directly loaded onto a silica gel column (with CH₂Cl₂ as eluent) to isolate methyl (*S*)-2-(*tert*-butyldimethylsilyl)oxy-4,4-dicyano-4,11b-dihydro-3*H*-pyrido[2,1-*a*]isoquinoline-1-carboxylate **78a** (38 mg, 0.090 mmol, 90% yield). HPLC analysis of the enantioselective [3+3]-cycloaddition product **78a** on chiral stationary phase indicated an enantiomeric excess of 93% [Chiralpak OD-H; flow: 1 mL/min; hexanes/*i*-PrOH: 95:5; 254 nm; tR (minor) = 5.5 min; tR (major) = 6.2 min].

Sample Procedure for the Enantioselective [3+3]-Cycloaddition of Isoquinolinium/Pyridinium Methylides (70/69) and Enol Diazoacetate (59) in the Presence of a Lewis Base. To a 10-mL flame-dried Schlenk flask containing a magnetic stirring bar, [Rh₂(*S*-PTIL)₄(EtOAc)₂] (4.2 mg, 0.0030 mmol), isoquinolinium dicyanomethylide **70a** (20 mg, 0.10 mmol), 1.0 mL of toluene and CH₃CN (12 mg, 0.30 mmol) were added sequentially under a nitrogen atmosphere. Then the flask was capped by a rubber septum and the resulting solution was stirred at room temperature for 5 min before methyl 3-(*tert*-butyldimethylsilyl)oxy-2-diazobut-3-enoate **59a** (46 mg, 0.18 mmol) dissolved in 1.0 mL of toluene was added via syringe pump over 1 h. Stirring was continued at room temperature for 2 h after the completion of adding **59a**. Then the reaction solution was concentrated under reduced pressure. The residue was dissolved in CDCl₃ to determine the ratio of **78a** to **79a** by ¹H NMR spectroscopy. Then

the solution was directly loaded onto a silica gel column (with 1:1 of CH₂Cl₂:hexanes as eluents) to isolate methyl (*S*)-2-(*tert*-butyldimethylsilyl)oxy-4,4-dicyano-4,11b-dihydro-3*H*-pyrido[2,1-*a*]isoquinoline-1-carboxylate **78a** (26 mg, 0.062 mmol, 62% yield). HPLC analysis of **78a** on chiral stationary phase showed an enantiomeric excess of 93%.

Procedure for the Generation of Methyl 2-(*tert*-Butyldimethylsilyl)oxy-cycloprop-1-enecarboxylate (80a) in Toluene from Enol Diazoacetate (59a) by Rh₂(OAc)₄-catalyzed Dinitrogen Extrusion Reaction. To a flame-dried vial equipped with a magnetic stirring bar, Rh₂(OAc)₄ (0.9 mg, 0.0020 mmol) and 0.75 mL toluene were added sequentially under a nitrogen atmosphere and then capped with a rubber septum. The solution was stirred at room temperature while methyl 3-(*tert*-butyldimethylsilyl)oxy-2-diazobut-3-enoate **59a** (46 mg, 0.18 mmol) was added dropwise over 1 min. Rapid evolution of nitrogen occurred, and the yellow color of **59a** disappeared within 5 min. Complete consumption of enol diazoacetate **59a** and the generation of donor-acceptor cyclopropene **80a** were verified by ¹H NMR spectroscopy by the disappearance of the two vinyl protons [δ (ppm): 5.02 (d, *J* = 2.1 Hz, 1H), 4.27 (d, *J* = 2.1 Hz, 1H)] on enol diazoacetate **59** and the appearance of the methylene protons [δ (ppm): 1.88 (s, 2H)] from cyclopropene **80a**. The solution was filtered through a short pad (~1 cm) of BAKERBOND-CN silica (40 μ m Prep LC packing) to remove the dirhodium catalyst and the silica pad was washed with 0.25 ml toluene. The combined filtrates containing methyl 2-(*tert*-butyldimethylsilyl)oxy-cycloprop-1-enecarboxylate **80a** were used directly in the subsequent reactions.

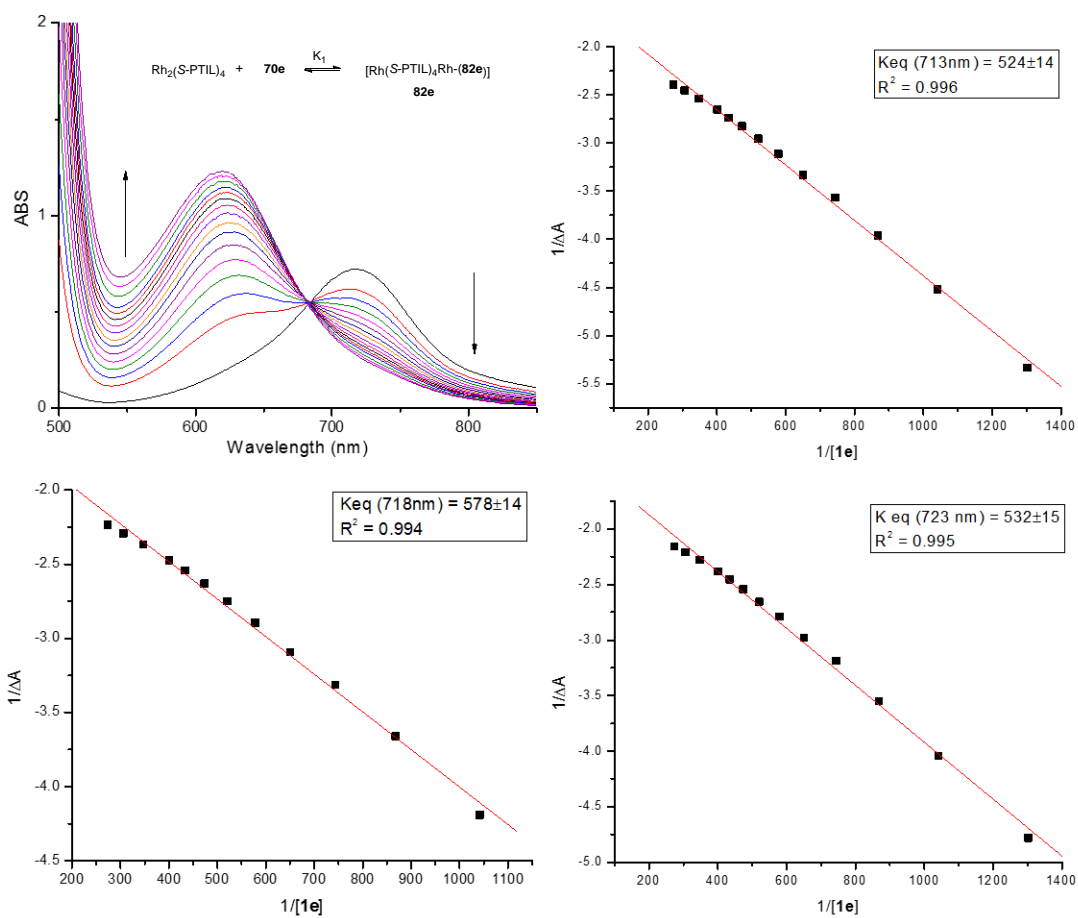
Sample Procedure for the Diastereoselective [3+2]-Cycloaddition of Isoquinolinium/Pyridinium Methylides (69/70) and cyclopropene 80. To the prepared toluene solution of methyl 2-(*tert*-butyldimethylsilyl)oxy-cycloprop-1-enecarboxylate **80a** at room temperature, isoquinolinium dicyanomethylide **70a** (20 mg, 0.10 mmol) was added as a solid under a nitrogen atmosphere. The resulting suspension was stirred at room temperature for 3 h during which time the mixture gradually became a homogeneous solution. The solution was then concentrated under reduced pressure and directly loaded onto a silica gel column (with 1:1 of CH₂Cl₂:hexanes as eluents) to isolate methyl (8a*SR*,9a*SR*,9b*SR*)-8a-(*tert*-butyldimethylsilyl)oxy-8,8-dicyano-8a,9,9a,9b-tetrahydro-8*H*-cyclopropa[3,4]pyrrolo[2,1-*a*]isoquinoline-9a-carboxylate **79a** (32 mg, 0.076 mmol, 76% yield).

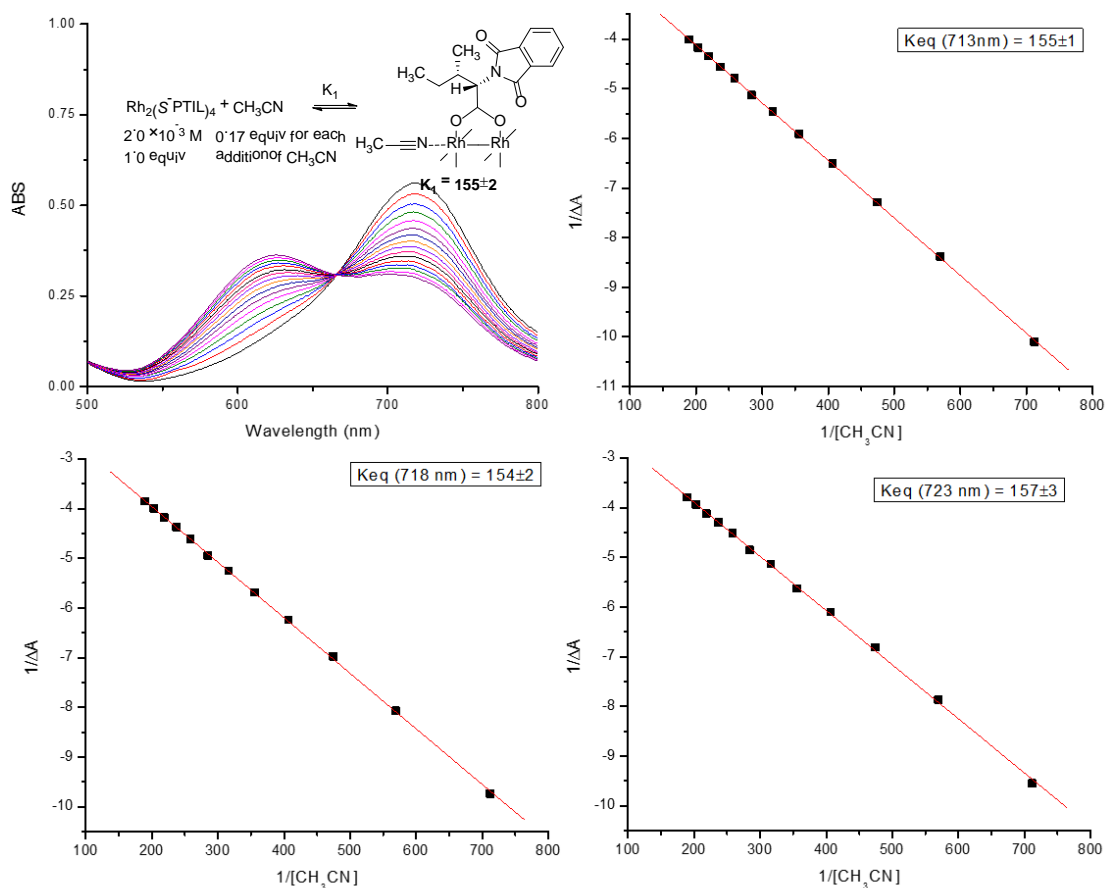
Sample Procedure for the Enantioselective [3+3]-Cycloaddition of Isoquinolinium/Pyridinium Methylides (69/70) and cyclopropene 80. To a 10-mL flame-dried Schlenk flask containing a magnetic stirring bar, [Rh₂(*S*-PTIL)₄(EtOAc)₂] (2.8 mg, 0.0020 mmol), isoquinolinium dicyanomethylide **70a** (20 mg, 0.10 mmol) and 1.0 mL of toluene were added sequentially under a nitrogen atmosphere. Then the flask was capped by a rubber septum and the resulting solution was stirred at room temperature. The prepared toluene solution of methyl 2-(*tert*-butyldimethylsilyl)oxy-cycloprop-1-enecarboxylate **80a** was added to the stirring mixture of [Rh₂(*S*-PTIL)₄(EtOAc)₂] and isoquinoline dicyanomethylide **70a** over 1 h via syringe pump. Stirring was continued at room temperature for 2 h after the completion of adding **80a**. Then the reaction solution was concentrated under reduced pressure and directly loaded

onto a silica gel column (with 1:1 of CH₂Cl₂:hexanes as eluents) to isolate methyl (*S*)-2-(*tert*-butyldimethylsilyloxy-4,4-dicyano-4,11b-dihydro-3*H*-pyrido[2,1-*a*]isoquinoline-1-carboxylate **78a** (32mg, 0.075 mmol, 75% yield). HPLC analysis of the enantioselective [3+3]-cycloaddition product **78a** on chiral stationary phase showed an enantiomeric excess of 93%.

Coordination Constant (K_1) Determination for Rh₂(*S*-PTIL)₄ and **70e or CH₃CN by UV-Vis Titration.** Rh₂(*S*-PTIL)₄(EtOAc)₂ was heated at 110 °C under high vacuum (0.1 Torr) for 3 h before storage inside an argon-atmosphere glove box, and the complete removal of axial EtOAc ligands was verified by ¹H NMR analysis through the disappearance of the peaks belong to EtOAc. A glass cell (1.0 cm path length) from Starna Cells, Inc., with screw top was used. Rh₂(*S*-PTIL)₄ (7.5 mg, 0.06 mmol) with no axial EtOAc was weighed into the glass cell inside the glovebox, and toluene (3.0 mL) was added into the glass cell. The glass was sealed inside the glove box and was then taken out into air. A toluene solution of **70e** or CH₃CN (2.0 × 10⁻¹ M) was prepared in a similar way. Absorption measurements were performed on a Carey 50 Bio UV-vis spectrometer in air. Prior to addition of the ligand solution, the UV-vis (500-800 nm) spectrum of Rh₂(*S*-PTIL)₄ was recorded. Then 5.0 μL of the ligand solution was added to the cell using a 10.0 μL syringe. The cell was inverted twice to ensure thorough mixing before the UV-vis spectrum was recorded at 20 °C. Fifteen additional aliquots (5.0 μL each) of the ligand solution were sequentially added to the cell over 20 min, and the total change in volume was less than 3%. Upon sequential addition of the ligand solutions, the color of the mixture turned from initial yellow-green to final deep red.

The UV-vis spectrum was recorded after the addition of each aliquot. Association constants were calculated by the method previously developed.¹²⁷





Control Experiment using Cycloaddition Product 78 or 79 as Lewis Base

Additive: Sample Procedure for the Enantioselective [3+3]-Cycloaddition of Isoquinolinium/Pyridinium Methylides (69/70) and Enol Diazoacetate 59 in the Presence of [3+3]-Cycloaddition Product 78 or [3+2]-Cycloaddition Product 79.

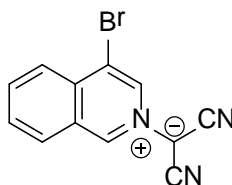
In a 10 mL flame-dried Schlenk flask charged with a magnetic stirring bar, $\text{Rh}_2(\text{S}^-\text{PTIL})_4$ (4.2 mg, 0.0030 mmol, 3 mol%), isoquinolinium dicyanomethylide **70a** (20 mg, 0.10 mmol), [3+3]-cycloaddition product **78g** (28 mg, 0.050 mmol) and 1.0 ml dry toluene were added sequentially under a nitrogen atmosphere. Then the flask was capped by a rubber septum and the resulting solution was stirred at room temperature for 5 min before enol diazoacetate **59a** (46 mg, 0.18 mmol) dissolved in 1.0 ml toluene was added via syringe pump over 1h. Stirring was continued at room temperature for

2h after the completion of adding **59a**. Then the solution was concentrated under reduced pressure, and the residue was analyzed by ^1H NMR to determine the product ratio (**78:79**).

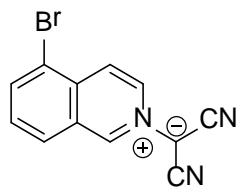
4.3 Characterization Data

Dirhodium(II) Tetrakis[*N*-phthaloyl-(*S*)-*iso*-leucinate] Bis(ethyl acetate)

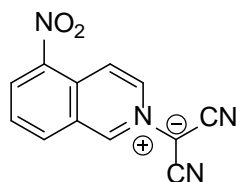
Adduct $[\text{Rh}_2(\text{S-PTIL})_4(\text{EtOAc})_2]$: ^1H NMR (400 MHz, CDCl_3) δ : 7.73 (dd, $J = 5.5$, 3.0 Hz, 8H), 7.64 (dd, $J = 5.5$, 3.0 Hz, 8H), 4.70 (d, $J = 8.0$ Hz, 4H), 4.15 (q, $J = 7.1$ Hz, 4H), 2.48 – 2.32 (comp, 4H), 2.05 (s, 6H), 1.49 – 1.32 (comp, 4H), 1.22 (t, $J = 7.1$ Hz, 6H), 0.97 (dd, $J = 10.4$, 5.5 Hz, 12H), 0.94 – 0.85 (comp, 4H), 0.81 (t, $J = 7.1$ Hz, 12H). ^{13}C NMR (100 MHz, CDCl_3) δ 187.9, 172.7, 167.5, 133.7, 131.9, 123.3, 60.8, 58.5, 34.8, 25.6, 21.0, 16.7, 14.1, 11.2. $[\alpha]_D^{23} = -32.0^\circ$ (c 0.08, CH_2Cl_2). HRMS (ESI $^+$): calcd for $\text{C}_{56}\text{H}_{58}\text{N}_4\text{O}_{17}\text{Rh}_2$ $[\text{M}+\text{H}_2\text{O}]^+$ 1264.1907, found 1264.1917.



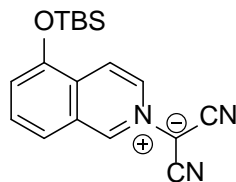
(4-Bromoisoquinolin-2-ium-2-yl)dicyanomethanide 70b: 43% yield. ^1H NMR (400 MHz, $\text{DMSO-}d_6$) δ : 9.42 (s, 1H), 8.48 (d, $J = 1.1$ Hz, 1H), 8.42 (d, $J = 8.2$ Hz, 1H), 8.13 (dd, $J = 8.2$, 1.1 Hz, 1H), 8.03 (ddd, $J = 8.2$, 7.0, 1.1 Hz, 1H), 7.94 (ddd, $J = 8.2$, 7.0, 1.1 Hz, 1H). ^{13}C NMR (100 MHz, $\text{DMSO-}d_6$) δ : 134.0, 133.6, 131.6, 130.6, 128.6, 125.7, 121.8, 118.3, 59.0. HRMS (ESI $^+$): calcd for $\text{C}_{12}\text{H}_7\text{BrN}_3$ $[\text{M}+\text{H}]^+$ 271.9823, found 271.9833.



(5-Bromoisoquinolin-2-ium-2-yl)dicyanomethanide 70c: 49% yield. ^1H NMR (400 MHz, DMSO- d^6) δ : 9.38 (d, $J = 1.7$ Hz, 1H), 8.50 (dd, $J = 7.3, 1.7$ Hz, 1H), 8.38 (d, $J = 8.6$ Hz, 1H), 8.28 (d, $J = 7.3$ Hz, 1H), 8.20 (dd, $J = 7.3, 0.9$ Hz, 1H), 7.74 (t, $J = 8.6$ Hz, 1H). ^{13}C NMR (100 MHz, DMSO- d^6) δ : 135.6, 133.4, 131.6, 130.2, 129.9, 129.5, 127.8, 124.5, 120.5, 118.2, 59.1. HRMS (ESI $^+$): calcd for $\text{C}_{12}\text{H}_7\text{BrN}_3$ $[\text{M}+\text{H}]^+$ 271.9823, found 271.9840.

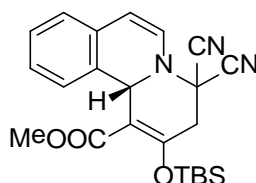


(5-Nitroisoquinolin-2-ium-2-yl)dicyanomethanide 70d: 63% yield. ^1H NMR (400 MHz, DMSO- d^6) δ : 9.50 (d, $J = 1.8$ Hz, 1H), 8.73 (d, $J = 8.5$ Hz, 1H), 8.67 (d, $J = 7.5$ Hz, 1H), 8.64 (dd, $J = 7.5, 1.8$ Hz, 1H), 8.59 (dd, $J = 7.5, 1.8$ Hz, 1H), 8.00 (t, $J = 8.5$ Hz, 1H). ^{13}C NMR (100 MHz, DMSO- d^6) δ : 144.2, 134.5, 133.0, 130.5, 123.0, 129.7, 129.4, 123.3, 121.4, 117.8, 59.5. HRMS (ESI $^+$): calcd for $\text{C}_{12}\text{H}_7\text{N}_4\text{O}_2$ $[\text{M}+\text{H}]^+$ 239.0569, found 239.0575.

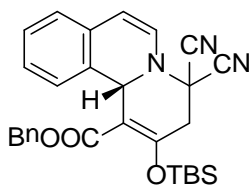


[5-(*tert*-Butyldimethylsilyloxy)isoquinolin-2-ium-2-yl]dicyanomethanide 70e: 59% yield. ^1H NMR (400 MHz, CDCl_3) δ : 8.94 (d, $J = 1.3$ Hz, 1H), 8.32 (dd, $J =$

7.8, 1.3 Hz, 1H), 8.17 (d, $J = 7.8$ Hz, 1H), 7.64 (t, $J = 8.3$ Hz, 1H), 7.50 (d, $J = 8.3$ Hz, 1H), 7.13 (d, $J = 7.8$ Hz, 1H), 1.09 (s, 9H), 0.35 (s, 6H). ^{13}C NMR (100 MHz, CDCl_3) δ 151.9, 132.6, 131.4, 130.6, 126.9, 126.2, 121.4, 119.6, 118.9, 118.5, 26.1, 18.8, 0.4, -3.9. HRMS (ESI⁺): calcd for $\text{C}_{18}\text{H}_{22}\text{N}_3\text{OSi}$ $[\text{M}+\text{H}]^+$ 324.1532, found 324.1539.

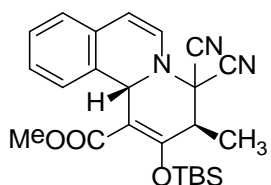


Methyl (S)-2-(tert-Butyldimethylsilyloxy)-4,4-dicyano-4,11b-dihydro-3H-pyrido[2,1-a]isoquinoline-1-carboxylate (78a). ^1H NMR (400 MHz, CDCl_3) δ : 7.30 (td, $J = 7.5, 1.5$ Hz, 1H), 7.24 (td, $J = 7.5, 1.5$ Hz, 1H), 7.16 (dd, $J = 7.5, 1.5$ Hz, 1H), 6.94 (d, $J = 7.5$ Hz, 1H), 6.69 (d, $J = 7.4$ Hz, 1H), 6.29 (d, $J = 7.4$ Hz, 1H), 5.15 (s, 1H), 3.70 (s, 3H), 3.17 (dd, $J = 16.6, 2.4$ Hz, 1H), 2.93 (dd, $J = 16.6, 1.5$ Hz, 1H), 1.02 (s, 9H), 0.37 (s, 3H), 0.29 (s, 3H). ^{13}C NMR (100 MHz, CDCl_3) δ : 165.2, 151.1, 132.6, 132.0, 130.8, 128.4, 127.9, 124.6, 124.2, 113.3, 112.7, 112.0, 109.1, 56.4, 52.1, 51.3, 41.6, 26.1, 18.8, -3.3, -3.7. 93% ee, HPLC: OD-H, 95% hexanes, 5% *i*-PrOH, 1.0 mL/min, 254 nm, 5.5 min (minor), 6.2 min (major). $[\alpha]_D^{23} = -164^\circ$ (c 1.3, CH_2Cl_2). HRMS (ESI⁺): calcd for $\text{C}_{23}\text{H}_{28}\text{N}_3\text{O}_3\text{Si}$ $[\text{M}+\text{H}]^+$ 422.1900, found 422.1913.

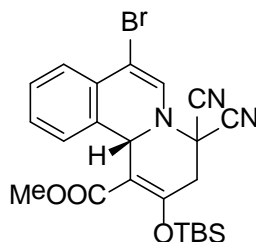


Benzyl (S)-2-(tert-Butyldimethylsilyloxy)-4,4-dicyano-4,11b-dihydro-3H-pyrido[2,1-a]isoquinoline-1-carboxylate (78b). ^1H NMR (400 MHz, CDCl_3) δ 7.28 – 7.18 (m, 4H), 7.16 – 7.08 (m, 3H), 7.04 (td, $J = 7.7, 1.3$ Hz, 1H), 6.82 (d, $J = 7.7$ Hz,

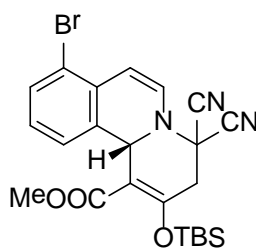
1H), 6.64 (d, $J = 7.4$ Hz, 1H), 6.24 (d, $J = 7.4$ Hz, 1H), 5.19 (d, $J = 12.3$ Hz, 1H), 5.14 (s, 1H), 5.07 (d, $J = 12.3$ Hz, 1H), 3.13 (dd, $J = 16.6, 2.4$ Hz, 1H), 2.90 (dd, $J = 16.6, 1.3$ Hz, 1H), 0.98 (s, 9H), 0.31 (s, 3H), 0.24 (s, 3H). ^{13}C NMR (100 MHz, CDCl_3) δ : 164.4, 151.3, 135.7, 132.5, 131.9, 130.5, 128.9, 128.8, 128.6, 128.3, 127.9, 124.6, 124.5, 113.5, 112.7, 112.0, 109.0, 66.8, 56.4, 51.3, 41.5, 26.1, 18.8, -3.3, -3.7. 93% ee, HPLC: OD-H, 95% hexanes, 5% *i*-PrOH, 1.0 mL/min, 254 nm, 10.0 min (minor), 12.0 min (major). $[\alpha]_D^{23} = -133^\circ$ (c 1.0, CH_2Cl_2). HRMS (ESI⁺): calcd for $\text{C}_{29}\text{H}_{32}\text{N}_3\text{O}_3\text{Si}$ $[\text{M}+\text{H}]^+$ 498.2213, found 498.2230.



Methyl (3R,11bS)-2-(*tert*-Butyldimethylsilyloxy)-4,4-dicyano-3-methyl-4,11b-dihydro-3H-pyrido[2,1-*a*]isoquinoline-1-carboxylate (78c). ^1H NMR (400 MHz, CDCl_3) δ : 7.29 (td, $J = 7.6, 0.6$ Hz, 1H), 7.21 (td, $J = 7.6, 1.3$ Hz, 1H), 7.15 (dd, $J = 7.3, 1.3$ Hz, 1H), 6.95 (d, $J = 7.3$ Hz, 1H), 6.72 (d, $J = 7.4$ Hz, 1H), 6.25 (d, $J = 7.4$ Hz, 1H), 5.08 (s, 1H), 3.72 (s, 3H), 2.86 (qd, $J = 6.8, 0.6$ Hz, 1H), 1.47 (d, $J = 6.8$ Hz, 3H), 1.06 (s, 9H), 0.33 (s, 3H), 0.31 (s, 3H). ^{13}C NMR (100 MHz, CDCl_3) δ : 165.8, 156.0, 133.1, 132.7, 131.1, 128.2, 127.6, 124.4, 123.4, 112.6, 112.1, 111.9, 107.4, 56.8, 56.7, 52.2, 45.3, 26.1, 18.7, 15.5, -3.1, -3.6. 82% ee, HPLC: OD-H, 99% hexanes, 1% *i*-PrOH, 1.0 mL/min, 254 nm, 6.0 min (minor), 7.6 min (major). $[\alpha]_D^{23} = -313^\circ$ (c 0.3, CH_2Cl_2). HRMS (ESI⁺): calcd for $\text{C}_{24}\text{H}_{30}\text{N}_3\text{O}_3\text{Si}$ $[\text{M}+\text{H}]^+$ 436.2056, found 436.2020.

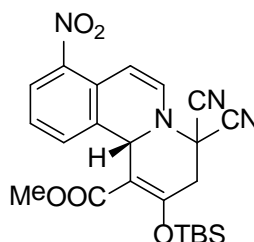


Methyl (S)-7-Bromo-2-(*tert*-butyldimethylsilyl)oxy-4,4-dicyano-4,11b-dihydro-3H-pyrido[2,1-*a*]isoquinoline-1-carboxylate (78d). ^1H NMR (400 MHz, CDCl_3) δ : 7.56 (dd, $J = 7.7, 1.2$ Hz, 1H), 7.41 (td, $J = 7.7, 0.7$ Hz, 1H), 7.34 (td, $J = 7.7, 1.2$ Hz, 1H), 6.99 (s, 1H), 6.92 (d, $J = 7.7$ Hz, 1H), 5.25 (s, 1H), 3.72 (s, 3H), 3.11 (dd, $J = 16.7, 2.1$ Hz, 1H), 2.97 (dd, $J = 16.7, 1.2$ Hz, 1H), 1.04 (s, 9H), 0.38 (s, 3H), 0.32 (s, 3H). ^{13}C NMR (100 MHz, CDCl_3) δ : 164.6, 151.6, 132.1, 131.9, 131.1, 129.5, 128.8, 125.0, 124.2, 112.3, 111.6, 109.0, 108.3, 56.3, 52.1, 50.2, 41.6, 26.2, 18.9, -3.2, -3.7. 96% ee, HPLC: OD-H, 97% hexanes, 3% *i*-PrOH, 1.0 mL/min, 254 nm, 5.2 min (minor), 5.6 min (major). $[\alpha]_{\text{D}}^{23} = -122^\circ$ (c 0.8, CH_2Cl_2). HRMS (ESI $^+$): calcd for $\text{C}_{23}\text{H}_{27}\text{BrN}_3\text{O}_3\text{Si}$ $[\text{M}+\text{H}]^+$ 500.1005, found 500.1009.

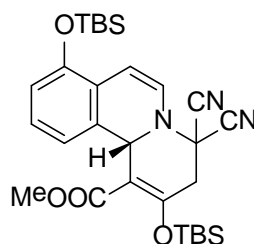


Methyl (S)-8-Bromo-2-(*tert*-butyldimethylsilyl)oxy-4,4-dicyano-4,11b-dihydro-3H-pyrido[2,1-*a*]isoquinoline-1-carboxylate (78e). ^1H NMR (400 MHz, CDCl_3) δ : 7.52 (d, $J = 7.9$ Hz, 1H), 7.09 (t, $J = 7.9$ Hz, 1H), 6.88 (dd, $J = 7.7, 0.7$ Hz, 1H), 6.82 (d, $J = 7.7$ Hz, 1H), 6.61 (dd, $J = 7.7, 0.7$ Hz, 1H), 5.11 (s, 1H), 3.70 (s, 3H), 3.18 (dd, $J = 16.6, 2.4$ Hz, 1H), 2.94 (dd, $J = 16.6, 1.1$ Hz, 1H), 1.03 (s, 9H), 0.37 (s, 3H), 0.30 (s, 3H). ^{13}C NMR (100 MHz, CDCl_3) δ : 164.9, 151.8, 133.6, 132.5, 132.5,

132.3, 128.6, 123.4, 120.4, 112.4, 111.8, 111.7, 108.5, 56.7, 52.2, 51.2, 41.6, 26.1, 18.8, -3.3, -3.7. 94% ee, HPLC: OD-H, 95% hexanes, 5% *i*-PrOH, 1.0 mL/min, 254 nm, 10.5 min (minor), 11.6 min (major). $[\alpha]_D^{23} = -281^\circ$ (*c* 0.5, CH₂Cl₂). HRMS (ESI⁺): calcd for C₂₃H₂₇BrN₃O₃Si [M+H]⁺ 500.1005, found 500.1012.

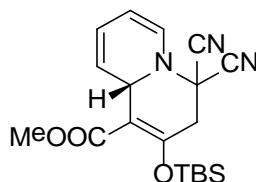


Methyl (S)-2-(*tert*-Butyldimethylsilyloxy)-4,4-dicyano-8-nitro-4,11b-dihydro-3H-pyrido[2,1-*a*]isoquinoline-1-carboxylate (78f). ¹H NMR (400 MHz, CDCl₃) δ 8.01 (d, *J* = 7.9 Hz, 1H), 7.35 (t, *J* = 7.9 Hz, 1H), 7.18 (dd, *J* = 7.9, 0.6 Hz, 1H), 7.07 (dd, *J* = 7.9, 0.6 Hz, 1H), 6.96 (d, *J* = 7.9 Hz, 1H), 5.14 (s, 1H), 3.71 (s, 3H), 3.21 (dd, *J* = 16.6, 2.4 Hz, 1H), 2.96 (dd, *J* = 16.6, 1.0 Hz, 1H), 1.04 (s, 9H), 0.39 (s, 3H), 0.32 (s, 3H). ¹³C NMR (100 MHz, CDCl₃) δ: 164.6, 152.6, 144.5, 136.4, 133.0, 129.2, 127.7, 127.4, 124.9, 112.1, 111.5, 107.8, 107.0, 56.5, 52.3, 51.0, 41.6, 26.0, 18.8, -3.2, -3.6. 95% ee, HPLC: IB-3, 90% hexanes, 9% *i*-PrOH, 1% EtOH, 1.0 mL/min, 254 nm, 6.7 min (major), 7.0 min (minor). $[\alpha]_D^{23} = -179^\circ$ (*c* 0.4, CH₂Cl₂). HRMS (ESI⁺): calcd for C₂₃H₂₇N₄O₅Si [M+H]⁺ 467.1751, found 467.1771.

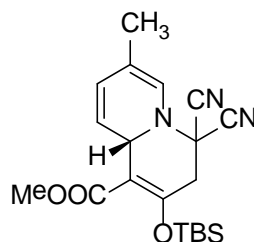


Methyl (S)-2,8-Bis(*tert*-butyldimethylsilyloxy)-4,4-dicyano-4,11b-dihydro-3H-pyrido[2,1-*a*]isoquinoline-1-carboxylate (78g). ¹H NMR (400 MHz, CDCl₃) δ

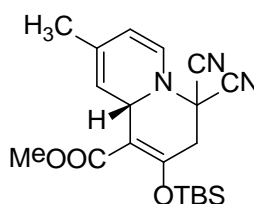
7.07 (t, $J = 8.0$ Hz, 1H), 6.73 (d, $J = 8.0$ Hz, 1H), 6.64 (d, $J = 8.0$ Hz, 1H), 6.52 (d, $J = 7.2$ Hz, 1H), 6.51 (d, $J = 7.2$ Hz, 1H), 5.04 (s, 1H), 3.68 (s, 3H), 3.13 (dd, $J = 16.5, 2.5$ Hz, 1H), 2.89 (dd, $J = 16.5, 1.2$ Hz, 1H), 1.06 (s, 9H), 1.02 (s, 9H), 0.36 (s, 3H), 0.28 (s, 3H), 0.26 (s, 3H), 0.24 (s, 3H). ^{13}C NMR (100 MHz, CDCl_3) δ : 164.9, 150.8, 150.3, 132.7, 131.1, 128.3, 124.2, 118.7, 117.2, 112.6, 111.8, 109.4, 108.9, 56.5, 51.9, 51.3, 41.6, 26.3, 26.2, 18.9, 18.8, -3.3, -3.7, -3.7, -3.8. 95% ee, HPLC: IC-3, 99% hexanes, 1% *i*-PrOH, 1.0 mL/min, 254 nm, 5.0 min (minor), 6.7 min (major). $[\alpha]_D^{23} = -330^\circ$ (*c* 1.0, CH_2Cl_2). HRMS (ESI⁺): calcd for $\text{C}_{29}\text{H}_{42}\text{N}_3\text{O}_4\text{Si}_2$ $[\text{M}+\text{H}]^+$ 552.2714, found 552.2701.



Methyl (S)-2-(tert-Butyldimethylsilyl)oxy-4,4-dicyano-4,9a-dihydro-3H-quinolizine-1-carboxylate (78h). ^1H NMR (400 MHz, CDCl_3) δ : 6.57 (d, $J = 7.7$ Hz, 1H), 6.08 (dddd, $J = 9.1, 5.2, 2.8, 0.7$ Hz, 1H), 5.64 (ddd, $J = 7.7, 5.2, 1.4$ Hz, 1H), 5.43 (dddd, $J = 9.1, 2.8, 1.4, 0.9$ Hz, 1H), 4.68 (s, 1H), 3.78 (s, 3H), 3.15 (dd, $J = 16.7, 3.1$ Hz, 1H), 2.79 (dd, $J = 16.7, 1.8$ Hz, 1H), 1.00 (s, 9H), 0.30 (s, 3H), 0.24 (s, 3H). ^{13}C NMR (100 MHz, CDCl_3) δ : 164.6, 145.0, 132.1, 124.5, 122.0, 112.5, 111.1, 110.2, 109.8, 52.5, 52.0, 51.9, 41.1, 26.0, 18.7, -3.4, -3.7. 87% ee, HPLC: OD-H, 99% hexanes, 1% *i*-PrOH, 1.0 mL/min, 254 nm, 6.7 min (major), 7.5 min (minor). $[\alpha]_D^{23} = -350^\circ$ (*c* 0.6, CH_2Cl_2). HRMS (ESI⁺): calcd for $\text{C}_{19}\text{H}_{26}\text{N}_3\text{O}_3\text{Si}$ $[\text{M}+\text{H}]^+$ 372.1743, found 372.1759.

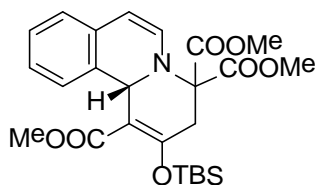


Methyl (S)-2-(tert-Butyldimethylsilyl)oxy-4,4-dicyano-7-methyl-4,9a-dihydro-3H-quinolizine-1-carboxylate (78i). ^1H NMR (400 MHz, CDCl_3) δ : 6.30 (s, 1H), 6.00 (ddd, $J = 9.2, 2.5, 0.8$ Hz, 1H), 5.48 (dd, $J = 9.2, 2.5$ Hz, 1H), 4.57 (p, $J = 2.5$ Hz, 1H), 3.78 (s, 3H), 3.10 (dd, $J = 16.8, 3.0$ Hz, 1H), 2.81 (dd, $J = 16.8, 1.4$ Hz, 1H), 1.87 (d, $J = 1.4$ Hz, 3H), 1.00 (s, 9H), 0.29 (s, 3H), 0.24 (s, 3H). ^{13}C NMR (100 MHz, CDCl_3) δ : 164.7, 150.2, 128.2, 127.4, 122.6, 120.4, 113.1, 111.4, 109.9, 52.8, 51.9, 51.7, 41.2, 26.0, 18.7, 17.9, -3.4, -3.7. 86% ee, HPLC: IB-3, 97% hexanes, 3% CH_2Cl_2 , 1.0 mL/min, 254 nm, 10.5 min (major), 17.5 min (minor). $[\alpha]_D^{23} = -336^\circ$ (c 0.6, CH_2Cl_2). HRMS (ESI $^+$): calcd for $\text{C}_{20}\text{H}_{28}\text{N}_3\text{O}_3\text{Si}$ $[\text{M}+\text{H}]^+$ 386.1900, found 386.1883.

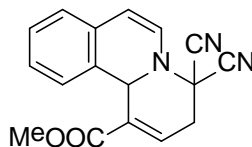


Methyl (S)-2-(tert-Butyldimethylsilyl)oxy-4,4-dicyano-8-methyl-4,9a-dihydro-3H-quinolizine-1-carboxylate (78j). ^1H NMR (400 MHz, CDCl_3) δ 6.52 (d, $J = 7.5$ Hz, 1H), 5.50 (dd, $J = 7.5, 1.9$ Hz, 1H), 5.08 (s, 1H), 4.63 (s, 1H), 3.79 (s, 3H), 3.11 (dd, $J = 16.6, 3.2$ Hz, 1H), 2.76 (dd, $J = 16.6, 1.9$ Hz, 1H), 1.82 (t, $J = 1.9$ Hz, 3H), 1.00 (s, 9H), 0.30 (s, 3H), 0.24 (s, 3H). ^{13}C NMR (100 MHz, CDCl_3) δ : 164.36, 149.30, 133.22, 131.53, 116.98, 112.93, 112.47, 110.92, 110.80, 52.94, 51.76, 41.25,

26.08, 20.21, 18.75, -3.35, -3.73. 74% ee, HPLC: IB-3, 97% hexanes, 3% CH₂Cl₂, 1.0 mL/min, 254 nm, 9.6 min (major), 11.2 min (minor). $[\alpha]^{23}_{\text{D}} = -287^{\circ}$ (*c* 0.4, CH₂Cl₂). HRMS (ESI⁺): calcd for C₂₀H₂₈N₃O₃Si [M+H]⁺ 386.1900, found 386.1889.

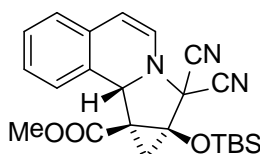


Trimethyl (S)-2-(*tert*-Butyldimethylsilyl)oxy-3H-pyrido[2,1a]isoquinoline-1,4,4(11bH)-tricarboxylate (78k). ¹H NMR (400 MHz, CDCl₃) δ : 7.15 (td, *J* = 7.5, 0.8 Hz, 1H), 7.08 (td, *J* = 7.5, 1.4 Hz, 1H), 7.01 (dd, *J* = 7.5, 1.4 Hz, 1H), 6.81 (dd, *J* = 7.5, 0.8 Hz, 1H), 6.39 (d, *J* = 7.5 Hz, 1H), 5.87 (d, *J* = 7.5 Hz, 1H), 5.00 (s, 1H), 3.86 (s, 3H), 3.72 (s, 3H), 3.63 (s, 3H), 2.95 (dd, *J* = 16.1, 2.4 Hz, 1H), 2.86 (dd, *J* = 16.1, 1.2 Hz, 1H), 1.02 (s, 9H), 0.34 (s, 3H), 0.27 (s, 3H). ¹³C NMR (100 MHz, CDCl₃) δ : 168.89, 168.50, 165.78, 155.90, 135.74, 134.18, 131.05, 127.35, 126.14, 123.56, 123.19, 107.18, 106.53, 70.88, 56.89, 53.62, 53.44, 51.49, 38.98, 26.25, 18.88, -3.23, -3.71. 52% ee, HPLC: IB-3, 98% hexanes, 2% *i*-PrOH, 1.0 mL/min, 254 nm, 7.0 min (minor), 7.8 min (major). $[\alpha]^{23}_{\text{D}} = -117^{\circ}$ (*c* 0.1, CH₂Cl₂). HRMS (ESI⁺): calcd for C₂₅H₃₄NO₇Si [M+H]⁺ 488.2105, found 488.2140.

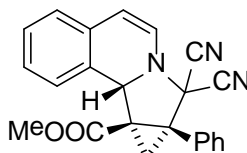


Methyl 4,4-Dicyano-4,11b-dihydro-3H-pyrido[2,1-a]isoquinoline-1-carboxylate (78l). ¹H NMR (400 MHz, CDCl₃) δ : 7.32 (td, *J* = 7.6, 0.7 Hz, 1H), 7.26 (td, *J* = 7.6, 1.5 Hz, 1H), 7.19 (dd, *J* = 3.5, 1.5 Hz, 1H), 7.17 (dd, *J* = 4.6, 1.5 Hz, 1H), 6.82 (dd, *J* = 7.6, 0.5 Hz, 1H), 6.75 (d, *J* = 7.4 Hz, 1H), 6.38 (d, *J* = 7.4 Hz, 1H), 5.06

(s, 1H), 3.85 (s, 3H), 3.19 (dd, $J = 4.6, 2.5$ Hz, 2H). ^{13}C NMR (100 MHz, CDCl_3) δ : 165.6, 132.8, 132.4, 131.6, 131.1, 129.3, 128.6, 128.0, 124.7, 124.4, 114.3, 113.1, 112.4, 55.7, 53.0, 49.8, 36.4. HRMS (ESI⁺): calcd for $\text{C}_{17}\text{H}_{14}\text{N}_3\text{O}_2$ [M+H]⁺ 292.1086, found 292.1096.



Methyl (8aSR,9aSR,9bSR)-8a-(tert-Butyldimethylsilyl)oxy-8,8-dicyano-8a,9,9a,9b-tetrahydro-8H-cyclopropa[3,4]pyrrolo[2,1-a]isoquinoline-9a-carboxylate (79a). ^1H NMR (400 MHz, CDCl_3) δ : 7.28 (tdd, $J = 7.5, 1.4, 0.7$ Hz, 1H), 7.22 (td, $J = 7.5, 1.4$ Hz, 1H), 7.10 (dd, $J = 7.5, 1.4$ Hz, 1H), 6.91 (d, $J = 7.5$ Hz, 1H), 6.47 (d, $J = 7.5$ Hz, 1H), 5.93 (d, $J = 7.5$ Hz, 1H), 5.42 (s, 1H), 3.88 (s, 3H), 2.34 (d, $J = 7.3$ Hz, 1H), 1.91 (dd, $J = 7.3, 0.5$ Hz, 1H), 1.00 (s, 9H), 0.40 (s, 3H), 0.32 (s, 3H). ^{13}C NMR (100 MHz, CDCl_3) δ : 167.2, 132.7, 128.7, 128.3, 128.0, 127.8, 125.2, 124.2, 112.6, 111.7, 109.4, 73.6, 60.8, 60.2, 53.3, 35.9, 25.8, 18.8, 18.4, -3.2, -3.6. HRMS (ESI⁺): calcd for $\text{C}_{23}\text{H}_{28}\text{N}_3\text{O}_3\text{Si}$ [M+H]⁺ 422.1900, found 422.1939.



Methyl (8aSR,9aRS,9bSR)-8,8-Dicyano-8a-phenyl-8a,9,9a,9b-tetrahydro-8H-cyclopropa[3,4]pyrrolo[2,1-a]isoquinoline-9a-carboxylate (79b): ^1H NMR (400 MHz, CDCl_3) δ : 7.56 – 7.44 (comp, 5H), 7.31 (tq, $J = 7.5, 0.6$ Hz, 1H), 7.24 (td, $J = 7.5, 1.4$ Hz, 1H), 7.14 (dd, $J = 7.5, 1.4$ Hz, 1H), 7.01 (t, $J = 5.5$ Hz, 1H), 6.52 (d, $J = 7.5$ Hz, 1H), 5.98 (d, $J = 7.5$ Hz, 1H), 5.61 (s, 1H), 4.18 (q, $J = 7.1$ Hz, 2H), 2.21 (d,

$J = 6.3$ Hz, 1H), 2.16 (d, $J = 6.3$ Hz, 1H), 1.08 (t, $J = 7.1$ Hz, 3H). ^{13}C NMR (100 MHz, CDCl_3) δ : 168.1, 132.6, 131.6, 130.6, 130.4, 129.5, 128.75, 128.7, 128.2, 127.8, 125.2, 124.5, 112.2, 112.2, 109.5, 62.4, 61.8, 61.2, 47.0, 37.9, 17.8, 14.3. HRMS (ESI⁺): calcd for $\text{C}_{23}\text{H}_{18}\text{N}_3\text{O}_2$ [M+H]⁺ 368.1399, found 368.1437.

NMR graphs, HPLC chromatograms and X-ray single crystal analysis data can be obtained from the supporting information of the paper published in the *Journal of the American Chemical Society*: Xu, X.; Zavalij, P. Y.; Doyle, M. P. *J. Am. Chem. Soc.* **2013**, *135*, 12439-12447.

V. Reference

- (1) Davies, H. M.; Morton, D. *Chem. Soc. Rev.* **2011**, *40*, 1857.
- (2) Doyle, M. P.; McKervey, M. A. *Chem. Comm.* **1997**, 983.
- (3) Davies, H. M. L.; Beckwith, R. E. J. *Chem. Rev.* **2003**, *103*, 2861.
- (4) Doyle, M. P.; Duffy, R.; Ratnikov, M.; Zhou, L. *Chem. Rev.* **2010**, *110*, 704.
- (5) Ye, T.; McKervey, M. A. *Chem. Rev.* **1994**, *94*, 1091.
- (6) Cotton, F. A.; DeBoer, B. G.; LaPrade, M. D.; Pipal, J. R.; Ucko, D. *Acta Crystallographica* **1971**, *B27*, 1664.
- (7) Chifotides, H. T.; Dunbar, K. R., Chifotides, H. T.; Dunbar, K. R. *In Multiple Bonds Between Metal Atoms; 3rd ed.; Cotton, F. A.; Murillo, C. A.; Walton, R. A. Eds.; Springer: New York, 2005.*
- (8) Doyle, M. P.; A., M.; Ye, T. *Modern Catalytic Methods for Organic Synthesis with Diazo Compounds: From Cyclopropanes to Ylides; Wiley-Interscience: New York, 1998.*
- (9) Müller, P.; Gränicher, C. *Helv. Chim. Acta* **1993**, *76*, 521.
- (10) Müller, P.; Gränicher, C. *Helv. Chim. Acta* **1995**, *78*, 129.

- (11) Müller, P.; Pautex, N.; Doyle, M. P.; Bagheri, V. *Helv. Chim. Acta* **1990**, *73*, 1233.
- (12) Doyle, M. P. *J. Org. Chem.* **2006**, *71*, 9253.
- (13) Welch, C. J.; Tu, Q.; Wang, T.; Raab, C.; Wang, P.; Jia, X.; Bu, X.; Bykowski, D.; Hohenstaufen, B.; Doyle, M. P. *Adv. Synth. Catal.* **2006**, *348*, 821.
- (14) Yoon, T. P.; Jacobsen, E. N. *Science* **2003**, *299*, 1691.
- (15) Doyle, M. P.; Ratnikov, M.; Liu, Y. *Org. Biomol. Chem.* **2011**, *9*, 4007.
- (16) Estevan, F.; Lahuerta, P.; Perez-Prieto, J.; Sanau, M.; Stiriba, S.-E.; Ubeda, M. A. *Organometallics* **1997**, *16*, 880.
- (17) Barberis, M.; Estevan, F.; Lahuerta, P.; Perez-Prieto, J.; Sanau, M. *Inorg. Chem.* **2001**, *40*, 4226.
- (18) Estevan, F. L., P.; Perez-Prieto, J.; Pereira, I.; Stiriba, S.-E. *Organometallics* **1998**, *17*, 3442.
- (19) Lloret, J.; Carbo, J. J.; Bo, C.; Lledos, A.; Perez-Prieto, J. *Organometallics* **2008**, *27*, 2873.
- (20) Kennedy, M.; McKervey, M. A.; Maguire, A. R.; Roos, G. H. P. *Chem. Comm.* **1990**, 361.
- (21) Davies, H. M. L. *Eur. J. Org. Chem.* **1999**, 2459.
- (22) Davies, H. M.; Nikolai, J. *Org. Biomol. Chem.* **2005**, *3*, 4176.
- (23) Davies, H. M. L.; Manning, J. R. *Nature* **2008**, *451*, 417.
- (24) Hansen, J.; Davies, H. M. L. *Coord. Chem. Rev.* **2008**, *252*, 545.

- (25) Hansen, J.; Autschbach, J.; Davies, H. M. L. *J. Org. Chem.* **2009**, *74*, 6555.
- (26) Anada, M.; Kitagaki, S.; Hashimoto, S. *Heterocycles* **2000**, *52*, 875.
- (27) Reddy, R. P.; Lee, G. H.; Davies, H. M. L. *Org. Lett.* **2006**, *16*, 3437.
- (28) Qin, C.; Boyarskikh, V.; Hansen, J. H.; Hardcastle, K. I.; Musaev, D. G.; Davies, H. M. *J. Am. Chem. Soc.* **2011**, *133*, 19198.
- (29) Qin, C.; Davies, H. M. *J. Am. Chem. Soc.* **2013**, *135*, 14516.
- (30) Xu, X.; Lu, H.; Ruppel, J. V.; Cui, X.; Lopez de Mesa, S.; Wojtas, L.; Zhang, X. P. *J. Am. Chem. Soc.* **2011**, *133*, 15292.
- (31) Doyle, M. P.; Winchester, W. R.; Protopopova, M. N.; Kazala, A. P.; Westrum, L. J. *Org. Synth.* **1996**, *73*, 13.
- (32) Doyle, M. P.; Pieters, R. J.; Martin, S. F.; Austin, R. E.; Oalmann, C. J.; Müller, P. *J. Am. Chem. Soc.* **1991**, *113*, 1423.
- (33) Doyle, M. P.; Brandes, B. D.; Kazala, A. P.; Pieters, R. J.; Jarstfer, M. B.; Watkins, L. M.; Eagle, C. T. *Tetrahedron Lett.* **1990**, *31*, 6613.
- (34) Doyle, M. P.; Zhou, Q.-L.; Raab, C. E.; Roos, G. H. P.; Simonsen, S. H.; Lynch, V. *Inorg. Chem.* **1996**, *35*, 6064.
- (35) Doyle, M. P.; Davies, S. B.; Hu, W. *Org. Lett.* **2000**, *2*, 1145.
- (36) Doyle, M. P.; Phillips, I. M.; Hu, W. *J. Am. Chem. Soc.* **2001**, *123*, 5366.
- (37) Doyle, M. P.; Valenzuela, M.; Huang, P. *PNAS* **2004**, *101*, 5391.
- (38) Watanabe, Y.; Washio, T.; Krishnamurthi, J.; Anada, M.; Hashimoto, S. *Chem. Comm.* **2012**, *48*, 6969.

- (39) Wang, Y.; Wolf, J.; Zavalij, P.; Doyle, M. P. *Angew. Chem., Int. Ed.* **2008**, *47*, 1439.
- (40) Wang, X.; Weigl, C.; Doyle, M. P. *J. Am. Chem. Soc.* **2011**, *133*, 9572.
- (41) Hashimoto, S.; Watanabe, N.; Ikegami, S. *Tetrahedron Lett.* **1990**, *31*, 5173.
- (42) Oohara, T.; Nambu, H.; Anada, M.; Takeda, K.; Hashimoto, S. *Adv. Synth. Catal.* **2012**, *354*, 2331.
- (43) Goto, T.; Takeda, K.; Shimada, N.; Nambu, H.; Anada, M.; Shiro, M.; Ando, K.; Hashimoto, S. *Angew. Chem., Int. Ed.* **2011**, *50*, 6803.
- (44) Hashimoto, Y.; Itoh, K.; Kakehi, A.; Shiro, M.; Suga, H. *J. Org. Chem.* **2013**, *78*, 6182.
- (45) Shimada, N.; Hanari, T.; Kurosaki, Y.; Takeda, K.; Anada, M.; Nambu, H.; Shiro, M.; Hashimoto, S. *J. Org. Chem.* **2010**, *75*, 6039.
- (46) Suga, H.; Hashimoto, Y.; Yasumura, S.; Takezawa, R.; Itoh, K.; Kakehi, A. *J. Org. Chem.* **2013**, *78*, 10840.
- (47) Anada, M.; Kitagaki, S.; Hashimoto, S., *Heterocycles* **2000**, *52*, 875.
- (48) Krishnamurthi, J.; Nambu, H.; Takeda, K.; Anada, M.; Yamanob, A.; Hashimoto, S. *Org. Biomol. Chem.* **2013**, *11*, 5374.
- (49) Anada, M.; Tanaka, M.; Washio, T.; Yamawaki, M.; Abe, T.; Hashimoto, S. *Org. Lett.* **2007**, *9*, 4559.
- (50) Shimada, N.; Anada, M.; Nakamura, S.; Nambu, H.; Tsutsui, H.; Hashimoto, S. *Org. Lett.* **2008**, *10*, 3603.

- (51) Shimada, N.; Oohara, T.; Krishnamurthi, J.; Nambu, H.; Hashimoto, S.
Org. Lett. **2011**, *13*, 6284.
- (52) Shimada, N.; Hanari, T.; Kurosaki, Y.; Anada, M.; Nambu, H.;
Hashimoto, S. *Tetrahedron Lett.* **2010**, *51*, 6572.
- (53) Tanaka, M.; Kurosaki, Y.; Washio, T.; Anada, M.; Hashimoto, S.
Tetrahedron Lett. **2007**, *48*, 8799.
- (54) Minami, K.; Saito, H.; Tsutsui, H.; Nambu, H.; Anada, M.;
Hashimoto, S. *Adv. Synth. Catal.* **2005**, *347*, 1483.
- (55) Tsutsui, H.; Yamaguchi, Y.; Kitagaki, S.; Nakamura, S.; Anada, M.;
Hashimoto, S. *Tetrahedron: Asymmetry* **2003**, *14*, 817.
- (56) Saito, H.; Oishi, H.; Kitagaki, S.; Nakamura, S.; Anada, M.;
Hashimoto, S. *Org. Lett.* **2002**, *4*, 3887.
- (57) Tsutsui, H.; Shimada, N.; Abe, T.; Anada, M.; Nakajima, M.;
Nakamura, S.; Nambu, H.; Hashimoto, S. *Adv. Synth. Catal.* **2007**, *349*, 521.
- (58) Anada, M.; Tanaka, M.; Washio, T.; Yamawaki, M.; Abe, T.;
Hashimoto, S. *Org. Lett.* **2007**, *9*, 4559.
- (59) Yamawaki, M.; Tsutsui, H.; Kitagaki, S.; Anada, M.; Hashimoto, S.
Tetrahedron Lett. **2002**, *43*, 9561.
- (60) Kitagaki, S.; Yanamoto, Y.; Tsutsui, H.; Anada, M.; Nakajima, M.;
Hashimoto, S. *Tetrahedron Lett.* **2001**, *42*, 6361.
- (61) DeAngelis, A.; Dmitrenko, O.; Yap, G. P. A.; Fox, J. M. *J. Am. Chem.
Soc.* **2009**, *131*, 7230.

- (62) Boruta, D. T.; Dmitrenko, O.; Yap, G. P. A.; Foxa, J. M. *Chem. Sci.* **2013**, *3*, 1589.
- (63) Lindsay, V. N.; Lin, W.; Charette, A. B. *J. Am. Chem. Soc.* **2009**, *131*, 16383.
- (64) Lindsay, V. N.; Nicolas, C.; Charette, A. B. *J. Am. Chem. Soc.* **2011**, *133*, 8972.
- (65) Ghanem, A.; Gardiner, M. G.; Williamson, R. M.; Muller, P. *Chem.–Eur. J.*, **2010**, *16*, 3291.
- (66) DeAngelis, A.; Shurtleff, V. W.; Dmitrenko, O.; Fox, J. M. *J. Am. Chem. Soc.* **2011**, *133*, 1650.
- (67) Curtius, T. *Ber. Dtsch. Chem. Ges.* **1883**, *16*, 2230.
- (68) Regitz, M. *Angew. Chem., Int. Ed.* **1967**, *6*, 733.
- (69) Qian, Y.; Xu, X.; Wang, X.; Zavalij, P. J.; Hu, W.; Doyle, M. P. *Angew. Chem., Int. Ed.* **2012**, *51*, 5900.
- (70) Xu, X.; Zavalij, P. Y.; Doyle, M. P. *Angew. Chem., Int. Ed.* **2012**, *51*, 9829.
- (71) Xu, X.; Zavalij, P. Y.; Doyle, M. P. *Angew. Chem., Int. Ed.* **2013**, *52*, 12664.
- (72) Xu, X.; Leszczynski, J. S.; Mason, S. M.; Zavalij, P. Y.; Doyle, M. P. *Chem. Comm.* **2014**, *50*, 2462.
- (73) Xu, X.; Zavalij, P. J.; Doyle, M. P. *Chem. Comm.* **2013**, *49*, 10287.
- (74) Xu, X.; Zavalij, P. Y.; Doyle, M. P. *J. Am. Chem. Soc.* **2013**, *135*, 12439.

- (75) Davies, H. M. L.; Houser, J. H.; Thornley, C. *J. Org. Chem.* **1995**, *60*, 7529.
- (76) Truong, P. M.; Mandler, M. D.; Zavalij, P. Y.; Doyle, M. P. *Org. Lett.* **2013**, *15*, 3278.
- (77) Miege, F.; Meyer, C.; Cossy, J. *Beilstein J. Org. Chem.* **2011**, *7*, 717.
- (78) Archambeau, A.; Miege, F.; Meyer, C.; Cossy, J. *Angew. Chem., Int. Ed.* **2012**, *51*, 11540.
- (79) Wang, X.; Xu, X.; Zavalij, P. Y.; Doyle, M. P. *J. Am. Chem. Soc.* **2011**, *133*, 16402.
- (80) Linn, W. J.; Webster, O. W.; Benson, R. E. *J. Am. Chem. Soc.* **1965**, 3651.
- (81) Basktter, N.; Plunket, A. O. *Chem. Comm.* **1971**, 1578.
- (82) Padwa, A.; Beall, L. S.; Heidelbaugh, T. M.; Liu, B.; Sheehan, S. M. *J. Org. Chem.* **2000**, *65*, 2684.
- (83) Stearman, C. J.; Wilson, M.; Padwa, A. *J. Org. Chem.* **2009**, *74*, 3491.
- (84) Atsumoto, K.; Ono, Y. *Chem. Comm.* **1976**, 1045.
- (85) Zhu, C.; Yoshimura, A.; Ji, L.; Wei, Y.; Nemykin, V. N.; Zhdankin, V. *Org. Lett.* **2012**, *14*, 3170.
- (86) Kostik, E. I.; Abiko, A.; Oku, A. *J. Org. Chem.* **2001**, *66*, 1638.
- (87) Civjan, N.; O'Connor, S. E. *Alkaloids Natural Products in Chemical Biology*; John Wiley & Sons, Inc., Hoboken, NJ **2012**.
- (88) Scott, J. D.; Williams, R. M. *Chem. Rev.* **2002**, *102*, 1669.
- (89) Bentley, K. W. *Nat. Prod. Rep.* **2005**, *22*, 249.

- (90) Bentley, K. W. *Nat. Prod. Rep.* **2006**, *23*, 444.
- (91) Michael, J. P. *Nat. Prod. Rep.* **2008**, *25*, 139.
- (92) Chrzanowska, M.; Rozwadowska, M. D. *Chem. Rev.* **2004**, *104*, 3341.
- (93) Stöckigt, J.; Antonchick, A. P.; Wu, F.; Waldmann, H. *Angew. Chem., Int. Ed.* **2011**, *50*, 8538.
- (94) Perreault, S.; Rovis, T. *Chem. Soc. Rev* **2009**, *38*, 3149.
- (95) Itoh, T.; Yokoya, M.; Miyauchi, K.; Nagata, K.; Ohsawa, A. *Org. Lett.* **2006**, *8*, 1533.
- (96) Lalonde, M. P.; McGowan, M. A.; Rajapaksa, N. S.; Jacobsen, E. N. *J. Am. Chem. Soc.* **2013**, *135*, 1891.
- (97) Frisch, K.; Landa, A.; Saaby, S.; Jørgensen, K. A. *Angew. Chem., Int. Ed.* **2005**, *44*, 6058.
- (98) Takamura, M.; Funabashi, K.; Kanai, M.; Shibasaki, M. *J. Am. Chem. Soc.* **2000**, *122*, 6327.
- (99) Takamura, M.; Funabashi, K.; Kanai, M.; Shibasaki, M. *J. Am. Chem. Soc.* **2001**, *123*, 6801.
- (100) Funabashi, K.; Ratni, H.; Kanai, M.; Shibasaki, M. *J. Am. Chem. Soc.* **2001**, *123*, 10784.
- (101) Ichikawa, E.; Suzuki, M.; Yabu, K.; Albert, M.; Kanai, M.; Shibasaki, M. *J. Am. Chem. Soc.* **2004**, *126*, 11808.
- (102) Taylor, M. S.; Tokunaga, N.; Jacobsen, E. N. *Angew. Chem., Int. Ed.* **2005**, *44*, 6700.
- (103) Sun, Z.; Yu, S.; Ding, Z.; Ma, D. *J. Am. Chem. Soc.* **2007**, *129*, 9300.

- (104) Yamaoka, Y.; Miyabe, H.; Takemoto, Y. *J. Am. Chem. Soc.* **2007**, *129*, 6686.
- (105) Bandini, M.; Melloni, A.; Umani-Ronchi *Angew. Chem., Int. Ed.* **2004**, *43*, 550.
- (106) Taylor, M. S.; Jacobsen, E. N. *J. Am. Chem. Soc.* **2004**, *126*, 10558.
- (107) Uraguchi, D.; Sorimachi, K.; Terada, M. *J. Am. Chem. Soc.* **2004**, *126*, 11804.
- (108) Evans, D. A.; Fandrick, K. R.; Song, H. *J. Am. Chem. Soc.* **2005**, *127*, 8942.
- (109) Wang, D.; Chen, Q.; Lu, S.; Zhou, Y. *Chem. Rev.* **2012**, *112*, 2557.
- (110) Panne, P.; Fox, J. M. *J. Am. Chem. Soc.* **2007**, *129*, 22.
- (111) Zhu, C.; Yoshimura, A.; Ji, L.; Wei, Y.; Nemykin, V. N.; Zhdankin, V. *V. Org. Lett.* **2012**, *14*, 3170.
- (112) Fernández, N.; Carrillo, L.; Vicario, J. D.; Badía, D.; Reyes, E. *Chem. Comm.* **2011**, *47*, 12313.
- (113) Enders, D.; Shilvock, J. P. *Chem. Soc. Rev* **2000**, *29*, 359.
- (114) Wang, J.; Liu, X.; Feng, X. *Chem. Rev.* **2011**, *111*, 6947.
- (115) Xu, X.; Shabashov, D.; Zavalij, P. Y.; Doyle, M. P. *J. Org. Chem.* **2012**, *77*, 5313.
- (116) Xu, X.; Shabashov, D.; Zavalij, P. Y.; Doyle, M. P. *Org. Lett.* **2012**, *14*, 800.
- (117) Watanabe, N.; Anada, M.; Hashimoto, S.; Ikegami, S. *Synlett* **1994**, 1031.

- (118) Anada, M.; Hashimoto, S. *Tetrahedron Lett.* **1998**, *39*, 79.
- (119) Doyle, M. P.; Liu, Y.; Ratnikov, M. *Org. React.* **2013**, *80*, 1.
- (120) Barluenga, J.; Lonzi, G.; Riesgo, L.; López, L. A.; Tomás, M. *J. Am. Chem. Soc.* **2010**, *132*, 13200.
- (121) Kanemasa, S.; Takenaka, S.; Watanabe, H.; Tsuge, O. *J. Org. Chem.* **1989**, *54*, 420.
- (122) Ruano, J. L. G.; Fraile, A.; Martín, M. R.; González, G.; Fajardo, C.; Martín-Castro, A. M. *J. Org. Chem.* **2011**, *76*, 3296.
- (123) Wu, L.; Sun, J.; Yan, C. *Org. Biomol. Chem.* **2012**, *10*, 9452.
- (124) Liu, Y.; Zhang, Y.; Shen, Y.; Hu, H.; Xu, J. *Org. Biomol. Chem.* **2010**, *8*, 2449.
- (125) Katritzky, A. R.; Qiu, G.; Yang, B.; He, H. *J. Org. Chem.* **1999**, *64*, 7618.
- (126) Davies, H. M. L.; Stafford, D. G.; Doan, B. D.; Houser, J. H. *J. Am. Chem. Soc.* **1998**, *120*, 3326.
- (127) Xu, X.; Doyle, M. P. *Inorg. Chem.* **2011**, *50*, 7610.
- (128) Drago, R. S.; Long, J. R.; Cosmano, R. *Inorg. Chem.* **1981**, *20*, 2920.
- (129) Drago, R. S. *Inorg. Chem.* **1982**, *21*, 1697.
- (130) Drago, R. S.; Long, J. R.; Cosmano, R. *Inorg. Chem.* **1982**, *21*, 2196.
- (131) Chifotides, H. T.; Dunbar, K. R. *In Multiple Bonds Between Metal Atoms*, 3rd ed.; Cotton, F. A., Murillo, C. A., Walton, R. A., Eds.; Springer: New York, 2005; Chapter 12.
- (132) Doyle, M. P.; Ren, T. *Prog. Inorg. Chem.* **2001**, *49*, 113.

- (133) Trindade, A. F.; Coelho, J. A. S.; Afonso, C. A. M.; Veiros, L. F.; Gois, P. M. P. *ACS Catal.* **2012**, *2*, 370.
- (134) Pirrung, M. C.; Liu, H.; Morehead, A. T., Jr. *J. Am. Chem. Soc.* **2002**, *124*, 1014.
- (135) Wynne, D. C.; Olmstead, M. M.; Jessop, P. G. *J. Am. Chem. Soc.* **2000**, *122*, 7638.
- (136) Galan, B. R.; Gembicky, M.; Dominiak, P. M.; Keister, J. B.; Diver, S. T. *J. Am. Chem. Soc.* **2005**, *127*, 15702.
- (137) López, L. A.; Barrio, P.; Borge, J. *Organometal.* **2012**, *31*, 7844.
- (138) Baquero, E. A.; Silbestri, G. F.; Gómez-Sal, P.; Flores, J. C.; De Jesús, E. *Organometal.* **2013**, *32*, 2814.
- (139) Snyder, J. P.; Padwa, A.; Stengel, T.; Arduengo, A. J., III; Jockisch, A.; Kim, H. *J. Am. Chem. Soc.* **2001**, *123*, 11318.
- (140) Trindade, A. F.; Gois, P. M. P.; Veiros, L. F.; André, V.; Duarte, M. T.; Afonso, C. A. M.; Caddick, S.; Cloke, F. G. N. *J. Org. Chem.* **2008**, *73*, 4076.
- (141) Rubin, M.; Rubina, M.; Gevorgyan, V. *Chem. Rev.* **2007**, *107*, 3117.
- (142) Marek, I.; Simaan, S.; Masarwa, A. *Angew. Chem., Int. Ed.* **2007**, *46*, 7364.
- (143) Zhu, Z.; Wei, Y.; Shi, M. *Chem. Soc. Rev.* **2011**, *40*, 5534.
- (144) Müller, P.; Bernardinelli, G. R.; Allenbach, Y. F.; Ferri, M.; Flack, H. D. *Org. Lett.* **2004**, *6*, 1725.
- (145) Müller, P.; Fruit, C. *Chem. Rev.* **2003**, *103*, 2905.

Chapter 2: Catalytic [3+2]-Cycloaddition of Silyated Ketene

Imine with Enol Diazoacetate

I. Introduction

1.1 General Information for Ketene Imines

Ketene imines are highly reactive species that belong to a subclass of cumulenes, which hold at least two cumulative double bonds within the molecules, and they are very useful synthetic intermediates.¹⁻³ Due to their reactive nature, only a few synthetic methods are known to afford ketene imines and this shortage of methodologies for the formation of ketene imines has limited their uses in synthetic chemistry and chemical catalysis.⁴⁻⁹ However, during the last two decades, several highly reliable and practical synthetic approaches toward the synthesis¹⁰⁻¹³ or in situ generation of ketene imines^{13,14} have been developed, thereby enabling comprehensive studies on their chemical and physical properties as well as the use of ketene imine in synthesizing organic compounds in a concise and efficient way.^{8,9,15,16}

Ketene imines are structurally similar to allenes and ketenes. The dihedral angles between the $C=CR^1R^2$ and $C=N-R^3$ planes are close to 90° with $C=N-R^3$ angles proximating 120° (**Figure 2.1**).^{17,18} Although ketene imines are active intermediates and most often generated in situ, heteroatoms including silicon, phosphorous, and sulfur at the *N*-terminus, and conjugated functional groups, for instance, vinyl, aryl, and carbonyl, at the *C*-terminus, can provide sufficient stabilization to afford isolable,

even storable ketene imines.^{15,16} Ketene imines can undergo nucleophilic additions, radical additions, cycloaddition reactions, and rearrangements.^{8,9}

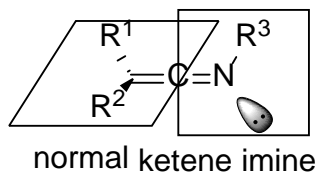
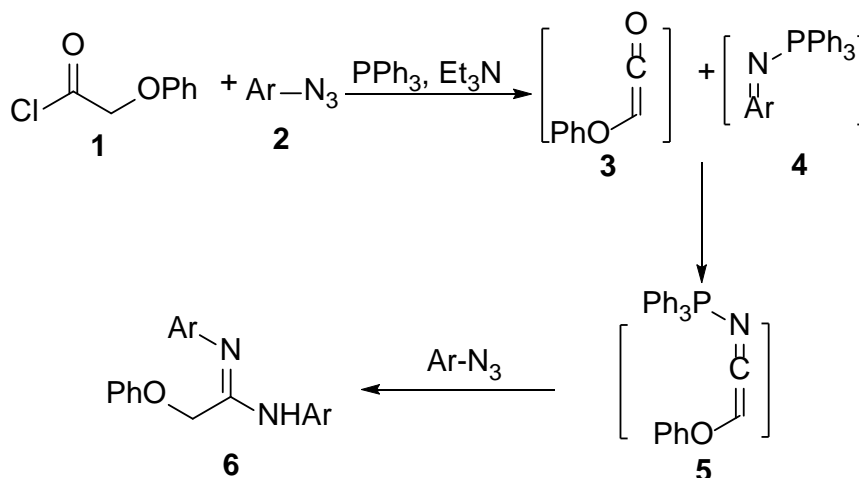


Figure 2.1 Structures for Ketene Imines.

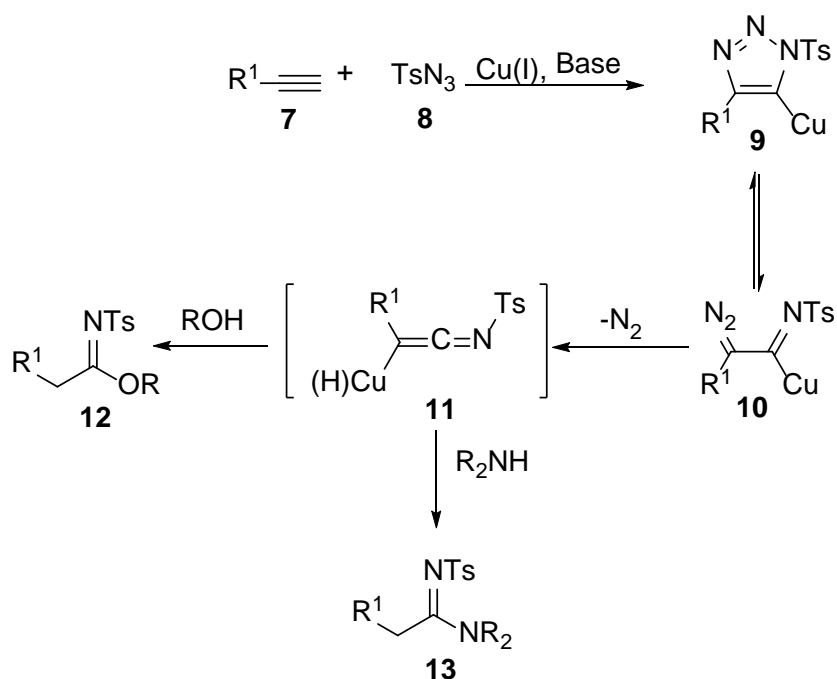
1.2 Representative Examples for the Preparation of Ketene Imine and Their Chemical Properties

The Wittig reaction is a high efficient means for the conversion of carbonyl groups into C=C or C=N bonds, and it has been used in the synthesis of ketene imines from ketenes.^{10,11} For instance, the condensation between the ketenes **3** and aza-Wittig reagents **4** generates highly reactive ketene imines **5** that react further with aryl azides **2** to afford amidines **6** (**Scheme 2.1**).¹⁰



Scheme 2.1 Ketene Imine Formation via Aza-Wittig Reaction.

Catalytic generation of ketene imines can be achieved between sulfonyl azides and terminal alkynes under Cu(I) catalysis (**Scheme 2.2**).¹³ Cu(I)-catalyzed azide/alkyne cycloaddition reaction reliably produces the 1-sulfonyl 1,2,3-triazole **9**, which is in equilibrium with the α -diazo imine **10**. Catalytic dinitrogen extrusion and the following hetero-Wolff rearrangement yield *N*-sulfonyl ketene imines **11**. Further trapping of the catalytically generated ketene imine species **11** by amines or alcohols provides functionalized amidines **12** and imidates **13** in good reaction yields.

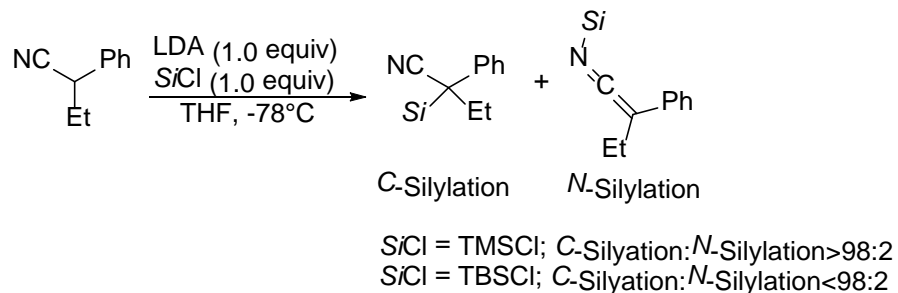


Scheme 2.2 Ketene Imine Generation via Hetero-Wolff Rearrangement of 1-Sulfonyl 1,2,3-Triazole.

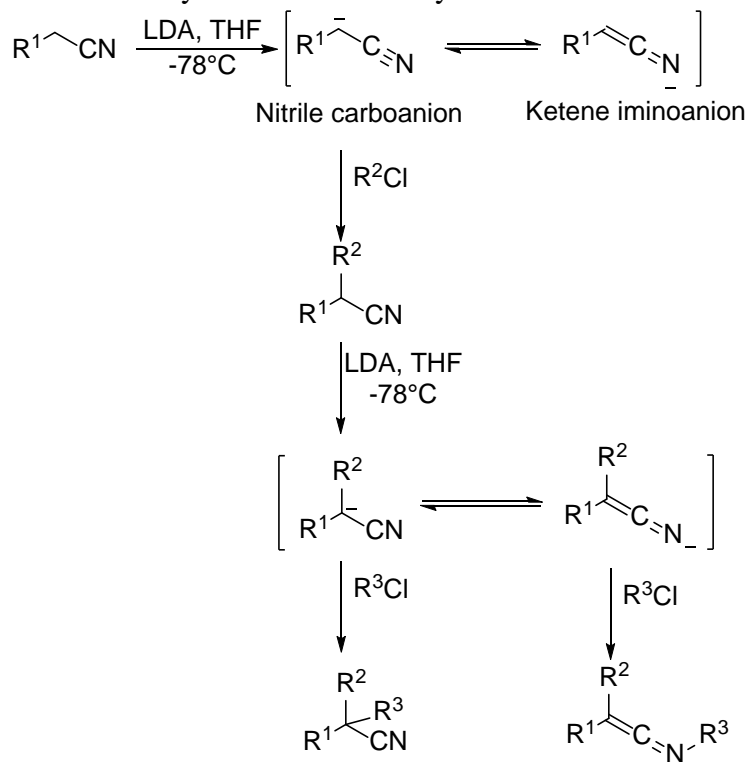
1.3 General Information and the Synthesis of Silylated Ketene Imines

Ambident anions can be produced by deprotonating nitriles.¹⁹⁻²¹ They react with electrophiles at either the *C*- or *N*-terminus (**Scheme 2.3**).^{22,23} The selective alkylation of nitrile carboanions at the *C*-terminus with alkyl halides has been used extensively for the synthesis of substituted nitriles,^{24,25} the further deprotonation of substituted

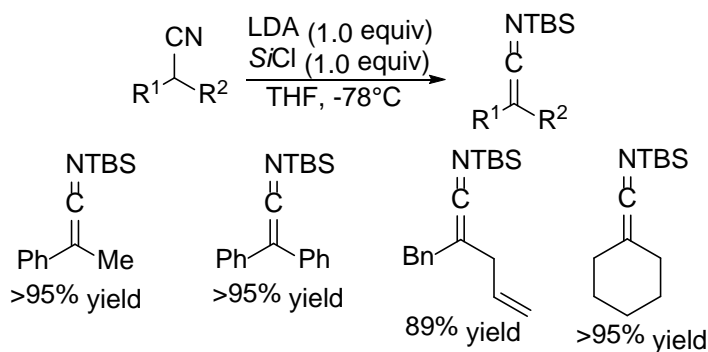
nitriles, and the subsequent selective *N*-silylation of the resulting substituted ketene iminoanion with electrophilic silylating reagents (TBSCl and others), produces silylated ketene imines (SKIs) (**Scheme 2.4**).^{24,25} This strategy has been the most used method to access to disubstituted SKIs from simple nitriles (**Scheme 2.5**).



Scheme 2.3 Selective *C*-Silylation versus *N*-Silylation.



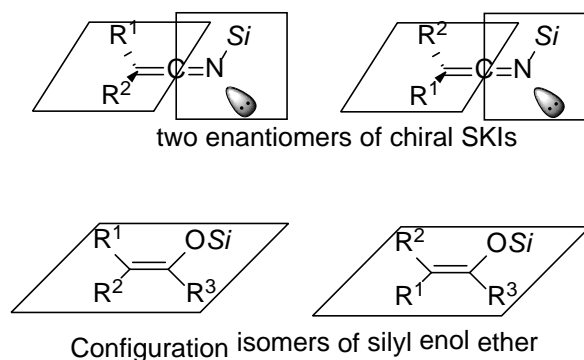
Scheme 2.4 Synthesis of Silylated Ketene Imine from Simple Nitriles.



Scheme 2.5 Preparation of TBS-substituted SKIs.

SKIs are nucleophiles that closely resemble silyl enol ethers,²⁶⁻²⁸ which are synthesized by the selective *O*-silylation of enolates. Silyl enol ethers can be viewed as enolate analogues;²⁹⁻³¹ SKIs can be similarly treated as the equivalents of α -cyanocarboanions.^{19-21,32} Moreover, the preparations of SKIs and silyl enol ethers are uniform as well, with both invoking deprotonation and subsequent silylation.

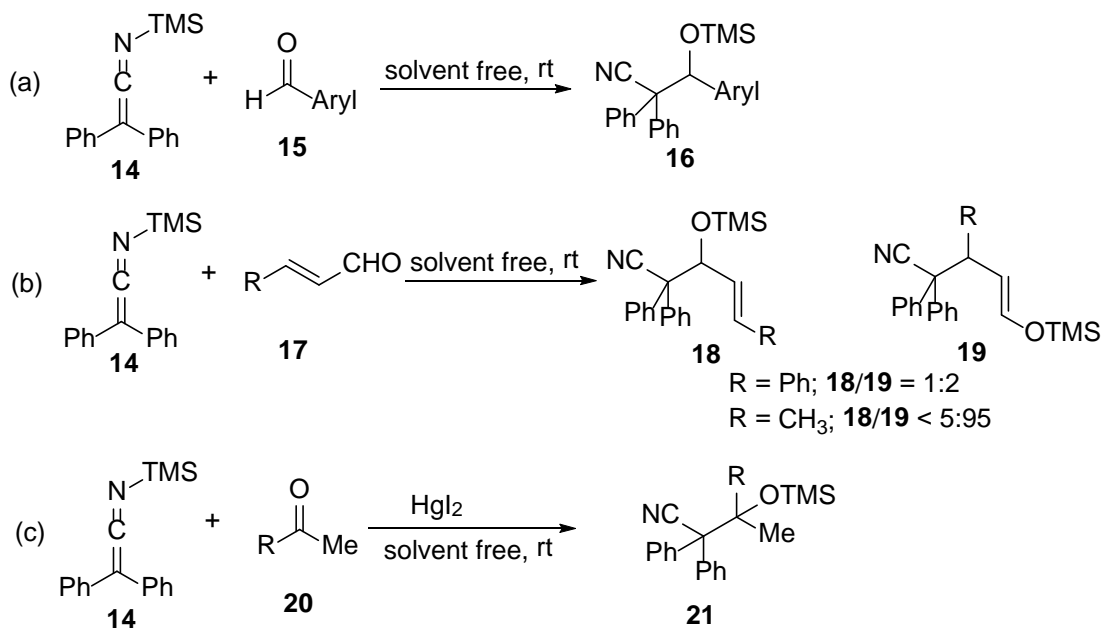
SKIs and silyl enol ethers are structurally different in spite of many shared features. One immediate unique characteristic of SKIs, unlike intrinsically achiral silyl enol ethers, is the axial chirality imparted by the pair of orthogonal substituent planes when R^1 is not equal to R^2 (**Scheme 2.6**).^{19,20}



Scheme 2.6 Structural Features for SKIs and Silyl Enol Ethers.

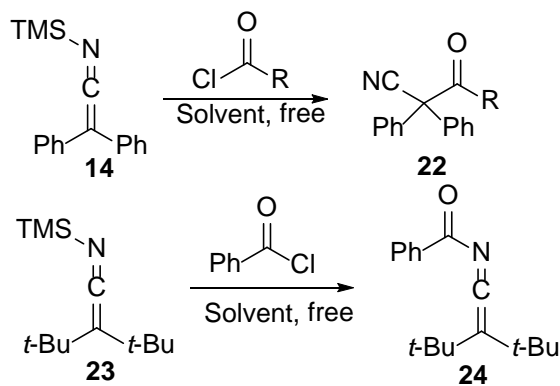
1.4 Reactions Involving Nucleophilic SKIs

Nucleophilic addition of SKIs to aldehydes is reported by Frainnet and co-workers.³⁷ In the absence of a catalyst, mixing *N*-(trimethylsilyl)diphenylketene imine **14** and benzaldehyde in their pure forms results in the generation of β -silyloxy nitrile **16** in quantitative yield (**Scheme 2.7**). As expected, electron-poor aromatic aldehydes also engaged in the addition reaction; however, the use of benzaldehyde having strong electron-donating substituents is not reported. Nevertheless, α,β -unsaturated aldehydes could also undergo the reaction with diphenyl ketene imine **14**, and selectivity in 1,2- to 1,4-addition appeared to be substrate-dependent.³⁷ While a 1:2 ratio of 1,2- to 1,4-addition products (**18** and **19**, respectively) was observed for cinnamaldehyde, the use of crotonaldehyde only afforded the 1,4-addition product **19** (**Scheme 2.7b**). The less electrophilic ketones could also be used as the electrophilic counterparts only when an activator was present.³⁷ For instance, the reaction of diphenyl ketene imine **14** with various ketones proceeded under catalysis of an equal molar amount of HgI₂ with significant enolization of ketones (**Scheme 2.7c**). Although, the reaction with ketones generated two vicinal quaternary carbons, the lack of efficiency and the enolization of the ketone under the reaction condition impaired the generality and synthetic uses of this process.



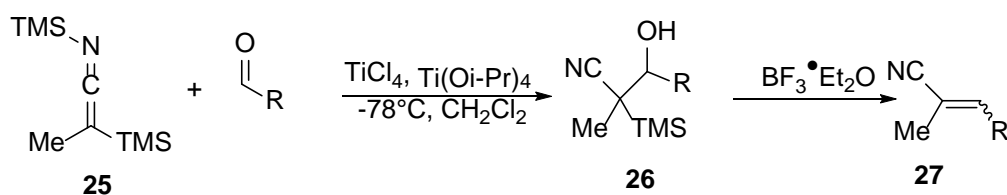
Scheme 2.7 Nucleophilic Addition of SKIs to Aldehydes and Ketones.

The acylation reaction of SKIs with acid chlorides has also been studied (**Scheme 2.8**).³⁸ Unlike the reaction with ketones, the highly electrophilic acid chlorides condense with SKIs smoothly at room temperature in the absence of a catalyst. The steric factors associated with the substituents attached to the terminal carbon influence the reaction outcome. For example, diphenyl ketene imines **14** reacts with acid chlorides to afford the β -nitrile ketones **22**, and the very bulky di-*tert*-butyl keteneimine **23** under the same condition only generates the *N*-benzoyl keteneimines **24**.



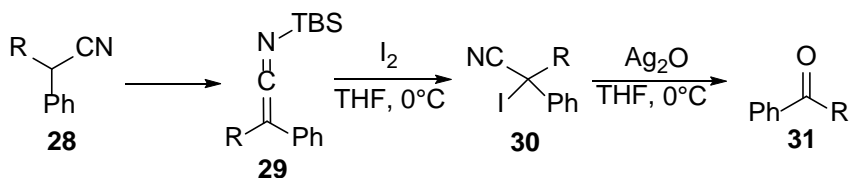
Scheme 2.8 Reactions of SKIs with Acid Chlorides.

Matsuda and co-workers have reported an interesting method for the preparation of vinyl nitriles by employing the SKI/aldehyde addition and the Lewis acid-catalyzed Peterson-type elimination (**Scheme 2.9**).³⁹ α -Silyl substituted SKI **34** reacts with an alkyl or aromatic aldehyde under catalysis by a mixture of TiCl_4 and $\text{Ti}(\text{O}i\text{-Pr})_4$ to provide the β -silyl alcohols **35** after aqueous workup. The β -silyl alcohols **35**, upon loss of TMSOH , rearranges to the vinyl nitriles **36** in good yields and moderate to excellent *E/Z* ratios in the presence of highly Lewis acidic BF_3 -etherate (**Scheme 2.9**).⁴⁰⁻⁴²



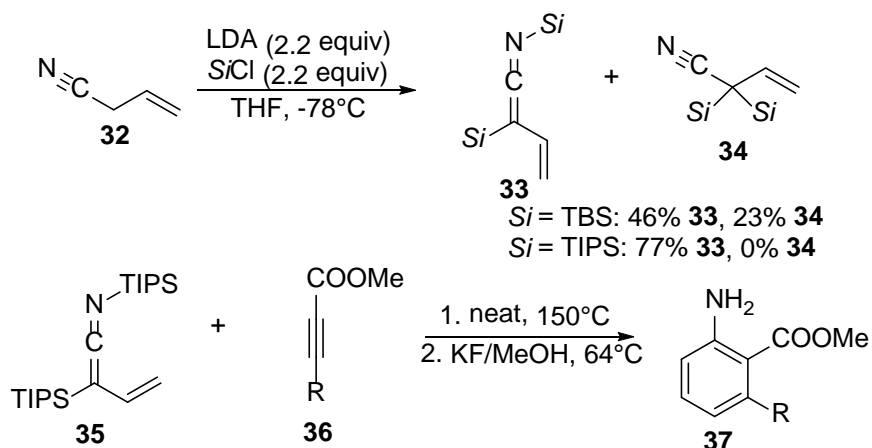
Scheme 2.9 Syntheses of Vinyl Nitriles from SKIs.

The conversion of a nitrile to a ketone can be achieved via a SKI intermediate (**Scheme 2.10**).⁴³ The SKIs **29** derived from the parent nitriles **28** react with iodine in the absence of a catalyst and result in the generation of β -iodonitriles **30**, which can subsequently be converted to ketones **31** upon treatment of Ag_2O .



Scheme 2.10 Conversion of Nitriles to Ketones through SKI Intermediates.

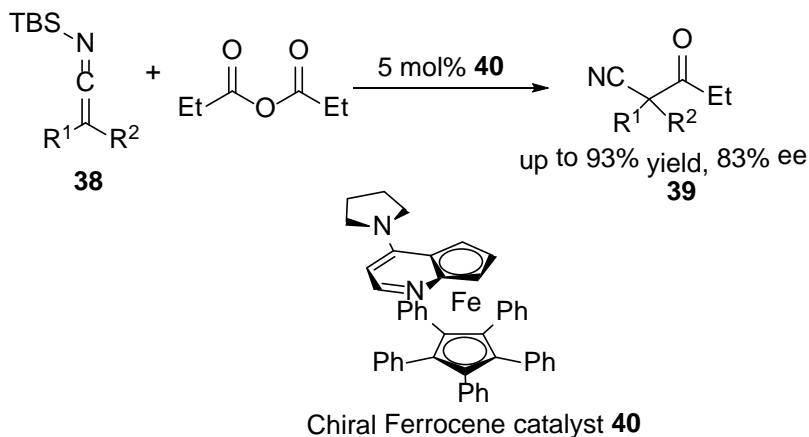
Vinyl nitrile **32**, when treated with 2.2 equivalents of a strong base (LDA) and sterically encumbered TIPSCI at a low temperature affords exclusively the *N*-TIPS vinyl SKI **33**, which reacts as a diene at high temperature with electron-deficient propargylic ester **36** to afford arenes **37** after fluorodesilylation reaction (**Scheme 2.11**).⁴⁴



Scheme 2.11 Cycloaddition Reaction of Vinyl SKIs with Propargylic Esters.

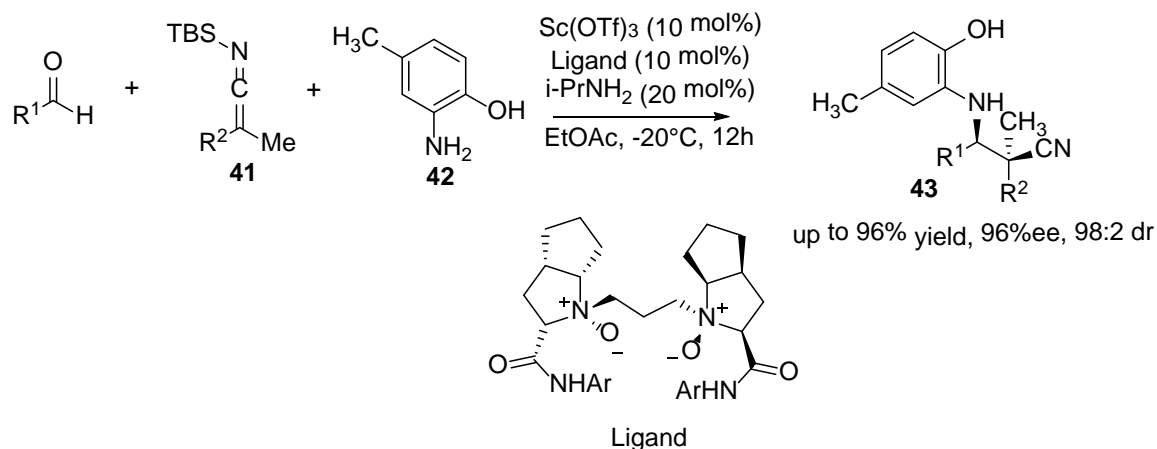
Although SKIs have been demonstrated to be highly potent nucleophiles in several studies, the first catalytic asymmetric reaction involving SKIs has surfaced recently. Fu and Mermerian have studied the acylation reaction of SKIs with acid anhydrides under catalysis of chiral pyridines (**Scheme 2.12**).⁴⁵⁻⁴⁷ The Lewis basic pyridine catalyst **40** could only deliver good yields and moderate to good enantioselectivities with aryl substituted SKIs **38** and propionic anhydride. The dialkyl-

substituted nucleophiles display no reactivity under the optimal conditions. Although electrophilic reagents such as cyanoformates and chloroformates exhibit good reactivities, the enantioselective outcomes for these reactions are much less satisfactory.



Scheme 2.12 A Planar Chiral Pyridine Complex Catalyzes Asymmetric Addition of SKIs to Acid Anhydrides.

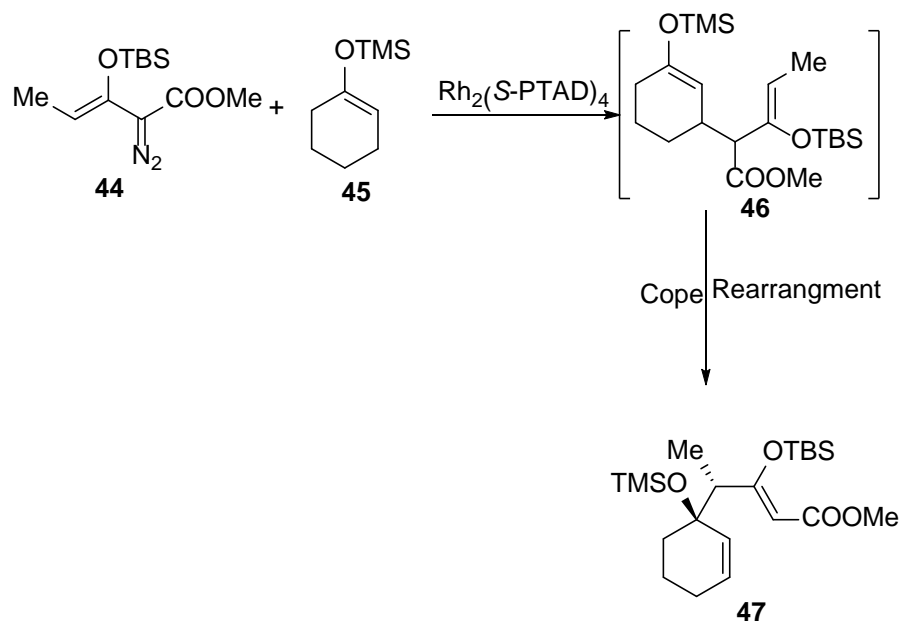
Very recently Feng and coworkers have reported an asymmetric Mannich-type reaction between in situ generated imines and TBS-substituted SKIs under chiral Lewis acid catalysis in excellent reaction yields, diastereoselectivity and enantioselectivity (**Scheme 2.13**).³² The base additive - *i*-PrNH₂ - is critical to achieving high enantio- and diastereocontrol. Its role in the reaction is believed to be deprotonation of the phenolic imine to give the corresponding imino phenolic oxide, which supposedly coordinates more tightly to the chiral Lewis acid catalyst than the phenolic imine. Although the enantioenriched products can be transformed into a variety of chiral molecules, deprotection of the *N*-protecting group requires a multistep derivatization of the optical active nitriles **43**.



Scheme 2.13 Chiral $\text{Sc}(\text{OTf})_3/\text{N}$ -Oxide Ligand Complex Promoted Asymmetric Mannich Addition of SKIs.

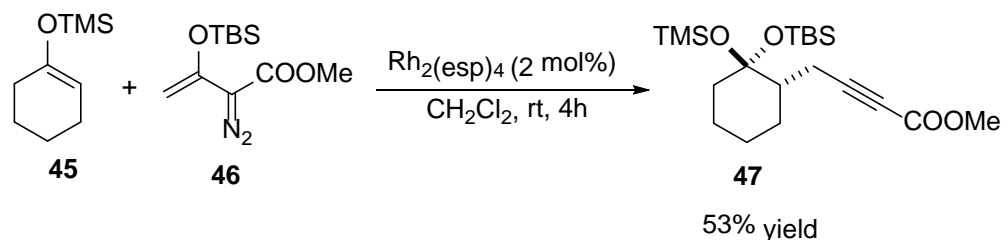
1.5 Reaction of Enol Diazoacetate with Silyl Enol Ether by Dirhodium Catalysis

Silyl enol ethers have previously been identified as alkene components in reactions with catalytically generated rhodium carbene intermediates.⁴⁸⁻⁵⁹ However, the diversities of this type of reaction are far beyond original anticipation. Davies and coworkers recognize that the nucleophilic silyl enol ether can be a highly effective counterpart in the allylic C-H insertion/Cope rearrangement reaction of methyl-substituted enol diazoacetate **44** (Scheme 2.14).⁴⁸⁻⁵¹ Interestingly, the corresponding cyclopropanation reaction⁶⁰ does not occur, which probably reflects the congested nature of the tri-substituted silyl enol ether. Under the catalysis by $\text{Rh}_2(\text{S-PTAD})_4$ exceptional levels of enantioselectivity and diastereoselectivity have been achieved along with good reaction yields.



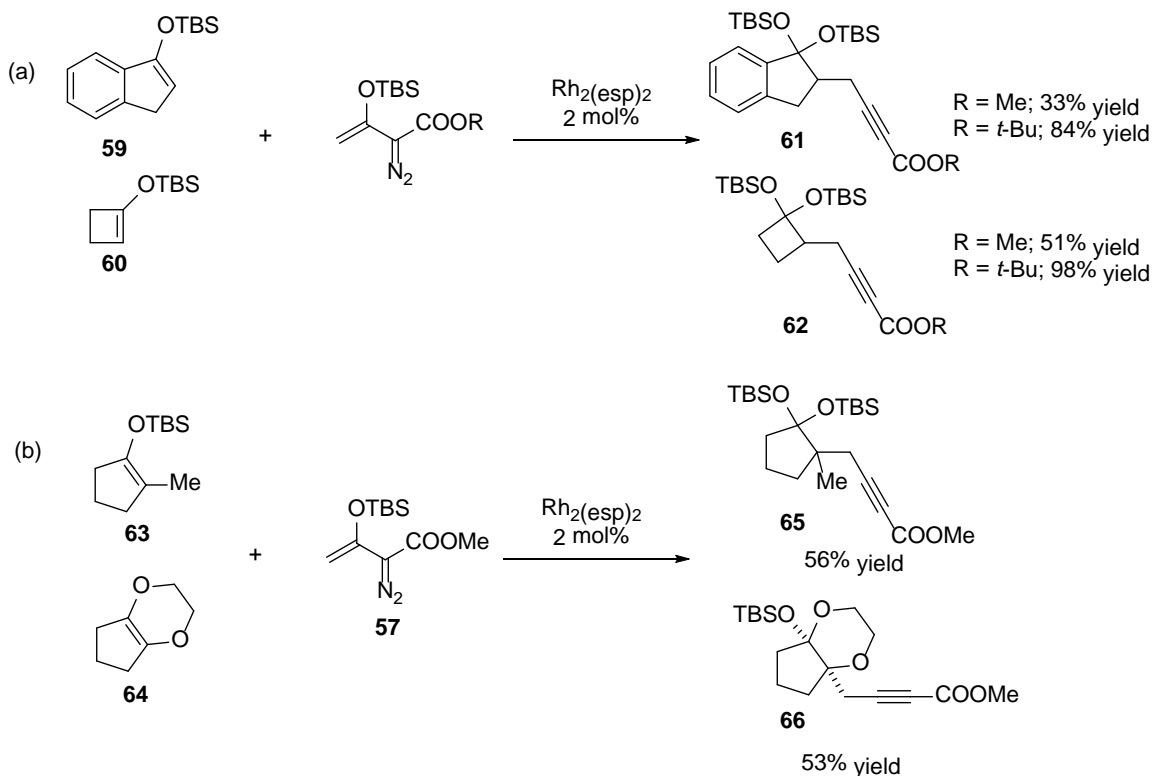
Scheme 2.14 Catalytic Enantioselective Allylic C-H insertion/Cope Rearrangement of Methyl-Substituted Enol Diazoacetate with Silyl Enol Ether.

Further studies of reactions with enol diazoacetate **46** surprisingly afford a completely different product that clearly comes from the selective vinylogous addition rather than carbene addition.⁶¹ Under catalysis by $\text{Rh}_2(\text{esp})_2$, the reaction of enol diazoacetate **46** with 1-(trimethylsiloxy)cyclohexene **45** produces alkynecarboxylate **47**, whose structure is unambiguously confirmed by X-ray analysis, in 53% yield and with complete diastereocontrol (**Scheme 2.15**).



Scheme 2.15 Alkynecarboxylate Formation through the Vinylogous Addition of Silyl Enol Ether over Carbene Addition to Unsubstituted Enol Diazoacetate.

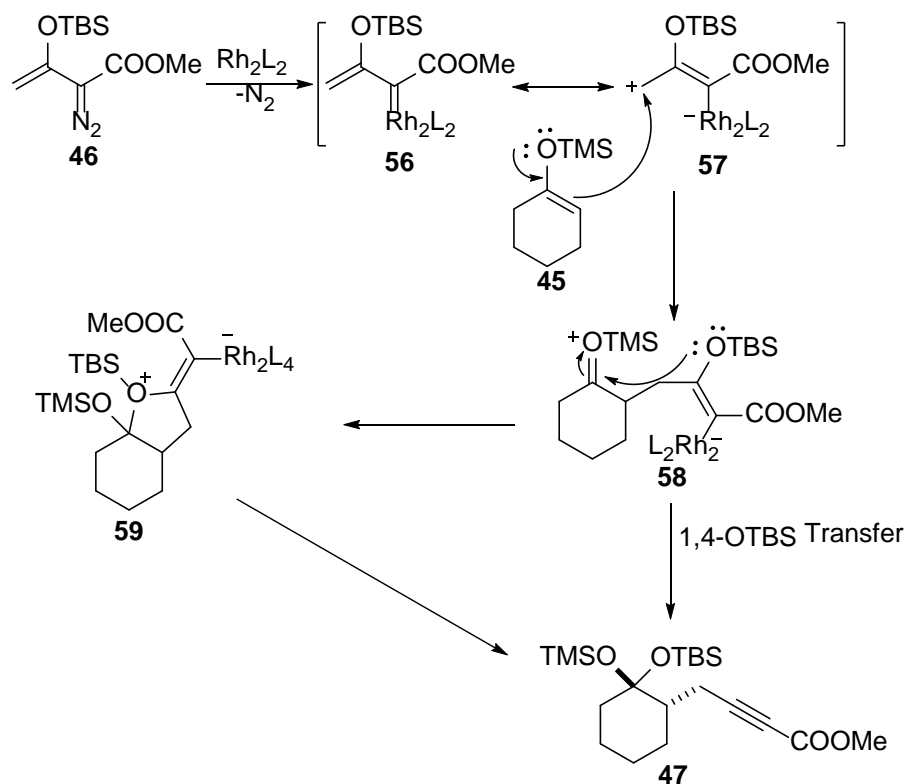
The reaction outcome evidently originates from the initial vinylogous addition of 1-(trimethylsiloxy)-cyclohexene to the rhodium enol carbene intermediate; however, subsequent stereoselective migration of OTBS group from the rhodium bound zwitterionic intermediate intermediate is exceptionally uncommon. The substrate scope study suggests that reaction yields are only moderate for most of the substrates tested, although consistently high diastereoselectivity could be achieved. The reaction for several substrates, for instance, siloxyindene **48** and siloxycyclobutene **49**, have shown clear competition from the carbene addition/Cope rearrangement and introducing the *tert*-butyl ester instead of a methyl ester dramatically enhances the selectivity toward alkynecarboxylate (**Scheme 2.16a**). Intriguingly, tetrasubstituted vinyl ethers such as **52** and **53** are also applicable to the reaction and the corresponding alkynoates generated containing two vicinal quaternary centers (**Scheme 2.16b**).



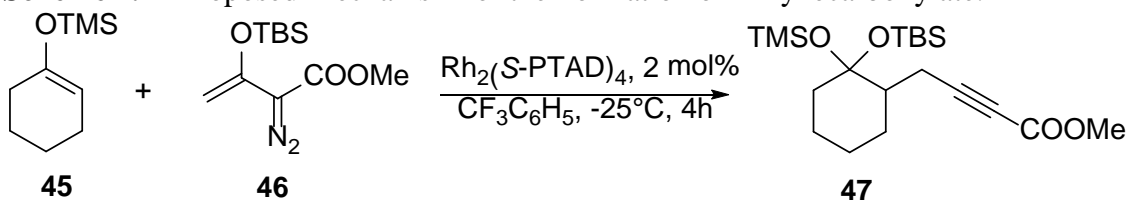
Scheme 2.16 (a) Enhanced Reactivity of *tert*-Butyl Enol Diazoacetate Compared to

Methyl Enol Diazoacetate. (b) Tetrasubstituted Silyl Enol Ethers are Viable Substrates for Alkynecarboxylate Formation.

A tentative mechanism proposed by Davies is shown in **Scheme 2.17**. The reaction outcome is in accordance with the rationale that the unsubstituted vinylogous position of the rhodium bound vinyl carbene **56** is crucial for the initial addition by the silyl enol ether **45**. The use of sterically demanding nucleophiles, essentially tri- and tetrasubstituted silyl enol ethers, enhances the vinylogous reactivity. Nucleophilic addition of the silyl enol ether **45** to rhodium bound 1,3-dipole equivalent **57** provides the zwitterionic intermediate **58**. Subsequent direct 1,4-siloxy group transfer with the concomitant release of dirhodium catalyst constitutes one possible reaction pathway. Alternatively, stepwise intramolecular addition of OTBS group to the oxocarbenium ion **58** via intermediate **59** followed by β -elimination yielded the same product (**47**). Rhodium-stabilized β -siloxyvinylcarbene has a strong tendency to adopt the *s-cis* conformation with the sterically encumbered siloxy group pointing away from the “wall” of the catalyst. This same conformation adopted by the rhodium bound enol carbene could facilitate β -elimination or migration of the OTBS group to afford the alkynoate product. In an attempt to develop the chiral variant for this transformation, only moderate levels of asymmetric induction by a chiral dirhodium carboxylate catalyst could be achieved (**Scheme 2.18**). Although with increasing ring size of the cyclic silyl enol ether higher enantioselectivity could be achieved, the highest ee obtained is still modest.



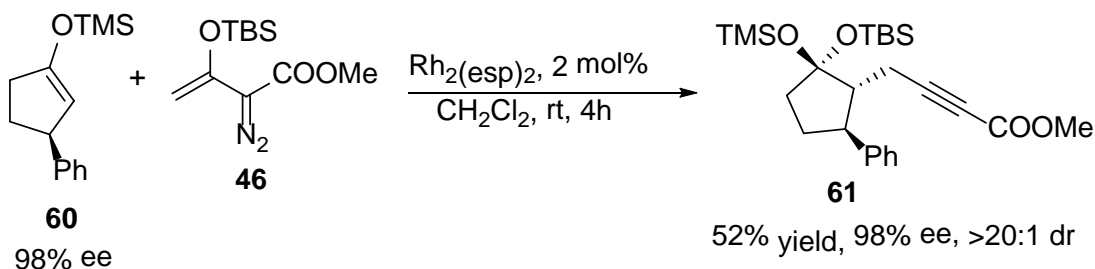
Scheme 2.17 Proposed Mechanism for the Formation of Alkynecarboxylate.



69% yield, 70% ee, >20:1 dr

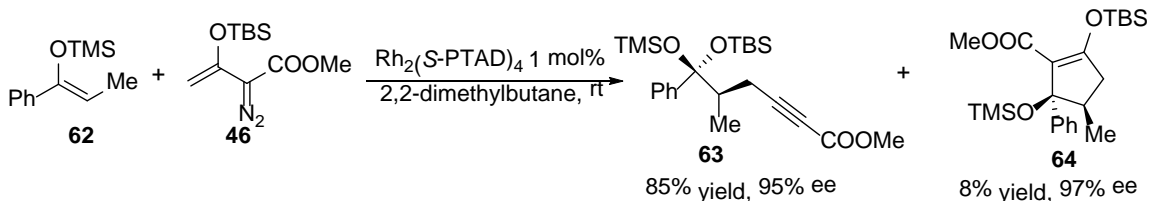
Scheme 2.18 Catalytic Asymmetric Synthesis of Alkynecarboxylate under The Catalysis by Rh₂(S-PTAD)₄.

In order to develop a highly enantioselective variant of this unusual transformation, the use of enantioenriched (*S*)-1-trimethylsilyloxy-3-phenylcyclopentene **71** (98% ee) as the silyl enol ether component results in the complete transfer of chirality to the alkyneate product with excellent diastereoselectivity (**Scheme 2.19**).



Scheme 2.19 Chirality Transfer from Optical Active Silyl Enol Ether to Alkynecarboxylate by Catalysis of $\text{Rh}_2(\text{esp})_2$.

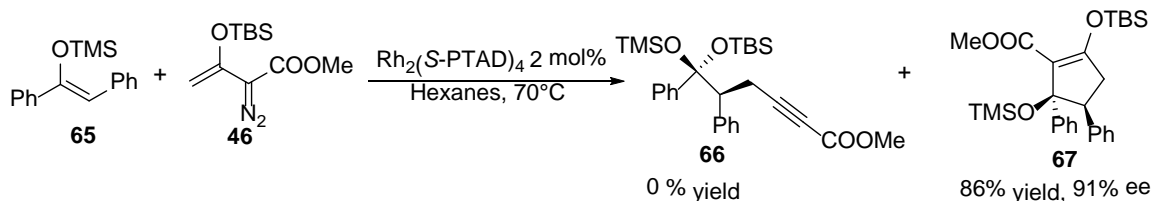
The use of stereodefined acyclic (*Z*)-silyl enol ethers **62** in the same reaction stated above delivers disiloxyketal alkynecarboxylate with the opposite diastereoselectivity in comparison to the cyclic system (**Scheme 2.20**).⁶² Strikingly, a small amount of highly substituted cyclopentene **64** is also isolated. More importantly, unlike the modest enantioselectivity obtained with cyclic silyl enol ethers, acyclic silyl enol ethers appear to offer better enantiocontrol, and up to 97% ee has been achieved when performing the reaction in 2,2-dimethylbutane with $\text{Rh}_2(\text{S-PTAD})_4$ used as the chiral catalyst. Notably, the high chemoselectivity toward the alkynecarboxylate was retained in the asymmetric reactions.



Scheme 2.20 Catalytic Enantioselective Synthesis of Alkynecarboxylate by Using Acyclic (*Z*)-Silyl Enol Ether.

The observation that performing the reaction at elevated temperatures is effective for promoting the formal [3+2]-cycloaddition reaction coupled with use of more sterically hindered silyl enol ethers leads to the disclosure of the optimal conditions for the enantioselective synthesis of highly substituted cyclopentenes

(Scheme 2.21). Although the authors attempt to rationalize the differential reaction outcome from the perspective of steric factors, no convincing evidence is provided to support such an understanding.



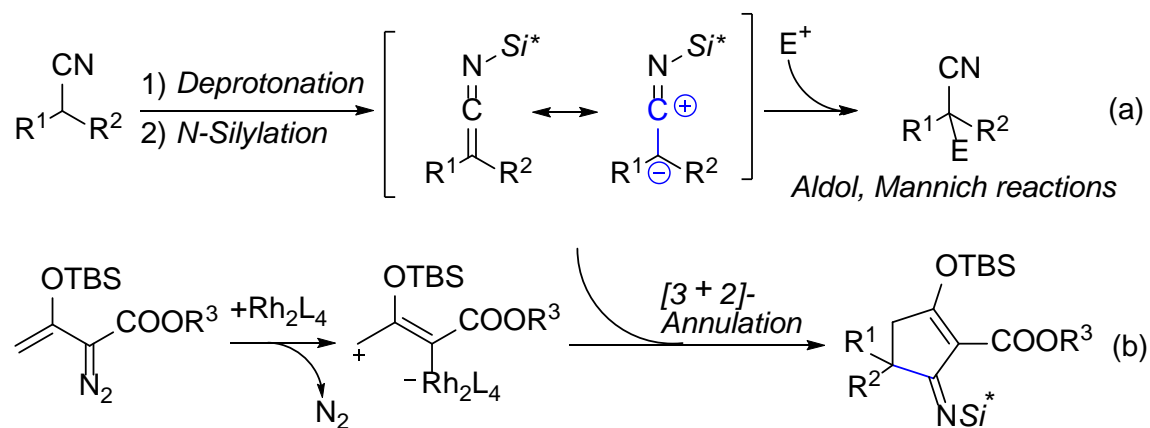
Scheme 2.21 Catalytic Enantioselective Formal [3+2]-Cycloaddition Between Acyclic (Z)-Silyl Enol Ether and Enol Diazoacetate.

1.6 Research Proposal

Cyclopentenones are ubiquitous structural frameworks of natural products and important pharmaceuticals.⁶³⁻⁶⁵ Both simple and highly functionalized cyclopentenones serve as building blocks for the construction of complex molecular architectures.⁶⁶ The Nazarov cyclization⁶⁷⁻⁷² and the Pauson-Khand reaction⁷²⁻⁷⁵ constitute powerful approaches for the synthesis of cyclopentenones. However, the need to use a stoichiometric amount of activator,⁶⁷⁻⁷⁵ the availability of starting materials⁶⁷⁻⁷⁰ and the often-harsh reaction conditions⁶⁷⁻⁷⁰ have limited the practicality of these methods. Recently, transition metal catalyzed annulation approaches to functionalized cyclopentenones have been reported,⁷⁶⁻⁸⁰ but the reported methods also have structural limitations; and none of them introduces an amino functional group into the product. Silylated ketene imines (SKIs),^{19,20} generated by the deprotonation and subsequent *N*-silylation of α -branched nitriles,^{22,24,25,43} are nucleophiles that can react with electrophilic counterparts to form a quaternary carbon center under Lewis acid³² or base^{23,45-47,81-85} catalysis (**Scheme 2.22a**); and, possibly due to the unique placement of a silyl group at the *N*-terminus, SKIs rarely undergo cycloaddition reactions,^{86,87} which

is in sharp contrast to their ketene and ketene imine analogues.²¹ However, the potential of SKIs to serve as dipole acceptors in such transformations has not been explored.

The chemistry of nucleophilic SKIs in combination with catalytically generated electrophilic metallated 1,3-dipole equivalents has not, to my knowledge, been previously documented.^{21,88} A highly efficient protocol for the assembly of enoldiazoacetates and SKIs under dirhodium catalysis to produce substituted 3-amino-2-cyclopentenones could be viable in light of this author's previous success in applying enoldiazoacetates in competitive [3+3]- and [3+2]-cycloadditions (**Scheme 2.22b**).



Scheme 2.22 (a) SKIs as Nucleophiles. (b) Formal [3+2]-Cycloaddition of SKIs and Enol Diazoacetate.

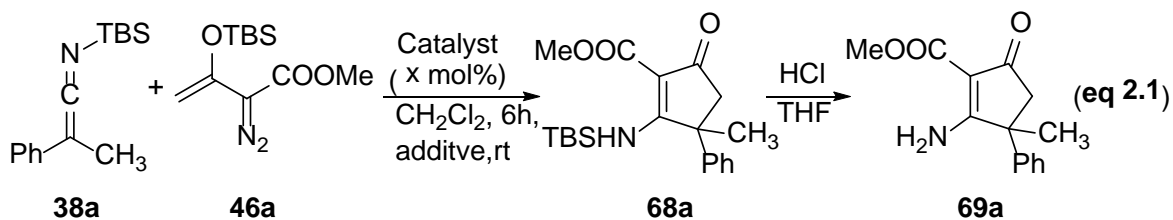
II. Results and Discussions

2.1 Results

The investigation was initiated by controlled addition of a solution of enol diazoacetate **46a** to the mixture of dirhodium catalyst and SKI **38a** in dichloromethane at room temperature. Results are reported in **Table 2.1**. By monitoring the reaction progress via TLC analysis and ¹H NMR spectroscopy,

the consumption of SKI **38a** and the formation of a new product **68a** (eq 2.1), whose structure was assigned by spectroscopic analysis to have originated from [3+2]-annulation, was observed. However, the isolated yield of **68a** was very low (<10%), and hydrolysis of SKI **38a** to the parent nitrile dominated. Adding activated 4Å MS to the reaction system dramatically increased the reaction yield by suppressing the proton desilylation of SKI **38a**, and the TBS-protected 3-amino-2-cyclopentenone **68a** was produced in excellent yield (Table 2.1, entry 2). Treatment of **68a** with a catalytic amount of aqueous HCl in THF cleaved the Si-N bond and provided the desilylated 3-amino-2-cyclopentenone product **69a** in quantitative yield. While the less soluble Rh₂(OAc)₄ gave a slightly lower product yield than did Rh₂(Oct)₄ (entry 3), Rh₂(OPiv)₄ with its sterically encumbered ligands was much less effective (entry 4). The more Lewis acidic catalyst Rh₂(TFA)₄ (entry 5), which was probably deactivated by the Lewis basic SKI **38a**,¹² only generated a trace amount of **68a**. The less Lewis acidic Rh₂(Cap)₄ did not catalyze the cycloaddition reaction, even at 80 °C in 1,2-dichloroethane (entry 6). Use of other transition metal catalysts, including Cu(OTf)₂ (entry 7) and AgSbF₆ (entry 8), only resulted in complex product mixtures under otherwise identical conditions without forming **68a**. The Lewis acid Sc(OTf)₃ showed no catalytic reactivity (entry 9).

Table 2.1 Optimization for the [3+2]-Cycloaddition Reaction.



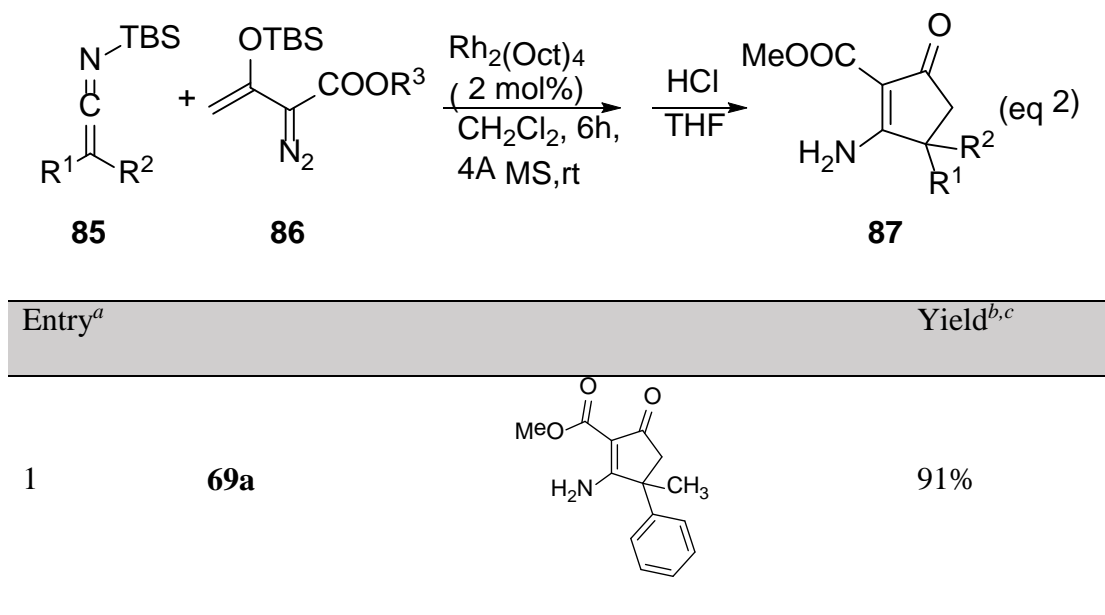
Entry ^a	Catalyst	Mol%	Additive ^b	Yield of 83 ^c
1	Rh ₂ (Oct) ₄	2 mol%	none	<10%
2	Rh ₂ (Oct) ₄	2 mol%	4 Å MS	91%
3	Rh ₂ (OAc) ₄	2 mol%	4 Å MS	87%
4	Rh ₂ (OPiv) ₄	2 mol%	4 Å MS	45%
5	Rh ₂ (TFA) ₄	2 mol%	4 Å MS	<10%
6 ^d	Rh ₂ (Cap) ₄	2 mol%	4 Å MS	<5%
7	Cu(OTf) ₂	5 mol%	4 Å MS	<5%
8	AgSbF ₆	5 mol%	4 Å MS	<5%
9	Sc(OTf) ₃	5 mol%	4 Å MS	No reaction

^aReactions were performed on 0.4 mmol of SKI **38a** (1.0 equivalent). Enoldiazoacetate **46a** (1.1 equivalent) in dichloromethane was added via syringe pump over 30 min. ^b4 Å MS was activated prior to use. ^cIsolated product yield after chromatography. ^dReaction performed at 80 °C in 1,2-dichloroethane.

Having identified the optimal reaction condition, a diverse array of substrates was surveyed to test the generality of this formal [3+2]-cycloaddition strategy, and results from this investigation are reported in **Table 2.2**. Changing the ester substituent of the enoldiazoacetate from methyl (entry 1) to benzyl (entry 2) shows minimal impact on the reaction outcome, and the resulting benzyl ester product was obtained in comparable reaction yield. Single crystal X-ray analysis of **69b** confirmed the structural assignment (**Figure 2.2**). Different aryl and alkyl substituents of the SKIs were well tolerated. Replacing the methyl group of SKI **38** with an ethyl group (entry 3) showed

marginal influence on the reaction yield. However, replacement of the methyl group with an isopropyl group (entry 4) significantly lowered the reaction yield. An SKI with an allyl group attached to the terminal carbon was also compatible with the reaction conditions, and no cyclopropanation product was observed (entry 5). Substituents with distinctive electronic properties on the phenyl ring were accommodated as well (entries 6-9). A SKI bearing a naphthyl, instead of a phenyl, group also underwent reaction (entry 10). Finally, SKIs derived from diphenylacetonitrile (entry 11) and cyclohexanecarbonitrile (entry 12) participated in the reaction and afforded the corresponding products in good yields. Overall, the [3+2]-annulation methodology represents a general approach for introducing a quaternary carbon onto the 3-amino-2-cyclopentenone skeleton.

Table 2.2 Substrate Scope for the Formal [3+2]-Cycloaddition Reaction.



2	69b		90%
3	69c		88%
4	69d		54%
5	69e		65%
6	69f		63%
7	69g		83%
8	69h		85%

9	69i		65%
10	69j		67%
11	69k		70%
12	69l		56%

^aReactions were performed on 0.4 mmol of SKI **38** (1.0 equivalent). Enoldiazoacetate **46** (1.1 equivalent) in dichloromethane was added via syringe pump over 30 min. ^bIsolated reaction yield. ^cReaction performed on 1.0 gram scale of **38a** afforded **69a** in comparable reaction yield (87%).

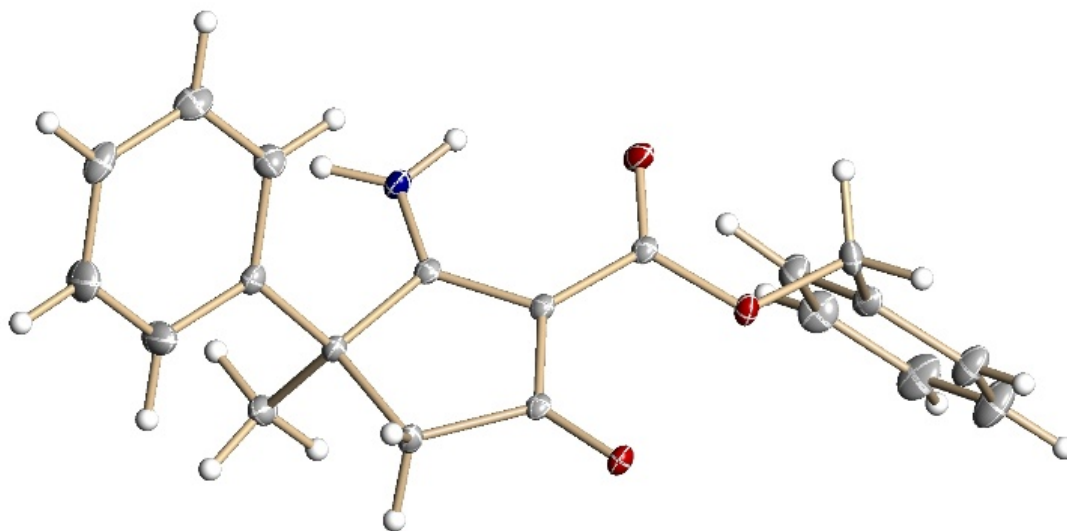
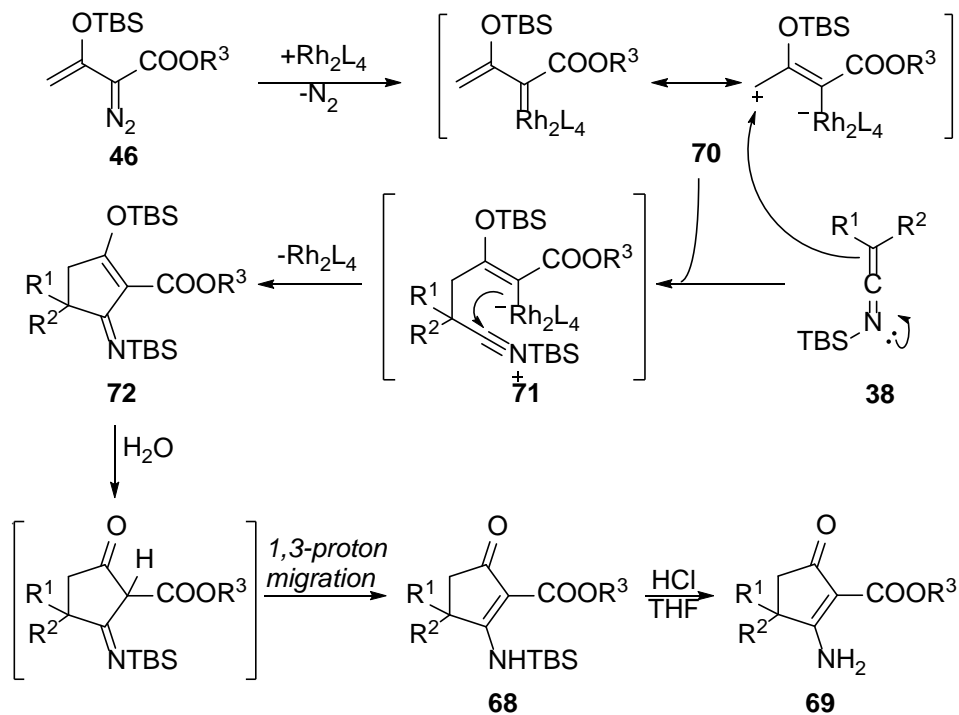


Figure 2.2 X-ray Crystal Structure of **69b** and CCDC 965494 Contains The Supplementary Crystallographic data. Thermal Ellipsoids Set at 30% Probability.

2.2 Discussion

The unusual outcome of the dirhodium(II)-catalyzed reaction is consistent with the mechanism that is outlined in **Scheme 2.23**. Dirhodium-catalyzed dinitrogen extrusion from **46** forms the electrophilic rhodium carbene intermediate **70** that preferentially undergoes vinylogous electrophilic addition to form nitrilium ion intermediate **71**. Intramolecular nitrilium ion addition to the nucleophilic vinylrhodium carbon center with release of the catalyst forms cyclopentane-imine **72**. The cyclopentane-imine **72** appears to be highly unstable and undergoes facile hydrolysis and subsequent 1,3-proton transfer reaction to yield the TBS-protected 3-amino-2-cyclopentenone **68**. In a control experiment, the triisopropylsilyl (TIPS)-substituted enoldiazoacetate engaged in the [3+2]-cycloaddition reaction and provided the identical TBS-substituted 3-amino-2-cyclopentenone **68**. This result is consistent with

hydrolysis of **72** occurring exclusively from oxygen rather than from nitrogen. Upon treating the product **68** with a catalytic amount of HCl, the 3-amino-2-cyclopentenone **69** is generated.



Scheme 2.23 The Proposed Mechanism for the [3+2]-Annulation Reaction.

This [3+2]-cyclization complements a recent report by Davies and coworkers for reactions of enoldiazoacetates with silylated enol ethers that involve vinylogous oxonium ion addition to the intermediate metal carbene, but in their case ring closure requires a bulky substituent on the vinyl ether to prevent OTBS transfer that forms propargylic products.

III. Conclusion

A catalytic [3+2]-cycloaddition reaction of SKIs and enoldiazoacetates with catalysis by dirhodium(II) carboxylates has been disclosed. This reaction proceeds

under mild conditions with remarkable functional group tolerance with structurally diverse 3-amino-2-cyclopentenones bearing a quaternary carbon at the 4-position produced in high reaction yields.

IV. Experimental Section

4.1 General Information

Experiments involving moisture and/or air sensitive components were performed in flame-dried glassware under a nitrogen atmosphere using freshly distilled solvents. Dichloromethane and 1,2-dichloroethane were dried over activated molecular sieves 4Å under argon and distilled prior to use. Commercial reagents and chromatography solvents (hexanes and ethyl acetate) were used without further purification. Thin layer chromatography (TLC) was carried out using EM Science silica gel 60 F254 plates. Chromatograms were analyzed by UV lamp (254 nm) or by development using cerium ammonium molybdate (CAM). Liquid chromatography was performed using a forced flow (flash chromatography) of the indicated system on silica gel (230-400 mesh). Proton nuclear magnetic resonance spectra (¹H NMR) were recorded on a Bruker AMX 400 spectrophotometer (in CDCl₃ or DMSO-*d*⁶ as solvent). Chemical shifts for ¹H NMR spectra are reported as δ in units of parts per million (ppm) downfield from SiMe₄ (δ = 0.00) and relative to the signal of chloroform-*d* (δ = 7.26, singlet) or DMSO-*d*⁶ (δ = 2.50, pentet). Multiplicities were given as: s (singlet); d (doublet); t (triplet); q (quartet); p (pentet); dd (doublet of doublets); ddd (doublet of doublet of doublets); dddd (doublet of doublet of doublet of doublets); dt (doublet of triplets); m (multiplet); comp (composite). The number of protons (n) for a given

resonance is indicated by nH . Coupling constants are reported as a J value in Hz. Carbon nuclear magnetic resonance spectra (^{13}C NMR) are reported in δ units of parts per million (ppm) downfield from $SiMe_4$ ($\delta = 0.00$) and relative to the central singlet for the signal of chloroform- d ($\delta = 77.00$, triplet) or $DMSO-d^6$ ($\delta = 39.50$, septet). High-resolution mass spectra (HRMS) were obtained on a JEOL AccuTOF-ESI mass spectrometer using CsI as the standard.

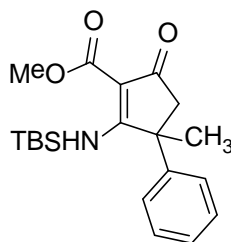
Molecular sieves 4\AA (powder, ~ 325 mesh), $Sc(OTf)_3$, $AgSbF_6$, $Cu(OTf)_2$ were purchased from Sigma-Aldrich. $Rh_2(OAc)_4$ and $Rh_2(Oct)_4$ were obtained from Pressure Chemical and Johnson Matthey, respectively. $Rh_2(Cap)_4$ was prepared according to established protocol.²⁹ Silylated ketene imines **38** were synthesized according to literature procedures.^{81, 83, 84} Enol diazoacetate **46**¹³ was prepared by the known method.

4.2 Experimental Procedure

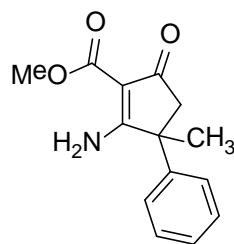
Sample procedure for the [3+2]-annulation of silylated ketene imine 38 and enol diazoacetate 46: A 10-mL Schlenk tube charged with 4\AA molecular sieves (200 mg) and a magnetic stirring bar was heated by an oil bath at $200\text{ }^\circ\text{C}$ under high vacuum (0.05 Torr) for 30 min. Then the Schlenk tube was cooled to room temperature with high vacuum (0.05 Torr) persisting. $Rh_2(Oct)_4$ (6.3 mg, 0.0080 mmol) was added to the Schlenk tube under a positive nitrogen atmosphere and the Schlenk tube was then sealed by a rubber septum. Dichloromethane (2.0 mL) and silylated ketene imine **38a** (102 mg, 0.40 mmol) were added sequentially by syringe at room temperature. The resulting green solution was stirred at room temperature while enol diazoacetate **46a** (113 mg, 0.44 mmol) dissolved in 2.0 ml dichloromethane was added to the Schlenk tube via syringe pump over 30 min. The reaction was continued for 6h with stirring.

Then the reaction mixture was filtrated through a short pad of celite. The celite pad was washed with ~1 ml EtOAc three times, and the combined filtrate was concentrated under reduced pressure. The residue was purified by column chromatography to afford the TBS-protected product **68a** together with a small amount of **69a**. The two fractions were combined and dissolved in 1.0 ml THF. Two droplets (~ 0.05 ml) of 1.0 M aqueous HCl were added to the resulting THF solution, which was further stirred for 5 min at room temperature. The THF solution was concentrated under reduced pressure and the solid residue was washed with ~3 ml of hexanes to afford the 3-aminocyclopentenone **69a** (89 mg, 91% yield).

4.3 Characterization Data

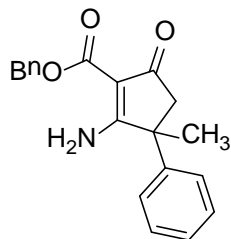


Methyl 2-(tert-Butyldimethylsilyl)amino-3-methyl-5-oxo-3-phenylcyclopent-1-enecarboxylate (68a). ^1H NMR (400 MHz, CDCl_3) δ 9.64 (s, 1H), 7.38 – 7.30 (comp, 2H), 7.30 – 7.19 (comp, 3H), 3.90 (s, 3H), 2.57 (s, 2H), 1.77 (s, 3H), 0.93 (s, 9H), 0.09 (s, 3H), -0.55 (s, 3H). ^{13}C NMR (100 MHz, CDCl_3) δ 196.8, 193.4, 167.7, 144.1, 128.9, 127.2, 126.0, 105.5, 55.8, 51.3, 47.1, 25.6, 24.6, 17.5, -2.6, -4.8. HRMS (ESI⁺): calcd for $\text{C}_{20}\text{H}_{30}\text{NO}_3\text{Si}$ [M+H]⁺ 360.1989, found 360.1970.



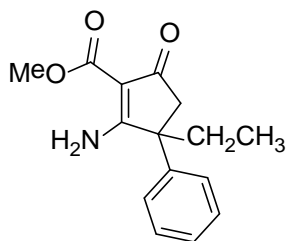
Methyl 2-Amino-3-methyl-5-oxo-3-phenylcyclopent-1-enecarboxylate

(69a). ^1H NMR (400 MHz, CDCl_3) δ 8.44 (br s, 1H), 7.40 – 7.33 (comp, 2H), 7.33 – 7.25 (comp, 3H), 5.59 (br s, 1H), 3.87 (s, 3H), 2.71 (d, $J = 18.0$ Hz, 1H), 2.58 (d, $J = 18.0$ Hz, 1H), 1.75 (s, 3H). ^{13}C NMR (100 MHz, CDCl_3) δ 196.7, 187.9, 166.5, 142.7, 129.1, 127.6, 126.0, 102.1, 53.2, 51.4, 45.6, 25.0. HRMS (ESI $^+$): calcd for $\text{C}_{14}\text{H}_{16}\text{NO}_3$ $[\text{M}+\text{H}]^+$ 246.1125, found 246.1133.



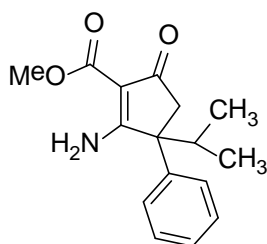
Benzyl 2-Amino-3-methyl-5-oxo-3-phenylcyclopent-1-enecarboxylate

(69b). ^1H NMR (400 MHz, CDCl_3) δ 8.35 (br s, 1H), 7.53 (dd, $J = 7.9, 0.9$ Hz, 2H), 7.42 – 7.27 (comp, 8H), 5.59 (br s, 1H), 5.38 (s, 2H), 2.72 (d, $J = 18.0$ Hz, 1H), 2.59 (d, $J = 18.0$ Hz, 1H), 1.75 (s, 3H). ^{13}C NMR (100 MHz, CDCl_3) δ 196.5, 187.7, 165.6, 142.8, 136.4, 129.0, 128.5, 127.8, 127.7, 127.6, 126.1, 102.1, 65.5, 53.3, 45.6, 25.0. HRMS (ESI $^+$): calcd for $\text{C}_{20}\text{H}_{20}\text{NO}_3$ $[\text{M}+\text{H}]^+$ 322.1438, found 322.1450.



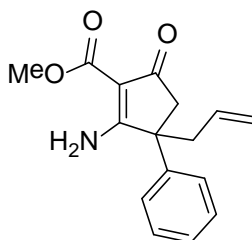
Methyl 2-Amino-3-ethyl-5-oxo-3-phenylcyclopent-1-enecarboxylate (69c).

^1H NMR (400 MHz, CDCl_3) δ 8.49 (br s, 1H), 7.38 – 7.31 (comp, 2H), 7.31 – 7.22 (comp, 3H), 5.92 (br s, 1H), 3.85 (s, 3H), 2.60 (d, $J = 18.2$ Hz, 1H), 2.53 (d, $J = 18.2$ Hz, 1H), 2.24 (dq, $J = 14.6, 7.3$ Hz, 1H), 2.08 (dq, $J = 14.6, 7.3$ Hz, 1H), 0.94 (t, $J = 7.3$ Hz, 3H). ^{13}C NMR (100 MHz, CDCl_3) δ 197.6, 186.5, 166.7, 143.6, 129.5, 127.9, 126.6, 104.1, 51.7, 50.1, 49.9, 29.1, 8.8. HRMS (ESI $^+$): calcd for $\text{C}_{15}\text{H}_{18}\text{NO}_3$ $[\text{M}+\text{H}]^+$ 260.1281, found 260.1288.



Methyl 2-Amino-3-isopropyl-5-oxo-3-phenylcyclopent-1-enecarboxylate (69d).

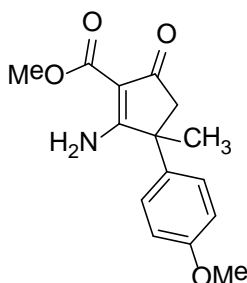
^1H NMR (400 MHz, CDCl_3) δ 8.48 (br s, 1H), 7.44 – 7.35 (comp, 4H), 7.34 – 7.29 (m, 1H), 5.61 (br s, 1H), 3.87 (s, 3H), 2.79 (dq, $J = 13.3, 6.6$ Hz, 1H), 2.74 (d, $J = 18.5$ Hz, 1H), 2.68 (d, $J = 18.5$ Hz, 1H), 1.06 (d, $J = 6.6$ Hz, 3H), 1.00 (d, $J = 6.6$ Hz, 3H). ^{13}C NMR (100 MHz, CDCl_3) δ 198.0, 186.8, 166.9, 142.2, 129.7, 127.9, 126.9, 103.0, 53.5, 51.8, 45.3, 30.8, 18.7, 17.8. HRMS (ESI $^+$): calcd for $\text{C}_{16}\text{H}_{20}\text{NO}_3$ $[\text{M}+\text{H}]^+$ 274.1438, found 274.1450.



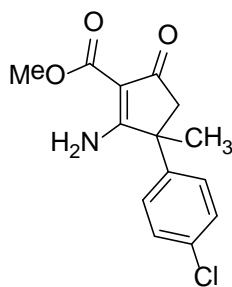
Methyl 3-Allyl-2-amino-5-oxo-3-phenylcyclopent-1-enecarboxylate (69e).

^1H NMR (400 MHz, CDCl_3) δ 8.54 (br s, 1H), 7.45 – 7.36 (comp, 2H), 7.36 – 7.29

(comp, 3H), 5.79 – 5.56 (comp, 2H), 5.27 (dd, $J = 16.9, 1.4$ Hz, 1H), 5.21 (dd, $J = 10.1, 1.4$ Hz, 1H), 3.89 (s, 3H), 2.99 – 2.81 (m, 2H), 2.75 (d, $J = 18.1$ Hz, 1H), 2.61 (d, $J = 18.1$ Hz, 1H). ^{13}C NMR (100 MHz, CDCl_3) δ 197.0, 186.0, 166.8, 142.8, 132.0, 129.6, 128.1, 126.6, 121.2, 104.1, 51.8, 50.4, 49.3, 41.2. HRMS (ESI⁺): calcd for $\text{C}_{16}\text{H}_{18}\text{NO}_3$ $[\text{M}+\text{H}]^+$ 272.1281, found 272.1293.

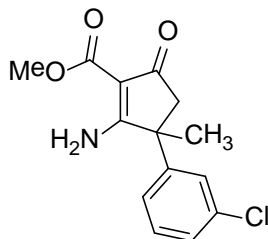


Methyl 2-Amino-3-(4-methoxyphenyl)-3-methyl-5-oxocyclopent-1-ene-carboxylate (69f). ^1H NMR (400 MHz, CDCl_3) δ 8.41 (br s, 1H), 7.20 (d, $J = 8.0$ Hz, 2H), 6.88 (d, $J = 8.0$ Hz, 2H), 5.53 (br s, 1H), 3.88 (s, 3H), 3.80 (s, 3H), 2.70 (d, $J = 18.0$ Hz, 1H), 2.57 (d, $J = 18.0$ Hz, 1H), 1.72 (s, 3H). ^{13}C NMR (100 MHz, CDCl_3) δ 197.3, 188.6, 166.9, 159.4, 135.0, 127.7, 114.8, 102.4, 55.8, 53.7, 51.8, 45.5, 25.8. HRMS (ESI⁺): calcd for $\text{C}_{15}\text{H}_{18}\text{NO}_4$ $[\text{M}+\text{H}]^+$ 276.1230, found 276.1243.

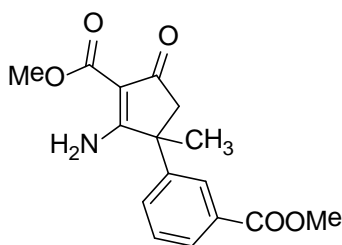


Methyl 2-Amino-3-(4-chlorophenyl)-3-methyl-5-oxocyclopent-1-ene-carboxylate (69g). ^1H NMR (400 MHz, CDCl_3) δ 8.46 (br s, 1H), 7.34 (dt, $J = 8.8, 2.7$ Hz, 2H), 7.22 (dt, $J = 8.8, 2.7$ Hz, 2H), 5.64 (br s, 1H), 3.88 (s, 3H), 2.65 (d, $J = 18.0$

Hz, 1H), 2.57 (d, $J = 18.0$ Hz, 1H), 1.74 (s, 3H). ^{13}C NMR (100 MHz, CDCl_3) δ 196.7, 187.7, 166.8, 141.8, 134.1, 129.7, 127.9, 102.6, 53.5, 51.9, 45.7, 25.3. HRMS (ESI⁺): calcd for $\text{C}_{14}\text{H}_{15}\text{ClNO}_3$ $[\text{M}+\text{H}]^+$ 280.0735, found 280.0737.

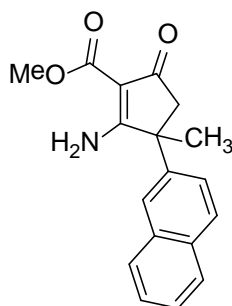


Methyl 2-Amino-3-(3-chlorophenyl)-3-methyl-5-oxocyclopent-1-ene-1-carboxylate (69h). ^1H NMR (400 MHz, $\text{DMSO}-d_6$) δ 8.51 (br s, 1H), 8.47 (br s, 1H), 7.40 (dd, $J = 14.7, 7.9$ Hz, 1H), 7.37 – 7.33 (m, 1H), 7.31 (t, $J = 1.8$ Hz, 1H), 7.20 (dt, $J = 7.9, 1.8$ Hz, 1H), 3.68 (s, 3H), 2.46 (d, $J = 17.7$ Hz, 1H), 2.33 (d, $J = 17.7$ Hz, 1H), 1.70 (s, 3H). ^{13}C NMR (100 MHz, $\text{DMSO}-d_6$) δ 194.4, 185.9, 165.1, 147.3, 133.1, 130.5, 126.8, 125.8, 124.7, 99.8, 52.9, 50.2, 45.1, 23.6. HRMS (ESI⁺): calcd for $\text{C}_{14}\text{H}_{15}\text{ClNO}_3$ $[\text{M}+\text{H}]^+$ 280.0735, found 280.0739.

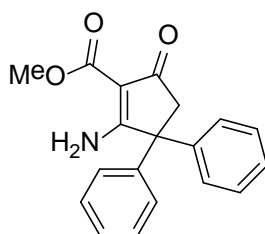


Methyl 3-[2-Amino-3-(methoxycarbonyl)-1-methyl-4-oxocyclopent-2-en-1-yl]benzoate (69i). ^1H NMR (400 MHz, CDCl_3) δ 8.47 (br s, 1H), 8.03 – 7.92 (comp, 2H), 7.51 – 7.44 (comp, 2H), 5.50 (br s, 1H), 3.93 (s, 3H), 3.89 (s, 3H), 2.71 (d, $J = 18.1$ Hz, 1H), 2.62 (d, $J = 18.1$ Hz, 1H), 1.80 (s, 3H). ^{13}C NMR (100 MHz, CDCl_3) δ 196.7, 187.6, 167.0, 166.9, 143.7, 131.4, 131.1, 129.8, 129.4, 127.4, 102.8, 53.5, 52.8,

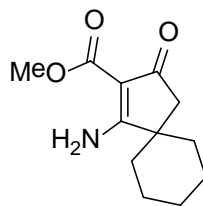
51.9, 46.0, 25.4. HRMS (ESI⁺): calcd for C₁₆H₁₈NO₅ [M+H]⁺ 304.1179, found 304.1190.



Methyl 2-Amino-3-methyl-3-(naphthalen-2-yl)-5-oxocyclopent-1-enecarboxylate (69j). ¹H NMR (400 MHz, CDCl₃) δ 8.40 (br d, *J* = 2.9 Hz, 1H), 7.82 – 7.68 (comp, 4H), 7.50 – 7.39 (comp, 2H), 7.16 (dd, *J* = 8.7, 2.0 Hz, 1H), 6.34 (br d, *J* = 2.9 Hz, 1H), 3.81 (s, 3H), 2.57 (d, *J* = 18.1 Hz, 1H), 2.37 (d, *J* = 18.1 Hz, 1H), 1.74 (s, 3H). ¹³C NMR (100 MHz, CDCl₃) δ 197.4, 188.4, 166.7, 140.5, 133.4, 132.7, 129.5, 128.3, 127.9, 127.1, 126.9, 125.1, 124.4, 102.2, 53.2, 51.7, 46.1, 25.1. HRMS (ESI⁺): calcd for C₁₈H₁₈NO₃ [M+H]⁺ 296.1281, found 296.1266.



Methyl 2-Amino-5-oxo-3,3-diphenylcyclopent-1-enecarboxylate (69k). ¹H NMR (400 MHz, CDCl₃) δ 8.71 (br d, *J* = 2.5 Hz, 1H), 7.39 – 7.26 (comp, 6H), 7.26 – 7.21 (comp, 4H), 5.99 (br d, *J* = 2.5 Hz, 1H), 3.83 (s, 3H), 3.12 (s, 2H). ¹³C NMR (100 MHz, CDCl₃) δ 195.8, 184.4, 166.3, 142.8, 128.8, 127.7, 127.5, 102.6, 55.8, 54.0, 51.3. HRMS (ESI⁺): calcd for C₁₉H₁₈NO₃ [M+H]⁺ 308.1281, found 308.1273.



Methyl 1-Amino-3-oxospiro[4.5]dec-1-ene-2-carboxylate (69I). ^1H NMR (400 MHz, CDCl_3) δ 8.63 (br s, 1H), 6.28 (br s, 1H), 3.83 (s, 3H), 2.36 (s, 2H), 1.83 – 1.71 (comp, 3H), 1.66 – 1.51 (comp, 4H), 1.49 – 1.32 (comp, 2H), 1.30 – 1.14 (m, 1H). ^{13}C NMR (100 MHz, CDCl_3) δ 197.3, 189.5, 167.2, 101.1, 51.6, 46.5, 43.5, 35.6, 25.5, 23.1. HRMS (ESI $^+$): calcd for $\text{C}_{12}\text{H}_{18}\text{NO}_3$ $[\text{M}+\text{H}]^+$ 224.1281, found 224.1288.

NMR graphs, HPLC chromatograms and X-ray single crystal analysis data can be obtained from the supporting information of the paper published in the *Chemical Communications*: Xu, X.; Leszczynski, J. S.; Mason, S. M.; Zavalij, P. Y.; Doyle, M. P. *Chem. Commun.*, **2014**, 50, 2462-2464.

V. Reference

- (1) Patai, S. *The Chemistry of Ketenes, Allenes and Related Compounds*, Wiley, New York, **1980**.
- (2) Schuster, H. F.; Coppola, G. M. *Allenenes in Organic Synthesis*, Wiley, New York, **1984**.
- (3) Tidwell, T. T. *Ketenes*, Wiley, New York, **1995**.
- (4) Krow, G. R. *Angew. Chem., Int. Ed.* **1971**, 10, 435.
- (5) Lu, P.; Wang, Y. *Synlett* **2010**, 2, 165.
- (6) Kim, S. H.; Park, S. H.; Choi, J. H.; Chang, S. *Chem.–Asian J.* **2011**, 6, 2618.
- (7) Yoo, E. J.; Chang, S. *Curr. Org. Chem.* **2009**, 13, 1766.
- (8) Perst, H. *Science of Synthesis* **2006**, 23, 781.

- (9) Kollenz, G. *Science of Synthesis* **2006**, 23, 351.
- (10) Cheng, Y.; Ma, Y.; Wang, X.; Mo, J. *J. Org. Chem.* **2009**, 74, 850.
- (11) Yang, Y.; Shou, W.; Hong, D.; Wang, Y. *J. Org. Chem.* **2008**, 73, 3574.
- (12) Cheng, L.; Cheng, Y. *Tetrahedron* **2007**, 63, 9359.
- (13) Bae, I.; Han, H.; Chang, S. *J. Am. Chem. Soc.* **2005**, 127, 2038.
- (14) Coffinier, D.; Kaim, L. E.; Grimaud, L. *Org. Lett.* **2009**, 11, 1825.
- (15) Sung, K. *J. Chem. Soc., Perkin Trans. 2*, **2000**, 847.
- (16) K. Sung *J. Chem. Soc., Perkin Trans. 2*, **1999**, 1169.
- (17) Wolf, R.; Wong, M. W.; Kennard, C. H. L.; Wentrup, C. *J. Am. Chem. Soc.* **1995**, 117, 6789.
- (18) Wolf, R.; S. Stadtmüller; Wong, M. W.; Barbieux-Flammang, M.; Flammang, R.; C. Wentrup *Chem.–Eur. J.* **1996**, 2, 1318.
- (19) Beutner, G. L.; Denmark, S. E. *Angew. Chem., Int. Ed.* **2013**, 52, 9086.
- (20) Denmark, S. E.; Wilson, T. W. *Angew. Chem., Int. Ed.* **2012**, 51, 9980.
- (21) Lu, P.; Wang, Y. *Chem. Soc. Rev.* **2012**, 41, 5687.
- (22) Arseniyadis, S.; Kyler, K. S.; Watt, D. S. *Org. React.* **1984**, 31, 3.
- (23) Newman, M. S.; Fukunaga, T.; Miwa, T. *J. Am. Chem. Soc.* **1960**, 82, 873.
- (24) Watt, D. S. *Synth. Commun.* **1974**, 4, 127.
- (25) Watt, D. S. *J. Org. Chem.* **1974**, 39, 2799.
- (26) Brownbridge, P. *Synthesis* **1983**, 1.
- (27) Brownbridge, P. *Synthesis* **1983**, 85.

- (28) Kita, Y.; Tamura, O.; Tamura, Y. *J. Synth. Org. Chem. Jpn.* **1986**, *44*, 1118.
- (29) Narasaka, K.; Soai, K.; Mukaiyam, T. *Chem. Lett* **1974**, 1223.
- (30) Oare, D. A.; Heathcock, C. H. *Top. Stereochem.* **1991**, *20*, 87.
- (31) Oare, D. A.; Heathcock, C. H. *Top. Stereochem.* **1989**, *19*, 227.
- (32) Zhao, J.; Liu, X.; Luo, W.; Xie, M.; Lin, L.; Feng, X. *Angew. Chem., Int. Ed.* **2013**, *52*, 3473.
- (33) Denissova, I.; Barriault, L. *Tetrahedron* **2003**, *59*, 10105.
- (34) Douglas, C. J.; Overman, L. E. *Proc. Natl. Acad. Sci.* **2004**, *101*, 5363.
- (35) Trost, B. M.; Jiang, C. *Synthesis* **2006**, 369.
- (36) Das, J. P.; Marek, I. *Chem. Comm.* **2011**, *47*, 4593.
- (37) Cazeau, P.; Llonch, J. P.; Simonin-Dabescat, F.; Frainnet, E. *J. Organomet. Chem.* **1976**, *105*, 145.
- (38) Cazeau, P.; Llonch, J. P.; Simonin-Dabescat, F.; Frainnet, E. *J. Organomet. Chem.* **1976**, *105*, 157.
- (39) Okada, H.; Matsuda, I.; Izumi, Y. *Chem. Lett* **1983**, 97.
- (40) Hudrlik, P. F.; Peterson, D. *J. Am. Chem. Soc.* **1975**, *97*, 1464.
- (41) Hudrlik, P. F.; Peterson, D.; Rona, R. J. *J. Org. Chem.* **1975**, *40*, 2263.
- (42) Ager, D. J. *Synthesis* **1984**, 384.
- (43) Freerksen, R. W.; Selikson, S. J.; Wroble, R. R.; Kyler, K. S.; Watt, D. *S. J. Org. Chem.* **1983**, *48*, 4087.
- (44) Differding, E.; Vandavelde, O.; Roekens, B.; Van, T. T.; Ghosez, L. *Tetrahedron Lett.* **1987**, *28*, 397.

- (45) Mermerian, A. H.; Fu, G. C. *J. Am. Chem. Soc.* **2003**, *125*, 4050.
- (46) Mermerian, A. H.; Fu, G. C. *J. Am. Chem. Soc.* **2005**, *127*, 5604.
- (47) Mermerian, A. H.; Fu, G. C. *Angew. Chem., Int. Ed.* **2005**, *44*, 949.
- (48) Davies, H. M. L.; Ahmed, G.; Churchill, M. R. *J. Am. Chem. Soc.* **1996**, *118*, 10774.
- (49) Davies, H. M. L.; Matasi, J. J.; Hodges, L. M.; Huby, N. J. S.; Thornley, C.; Kong, N.; Houser, J. H. *J. Org. Chem.* **1997**, *62*, 1095.
- (50) Reddy, R. P.; Davies, H. M. L. *J. Am. Chem. Soc.* **2007**, *129*, 10312.
- (51) Schwartz, B. D.; Denton, J. R.; Lian, Y.; Davies, H. M. L.; Williams, C. M. *J. Am. Chem. Soc.* **2009**, *131*, 8329.
- (52) Davies, H. M. L.; Saikali, E.; Clark, T. J.; Chee, E. H. *Tetrahedron Lett.* **1990**, *31*, 6299.
- (53) Davies, H. M. L.; Saikali, E.; Young, W. B. *J. Org. Chem.* **1991**, *56*, 5696.
- (54) Davies, H. M. L.; Hu, B.; Saikali, E.; Bruzinski, P. R. *J. Org. Chem.* **1994**, *59*, 4535.
- (55) Sevryugina, Y.; B. Weaver; Hansen, J.; Thompson, J.; Davies, H. M. L.; Petrukhina, M. A. *Organometallics* **2008**, *27*, 1750.
- (56) Y. Lian; Davies, H. M. L. *Org. Lett.* **2010**, *12*, 924.
- (57) Hansen, J. H.; Davies, H. M. L. *Chem. Sci.* **2011**, *2*, 457.
- (58) Lian, Y.; Davies, H. M. L. *Org. Lett.* **2012**, *14*, 1934.
- (59) Morton, D.; Dick, A. R.; Ghosh, D.; Davies, H. M. L. *Chem. Comm.* **2012**, *48*, 5838.

- (60) Muller, P.; Bernardinelli, G.; Allenbach, Y. F.; Ferri, M.; Flack, H. D. *Org. Lett.* **2004**, *6*, 1725.
- (61) Valette, D.; Lian, Y.; Haydek, J. P.; Hardcastle, K. I.; Davies, H. M. *Angew. Chem., Int. Ed.* **2012**, *51*, 8636.
- (62) Smith, A. G.; Davies, H. M. *J. Am. Chem. Soc.* **2012**, *134*, 18241.
- (63) Marks, F.; Furstenberger, G. *Prostaglandins, Leukotrienes and Other Eicosanoids, From Biogenesis to Clinical Application, Wiley-VCH* **1999**.
- (64) Straus, D. S.; Glass, C. K. *Med. Res. Rev.* **2001**, *21*, 185.
- (65) Roberts, S. M.; Santoro, M. G.; Sickle, E. S. *J. Chem. Soc., Perkin Trans. 1* **2002**, 1735.
- (66) Rezgui, F.; Amrib, H.; Gated, M. M. E. *Tetrahedron* **2003**, 1369.
- (67) Tius, M. A. *Acc. Chem. Res.* **2003**, *36*, 284.
- (68) Kurteva, V. B.; Afonso, C. A. M. *Chem. Rev.* **2009**, *109*, 6809.
- (69) T. N. Grant; Rieder, C. J.; West, F. G. *Chem. Comm.* **2009**, 5676.
- (70) Harmata, M. *Chem. Comm.* **2010**, *46*, 8886.
- (71) Schore, N. E. *Org. React.* **1991**, *40*, 1.
- (72) Brummond, K. M.; Kent, J. L. *Tetrahedron* **2000**, *56*, 3263.
- (73) Gibson, S. E.; Stevenazzi, A. *Angew. Chem., Int. Ed.* **2003**, *42*, 1800.
- (74) Gibson, S. E.; Mainolfi, N. *Angew. Chem., Int. Ed.* **2005**, *44*, 3022.
- (75) Reddy, L. V. R.; Kumar, V.; Sagar, R.; Shaw, A. K. *Chem. Rev.* **2013**, *113*, 3605.
- (76) Barluenga, J.; Barrio, P.; Riesgo, L.; Lopez, L. A.; Tomas, M. *J. Am. Chem. Soc.* **2007**, *129*, 14422.

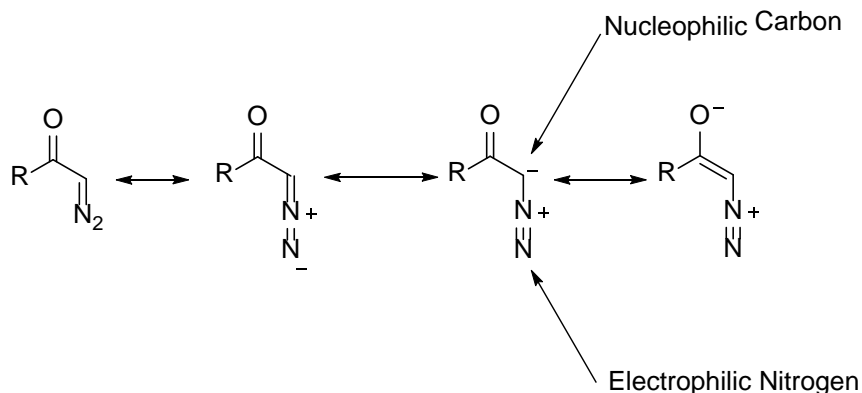
- (77) Davie, C. P.; Danheiser, R. L. *Angew. Chem., Int. Ed.* **2005**, *44*, 5867.
- (78) X. Shi; Gorin, D. J.; Toste, F. D. *J. Am. Chem. Soc.* **2005**, *127*, 5802.
- (79) Zhang, L.; Wang, S. *J. Am. Chem. Soc.* **2006**, *128*, 1442.
- (80) Jenkins, A. D.; Herath, A.; Song, M.; Montgomery, J. *J. Am. Chem. Soc.* **2011**, *133*, 14460.
- (81) Denmark, S. E.; Wynn, T.; Beutner, G. L. *J. Am. Chem. Soc.* **2002**, *124*, 13405.
- (82) Denmark, S. E.; Jr., J. R. H. *Org. Lett.* **2003**, *5*, 2303.
- (83) Denmark, S. E.; Beutner, G. L.; Wynn, T.; Eastgate, M. D. *J. Am. Chem. Soc.* **2005**, *127*, 3774.
- (84) Denmark, S. E.; Wilson, T. W.; Burk, M. T.; Jr., J. R. H. *J. Am. Chem. Soc.* **2007**, *129*, 14864.
- (85) Notte, G. T.; Vu, J. M. B.; Leighton, J. L. *Org. Lett.* **2011**, *13*, 816.
- (86) Alonso-Gomez, J. L.; Pazos, Y.; Navarro-Vazquez, A.; Lugtenburg, J.; Cid, M. M. *Org. Lett.* **2005**, *7*, 3773.
- (87) Navarro-Vazquez, A.; Alonso-Gomez, J.; Lugtenburg, J.; Cid, M. M. *Tetrahedron* **2010**, *66*, 3855.
- (88) Allen, A. D.; Tidwell, T. T. *Chem. Rev.* **2013**, *113*, 7287.

Chapter 3: Catalyst Controlled Selective 1,2-Migrations from α -Diazoacetates.

I. Introduction

1.1. General Information for α -Diazo Carbonyl compounds in Nucleophilic Addition Reactions.

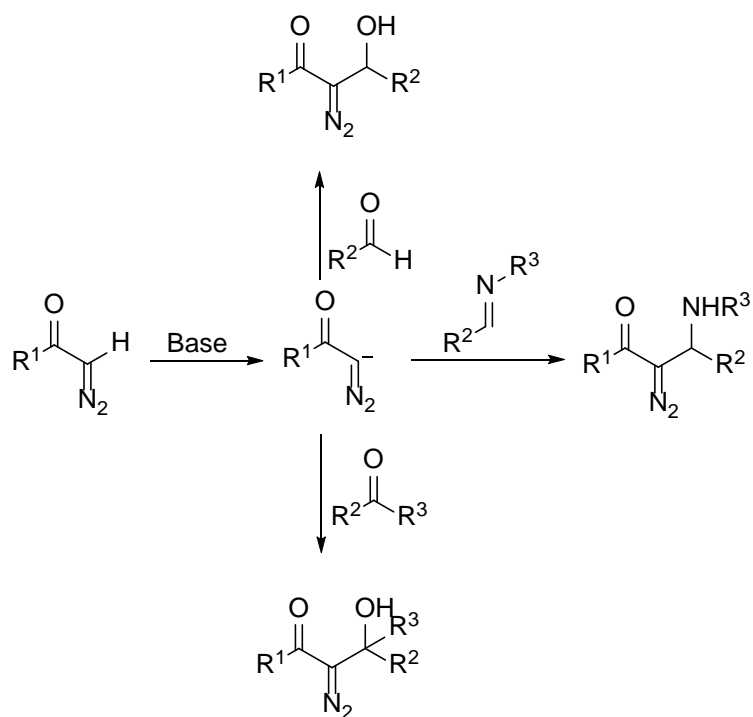
α -Diazo carbonyl compounds can react with both electrophiles and nucleophiles (**Scheme 3.1**).¹ While it is obvious that nucleophilic addition reaction of α -diazo carbonyl compounds occurs at the α -carbon position,² the terminal nitrogen, perhaps counterintuitively, is electrophilic.^{3,4}



Scheme 3.1 The Resonance Structures for an α -Diazo Carbonyl Compound.

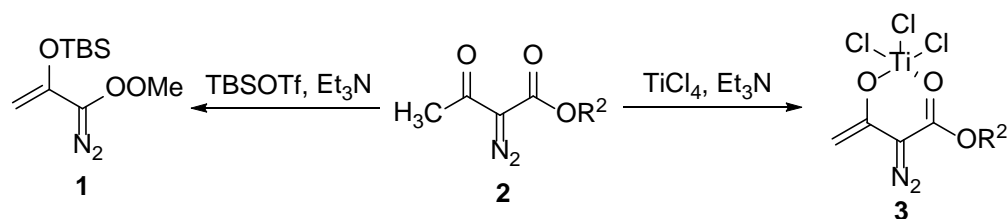
The relatively high acidity for the α -proton of α -diazo carbonyl compounds ($pK_a \sim 13$ for ethyl diazoacetate)^{1,5} enables generation of the corresponding carbanion which bears a diazo group under basic conditions.⁵ This carbanion is highly reactive towards nucleophilic addition to imines, aldehydes and ketones without a catalyst.⁶ More importantly, during these transformations, the diazo group remains intact and

thereby enables the synthesis of complex α -diazo carbonyl compounds from readily available α -diazo ketones or esters (**Scheme 3.2**).



Scheme 3.2 Construction of Complex α -Diazocarbonyl Compounds from α -Diazo Ketones or Esters.

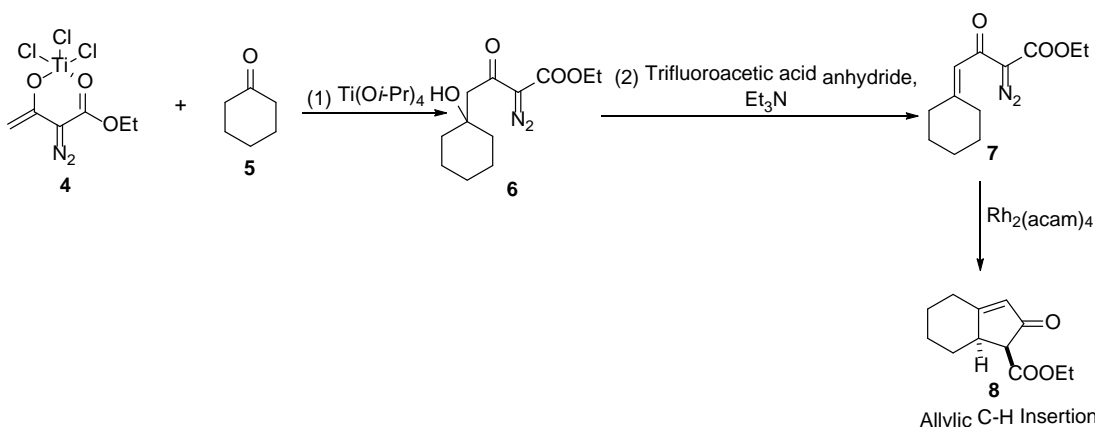
More intriguingly, Ti- or Si-enol diazoacetates can be generated from α -diazo- β -ketoesters with great ease (**Scheme 3.3**).⁷⁻¹⁰ Although the Ti-enol diazoacetates are generated in situ and used directly, the TBS-substituted enol diazoacetates, as stated in the previous chapters, are stable; and they do not undergo the intramolecular [1,5]-cyclization (**Scheme 1.16**) which is commonly observed for vinyl diazoacetates.¹¹ Both Ti- and Si-enol diazoacetates are nucleophilic and they serve as versatile precursors for the introduction of the α -diazo- β -ketoester scaffold in Lewis acid catalyzed reactions.⁸⁻



Scheme 3.3 Generation of Si- and Ti-enol Diazoacetate from α -Diazo- β -ketoesters.

1.2 Ti(IV)-enol Diazoacetates in Nucleophilic Additions.

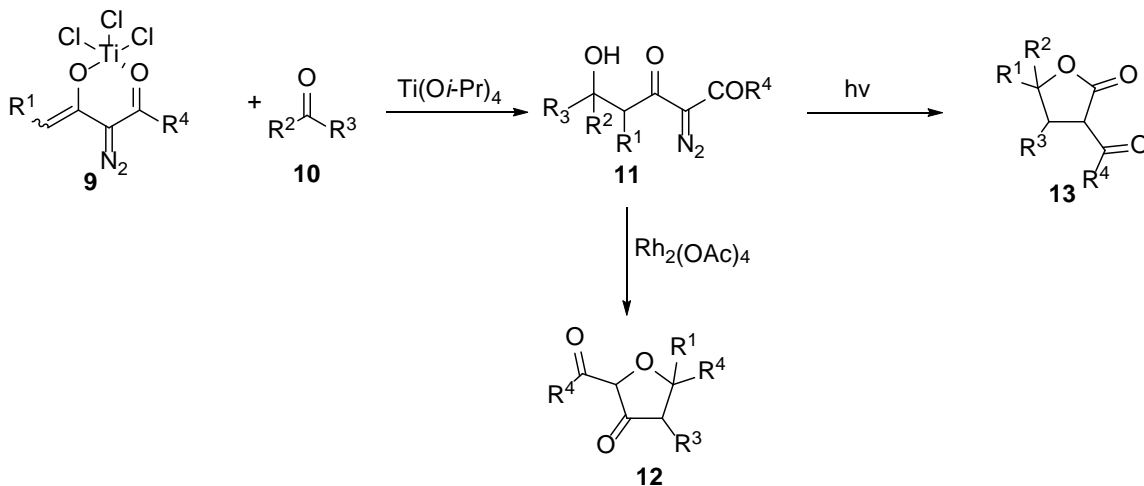
As reported by Calter and co-workers, while Ti-enol diazoacetate **4** and aldehydes react smoothly in the absence of a catalyst,⁸ the same reaction for ketones is very sluggish.^{9,10} The use of Lewis acid promoter-Ti(O*i*-Pr)₄ effectively enhances the reaction rate, and the tertiary alcohol product **6** is obtained in good reaction yields. Dehydration of the reaction product **6** at room temperature produces the γ,δ -unsaturated β -keto- α -diazoester **7**, which undergoes intramolecular allylic C-H insertion reaction to provide bicyclic fused cyclopentenones **8** in good yields (**Scheme 3.4**).



Scheme 3.4 Ti(O*i*-Pr)₄-catalyzed Addition of Ti-enol Diazoacetate to Ketones and Subsequent Intramolecular Allylic C-H Insertion.

Wang and coworkers have investigated a similar transformation with a γ -substituted Ti-enol diazoacetate **9**.¹² As expected, the addition reaction with ketones occurs through activation by Ti(O*i*-Pr)₄. Subsequent treatment of the resulting α -diazo-

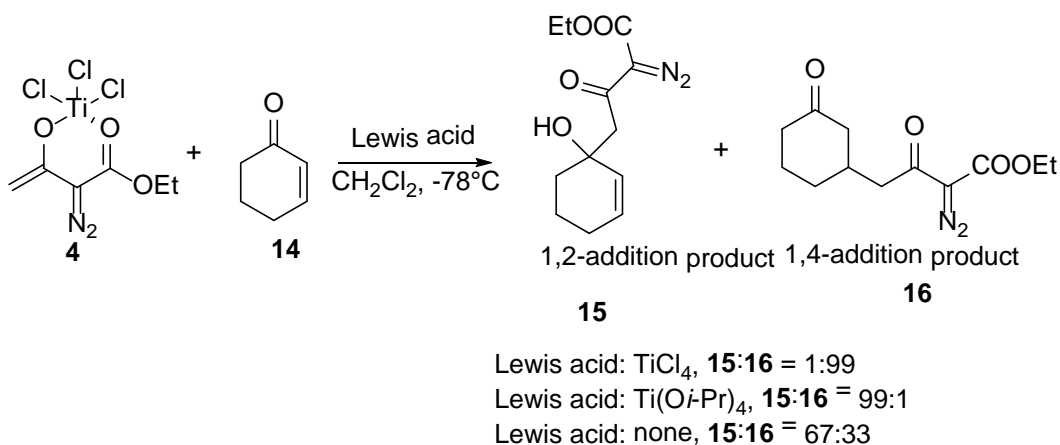
β -ketoester **11** with a catalytic amount of $\text{Rh}_2(\text{OAc})_4$ in refluxing toluene generates exclusively the intramolecular O-H insertion product **13**. Alternatively, photon-irradiation of the addition product **11** induces the Wolff rearrangement and affords a ketene intermediate which is intramolecularly trapped by OH group to produce the lactone product **13** (Scheme 3.5).



Scheme 3.5 Addition of Ti-enol Diazoacetate to Ketones and Subsequent Intramolecular OH-insertion or Lactone Formation.

Addition of enol diazoacetate to α,β -unsaturated carbonyl substrates invariably encounters competition between 1,4- and 1,2-addition. As demonstrated by Wang and coworker,¹³ the use of Ti-enol diazoacetate **4** with judicious selection of the promoter results in the complete selectivity reversal from 1,4- to 1,2-addition. While in the absence of any Lewis acid promoter, a 67:33 ratio for 1,2-/1,4-addition (**15:16**) was observed, the use of one equivalent of $\text{Ti}(\text{O}i\text{-Pr})_4$ enhances the selectivity to 99:1. Remarkably, a complete reversal of selectivity preference to 1:99 for 1,2-/1,4-addition (**15:16**) is achieved when switching to 1 equivalent TiCl_4 as the promoter (Scheme 3.6). Although the authors propose that the selectivity preference in the TiCl_4 -promoted reaction can be understood by considering the formation of a dimetallic species

between TiCl_4 and Ti-enol diazoacetate, such an explanation obviously overlooks the mechanistic complexity of Ti-catalyzed or -promoted reactions.¹⁴



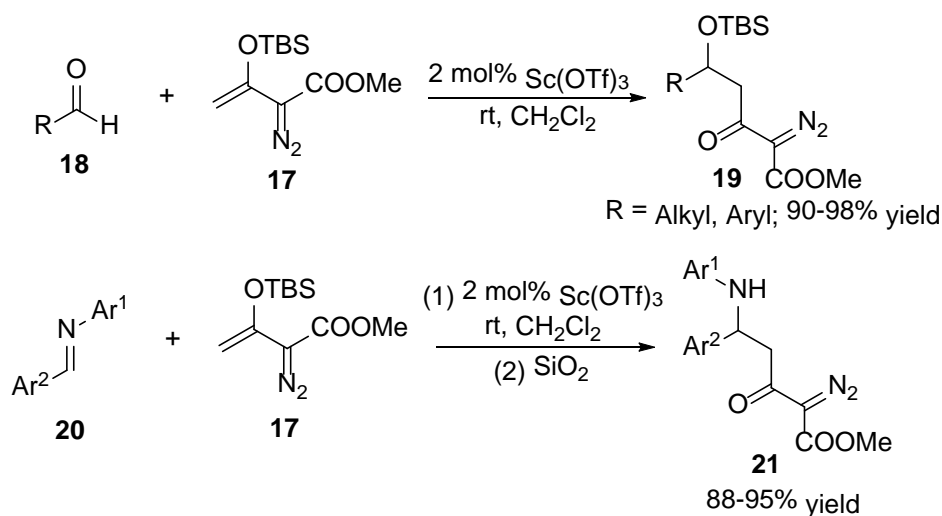
Scheme 3.6 Selectivity Reversal in Ti-promoted Addition of Ti-enol diazoacetate to α,β -Unsaturated Ketones.

1.3 Si-enol Diazoacetate in Nucleophilic Additions.

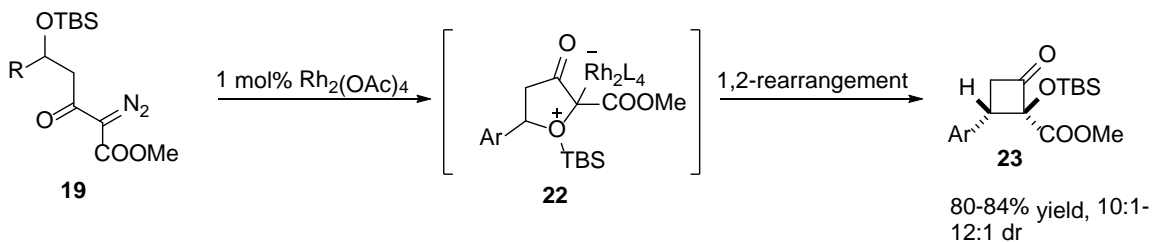
The use of Si-enol diazoacetate in nucleophilic addition reactions dates back to 1981.⁷ Since this initial report, several isolated studies have also emerged.¹⁵ It is from the recent efforts of Doyle and coworkers that systematic surveys of the behaviors of these highly valuable nucleophiles have become available.^{4,11,16-23} As stated previously, unlike Ti-enol diazoacetates, Si-enol diazoacetates are easy to handle and less susceptible to hydrolysis. Notably, for those reactions that involve Si-enol diazoacetates, intramolecular migration of silyl group often occurs and this feature, when coupled with the use of appropriate catalyst in the subsequent dinitrogen extrusion reaction, can yield totally unexpected reaction outcomes.²³

The Mukaiyama-Adol addition of Si-enol diazoacetate **17** to both aromatic and aliphatic aldehydes has been reported by Doyle in 2005 (**Scheme 3.7**).¹¹ In contrast to the previously established protocol which employs Ti-enol diazoacetate as the

substrate, the use of Si-enol diazoacetate **17** offers several advantages. First of all, as low as 2 mol% $\text{Sc}(\text{OTf})_3$ is sufficient to reach full conversion of the starting materials. Secondly, the reaction conditions are mild and operationally simple, while in $\text{Ti}(\text{O}i\text{-Pr})_4$ - or BF_3 -catalyzed reactions performing the reaction at -78°C is necessary to suppress byproduct generation. Finally, the resulting product, upon treatment with a catalytic amount of $\text{Rh}_2(\text{OAc})_4$, undergoes intramolecular oxonium ylide formation and subsequent 1,2-Stevens rearrangement with high diastereoselectivity (**Scheme 3.8**).



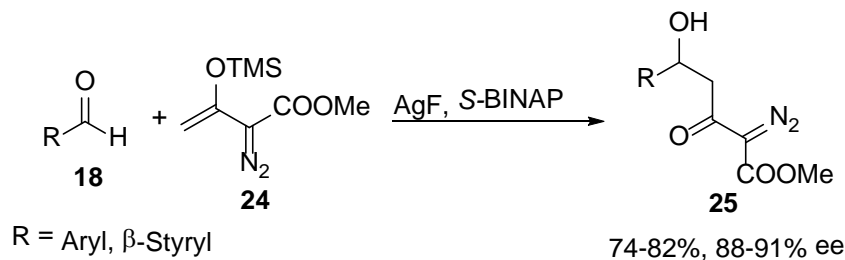
Scheme 3.7 $\text{Sc}(\text{OTf})_3$ -catalyzed Mukaiyama Aldol Addition of Si-enol Diazoacetate to Aldehydes and Imines.



Scheme 3.8 $\text{Rh}_2(\text{OAc})_4$ -Catalyzed Intramolecular Oxonium Ylide Formation/1,2-Stevens Rearrangement.

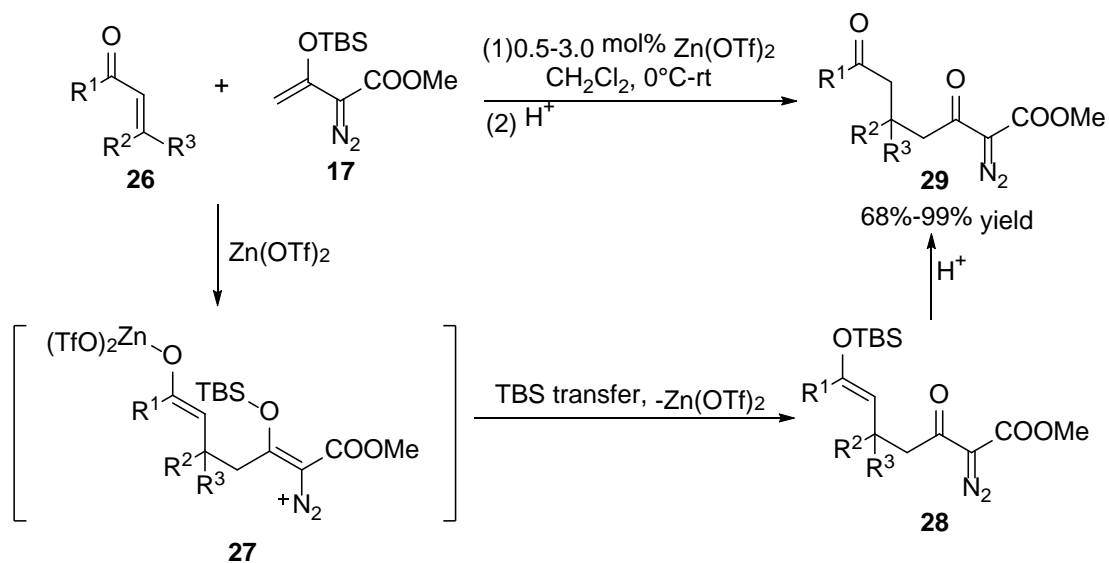
In an effort to render the catalytic Mukaiyama-Aldol addition reaction asymmetric, a quick survey of three asymmetric catalytic systems reveals that the

Ag/BINAP catalytic system can offer superior enantiocontrol.¹⁷ With the use of the more reactive TMS-enol diazoacetate in combination with fluoride activation, consistently good reaction yields could be obtained with aryl- and cinnmyl aldehyde at -20°C (**Scheme 3.9**).



Scheme 3.9 Catalytic Asymmetric Mukaiyama Aldol Reactions for TMS-enol Diazoacetate.

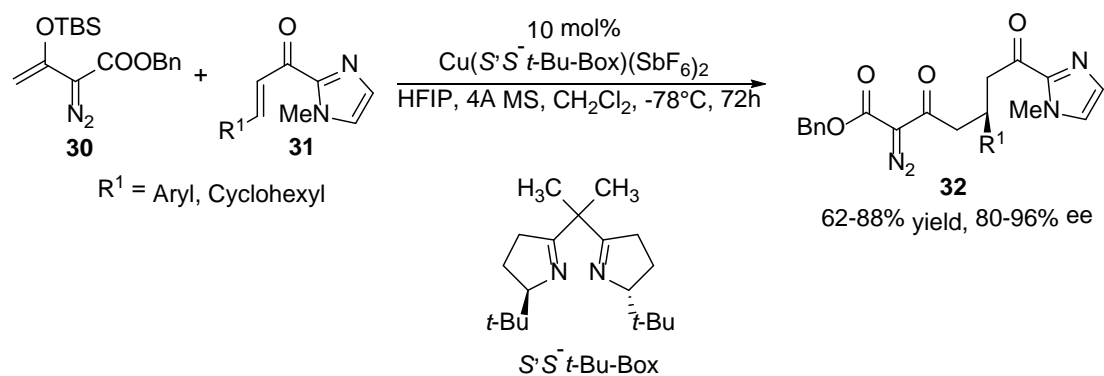
The Mukaiyama-Michael reaction is the condensation between silyl enol ethers and α,β -unsaturated carbonyl compounds and it represents a suitable extension of the Mukaiyama-Aldol reaction.¹⁸ Studies of the Mukaiyama Michael addition between cyclohexenone and TBS-enol diazoacetate **17** under Lewis acid catalysis suggest that $\text{Sc}(\text{OTf})_3$, the optimal catalyst for Mukaiyama-aldol reactions of TBS-enol diazoacetate, only provides moderate yields for the desired addition products after acidic workup. The sluggish reaction rate and proton desilylation of TBS-enol diazoacetate **17** to methyl diazoacetoacetate account for the moderate reaction yield. A survey of several mild Lewis acids identifies the inexpensive zinc(II) triflate as the preferred catalyst, which gives an improved yield to 79%. The use of excess TBS-enol diazoacetate **17** (1.5 equiv) further enhances the reaction yield to 96%. Notably, the catalyst loading of $\text{Zn}(\text{OTf})_2$ can be reduced to as low as 0.1 mol% while maintaining the excellent reaction yield (94%). The optimal reaction conditions are extended to a series of cyclic and acyclic enones with uniformly high reaction yields (**Scheme 3.10**).



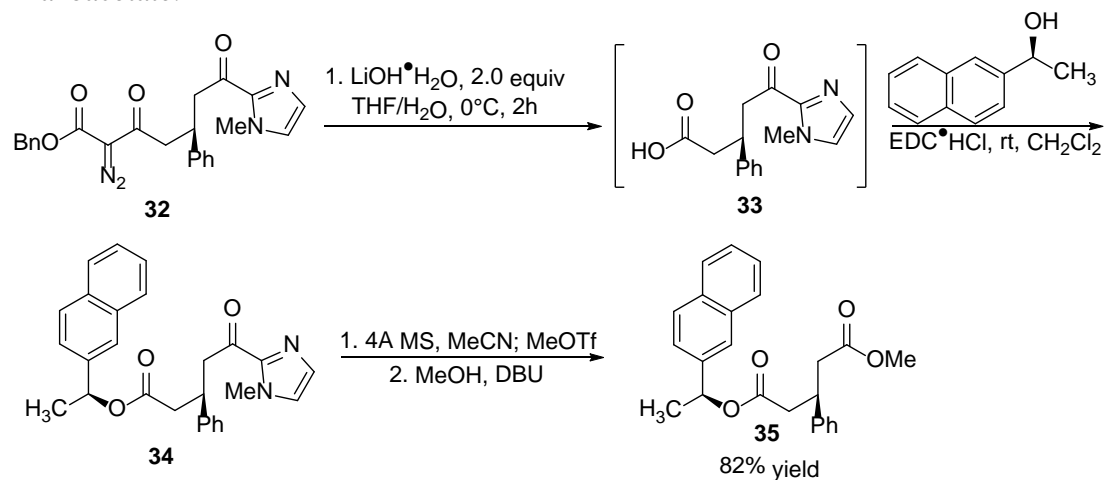
Scheme 3.10 Mukaiyama-Michael Addition of TBS-enol Diazoacetate to Cyclic and Acyclic enones.

Initial attempts to develop the asymmetric variant of the Mukaiyama-Michael addition reaction by the use of TBS-enol diazoacetate **17** and *N*-oxazolidinone-derivatized α,β -unsaturated carbonyl compounds were not successful with catalysis by several Cu(II)-based chiral Lewis acids.²¹ This lack of reactivity is attributed to the strong basicity of *N*-oxazolidinone group, but use of less basic α,β -unsaturated 2-acylimidazole **31** showed enhanced reactivity. After careful screening of a series of chiral bisoxazoline ligands, (*S,S*)-*t*-Bu-Box was identified to be the most effective one for enantiocontrol. Under the assistance of 1 equiv hexafluoroisopropyl alcohol, benzyl 3-(*tert*-butyldimethylsilyl)oxy-2-diazobut-3-enoate **30** gave exceptional enantioselectivity together with a good reaction yield (**Scheme 3.11**). This methodology has been demonstrated to be general applicable to a number of α,β -unsaturated 2-acylimidazoles with consistently high enantiocontrol. The synthesis of optical active 3-phenylpentanedioic acid diesters **35** was achieved by derivatization of

the resulting Mukaiyama-Michael addition product **32** without loss of enantioselectivity (**Scheme 3.12**).



Scheme 3.11 Catalytic Asymmetric Mukaiyama-Michael Addition of TBS-enol Diazoacetate.



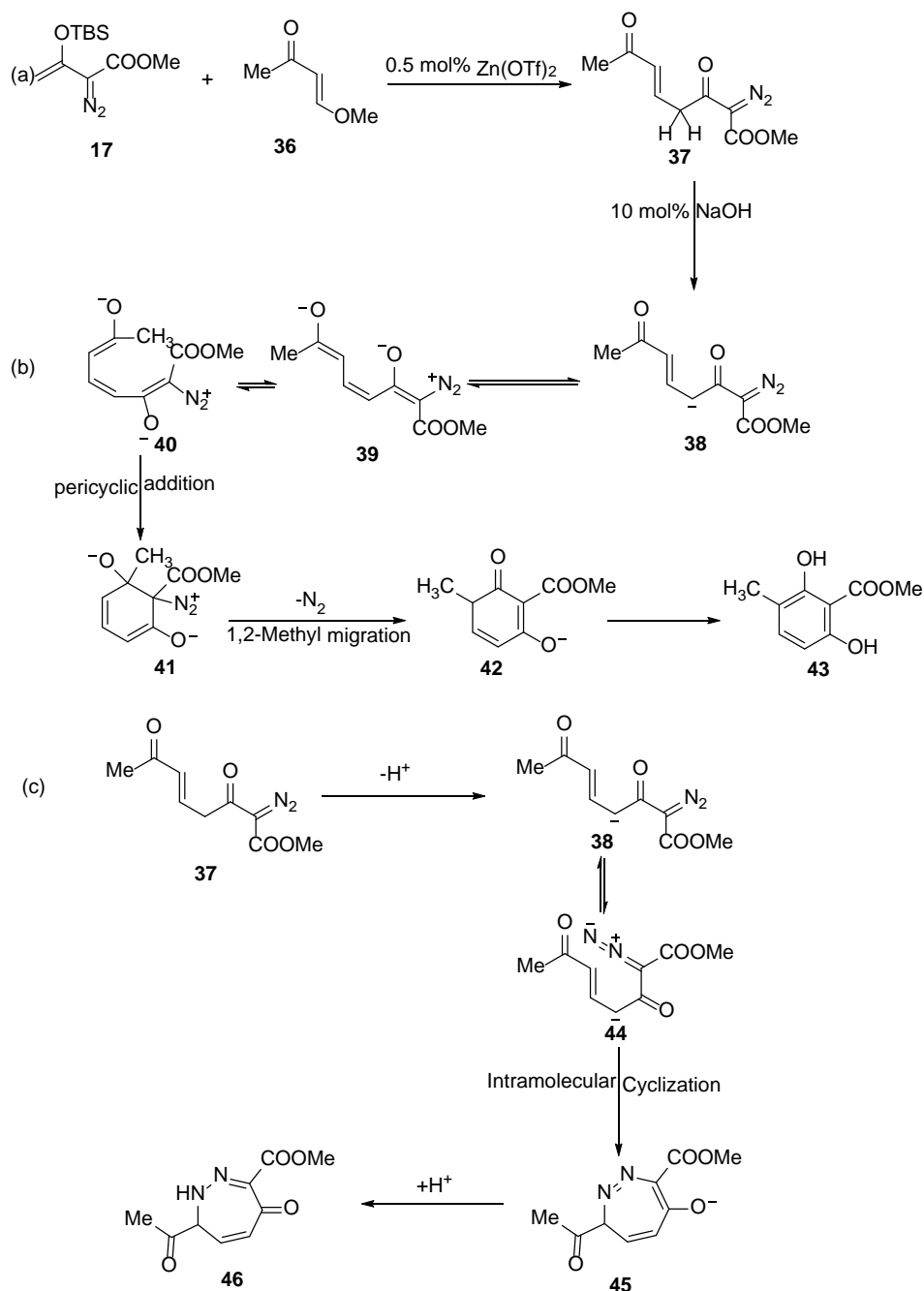
Scheme 3.12 Synthesis of Enantioenriched 3-Phenyl Pentanedioic Acid Diesters.

The outstanding synthetic power of the Mukaiyama-Michael addition using enol diazoacetates has enabled the construction of highly functionalized β -keto- α -diazo carbonyl compounds in a straightforward and efficient manner, and two recent intriguing examples of this kind have allowed for exceptionally rapid buildup of molecular complexity within only a few steps.^{4,16} The Lewis acid catalyzed addition of TBS-enol diazoacetate **17** to *trans*-4-methoxy-3-buten-2-one **36** affords the β -keto- α -diazoester **37** (**Scheme 3.13**).⁴ In the presence of a catalytic amount of NaOH, a

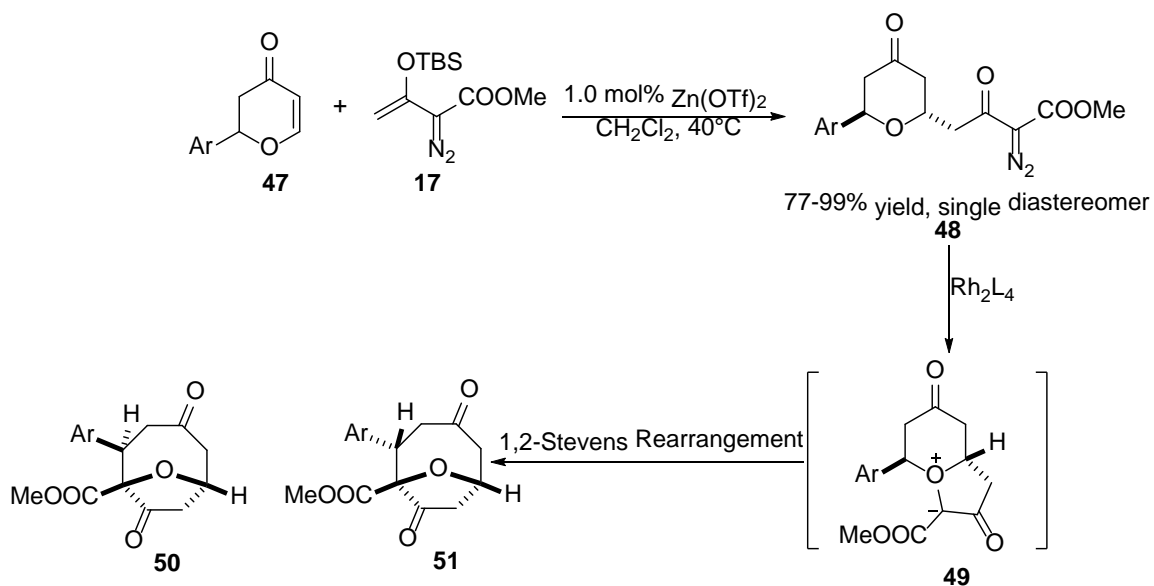
resorcinol product **43** is generated in high isolated yield. A plausible mechanistic proposal states that the conjugated enolate anion **38** generated by deprotonation of the most acidic proton by NaOH from β -keto- α -diazoester **37** is the key intermediate in this transformation. The conjugated enolate anion **38** isomerizes into the conjugated triene **40**, which is appropriately placed for pericyclization. The resulting diazonium ion intermediate **41** undergoes the dinitrogen extrusion with concomitant 1,2-methyl migration and eventually tautomerizes to the resorcinol product **43** in a good yield. Interestingly, when changing the methyl ester of the highly functionalized β -keto- α -diazoester to the corresponding isopropyl, *tert*-butyl, and benzyl ester, a 1,2-diazepine **46** is formed as a minor product. The formation of this product clearly comes from nucleophilic addition to the terminal nitrogen of the diazo group and subsequent rearrangement (**Scheme 3.13c**).

In another example, the Lewis acid catalyzed Mukaiyama Michael addition of TBS-enol diazoacetate **17** to pyranones **47** furnishes highly functionalized diazoester **48** with complete diastereoselectivity.¹⁶ Treating the diazoester with a catalytic amount of dirhodium catalyst forms an oxonium ylide intermediate, which undergoes a 1,2-Stevens rearrangement to produce highly functionalized oxabicyclo[4.2.1]nonane **50** and **51** (**Scheme 3.14**).

In these two examples access to highly functionalized diazoacetates would be very difficult without using the Lewis acid catalyzed Mukaiyama-Michael addition reaction. This approach to prepare highly functionalized diazoesters has great potential that is yet to be further explored.

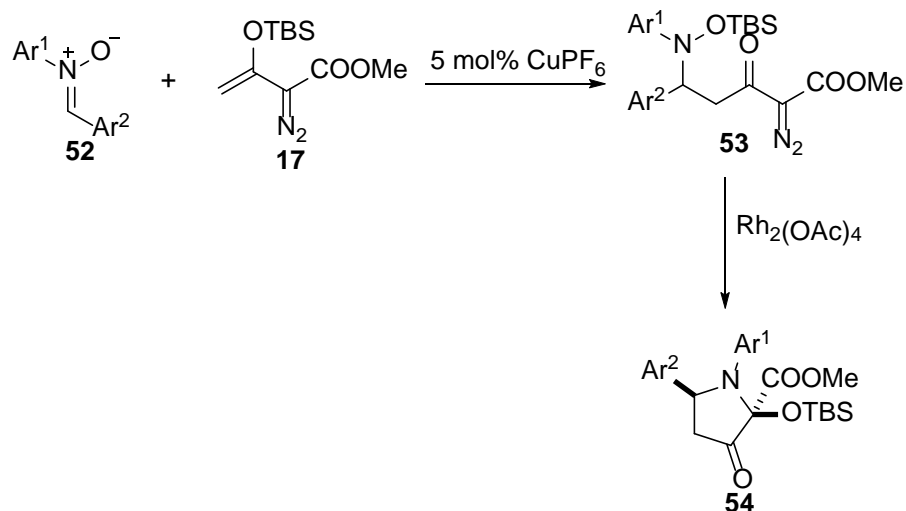


Scheme 3.13 (a) Mukaiyama-Michael Addition of TBS-enol Diazoacetate to *trans*-4-methoxy-3-buten-2-one. (b) NaOH-Catalyzed Denitrogenative Cyclization of Highly Functionalized β -Keto- α -diazoesters to Produce Resorcinol. (c) NaOH-Catalyzed Rearrangement of Highly Functionalized β -Keto- α -diazoesters to Furnish 1,2-Diazepine.

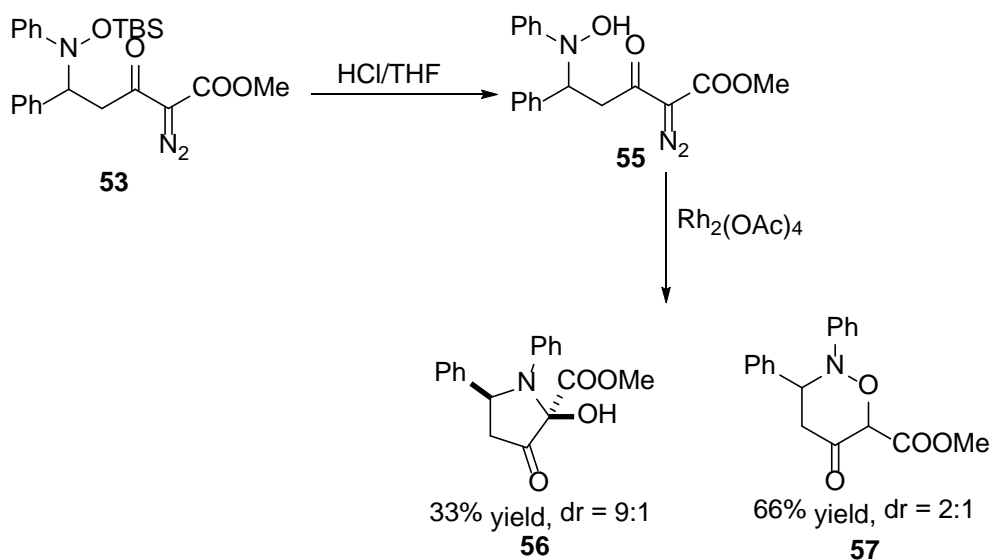


Scheme 3.14 Diastereoselective Mukaiyama Michael Addition of TBS-enol Diazoacetate to Pyranones, Dirhodium-catalyzed Oxonium Ylide Formation and 1,2-Stevens Rearrangement.

The use of diaryl nitron **52** as Mukaiyama-Mannich acceptor has also been studied. The reaction is effectively catalyzed by 5 mol% CuPF₆ at 0°C and catalytic dinitrogen extrusion of the resulting product **53** with Rh₂(OAc)₄ furnishes a substituted pyrrole **54** that could be formally viewed as coming from the N-O bond insertion of a rhodium carbene (**Scheme 3.15**).²³ The same reaction applied to the desilylated product **55** results mainly in the formation of the intramolecular OH-insertion product **57** with low diastereoselectivity (**Scheme 3.16**).



Scheme 3.15 Mukaiyama-Mannich Addition of TBS-enol Diazoacetate with Diaryl Nitrones and the Following Catalytic Formal N-O Insertion Reaction.



Scheme 3.16 Competitive OH-Insertion versus Formal N-O-Insertion.

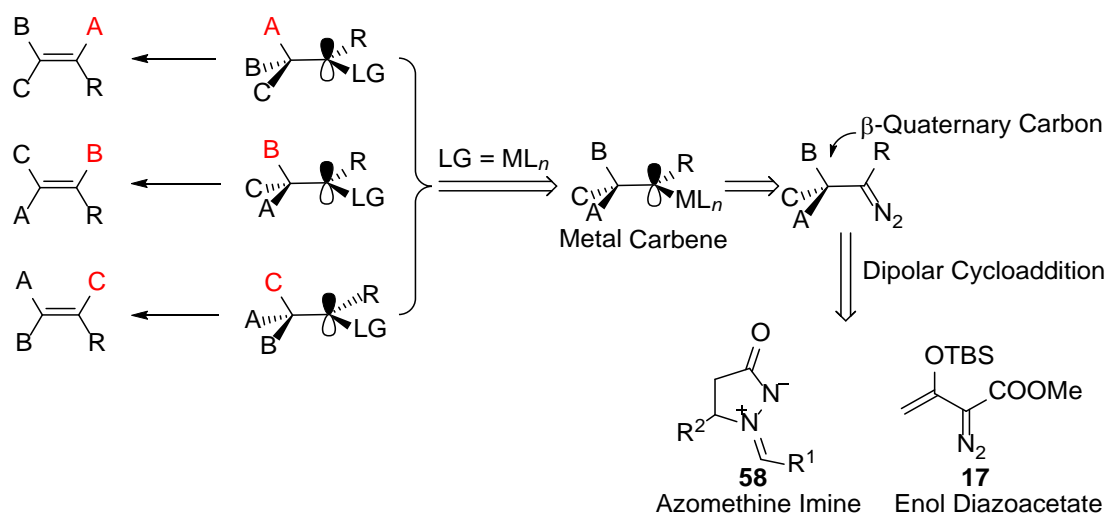
1.4 Research Proposal.

1,2-Migration to an electrophilic carbon center is a common transformation in organic chemistry that has been widely investigated for its intriguing mechanistic features²⁴⁻²⁷ and extensive occurrence in catalysis.²⁸⁻³² Among the reactions that

encompass these 1,2-migrations are the semipinacol rearrangement and its multiple variants,³³⁻³⁵ solvolysis reactions²⁷ that include Wagner-Meerwein rearrangements,³⁶⁻⁴⁰ ring-enlargement reactions⁴¹⁻⁴⁵ and, more recently, gold-catalyzed migrations.⁴⁶⁻⁵³ With free rotation around the C–C bond to the electrophilic carbon, migration of A, B, or C is dependent upon migratory aptitude as well as on the spacial positioning of the migrating group relative to the electrophilic center (**Scheme 3.17**).^{24,25,36,38} In general, although highly selective migrations are most desirable, competition between two migrating groups is commonly observed.^{26,26,33,35,42,43,48-50,52} In these reactions the product that is formed is dependent on the structure of the reactant,^{36,38,40} and external control of which group migrates has long been problematic.^{35,42,43,48-50,52} Catalytically generated metal carbenes from α -diazo carbonyl compounds are highly electrophilic, and 1,2-migration occurs if a saturated carbon is directly bonded to the carbene center.^{54,55} However, examples of catalyst-controlled migrations are rarely encountered,^{56,57} and effective catalyst-controlled selectivity in these transformations remains unsolved.⁵⁸

Reported results from Doyle and coworkers have presented diverse catalyst-dependent outcomes from reactions of enol diazoacetates with α,β -unsaturated aldehydes¹⁰ and with nitrones.¹¹ Could a catalytically generated metal carbene intermediate with an adjacent saturated carbon atom be induced by different catalysts to undergo selective 1,2-migration by each of its substituents? In order to answer this question, facile access to α -diazocompounds bearing β -quaternary carbons was the first objective. Inspired by the success of using enol diazoacetates in Lewis acid catalyzed reactions,¹² I envisioned that construction of α -diazo compounds could be

accomplished by [3+2]-cycloaddition of dipolar species and an enol diazoacetate (Scheme 3.17). Azomethine imines **58** are promising candidates since they are stable, easily accessible dipolar compounds and precursors for the synthesis of dinitrogen-fused heterocyclic rings,⁵⁹⁻⁶⁹ which display broad biological activities.⁷⁰⁻⁷² If the [3+2]-cycloaddition reactions of azomethine imines **58** with enol diazoacetate **17** indeed occur under Lewis acid catalysis, the resulting diazoester will have the β -quaternary carbon directly bound to carbon, nitrogen, and oxygen substituents that are poised to rearrange to an adjacent electrophilic carbon. With the use of different metal catalysts, direct migration by carbon, nitrogen, and oxygen substituents could be achieved with a high degree of selectivity to generate a diverse array of highly functionalized fused-ring heterocyclic compounds in an efficient and controllable manner.

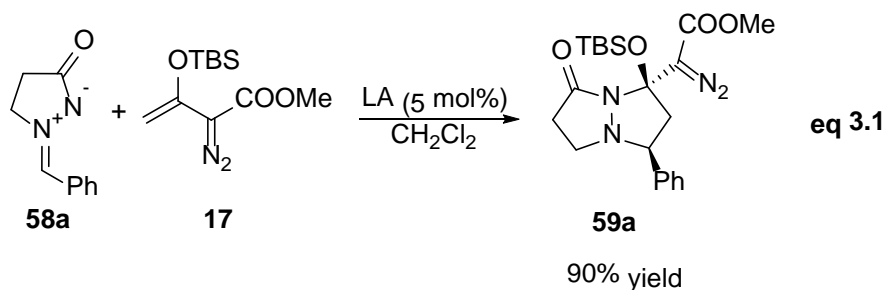


Scheme 3.17 Stereoelectronic Factors Influencing 1,2-Migration and the Strategy for the Synthesis of α -Diazoacetates Bearing β -Quaternary Carbons.

II. Results and Discussions

I initiated our study with the Lewis acid catalyzed reaction between azomethine imines **58** ($R^2 = H$) and enol diazoacetate **17** by using $Sc(OTf)_3$ (eq **3.1**). Highly

diastereoselective [3+2]-cycloaddition occurred with the pendant phenyl and TBSO groups *cis* as confirmed by X-ray analysis (**Figure 3.1**). Further investigations with 5-phenyl-azomethine imines **58** ($R^2 = \text{Ph}$) revealed that $\text{In}(\text{OTf})_3$ afforded a higher level of diastereoselectivity than $\text{Sc}(\text{OTf})_3$ (**Table 3.1**). As shown in **Table 3.2**, azomethine imines containing electron-withdrawing (entries 3, 9, 11 and 12) and electron-donating substituents (entries 2, 4, 5 and 10) on the phenyl rings afford the desired products in high isolated yields. Furthermore, substituents at the *para*- (entries 2-3, 5, 9-11), *meta*- (entry 12) and *ortho*- (entry 4) positions on the phenyl rings are well tolerated. Azomethine imines derived from cinnamaldehyde (entry 7) and from cyclohexylcarboxaldehyde (entries 6 and 13) show similar reactivity profiles as those derived from aromatic aldehydes, and all substrates shown in **Table 3.2** afford the cycloaddition products with complete diastereocontrol.



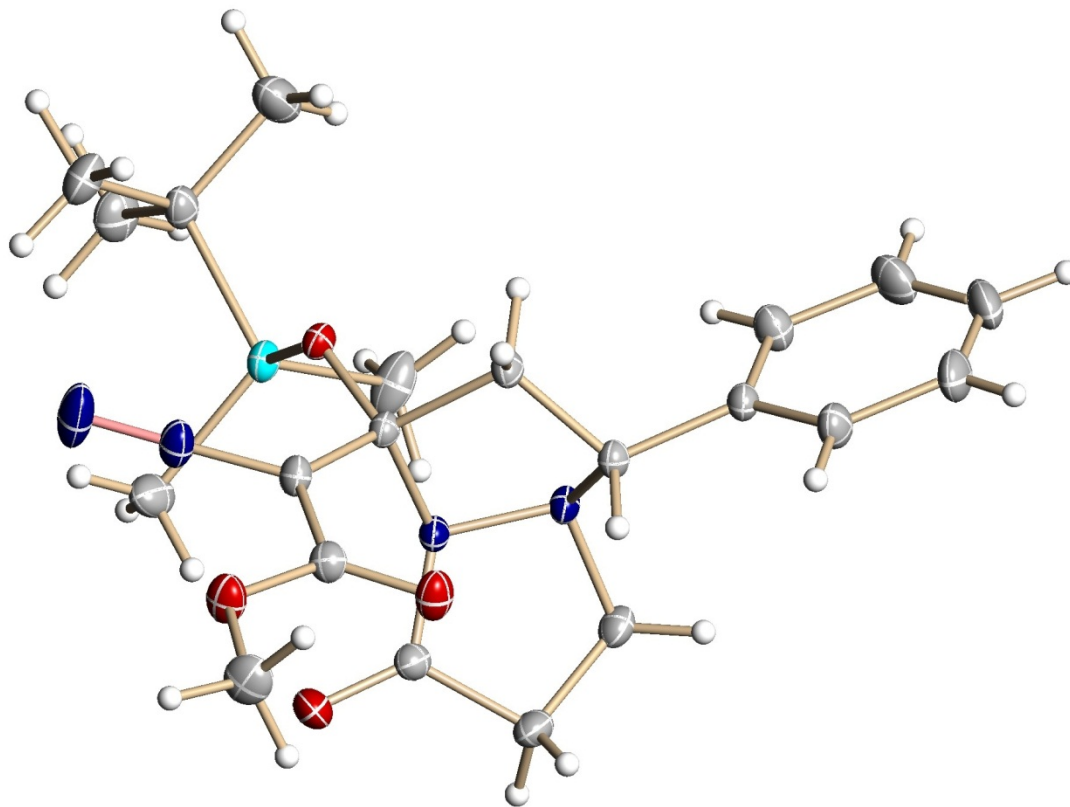
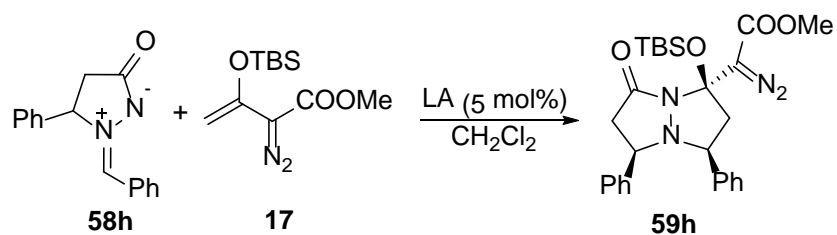


Figure 3.1 X-Ray Single Crystal Structure for **59a**.

Table 3.1 Lewis Acid Catalyst Screening for Formation of **59h** from **58h**.



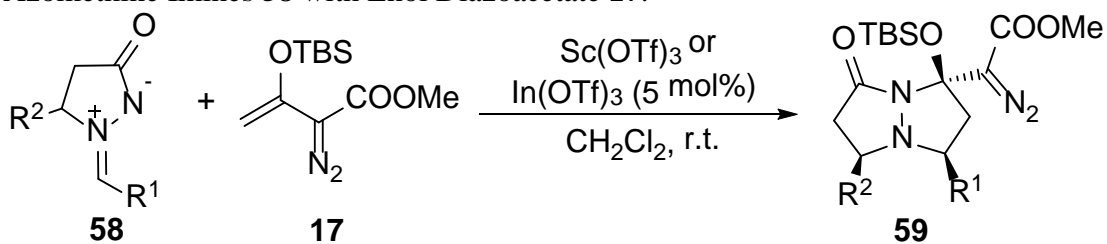
Entry ^a	Lewis acid	Time	Yield ^b	dr (<i>cis:trans</i>) ^c
1	Mg(OTf) ₂	12h	no reaction	--
2	Zn(OTf) ₂	3h	78%	>20:1
3	In(OTf) ₃	12h	81%	>20:1
4	Sc(OTf) ₃	12h	73%	~1:1
5	La(OTf) ₃	12h	68%	~1:1

6	Yb(OTf) ₃	12h	Trace	--
7	Cu(SbF ₆) ₂	3h	76%	>20:1

^aReaction performed with 0.25 mmol of azomethine imine **58** (1.0 eq) and enol diazoacetate **17** (1.8 eq) with 5 mol% Lewis acid in CH₂Cl₂ at room temperature.

^bYields reported are isolated yields. ^cdr is determined by ¹H NMR analysis of the reaction mixture.

Table 3.2 Lewis Acid Catalyzed Diastereoselective [3+2]-Cycloaddition of Azomethine Imines **58** with Enol Diazoacetate **17**.



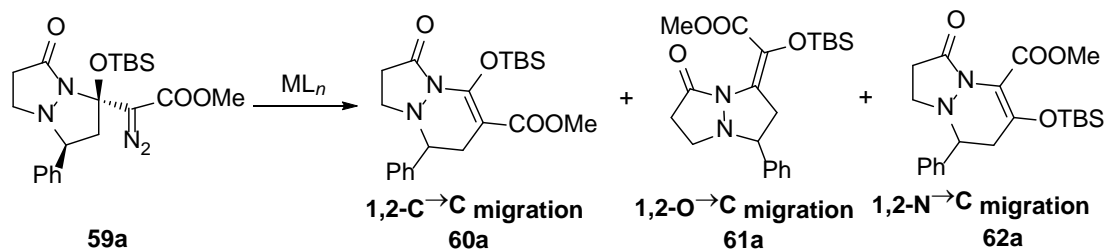
entry ^a	R ¹	R ²	59 ^d	yield, % ^e
1 ^b	Ph	H	59a	90
2 ^b	4-MeC ₆ H ₄	H	59b	74
3 ^b	4-ClC ₆ H ₄	H	59c	78
4 ^b	2-MeOC ₆ H ₄	H	59d	65
5 ^b	4-MeOC ₆ H ₄	H	59e	69
6 ^b	Cyclohexyl	H	59f	80
7 ^b	(<i>E</i>)-Ph-CH=CH-	H	59g	67
8 ^c	Ph	Ph	59h	81
9 ^c	4-NO ₂ C ₆ H ₄	Ph	59i	66
10 ^c	4-MeOC ₆ H ₄	Ph	59j	71
11 ^c	4-BrC ₆ H ₄	Ph	59k	78
12 ^c	3-BrC ₆ H ₄	Ph	59l	72

^aReaction performed with 0.25 mmol of azomethine imine **58** (1.0 equiv) and enol diazoacetate **17** (1.8 equiv) in CH₂Cl₂ for 12h at room temperature. ^b5 mol% Sc(OTf)₃ used as catalyst. ^c5 mol% In(OTf)₃ used as catalyst. ^dSingle diastereomer obtained. ^eIsolated yields.

Having prepared highly functionalized α -diazoacetates **59** bearing quaternary carbons at the β -positions, I next investigated their transition-metal catalyzed dinitrogen extrusion and subsequent rearrangement of the catalytically generated metal carbene intermediates, and these results are reported in **Table 3.3**. In the reaction of **59a** with Rh₂(OAc)₄ three products were obtained in 90% combined yield, and these were determined by X-ray diffraction and/or spectroscopically to be those from 1,2-C \rightarrow C migration (**60a**, 58%), stereoselective 1,2-O \rightarrow C migration (**61a**, 25%) and 1,2-N \rightarrow C migration (**62a**, 17%). Using the more Lewis acidic Rh₂(tfa)₄ (entry 2) and Rh₂(pfb)₄ (entry 3) under the same conditions showed that the 1,2-N \rightarrow C migration pathway was inhibited in favor of 1,2-C \rightarrow C and -O \rightarrow C migrations with approximately 3:1 selectivity. In contrast, performing this reaction with the less Lewis acidic Rh₂(cap)₄ in ClCH₂CH₂Cl at 80°C revealed that both the 1,2-N \rightarrow C and 1,2-O \rightarrow C migration pathways were suppressed, and 1,2-C \rightarrow C migration was dominant (entry 4). In a control experiment, where the same reaction was conducted with Rh₂(OAc)₄ (entry 5) under otherwise identical conditions as that with Rh₂(cap)₄, comparable selectivity to the reaction performed in CH₂Cl₂ at 40°C (entry 1) was shown but with much lower selectivity than with Rh₂(cap)₄ (entry 4). The use of Rh₂(piv)₄ and Rh₂(esp)₂ that contain sterically bulky ligands gave high selectivities for both 1,2-N \rightarrow C and 1,2-O \rightarrow C migrations (entries 6 and 7). In contrast, copper and silver catalysts display

distinctive and virtually exclusive selectivity for 1,2-N→C migration (entries 8-11) compared with dirhodium complexes. Thus, catalysts derived from different metals (Rh and Cu) direct competitive 1,2-C→C and 1,2-N→C migration pathways with high selectivities, and the 1,2-C→C migration product **60a** and the 1,2-N→C migration product **62a** can be obtained with high yields under catalysis of Rh₂(cap)₄ and CuPF₆ respectively. 1,2-C→C and 1,2-O→C migrations appear to be linked, but highly selective catalyst-directed 1,2-O→C migration could not be achieved with **59a**.

Table 3.3 Catalyst Screening with **59a** for Selective 1,2-C→C, -O→C and -N→C Migrations.



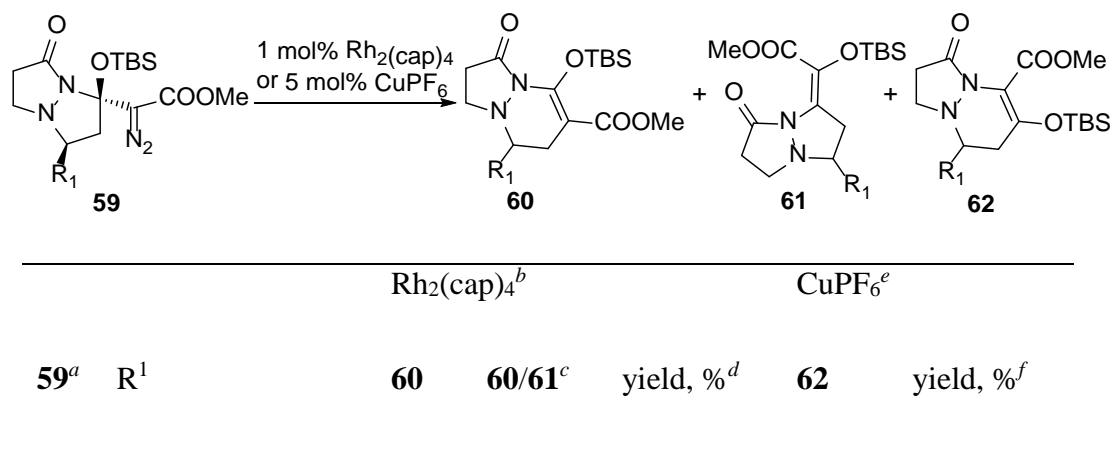
entry ^a	catalyst	temp	solvent	time, h	60a : 61a ^d : 62a ^e	yield, % ^f
1 ^b	Rh ₂ (OAc) ₄	40°C	CH ₂ Cl ₂	3	58:25:17	90
2 ^b	Rh ₂ (tfa) ₄	40°C	CH ₂ Cl ₂	3	78:22:–	94
3 ^b	Rh ₂ (pfb) ₄	40°C	CH ₂ Cl ₂	3	71:29:–	91
4 ^b	Rh ₂ (cap) ₄	80°C	(CH ₂ Cl) ₂	3	78:9:13	93
5 ^b	Rh ₂ (OAc) ₄	80°C	(CH ₂ Cl) ₂	3	61:25:14	85
6 ^b	Rh ₂ (piv) ₄	40°C	CH ₂ Cl ₂	3	12:39:49	82

7 ^b	Rh ₂ (esp) ₂	40°C	CH ₂ Cl ₂	3	20:39:41	87
8 ^c	Cu(OTf) ₂	rt	CH ₂ Cl ₂	12	–:–:100	70
9 ^c	Cu(hfacac) ₂	rt	CH ₂ Cl ₂	12	9: –:91	88
10 ^c	AgBF ₄	rt	CH ₂ Cl ₂	12	–:–:100	40
11 ^c	CuPF ₆	rt	CH ₂ Cl ₂	12	–:–:100	86

^aReaction performed with 0.1 mmol of **59a**. ^b1 mol% Rh₂L_n catalyst was used. ^c5 mol% catalyst was used. ^d**61a** was obtained as the (*E*)-configuration exclusively. ^eRatios determined by ¹H NMR analysis of reaction mixtures. ^fYields reported are combined yields of **60a**, **61a** and **62a**.

The influence of R¹ on the selective 1,2-C→C migration catalyzed by Rh₂(cap)₄ and the 1,2-N→C migration catalyzed by CuPF₆ was investigated, and these results are summarized in **Table 3.4**. Reactions performed with CuPF₆ as catalyst uniformly afford the 1,2-N→C migration product, and Rh₂(cap)₄ promotes the 1,2-C→C migration process with high selectivities but without significant dependence on R¹.

Table 3.4 Selective 1,2-C→C and -N→C migrations of **59** catalyzed by Rh₂(cap)₄ and CuPF₆.



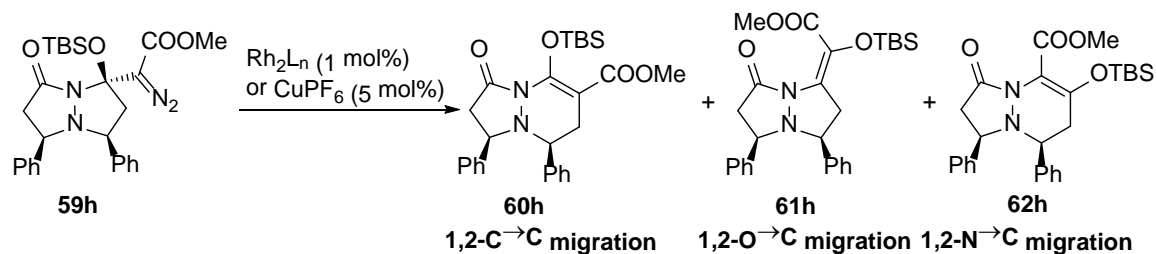
59a	Ph	60a	85:15	85	62a	86
59b	4-MeC ₆ H ₄	60b	89:11	81	62b	85
59c	4-ClC ₆ H ₄	60c	88:12	83	62c	80
59d	2-MeOC ₆ H ₄	60d	81:19	79	62d	86
59e	4-MeOC ₆ H ₄	60e	88:12	86	62e	78
59f	Cyclohexyl	60f	87:13	88	62f	77
59g	(<i>E</i>)-Ph-CH=CH-	60g	86:14	85	62g	84

^aReaction performed with 0.1 mmol of **59**. ^bReaction performed with 1.0 mol% of Rh₂(cap)₄ in ClCH₂CH₂Cl at 80°C for 3h. ^cRatios determined by ¹H NMR analysis of crude reaction mixtures. ^dYields reported are combined (**60**+**61**) yields. ^eReaction performed with 5 mol% of CuPF₆ in CH₂Cl₂ for 12h at room temperature. ^fYields reported are isolated yields of **60**.

In an effort to selectively achieve 1,2-C→C migration, 1,2-O→C migration, and 1,2-N→C migration with different catalysts, diazoacetate **59h**, which has an additional phenyl group on the pyrazolidinone ring, was subjected to the same series of catalytic reactions (**Table 3.5**). With 1 mol% of Rh₂(OAc)₄, the formation of the 1,2-C→C migration product **60h** and the stereoselective 1,2-O→C migration product **61h** occurred without evidence for formation of the 1,2-N→C migration product **62h** (eq 4). Once again, Rh₂(cap)₄ selected the 1,2-C→C migration pathway (entry 6), and CuPF₆ effected exclusive 1,2-N→C migration (entry 9). Consistent with entries 6 and 7 in **Table 3.3**, but more dramatic, increasing the steric size of the ligand by using Rh₂(piv)₄ (entry 4) significantly enhances the reaction selectivity towards the formation

of the 1,2-O→C migration product **61h**, and this outcome is mirrored with the use of Rh₂(esp)₄ (entry 5) but in higher overall yield. Hence, by simply changing the ligand attachments to the dirhodium centers, the competing 1,2-C→C and 1,2-O→C migrations become dominant through the catalysis by Rh₂(esp)₂ [or Rh₂(piv)₄] and Rh₂(cap)₄, respectively; and the 1,2-O→C migration product **62h**, which was not detected in dirhodium complex catalyzed reactions, was the sole migration outcome with catalysis by CuPF₆. In addition, as shown in **Table 3.6**, these reactions have the same selectivities irrespective of the electronic nature of the substituents on the phenyl ring of R¹ even when cyclohexyl is used in place of aryl.

Table 3.5 Catalyst Screening with **59h** for Selective 1,2-C→C, -O→C and -N→C Migrations.



entry ^a	catalyst	solvent	time, h	60h:61h^d:62h^e	yield, % ^f
1 ^b	Rh ₂ (OAc) ₄	CH ₂ Cl ₂	3	60:40:–	91
2 ^b	Rh ₂ (Oct) ₄	CH ₂ Cl ₂	3	43:57:–	88
3 ^b	Rh ₂ (OBz) ₄	CH ₂ Cl ₂	3	25:75:–	82
4 ^b	Rh ₂ (piv) ₄	CH ₂ Cl ₂	3	12:88:–	74
5 ^b	Rh ₂ (esp) ₂	CH ₂ Cl ₂	3	15:85:–	88
6 ^b	Rh ₂ (cap) ₄	(CH ₂ Cl) ₂	1	91:9:–	86

7 ^b	Rh ₂ (tfa) ₄	CH ₂ Cl ₂	3	69:31:–	81
8 ^b	Rh ₂ (pfb) ₄	CH ₂ Cl ₂	3	64:36:–	79
9 ^c	CuPF ₆	CH ₂ Cl ₂	12	–:–:100	72

^aReactions performed with 0.1 mmol of **59h**. ^bReaction performed with 1.0 mol% of Rh₂L_n as catalyst. ^cReaction performed with 5.0 mol% CuPF₆. ^d**61h** was obtained in the (*E*)-configuration exclusively. ^eRatio determined by ¹H NMR analysis of crude reaction mixture. ^fYields reported are combined yields of **60h**, **61h** and **62h**.

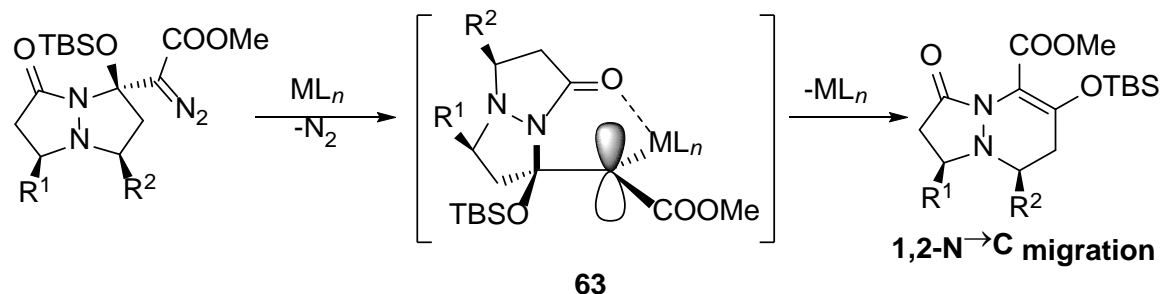
Table 3.6 Substrate Scope for Ligand-induced Divergent 1,2-C→C and -O→C Migrations.

		Rh ₂ (cap) ₄ ^b			Rh ₂ (esp) ₂ ^c		
59^a	R ¹	60	60/61^d	Yield, % ^e	61^f	60/61^d	Yield, % ^e
59h	Ph	60h	91:9	91%	61h	15:85	88%
59i	4-NO ₂ C ₆ H ₄	60i	97:3	90%	61i	16:84	86%
59j	4-MeOC ₆ H ₄	60j	96:4	92%	61j	17:83	85%
59k	4-BrC ₆ H ₄	60k	93:7	93%	61k	10:90	85%

59l	3-BrC ₆ H ₄	60l	88:12	91%	61l	14:86	82%
59m	Cyclohexyl	60m	75:25	86%	61m	15:85	92%

^aReaction performed with 0.1 mmol of **59** with 1.0 mol% Rh₂L_n as catalyst. ^bReaction performed in ClCH₂CH₂Cl at 80°C for 1h. ^cReaction performed in CH₂Cl₂ at room temperature for 3h. ^dRatios determined by ¹H NMR analysis of crude reaction mixture. ^eYields reported are combined yields of **60** and **61**. ^f**61** was obtained in the (*E*)-configuration exclusively.

Competition between formation of **60** (1,2-C→C migration) and **61** (1,2-O→C migration) is linked in dirhodium catalyzed reactions, and the causes for selectivity may be attributed to the steric [e.g., results with Rh₂(piv)₄ and Rh₂(esp)₂] and electronic [results with Rh₂(cap)₄] factors. However, the unexpected 1,2-N→C migration from **59**, which is formally an amide nitrogen migration, stands out as exceptionally favourable when copper, rather than dirhodium, catalysts are employed. This heightened selectivity for **62** may be due to coordination of the copper carbene intermediate with the carbonyl oxygen of the pyrazolidinone ring (**63** in Scheme 3.18) – a complexation that is not expected with the coordinatively saturated dirhodium complexes.¹⁶ Consequently, the overall 1,2-N→C migration is facilitated by transition metal catalysts with open coordination sites.



Scheme 3.18 Directing Effect in Cu-catalyzed 1,2-N→C Migration.

III. Conclusion

In summary, I have discovered catalyst-controlled highly selective 1,2-C→C, -O→C and -N→C migrations of β -methylene- β -silyloxy- β -amido- α -diazoacetates. The key to achieving this unique display of differential selectivities relies on steric and stereoelectronic control by their catalytically generated metal carbenes. These rearrangement reactions produce a variety of highly functionalized dinitrogen-fused heterocyclic compounds.

IV. Experimental Section

4.1 General Information

Experiments involving moisture and/or air sensitive components were performed in oven-dried glassware under a nitrogen atmosphere using freshly distilled solvents. CH_2Cl_2 and $\text{ClCH}_2\text{CH}_2\text{Cl}$ were dried over activated molecular sieves and distilled prior to use. Commercial reagents and solvents (hexanes and ethyl acetate) were used without further purification. Thin layer chromatography (TLC) was carried out using EM Science silica gel 60 F254 plates. The chromatogram was analyzed by UV lamp (254 nm), or by development using cerium ammonium molybdate (CAM). Liquid chromatography was performed using a forced flow (flash chromatography) of the indicated system on silica gel (230-400 mesh). Proton nuclear magnetic resonance spectra (^1H NMR) were recorded on a Bruker AMX 400 spectrophotometer (in CDCl_3 as solvent). Chemical shifts for ^1H NMR spectra are reported as δ in units of parts per million (ppm) downfield from SiMe_4 ($\delta = 0.00$) and relative to the signal of chloroform-*d* ($\delta = 7.26$, singlet). Multiplicities were given as: s (singlet); d (doublet); t (triplet); q

(quartet); dd (doublet of doublets); ddd (doublet of doublet of doublets); dddd (doublet of doublet of doublet of doublets); dt (doublet of triplets); m (multiplet). The number of protons (n) for a given resonance is indicated by nH. Coupling constants are reported as a *J* value in Hz. Carbon nuclear magnetic resonance spectra (¹³C NMR) are reported as δ in units of parts per million (ppm) downfield from SiMe₄ (δ = 0.00) and relative to the signal of chloroform-*d* (δ = 77.00, triplet). High-resolution mass spectra (HRMS) were obtained on a JEOL AccuTOF-ESI mass spectrometer using CsI as the standard. Sc(OTf)₃, In(OTf)₃, Cu(OTf)₂, Cu(hfacac)₂, CuPF₆(CH₃CN)₄, AgBF₄, Rh₂(esp)₄ were purchased from Aldrich. Rh₂(OAc)₄ was purchased from Pressure chemicals. Azomethine imines **58a-m**⁵⁹⁻⁶⁹ and enol diazoacetate **17**^{4,5} were prepared according to known procedures.

4.2 Experimental Procedure

General Procedure for Diastereoselective [3+2]-Cycloaddition of Azomethine Imines (58a-58g) and Enol Diazoacetate 2. In a 10 ml flame-dried Schlenk flask charged with a magnetic stirring bar, Sc(OTf)₃ (6.2 mg, 0.0125 mmol), azomethine imine **58a** (43.5 mg, 0.25 mmol) and 1.0 mL dry CH₂Cl₂ were added sequentially under a nitrogen atmosphere. Then the flask was capped by a rubber septum and the resulting solution was stirred at room temperature for 5 min before enol diazoacetate **17** (116.0 mg, 0.45 mmol) was added. Stirring was continued at room temperature for 12h. Then the reaction mixture was concentrated under reduced pressure and directly loaded onto a silica gel column (with 1:5 of ethyl acetate/hexanes as eluents) to isolate product **59a** as a yellow solid in 97.0 mg (90% yield).

General Procedure for the Diastereoselective [3+2]-Cycloaddition of Azomethine Imines (58h-58m) and Enol Diazoacetate 17: In a 10 ml flame-dried Schlenk flask charged with a magnetic stirring bar, In(OTf)₃ (7.0 mg, 0.0125 mmol), azomethine imine **58h** (62.5 mg, 0.25 mmol) and 1.0 mL dry CH₂Cl₂ were added sequentially under a nitrogen atmosphere. The flask was capped by a rubber septum and the resulting solution was stirred at room temperature for 5 min before enol diazoacetate **17** (116.0 mg, 0.45 mmol) was added. Stirring was continued at room temperature for 12h. Then the reaction mixture was concentrated under reduced pressure and directly loaded onto a silica gel column (with 1:7 of ethyl acetate/hexanes as eluents) to isolate product **59h** as a yellow solid in 103.0 mg (81% yield).

General Procedure for Rh₂(cap)₄ Catalyzed 1,2-C→C Migration: Rh₂(cap)₄ (0.7 mg, 0.001mmol) was added to a 5 ml flame-dried two-neck round-bottom flask under a nitrogen atmosphere. Then the flask was fitted with a condenser and a rubber septum, and 1.0 mL of dry CH₂Cl₂ was added through the septum. The resulting solution was heated to 80°C under a nitrogen atmosphere and a solution of diazoacetate **59a** (43.0 mg, 0.1 mmol) in 1.0 mL of dry CH₂Cl₂ was then added through the septum over 1h by syringe pump. After completion of addition, the reaction mixture was stirred for another 3h under reflux. Then the solution was cooled to room temperature, and solvent was removed under reduced pressure. The desired 1,2-C→C migration product **60a** was obtained by flash column chromatography (with 1:10 of ethyl acetate/hexanes as eluent) as a white solid (29.3 mg, 72% yield).

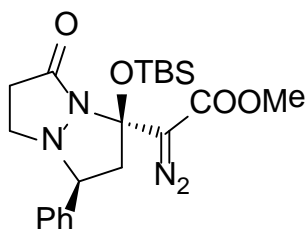
General Procedure for Rh₂(esp)₂ Catalyzed Selective 1,2-O→C Migrations: Rh₂(esp)₂ (0.8 mg, 0.001 mmol) was added to a flame-dried vial charged

with a magnetic stirring bar under a nitrogen atmosphere. The vial was then capped with a rubber septum, and 1.0 mL of dry CH₂Cl₂ was added to the vial. The resulting solution was stirred while a solution of diazoacetate **59a** (50.7 mg, 0.1 mmol) in 1.0 mL of dry dichloromethane was added over 1h by syringe pump. After completion of addition, the reaction mixture was stirred for another 3h at room temperature. The reaction product **61a** was obtained by flash column chromatography (with 1:5 of ethyl acetate/hexanes as eluents) in 38.0 mg (75% yield) as a white solid.

General Procedure for CuPF₆ Catalyzed Selective 1,2-N→C Migrations:

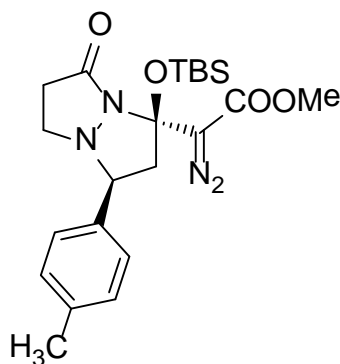
CuPF₆ (1.0 mg, 0.005 mmol) was added to a flame-dried vial under a nitrogen atmosphere. Then the vial was capped by a rubber septum and 1.0 mL of dry CH₂Cl₂ was added. The resulting solution was stirred while a solution of diazoacetate **59a** (43.0 mg, 0.1 mmol) in 1.0 mL of dry dichloromethane was added by syringe pump over 1h at room temperature. After completion of addition, the reaction mixture was stirred for another 12h at room temperature. The desired 1,2-N→C migration product **62a** was obtained by flash column chromatography (1:3 of ethyl acetate/hexanes as eluent) in 35.0 mg (86% yield) as a white solid.

4.3 Characterization Data

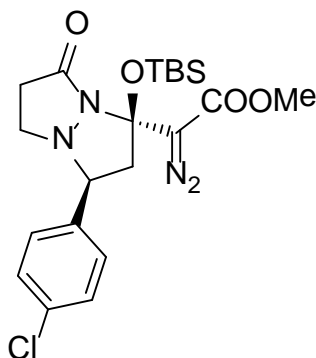


Methyl 2-[(1R,3S)-1-(tert-Butyldimethylsilyl)oxy-7-oxo-3-phenylhexahydro-1H-pyrazolo[1,2-a]pyrazol-1-yl]-2-diazoacetate (59a**):** 90% yield, ¹H NMR

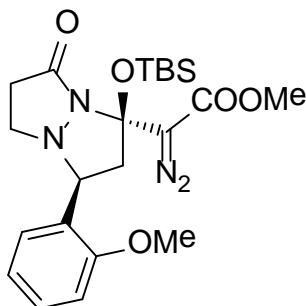
(400 MHz, CDCl₃) δ : 7.51 – 7.43 (m, 2H), 7.43 – 7.29 (m, 3H), 4.44 (dd, $J = 11.2, 6.8$ Hz, 1H), 3.78 (s, 3H), 3.46 (ddd, $J = 9.8, 8.3, 4.8$ Hz, 1H), 3.23 (dd, $J = 13.5, 6.8$ Hz, 1H), 2.91 (ddd, $J = 11.2, 9.8, 8.9$ Hz, 1H), 2.83 – 2.68 (m, 2H), 2.62 (dd, $J = 13.5, 11.2$ Hz, 1H), 0.90 (s, 9H), 0.39 (s, 3H), 0.23 (s, 3H). ¹³C NMR (100 MHz, CDCl₃) δ : 166.6, 165.3, 138.1, 128.7, 127.9, 127.2, 83.2, 70.7, 55.9, 51.4, 49.3, 34.8, 25.6, 17.9, -3.3, -4.2. HRMS (ESI⁺): calcd for C₂₁H₃₁N₄O₄Si [M+H]⁺ 431.2115, found 431.2121.



Methyl 2-[(1R,3S)-1-(*tert*-Butyldimethylsilyloxy)-7-oxo-3-(*p*-tolyl)-hexahydro-pyrazolo[1,2-*a*]pyrazol-1-yl]-2-diazoacetate (59b): 74% yield, ¹H NMR (400 MHz, CDCl₃) δ : 7.36 (d, $J = 8.0$ Hz, 2H), 7.20 (d, $J = 8.0$ Hz, 2H), 4.40 (dd, $J = 11.2, 6.8$ Hz, 1H), 3.78 (s, 3H), 3.45 (ddd, $J = 9.7, 8.3, 4.9$ Hz, 1H), 3.21 (dd, $J = 13.5, 6.8$ Hz, 1H), 2.90 (dt, $J = 11.2, 9.7$ Hz, 1H), 2.79-2.67 (m, 2H), 2.61 (dd, $J = 13.5, 11.2$ Hz, 1H), 2.37 (s, 3H), 0.90 (s, 9H), 0.39 (s, 3H), 0.23 (s, 3H). ¹³C NMR (100 MHz, CDCl₃) δ : 166.5, 165.2, 137.7, 135.0, 129.4, 127.2, 83.2, 70.5, 55.9, 51.4, 49.3, 34.9, 25.6, 21.0, 17.9, -3.3, -4.2. HRMS (ESI⁺): calcd for C₂₂H₃₃N₄O₄Si [M+H]⁺ 445.2271, found 445.2283.

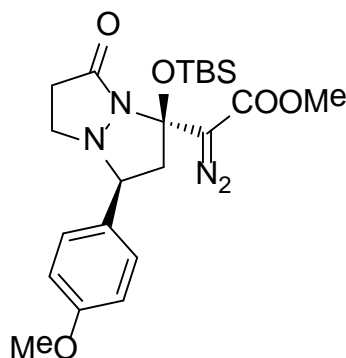


Methyl 2-[(1RS,3SR)-1-(*tert*-Butyldimethylsilyloxy)-3-(4-chlorophenyl)-7-oxo-hexahydropyrazolo[1,2-a]pyrazol-1-yl]-2-diazoacetate (59c): 78% yield, ^1H NMR (400 MHz, CDCl_3) δ : 7.41 (d, $J = 8.7$ Hz, 2H), 7.36 (d, $J = 8.7$ Hz, 2H), 4.43 (dd, $J = 11.0, 6.8$ Hz, 1H), 3.78 (s, 3H), 3.46 (ddd, $J = 10.0, 8.3, 4.8$ Hz, 1H), 3.21 (dd, $J = 13.5, 6.8$ Hz, 1H), 2.89 (dt, $J = 11.0, 10.0$ Hz, 1H), 2.83-2.68 (m, 2H), 2.56 (dd, $J = 13.5, 11.0$ Hz, 1H), 0.90 (s, 9H), 0.37 (s, 3H), 0.22 (s, 3H). ^{13}C NMR (100 MHz, CDCl_3) δ : 166.6, 165.4, 136.7, 133.7, 129.0, 128.6, 83.3, 70.0, 56.0, 51.5, 49.3, 34.8, 25.6, 18.0, -3.2, -4.1. HRMS (ESI $^+$): calcd for $\text{C}_{21}\text{H}_{30}\text{ClN}_4\text{O}_4\text{Si}$ $[\text{M}+\text{H}]^+$ 465.1725, found 465.1759.

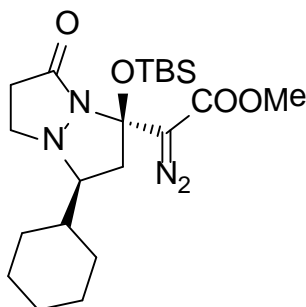


Methyl 2-[(1RS,3SR)-1-(*tert*-Butyldimethylsilyloxy)-3-(2-methoxyphenyl)-7-oxohexahydropyrazolo[1,2-a]pyrazol-1-yl]-2-diazoacetate (59d): 65% yield, ^1H NMR (400 MHz, CDCl_3) δ : 7.64 (dd, $J = 7.6, 1.4$ Hz, 1H), 7.27 (td, $J = 8.2, 1.4$ Hz, 1H), 7.00 (td, $J = 7.6, 0.8$ Hz, 1H), 6.88 (dd, $J = 8.2, 0.8$ Hz, 1H), 4.72 (dd, $J = 11.0,$

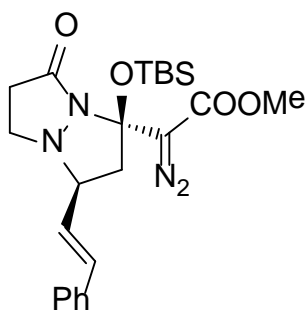
7.0 Hz, 1H), 3.83 (s, 3H), 3.79 (s, 3H), 3.53 (ddd, $J = 10.0, 7.0, 5.6$ Hz, 1H), 3.39 (dd, $J = 13.6, 7.0$ Hz, 1H), 2.88 (dt, $J = 11.0, 10.0$ Hz, 1H), 2.78-2.64 (m, 2H), 2.44 (dd, $J = 13.5, 11.0$ Hz, 1H), 0.85 (s, 9H), 0.30 (s, 3H), 0.21 (s, 3H). ^{13}C NMR (100 MHz, CDCl_3) δ : 166.6, 165.6, 157.8, 128.7, 127.4, 126.8, 121.1, 110.7, 83.4, 64.9, 55.8, 54.2, 51.9, 50.5, 35.7, 26.0, 18.4, -2.9, -3.7. HRMS (ESI+): calcd for $\text{C}_{22}\text{H}_{33}\text{N}_4\text{O}_5\text{Si}$ $[\text{M}+\text{H}]^+$ 461.2220, found 461.2242.



Methyl 2-[(1RS,3SR)-1-(*tert*-Butyldimethylsilyl)oxy-3-(4-methoxyphenyl)-7-oxohexahydropyrazolo[1,2-a]pyrazol-1-yl]-2-diazoacetate (59e): 69% yield, ^1H NMR (400 MHz, CDCl_3) δ : 7.38 (d, $J = 8.8$ Hz, 2H), 6.91 (d, $J = 8.8$ Hz, 2H), 4.37 (dd, $J = 11.2, 6.7$ Hz, 1H), 3.82 (s, 3H), 3.78 (s, 3H), 3.43 (ddd, $J = 9.7, 8.8, 4.7$ Hz, 1H), 3.18 (dd, $J = 13.5, 6.7$ Hz, 1H), 2.89 (ddd, $J = 11.2, 9.7, 8.8$ Hz, 1H), 2.81-2.66 (m, 2H), 2.60 (dd, $J = 13.5, 11.2$ Hz, 1H), 0.90 (s, 9H), 0.39 (s, 3H), 0.22 (s, 3H). ^{13}C NMR (100 MHz, CDCl_3) δ : 167.0, 165.8, 159.8, 130.3, 128.9, 114.5, 83.6, 70.7, 56.4, 55.7, 51.9, 49.6, 35.3, 26.0, 18.4, -2.8, -3.7. HRMS (ESI+): calcd for $\text{C}_{22}\text{H}_{33}\text{N}_4\text{O}_5\text{Si}$ $[\text{M}+\text{H}]^+$ 461.2220, found 461.2231.

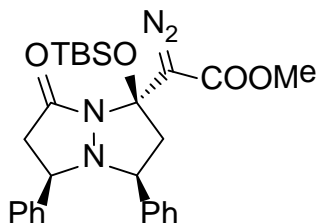


Methyl 2-[(1R,3SR)-1-(*tert*-Butyldimethylsilyloxy)-3-cyclohexyl-7-oxo-hexahydropyrazolo[1,2-a]pyrazol-1-yl]-2-diazoacetate (59f): 80% yield, ^1H NMR (400 MHz, CDCl_3) δ : 3.74 (s, 3H), 3.60 (td, $J = 8.8, 1.8$ Hz, 1H), 3.07 (dt, $J = 10.6, 7.1$ Hz, 1H), 3.03-2.83 (m, 2H), 2.74 (ddd, $J = 16.0, 13.1, 8.8$ Hz, 1H), 2.60 (ddd, $J = 16.0, 8.8, 1.8$ Hz, 1H), 2.39 (dd, $J = 13.1, 10.6$ Hz, 1H), 1.94-1.64 (m, 5H), 1.54-1.39 (m, 1H), 1.36-1.08 (m, 3H), 1.10-0.94 (m, 2H), 0.89 (s, 9H), 0.30 (s, 3H), 0.16 (s, 3H). ^{13}C NMR (100 MHz, CDCl_3) δ : 165.1, 164.7, 82.1, 72.4, 53.7, 51.4, 50.6, 41.0, 36.0, 30.8, 29.1, 26.4, 26.1, 26.1, 25.6, 18.0, -3.4, -4.2. HRMS (ESI $^+$): calcd for $\text{C}_{21}\text{H}_{37}\text{N}_4\text{O}_4\text{Si}$ $[\text{M}+\text{H}]^+$ 437.2584, found 437.2563.

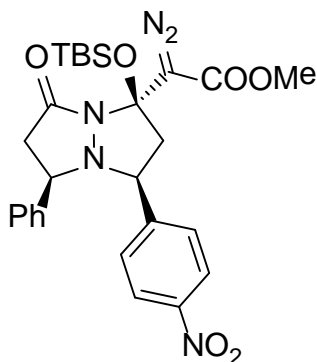


Methyl 2-[(1R,3SR)-1-(*tert*-Butyldimethylsilyloxy)-7-oxo-3-((*E*)-styryl)-hexahydropyrazolo[1,2-a]pyrazol-1-yl]-2-diazoacetate (59g): 67% yield, ^1H NMR (400 MHz, CDCl_3) δ : 7.48-7.24 (m, 5H), 6.68 (d, $J = 15.9$ Hz, 1H), 6.07 (dd, $J = 15.9, 8.4$ Hz, 1H), 3.99 (dt, $J = 10.8, 7.7$ Hz, 1H), 3.78 (s, 3H), 3.53 (ddd, $J = 9.8, 8.4, 4.6$ Hz, 1H), 3.09 (dd, $J = 13.6, 6.9$ Hz, 1H), 2.97 (ddd, $J = 10.8, 9.8, 9.0$ Hz, 1H), 2.81-

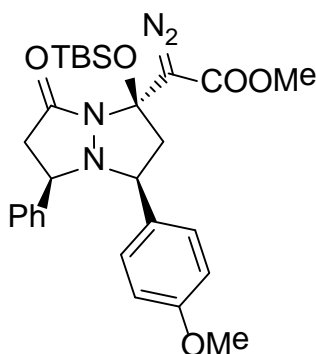
2.61 (m, 2H), 2.56 (dd, $J = 13.6, 10.8$ Hz, 1H), 0.91 (s, 9H), 0.37 (s, 3H), 0.20 (s, 3H).
 ^{13}C NMR (100 MHz, CDCl_3) δ : 166.8, 165.8, 136.7, 134.2, 129.1, 128.4, 127.0, 126.9, 83.4, 70.3, 53.5, 51.9, 49.8, 35.4, 26.2, 26.1, 25.9, 18.4, -2.9, -3.7. HRMS (ESI+): calcd for $\text{C}_{23}\text{H}_{33}\text{N}_4\text{O}_4\text{Si}$ $[\text{M}+\text{H}]^+$ 457.2271, found 457.2296.



Methyl 2-[(1R,3SR,5RS)-1-(*tert*-Butyldimethylsilyl)oxy-7-oxo-3,5-diphenyl-hexahydropyrazolo[1,2-a]pyrazol-1-yl]-2-diazoacetate (59h): 81% yield, ^1H NMR (CDCl_3 , 400 MHz) δ : 7.25-7.23 (m, 2H), 7.20-7.17 (m, 2H), 7.14-7.07 (m, 6H), 4.66 (dd, $J = 11.6, 7.2$ Hz, 1H), 4.28 (dd, $J = 11.6, 8.8$ Hz, 1H), 3.84 (s, 3H), 3.27 (dd, $J = 14.0, 7.2$ Hz, 1H), 3.09 (dd, $J = 16.8, 8.8$ Hz, 1H), 2.92 (dd, $J = 16.8, 11.6$ Hz, 1H), 2.74 (dd, $J = 14.0, 11.6$ Hz, 1H), 0.94 (s, 9H), 0.49 (s, 3H), 0.35 (s, 3H); ^{13}C NMR (CDCl_3 , 100 MHz) δ : 165.4, 164.8, 139.1, 137.5, 128.1, 128.1, 127.7, 127.6, 127.6, 127.4, 82.8, 71.9, 68.7, 65.2, 56.3, 51.6, 44.4, 25.7, 18.1, -3.0, -4.0; HRMS (ESI+): calcd for $\text{C}_{27}\text{H}_{35}\text{N}_4\text{O}_4\text{Si}$ $[\text{M}+\text{H}]^+$ 507.2428, found 507.2428.



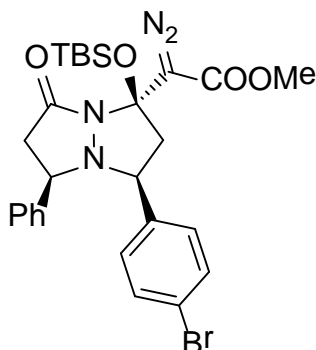
Methyl 2-[(1*RS*,3*SR*,5*RS*)-1-(*tert*-Butyldimethylsilyl)oxy-3-(4-nitrophenyl)-7-oxo-5-phenylhexahydropyrazolo[1,2-*a*]pyrazol-1-yl]-2-diazoacetate (59i): 66% yield, ¹H NMR (CDCl₃, 400 MHz) δ: 7.93 (d, *J* = 8.8 Hz, 2H), 7.37 (d, *J* = 8.8 Hz, 2H), 7.20-7.13 (m, 5H), 4.80 (dd, *J* = 11.6, 7.2 Hz, 1H), 4.27 (dd, *J* = 12.4, 8.4 Hz, 1H), 3.83 (s, 3H), 3.31 (dd, *J* = 11.6, 7.2 Hz, 1H), 3.02-2.95 (m, 2H), 2.64 (dd, *J* = 12.4, 11.2 Hz, 1H), 0.92 (s, 9H), 0.46 (s, 3H), 0.33 (s, 3H); ¹³C NMR (CDCl₃, 100 MHz) δ: 165.5, 164.4, 147.2, 145.5, 138.1, 128.4, 128.3, 128.2, 127.5, 123.3, 82.7, 70.8, 69.8, 65.1, 56.3, 51.6, 44.4, 25.6, 18.0, -3.0, -4.0; HRMS (ESI⁺): calcd for C₂₇H₃₄N₅O₆Si [M+H]⁺ 552.2278, found 552.2283.



Methyl 2-[(1*RS*,3*SR*,5*RS*)-1-(*tert*-Butyldimethylsilyl)oxy-3-(4-methoxyphenyl)-7-oxo-5-phenylhexahydropyrazolo[1,2-*a*]pyrazol-1-yl]-2-diazoacetate (59j): 71% yield, ¹H NMR (CDCl₃, 400 MHz) δ: 7.17-7.11 (m, 7H), 6.64 (d, *J* = 8.8 Hz, 2H), 4.60 (dd, *J* = 11.6, 6.8 Hz, 1H), 4.26 (dd, *J* = 10.0, 8.4 Hz, 1H), 3.82 (s, 3H), 3.70 (s, 3H), 3.22 (dd, *J* = 10.0, 6.8 Hz, 1H), 3.08 (dd, *J* = 16.4, 8.4 Hz, 1H), 2.89 (dd, *J* = 16.4, 11.6 Hz, 1H), 2.70 (dd, *J* = 13.6, 11.2 Hz, 1H), 0.93 (s, 9H), 0.47 (s, 3H), 0.32 (s, 3H); ¹³C NMR (CDCl₃, 100 MHz) δ: 165.4, 164.9, 159.0, 139.3, 129.4, 128.8, 128.1,

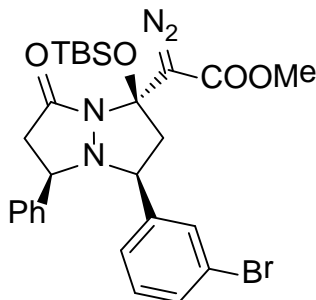
127.5, 127.3, 113.5, 82.8, 71.4, 68.3, 65.2, 56.2, 55.2, 51.5, 44.3, 25.7, 18.0, -3.0, -4.0;

HRMS (ESI+): calcd for C₂₈H₃₇N₄O₅Si [M+H]⁺ 537.2533, found 537.2542.



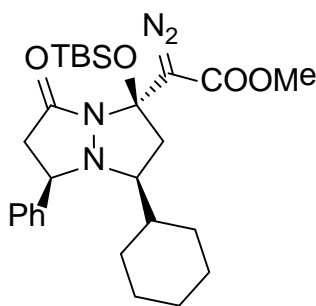
Methyl 2-[(1RS,3SR,5RS)-3-(4-Bromophenyl)-1-(*tert*-butyldimethylsilyl)-oxy-7-oxo-5-phenylhexahydropyrazolo[1,2-a]pyrazol-1-yl]-2-diazoacetate (59k):

78% yield, ¹H NMR (CDCl₃, 400 MHz) δ: 7.21-7.15 (m, 7H), 7.09 (d, *J* = 8.8 Hz, 2H), 4.63 (dd, *J* = 11.6, 7.6 Hz, 1H), 4.24 (dd, *J* = 12.4, 8.4 Hz, 1H), 3.82 (s, 3H), 3.25 (dd, *J* = 16.4, 7.6 Hz, 1H), 3.07 (dd, *J* = 16.4, 8.4 Hz, 1H), 2.93 (dd, *J* = 16.4, 11.6, Hz, 1H), 2.63 (dd, *J* = 16.4, 12.4, Hz, 1H), 0.92 (s, 9H), 0.45 (s, 3H), 0.32 (s, 3H); ¹³C NMR (CDCl₃, 100 MHz) δ: 165.9, 165.1, 139.2, 137.2, 134.9, 131.6, 129.6, 128.7, 128.3, 127.8, 121.8, 116.3, 83.2, 71.5, 69.3, 65.5, 56.7, 52.0, 44.7, 26.0, 18.4, -2.6, -3.6; HRMS (ESI+): calcd for C₂₇H₃₄BrN₄O₄Si [M+H]⁺ 585.1533, found 585.1499.



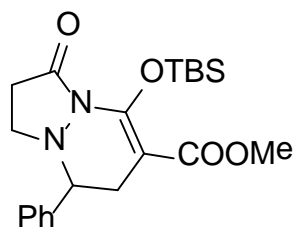
Methyl 2-[(1*RS*,3*SR*,5*RS*)-3-(3-Bromophenyl)-1-(*tert*-butyldimethylsilyl)-oxy-7-oxo-5-phenylhexahydropyrazolo[1,2-*a*]pyrazol-1-yl]-2-diazoacetate (59l):

72% yield, ^1H NMR (CDCl_3 , 400 MHz) δ : 7.38 (s, 1H), 7.23-7.11 (m, 7H), 6.96 (t, $J = 8.0$ Hz, 1H), 4.63 (dd, $J = 11.6, 7.2$ Hz, 1H), 4.25 (dd, $J = 11.6, 8.4$ Hz, 1H), 3.83 (s, 3H), 3.27 (dd, $J = 11.6, 7.2$ Hz, 1H), 3.03 (dd, $J = 16.4, 8.4$ Hz, 1H), 2.93 (dd, $J = 16.4, 8.4$ Hz, 1H), 2.67 (dd, $J = 16.4, 11.6$ Hz, 1H), 0.93 (s, 9H), 0.47 (s, 3H), 0.34 (s, 3H); ^{13}C NMR (CDCl_3 , 100 MHz) δ : 165.4, 164.5, 140.1, 138.5, 130.8, 130.6, 129.6, 128.2, 128.0, 127.5, 126.0, 122.1, 82.7, 71.0, 69.3, 56.2, 51.6, 44.4, 25.6, 18.0, -3.0, -4.0; HRMS (ESI $^+$): calcd for $\text{C}_{27}\text{H}_{34}\text{BrN}_4\text{O}_4\text{Si}$ $[\text{M}+\text{H}]^+$ 585.1533, found 585.1499.

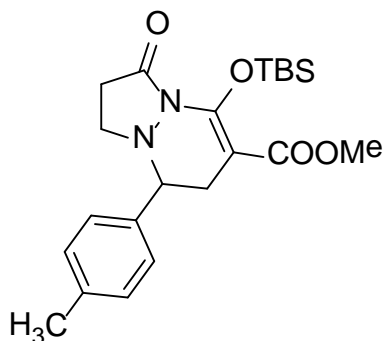


Methyl 2-[(1*RS*,3*SR*,5*RS*)-1-(*tert*-Butyldimethylsilyl)oxy-3-cyclohexyl-7-oxo-5-phenylhexahydropyrazolo[1,2-*a*]pyrazol-1-yl]-2-diazoacetate (59m): 56%

yield, ^1H NMR (CDCl_3 , 400 MHz) δ : 7.48-7.46 (m, 2H), 7.39-7.29 (m, 3H), 4.19 (dd, $J = 12.4, 8.0$ Hz, 1H), 3.75 (s, 3H), 3.46-3.40 (m, 1H), 2.96 (dd, $J = 12.4, 8.0$ Hz, 1H), 2.80-2.73 (m, 2H), 2.51 (dd, $J = 13.2, 7.2$ Hz, 1H), 1.66-1.50 (m, 5H), 1.04-0.75 (m, 15H), 0.40 (s, 3H), 0.27 (s, 3H); ^{13}C NMR (CDCl_3 , 100 MHz) δ : 165.2, 163.8, 140.2, 128.5, 128.0, 127.4, 82.4, 72.4, 70.3, 65.1, 51.4, 47.3, 45.9, 37.7, 30.6, 26.5, 26.5, 26.4, 25.8, 25.7, 18.0, -3.1, -4.1; HRMS (ESI $^+$): calcd for $\text{C}_{27}\text{H}_{41}\text{N}_4\text{O}_4\text{Si}$ $[\text{M}+\text{H}]^+$ 513.2897, found 513.2856.

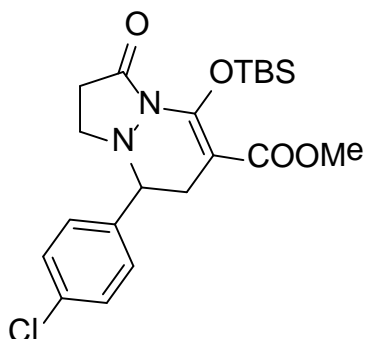


Methyl 5-(*tert*-Butyldimethylsilyloxy)-3-oxo-8-phenyl-2,3,7,8-tetrahydro-1H-pyrazolo[1,2-a]pyridazine-6-carboxylate (60b): 72% yield; ^1H NMR (400 MHz, CDCl_3) δ : 7.48-7.31 (m, 5H), 3.72 (s, 3H), 3.65 (dd, $J = 9.9, 4.6$ Hz, 1H), 3.22 (ddd, $J = 11.2, 8.7, 6.7$ Hz, 1H), 2.87-2.77 (m, 2H), 2.70 (dd, $J = 16.9, 9.9$ Hz, 1H), 2.63-2.33 (m, 2H), 1.07 (s, 9H), 0.25 (s, 3H), 0.23 (s, 3H). ^{13}C NMR (100 MHz, CDCl_3) δ : 171.0, 167.7, 149.0, 139.8, 129.4, 128.9, 128.3, 94.3, 66.6, 51.4, 47.3, 35.6, 31.5, 26.1, 18.7, -3.9, -3.8. HRMS (ESI⁺): calcd for $\text{C}_{21}\text{H}_{31}\text{N}_2\text{O}_4\text{Si}$ $[\text{M}+\text{H}]^+$ 403.2053, found 403.2060.

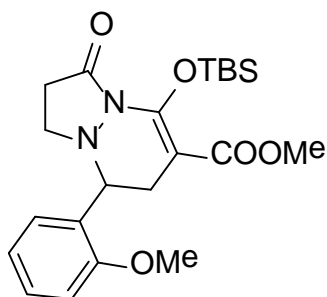


Methyl 5-(*tert*-Butyldimethylsilyloxy)-3-oxo-8-(*p*-tolyl)-2,3,7,8-tetrahydro-1H-pyrazolo[1,2-a]pyridazine-6-carboxylate (60b): 72% yield, ^1H NMR (400 MHz, CDCl_3) δ : 7.24 (d, $J = 8.3$ Hz, 2H), 7.20 (d, $J = 8.3$ Hz, 2H), 3.72 (s, 3H), 3.62 (dd, $J = 9.8, 4.6$ Hz, 1H), 3.21 (ddd, $J = 11.2, 8.7, 6.6$ Hz, 1H), 2.90-2.74 (m, 2H), 2.69 (dd, $J = 16.9, 9.8$ Hz, 1H), 2.60-2.41 (m, 2H), 2.38 (s, 3H), 1.07 (s, 9H), 0.25 (s, 3H), 0.23 (s, 3H). ^{13}C NMR (100 MHz, CDCl_3) δ : 171.0, 167.8, 148.9, 138.7, 136.7, 130.0, 128.2,

94.3, 66.3, 51.4, 47.2, 35.5, 31.6, 26.1, 21.6, 18.7, -3.79, -3.82. HRMS (ESI+): calcd for C₂₂H₃₃N₂O₄Si [M+H]⁺ 417.2210, found 417.2203.

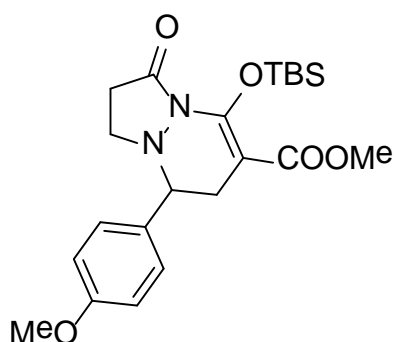


Methyl 5-(*tert*-Butyldimethylsilyloxy)-8-(4-chlorophenyl)-3-oxo-2,3,7,8-tetrahydro-1H-pyrazolo[1,2-a]pyridazine-6-carboxylate (60c): 73% yield, ¹H NMR (400 MHz, CDCl₃) δ: 7.38 (d, *J* = 8.0 Hz, 2H), 7.30 (d, *J* = 8.0 Hz, 2H), 3.72 (s, 3H), 3.64 (dd, *J* = 10.0, 4.5 Hz, 1H), 3.22 (ddd, *J* = 11.1, 8.7, 6.6 Hz, 1H), 2.80 (m, 2H), 2.64 (dd, *J* = 16.8, 10.0 Hz, 1H), 2.60-2.40 (m, 2H), 1.07 (s, 9H), 0.25 (s, 3H), 0.23 (s, 3H). ¹³C NMR (100 MHz, CDCl₃) δ: 170.7, 167.6, 149.0, 138.3, 134.7, 129.6, 129.6, 94.0, 65.9, 51.5, 47.3, 35.6, 31.5, 26.1, 18.7, -3.79, -3.81. HRMS (ESI+): calcd for C₂₁H₃₀ClN₂O₄Si [M+H]⁺ 437.1663, found 437.1689.

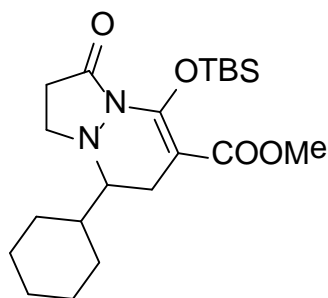


Methyl 5-(*tert*-Butyldimethylsilyloxy)-8-(2-methoxyphenyl)-3-oxo-2,3,7,8-tetrahydro-1H-pyrazolo[1,2-a]pyridazine-6-carboxylate (60d): 64% yield, ¹H NMR (400 MHz, CDCl₃) δ: 7.38 (dd, *J* = 7.6, 1.7 Hz, 1H), 7.35-7.27 (m, 1H), 7.03 (td,

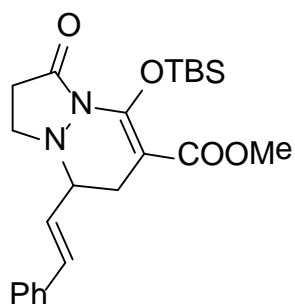
$J = 7.6, 0.9$ Hz, 1H), 6.93 (dd, $J = 8.3, 0.9$ Hz, 1H), 4.34 (dd, $J = 9.9, 4.6$ Hz, 1H), 3.86 (s, 3H), 3.72 (s, 3H), 3.28 (ddd, $J = 11.4, 8.6, 7.8$ Hz, 1H), 2.90 (ddd, $J = 11.4, 8.6, 6.8$ Hz, 1H), 2.76 (dd, $J = 16.8, 4.6$ Hz, 1H), 2.69-2.54 (m, 2H), 2.52-2.33 (m, 1H), 1.07 (s, 9H), 0.26 (s, 3H), 0.25 (s, 3H). ^{13}C NMR (100 MHz, CDCl_3) δ : 172.1, 167.8, 157.6, 148.9, 129.4, 128.6, 127.8, 121.7, 111.0, 94.8, 57.1, 56.0, 51.4, 46.6, 34.0, 31.6, 26.1, 18.8, -3.79, -3.83. HRMS (ESI+): calcd for $\text{C}_{22}\text{H}_{33}\text{N}_2\text{O}_5\text{Si}$ $[\text{M}+\text{H}]^+$ 433.2159, found 433.2133.



Methyl 5-(*tert*-Butyldimethylsilyloxy)-8-(4-methoxyphenyl)-3-oxo-2,3,7,8-tetrahydro-1H-pyrazolo[1,2-a]pyridazine-6-carboxylate (60e): 76% yield, ^1H NMR (400 MHz, CDCl_3) δ : 7.27 (d, $J = 8.7$ Hz, 2H), 6.93 (d, $J = 8.7$ Hz, 2H), 3.84 (s, 3H), 3.72 (s, 3H), 3.61 (dd, $J = 9.8, 4.6$ Hz, 1H), 3.19 (ddd, $J = 11.1, 8.7, 6.6$ Hz, 1H), 2.90-2.74 (m, 2H), 2.68 (dd, $J = 16.9, 9.8$ Hz, 1H), 2.59-2.36 (m, 2H), 1.07 (s, 9H), 0.25 (s, 3H), 0.23 (s, 3H). ^{13}C NMR (100 MHz, CDCl_3) δ : 171.0, 167.8, 160.1, 148.9, 131.6, 129.4, 114.7, 94.3, 65.9, 55.7, 51.4, 47.1, 35.5, 31.6, 26.1, 18.7, -3.79, -3.82. HRMS (ESI+): calcd for $\text{C}_{22}\text{H}_{33}\text{N}_2\text{O}_5\text{Si}$ $[\text{M}+\text{H}]^+$ 433.2159, found 433.2130.

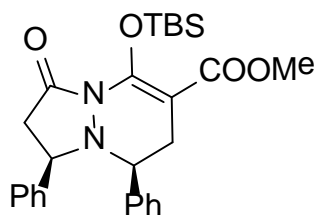


Methyl 5-(*tert*-Butyldimethylsilyloxy)-8-cyclohexyl-3-oxo-2,3,7,8-tetrahydro-1H-pyrazolo[1,2-a]pyridazine-6-carboxylate (60f): 77% yield, ^1H NMR (400 MHz, CDCl_3) δ : 3.72 (s, 3H), 3.48 (ddd, $J = 10.0, 8.3, 4.4$ Hz, 1H), 2.91 (td, $J = 10.0, 8.3$ Hz, 1H), 2.73-2.48 (m, 3H), 2.48-2.38 (m, 2H), 1.80 (m, 5H), 1.56 (m, 1H), 1.40-1.12 (m, 5H), 1.04 (s, 9H), 0.19 (s, 3H), 0.15 (s, 3H). ^{13}C NMR (100 MHz, CDCl_3) δ : 169.0, 168.4, 148.9, 92.9, 65.6, 51.4, 47.4, 39.1, 32.6, 30.5, 27.3, 27.1, 26.7, 26.6, 26.2, 25.3, 18.6, -3.78, -3.81. HRMS (ESI+): calcd for $\text{C}_{21}\text{H}_{37}\text{N}_2\text{O}_4\text{Si}$ $[\text{M}+\text{H}]^+$ 409.2523, found 409.2549.

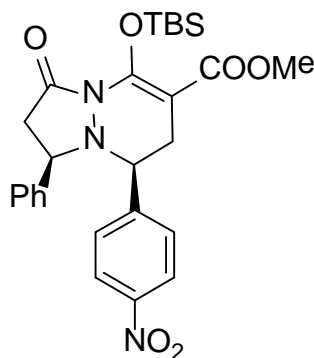


Methyl (*E*)-5-(*tert*-Butyldimethylsilyloxy)-3-oxo-8-styryl-2,3,7,8-tetrahydro-1H-pyrazolo[1,2-a]pyridazine-6-carboxylate (60g): 73% yield, ^1H NMR (400 MHz, CDCl_3) δ : 7.46-7.30 (m, 5H), 6.70 (d, $J = 15.9$ Hz, 1H), 6.09 (dd, $J = 15.9, 8.8$ Hz, 1H), 3.74 (s, 3H), 3.52-3.33 (m, 2H), 3.27 (dt, $J = 11.3, 8.8$ Hz, 1H), 2.72 (dd, $J = 16.8, 4.7$ Hz, 1H), 2.68 – 2.51 (m, 3H), 1.06 (s, 9H), 0.24 (s, 3H), 0.22 (s, 3H). ^{13}C NMR (100 MHz, CDCl_3) δ : 170.6, 167.3, 148.4, 135.9, 134.6, 128.7, 128.3,

126.5, 92.9, 64.1, 51.0, 46.5, 32.6, 31.1, 25.7, 18.3, -4.29, -4.33. HRMS (ESI+): calcd for C₂₃H₃₃N₂O₄Si [M+H]⁺ 429.2210, found 429.2230.

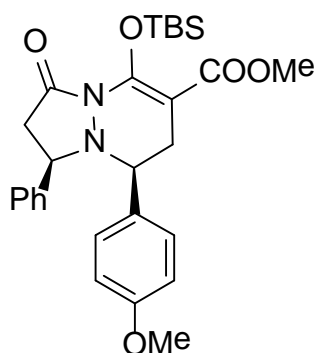


Methyl (1RS,8SR)-5-(tert-Butyldimethylsilyloxy)-3-oxo-1,8-diphenyl-2,3,7,8-tetrahydro-1H-pyrazolo[1,2-a]pyridazine-6-carboxylate (60h): 83% yield, ¹H NMR (CDCl₃, 400 MHz) δ: 7.34-7.23 (m, 10H), 4.32 (dd, *J* = 7.6, 3.2 Hz, 1H), 3.93 (t, *J* = 7.6 Hz, 1H), 3.72 (s, 3H), 3.22 (dd, *J* = 18.0, 9.6 Hz, 1H), 2.81 (d, *J* = 7.6 Hz, 1H), 2.71 (dd, *J* = 18.0, 3.2 Hz, 1H), 1.01 (s, 9H), 0.21 (s, 3H), 0.07 (s, 3H); ¹³C NMR (CDCl₃, 100 MHz) δ: 171.9, 167.0, 148.0, 141.1, 139.7, 128.9, 128.4, 128.4, 127.8, 127.4, 126.4, 95.1, 66.2, 57.7, 51.1, 37.5, 35.7, 25.6, 18.3, -4.3, -4.4; HRMS (ESI+): calcd for C₂₇H₃₅N₂O₄Si [M+H]⁺ 479.2366, found 479.2309.

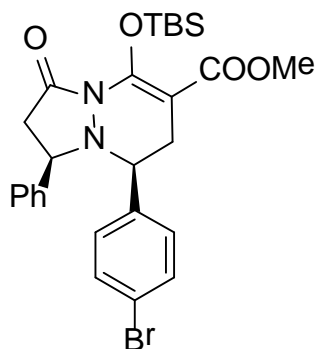


Methyl (1RS,8SR)-5-(tert-Butyldimethylsilyloxy)-8-(4-nitrophenyl)-3-oxo-1-phenyl-2,3,7,8-tetrahydro-1H-pyrazolo[1,2-a]pyridazine-6-carboxylate (60i): 87% yield, ¹H NMR (CDCl₃, 400 MHz) δ: 8.11 (d, *J* = 8.8 Hz, 2H), 7.48 (d, *J* = 8.8

Hz, 2H), 7.28-7.20 (m, 5H), 4.19 (dd, $J = 9.2, 4.4$ Hz, 1H), 4.05 (dd, $J = 9.2, 4.4$ Hz, 1H), 3.73 (s, 3H), 3.20 (dd, $J = 17.6, 8.8$, Hz, 1H), 2.83-2.68 (m, 3H), 1.02 (s, 9H), 0.22 (s, 3H), 0.11 (s, 3H); ^{13}C NMR (CDCl_3 , 100 MHz) δ : 170.4, 166.8, 148.1, 147.80, 146.8, 140.4, 128.8, 128.6, 127.8, 126.3, 123.9, 94.3, 66.0, 59.6, 51.2, 38.4, 35.4, 25.6, 18.3, -4.2, -4.3; HRMS (ESI+): calcd for $\text{C}_{27}\text{H}_{34}\text{N}_3\text{O}_6\text{Si}$ $[\text{M}+\text{H}]^+$ 524.2217, found 524.2269.

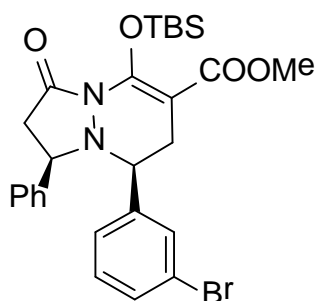


Methyl (1*RS*,8*SR*)-5-(*tert*-Butyldimethylsilyl)oxy-8-(4-methoxyphenyl)-3-oxo-1-phenyl-2,3,7,8-tetrahydro-1*H*-pyrazolo[1,2-*a*]pyridazine-6-carboxylate (60j): 88% yield, ^1H NMR (CDCl_3 , 400 MHz) δ : 7.31-7.21 (m, 7H), 6.83 (d, $J = 8.4$ Hz, 2H), 4.31 (dd, $J = 9.2, 3.2$, Hz, 1H), 3.86 (dd, $J = 8.4, 6.8$ Hz, 1H), 3.79 (s, 3H), 3.72 (s, 3H), 3.20 (dd, $J = 13.6, 9.2$ Hz, 1H), 2.78 (d, $J = 8.4$ Hz, 2H), 2.71 (dd, $J = 17.6, 3.2$ Hz, 1H), 1.00 (s, 9H), 0.20 (s, 3H), 0.06 (s, 3H); ^{13}C NMR (CDCl_3 , 100 MHz) δ : 171.8, 167.1, 159.6, 148.0, 141.2, 131.5, 129.0, 128.3, 127.3, 126.40, 114.3, 95.1, 65.6, 57.6, 55.3, 51.1, 37.6, 35.7, 25.6, 18.3, -4.3, -4.4; HRMS (ESI+): calcd for $\text{C}_{28}\text{H}_{37}\text{N}_2\text{O}_5\text{Si}$ $[\text{M}+\text{H}]^+$ 509.2472, found 509.2463.



Methyl (1RS,8SR)-8-(4-Bromophenyl)-5-(tert-butyldimethylsilyl)oxy-3-oxo-1-phenyl-2,3,7,8-tetrahydro-1H-pyrazolo[1,2-a]pyridazine-6-carboxylate

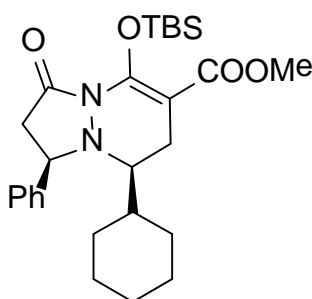
(60k): 87% yield, ^1H NMR (CDCl_3 , 400 MHz) δ : 7.40 (d, $J = 8.8$ Hz, 2H), 7.30-7.22 (m, 5H), 7.19 (d, $J = 8.8$ Hz, 2H), 4.25 (dd, $J = 8.0, 4.0$ Hz, 1H), 3.89 (dd, $J = 9.2, 4.0$ Hz, 1H), 3.72 (s, 3H), 3.20 (dd, $J = 17.6, 8.0$ Hz, 1H), 2.79-2.65 (m, 3H), 1.00 (s, 9H), 0.20 (s, 3H), 0.08 (s, 3H); ^{13}C NMR (CDCl_3 , 100 MHz) δ : 171.3, 166.9, 148.0, 140.8, 138.6, 132.0, 129.5, 128.4, 127.5, 126.3, 122.3, 94.7, 65.7, 58.4, 51.1, 37.9, 35.6, 25.6, 18.3, -4.3, -4.4; HRMS (ESI $^+$): calcd for $\text{C}_{27}\text{H}_{34}\text{BrN}_2\text{O}_4\text{Si}$ $[\text{M}+\text{H}]^+$ 557.1471, found 557.1473.



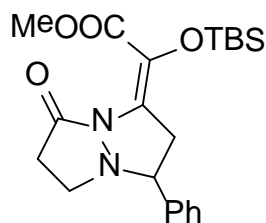
Methyl (1RS,8SR)-8-(3-Bromophenyl)-5-(tert-butyldimethylsilyl)oxy-3-oxo-1-phenyl-2,3,7,8-tetrahydro-1H-pyrazolo[1,2-a]pyridazine-6-carboxylate

(60l): 80% yield, ^1H NMR (CDCl_3 , 400 MHz) δ : 7.45 (t, $J = 1.6$ Hz, 1H), 7.40 (d, $J =$

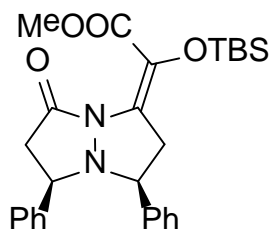
8.0 Hz, 1H), 7.31-7.23 (m, 6H), 7.16 (t, $J = 8.0$ Hz, 1H), 4.26 (dd, $J = 9.2, 4.0$ Hz, 1H), 3.88 (dd, $J = 9.2, 6.0$ Hz, 1H), 3.72 (s, 3H), 3.19 (dd, $J = 18.0, 9.2$ Hz, 1H), 2.78-2.68 (m, 3H), 1.01 (s, 9H), 0.20 (s, 3H), 0.09 (s, 3H); ^{13}C NMR (CDCl_3 , 100 MHz) δ : 171, 166.9, 148.0, 141.8, 140.7, 131.6, 131.1, 130.4, 128.5, 127.6, 126.4, 126.4, 126.4, 126.4, 122.8, 94.7, 66.0, 58.8, 51.1, 38.0, 35.5, 25.6, 18.3, -4.3, -4.4; HRMS (ESI⁺): calcd for $\text{C}_{27}\text{H}_{34}\text{BrN}_2\text{O}_4\text{Si}$ $[\text{M}+\text{H}]^+$ 557.1471, found 557.1473.



Methyl (1*RS*,8*SR*)-5-(*tert*-Butyldimethylsilyloxy)-8-cyclohexyl-3-oxo-1-phenyl-2,3,7,8-tetrahydro-1*H*-pyrazolo[1,2-*a*]pyridazine-6-carboxylate (60m): 65% yield, ^1H NMR (CDCl_3 , 400 MHz) δ : 7.48 (d, $J = 7.2$ Hz, 2H), 7.40 (t, $J = 7.2$ Hz, 2H), 7.33-7.28 (m, 1H), 4.56 (t, $J = 8.4$ Hz, 1H), 3.74 (s, 3H), 3.07 (dd, $J = 18.0, 11.6$ Hz, 1H), 2.87-2.84 (m, 1H), 2.73-2.59 (m, 2H), 2.34 (dd, $J = 16.4, 3.6$ Hz, 1H), 1.76-0.85 (m, 20H), 0.17 (s, 3H), 0.04 (s, 3H); ^{13}C NMR (CDCl_3 , 100 MHz) δ : 169.8, 167.5, 147.5, 140.6, 128.6, 127.8, 127.0, 94.9, 65.5, 59.2, 51.1, 39.6, 39.5, 30.1, 26.8, 26.4, 25.9, 25.7, 25.7, 25.6, 18.2, -4.4, -4.5; HRMS (ESI⁺): calcd for $\text{C}_{27}\text{H}_{41}\text{N}_2\text{O}_4\text{Si}$ $[\text{M}+\text{H}]^+$ 485.2836, found 485.2803.

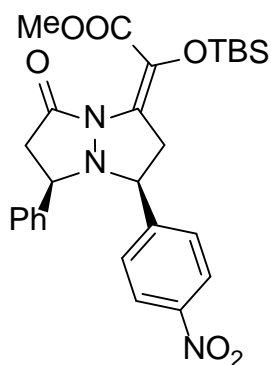


Methyl (E)-2-(tert-Butyldimethylsilyl)oxy-2-[7-oxo-3-phenyltetrahydro-pyrazolo-[1,2-a]pyrazol-1(5H)-ylidene]acetate (61a): 23% yield (Reaction catalyzed by 1 mol% $\text{Rh}_2(\text{OAc})_4$ at 40°C for 3h), ^1H NMR (400 MHz, CDCl_3) δ : 7.51-7.33 (m, 5H), 3.82 (s, 3H), 3.72 (dd, $J = 10.4, 7.0$ Hz, 1H), 3.59 (dt, $J = 12.0, 9.7$ Hz, 1H), 3.37 (dd, $J = 17.0, 7.0$ Hz, 1H), 3.06 (ddd, $J = 12.0, 9.7, 7.0$ Hz, 1H), 2.87 (dd, $J = 17.0, 10.4$ Hz, 1H), 2.82-2.63 (m, 2H), 0.94 (s, 9H), 0.23 (s, 3H), 0.17 (s, 3H). ^{13}C NMR (100 MHz, CDCl_3) δ : 171.6, 165.7, 137.9, 130.6, 129.3, 128.9, 128.2, 126.8, 69.3, 52.4, 45.5, 41.3, 31.4, 26.2, 18.8, -3.8, -4.0. HRMS (ESI+): calcd for $\text{C}_{21}\text{H}_{31}\text{N}_2\text{O}_4\text{Si}$ $[\text{M}+\text{H}]^+$ 403.2053, found 403.2066.



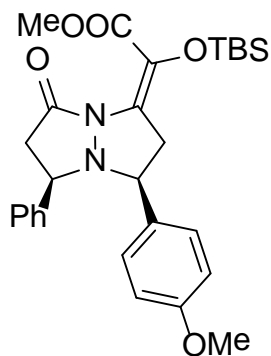
Methyl (E)-2-(tert-Butyldimethylsilyl)oxy-2-[(3SR,5RS)-7-oxo-3,5-diphenyltetrahydro-pyrazolo[1,2-a]pyrazol-1(5H)-ylidene]acetate (61h): 75% yield, ^1H NMR (CDCl_3 , 400 MHz) δ : 7.36-7.21 (m, 10H), 4.30 (dd, $J = 9.2, 7.2$ Hz, 1H), 3.88 (dd, $J = 10.0, 7.2$ Hz, 1H), 3.90 (m, 1H), 3.82 (s, 3H), 3.46 (dd, $J = 17.6, 7.2$ Hz, 1H), 3.27 (dd, $J = 17.6, 13.6$ Hz, 1H), 2.92-2.83 (m, 2H), 0.94 (s, 9H), 0.25 (s, 3H), 0.17 (s, 3H); ^{13}C NMR (CDCl_3 , 100 MHz) δ : 169.3, 165.3, 141.4, 137.5, 130.0, 128.6,

128.5, 128.3, 127.7, 127.5, 126.5, 125.7, 69.9, 62.3, 52.0, 40.9, 40.4, 25.8, 18.4, -4.2, -4.4; HRMS (ESI+): calcd for C₂₇H₃₅N₂O₄Si [M+H]⁺ 479.2366, found 479.2309.



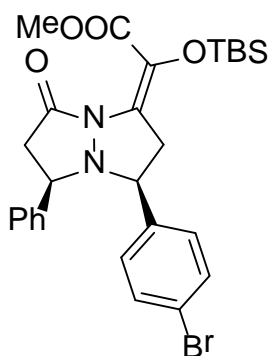
Methyl (*E*)-2-(*tert*-Butyldimethylsilyloxy)-2-[(3*SR*,5*RS*)-3-(4-nitrophenyl)-7-oxo-5-phenyltetrahydropyrazolo[1,2-*a*]pyrazol-1(5*H*)-ylidene]acetate (61i):

72% yield, ¹H NMR (CDCl₃, 400 MHz) δ: 8.11 (d, *J* = 8.8 Hz, 2H), 7.53 (d, *J* = 8.8 Hz, 2H), 7.32-7.23 (m, 5H), 4.27 (t, *J* = 8.8 Hz, 1H), 4.09 (dd, *J* = 10.0, 8.0 Hz, 1H), 3.84 (s, 3H), 3.54 (dd, *J* = 17.2, 8.0 Hz, 1H), 3.23 (dd, *J* = 17.2, 9.2 Hz, 1H), 2.97 (dd, *J* = 17.2, 8.0 Hz, 1H), 2.86 (dd, *J* = 17.2, 10.0 Hz, 1H), 0.92 (s, 9H), 0.25 (s, 3H), 0.15 (s, 3H); ¹³C NMR (CDCl₃, 100 MHz) δ: 167.7, 165.1, 147.7, 145.5, 140.2, 130.1, 128.7, 128.4, 128.0, 126.6, 124.0, 123.8, 68.9, 64.8, 52.0, 41.4, 40.9, 25.7, 18.4, -4.12, -4.4; HRMS (ESI+): calcd for C₂₇H₃₄N₃O₆Si [M+H]⁺ 524.2217, found 524.2269.



Methyl (E)-2-(tert-Butyldimethylsilyloxy)-2-[(3SR,5RS)-3-(4-methoxyphenyl)-7-oxo-5-phenyltetrahydropyrazolo[1,2-a]pyrazol-1(5H)-ylidene]acetate

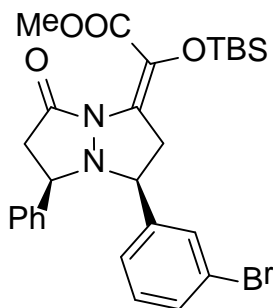
(61j): 71% yield, ^1H NMR (CDCl_3 , 400 MHz) δ : 7.31-7.22 (m, 7H), 6.82 (d, $J = 8.4$ Hz, 2H), 4.28 (dd, $J = 9.6, 6.4$ Hz, 1H), 3.83-3.81 (m, 1H), 3.79 (s, 3H), 3.78 (s, 3H), 3.36 (dd, $J = 16.8, 7.6$ Hz, 1H), 3.27 (dd, $J = 16.8, 7.6$ Hz, 1H), 2.89-2.82 (m, 2H), 0.94 (s, 9H), 0.25 (s, 3H), 0.16 (s, 3H); ^{13}C NMR (CDCl_3 , 100 MHz) δ : 169.5, 165.3, 159.6, 141.7, 130.0, 129.2, 128.8, 128.5, 127.4, 126.4, 125.9, 114.1, 69.4, 61.8, 55.3, 51.9, 40.9, 40.2, 25.8, 18.4, -4.2, -4.4; HRMS (ESI+): calcd for $\text{C}_{28}\text{H}_{37}\text{N}_2\text{O}_5\text{Si}$ $[\text{M}+\text{H}]^+$ 509.2472, found 509.2463.



Methyl (E)-2-[(3SR,5RS)-3-(4-Bromophenyl)-7-oxo-5-phenyltetrahydropyrazolo[1,2-a]pyrazol-1(5H)-ylidene]-2-(tert-butyl dimethylsilyloxy)acetate

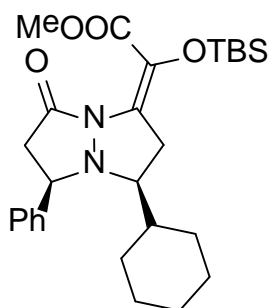
(61k): 77% yield, ^1H NMR (CDCl_3 , 400 MHz) δ : 7.40 (d, $J = 8.8$ Hz, 2H), 7.29-7.20 (m, 7H), 4.25 (dd, $J = 10.0, 3.6$ Hz, 1H), 3.86-3.84 (m, 1H), 3.81 (s, 3H), 3.39 (dd, $J = 8.0, 3.6$ Hz, 1H), 3.24 (dd, $J = 16.0, 8.0$ Hz, 1H), 2.90-2.77 (m, 2H), 0.93 (s, 9H), 0.24 (s, 3H), 0.15 (s, 3H); ^{13}C NMR (CDCl_3 , 100 MHz) δ : 168.9, 165.2, 141.1, 136.7, 131.8, 130.1, 129.2, 128.62, 127.7, 126.5, 125.1, 122.2, 69.1, 62.9, 52.0, 40.9, 40.6, 25.7, 18.4,

-4.2, -4.4; HRMS (ESI+): calcd for C₂₇H₃₄BrN₂O₄Si [M+H]⁺ 557.1471, found 557.1473.



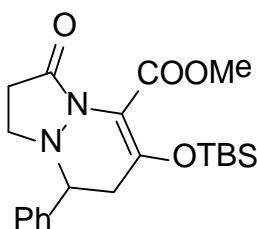
Methyl (E)-2-[(3SR,5RS)-3-(3-Bromophenyl)-7-oxo-5-phenyltetrahydropyrazolo[1,2-a]pyrazol-1(5H)-ylidene]-2-(tert-butyldimethylsilyl)oxy]acetate

(61l): 71% yield, ¹H NMR (CDCl₃, 400 MHz) δ: 7.48 (t, *J* = 1.6 Hz, 1H), 7.37-7.24 (m, 7H), 7.14 (t, *J* = 8.0 Hz, 1H), 4.25 (dd, *J* = 13.2, 10.8 Hz, 1H), 3.86 (dd, *J* = 10.8, 3.6 Hz, 1H), 3.82 (s, 3H), 3.46 (dd, *J* = 16.8, 8.0 Hz, 1H), 3.23 (dd, *J* = 16.8, 9.2 Hz, 1H), 2.94-2.80 (m, 3H), 0.94 (s, 9H), 0.24 (s, 3H), 0.16 (s, 3H); ¹³C NMR (CDCl₃, 100 MHz) δ: 168.8, 165.5, 141.13, 140.4, 131.7, 131.2, 130.6, 130.5, 129.0, 128.2, 127.0, 126.5, 125.1, 123.0, 69.6, 63.9, 52.4, 41.3, 41.3, 26.2, 18.8, -3.8, -4.0; HRMS (ESI+): calcd for C₂₇H₃₄BrN₂O₄Si [M+H]⁺ 557.1471, found 557.1473.

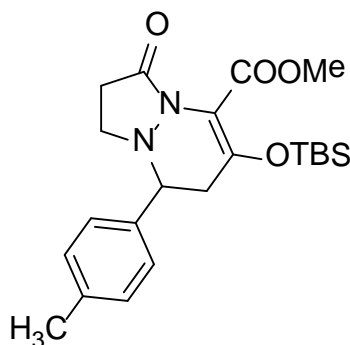


Methyl (E)-2-(tert-Butyldimethylsilyl)oxy-2-[(3SR,5RS)-3-cyclohexyl-7-oxo-5-phenyltetrahydropyrazolo[1,2-a]pyrazol-1(5H)-ylidene]acetate (61m): 78%

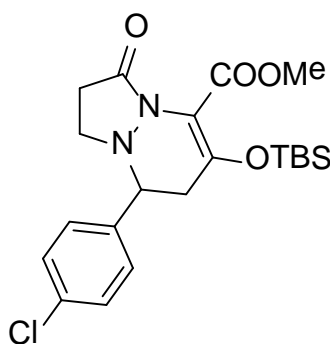
yield, ^1H NMR (CDCl_3 , 400 MHz) δ : 7.49 (d, $J = 7.2$ Hz, 2H), 7.40 (t, $J = 7.2$ Hz, 2H), 7.32-7.28 (m, 1H), 4.21 (dd, $J = 10.0, 8.8$ Hz, 1H), 3.79 (s, 3H), 3.05 (dd, $J = 16.4, 8.0$ Hz, 1H), 2.96-2.70 (m, 4H), 1.68-0.84 (m, 20H), 0.23 (s, 3H), 0.19 (s, 3H); ^{13}C NMR (CDCl_3 , 100 MHz) δ : 165.9, 165.3, 140.7, 129.4, 128.7, 128.0, 127.0, 125.0, 70.4, 67.5, 51.8, 43.1, 39.0, 32.4, 30.3, 26.8, 26.4, 26.3, 25.8, 18.4, -4.1, -4.4; HRMS (ESI⁺): calcd for $\text{C}_{27}\text{H}_{41}\text{N}_2\text{O}_4\text{Si}$ $[\text{M}+\text{H}]^+$ 485.2836, found 485.2803.



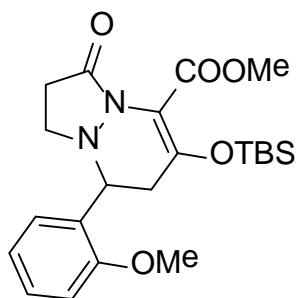
Methyl 6-(*tert*-Butyldimethylsilyl)oxy-3-oxo-8-phenyl-2,3,7,8-tetrahydro-1*H*-pyrazolo[1,2-*a*]pyridazine-5-carboxylate (62a): 86% yield, ^1H NMR (400 MHz, CDCl_3) δ : 7.47-7.31 (m, 5H), 3.98-3.73 (m, 4H), 3.39 (dt, $J = 11.6, 8.9$ Hz, 1H), 2.93 (s, 1H), 2.71-2.29 (m, 4H), 0.94 (s, 9H), 0.21 (s, 3H), 0.20 (s, 3H). ^{13}C NMR (100 MHz, CDCl_3) δ : 168.7, 161.9, 147.6, 139.2, 129.2, 128.7, 127.6, 113.3, 66.1, 51.9, 46.5, 39.9, 29.6, 25.4, 18.1, -3.8, -4.0. HRMS (ESI⁺): calcd for $\text{C}_{21}\text{H}_{31}\text{N}_2\text{O}_4\text{Si}$ $[\text{M}+\text{H}]^+$ 403.2053, found 403.2060.



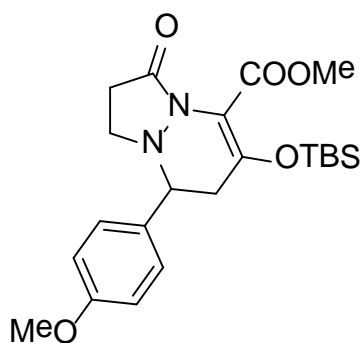
Methyl 6-(*tert*-Butyldimethylsilyloxy)-3-oxo-8-(*p*-tolyl)-2,3,7,8-tetrahydro-1H-pyrazolo[1,2-*a*]pyridazine-5-carboxylate (62b): 85% yield, ¹H NMR (400 MHz, CDCl₃) δ: 7.24 (s, 4H), 3.85 (m, 4H), 3.38 (dt, *J* = 11.6, 8.6 Hz, 1H), 2.98-2.88 (m, 1H), 2.70-2.41 (m, 4H), 2.40 (s, 3H), 0.95 (s, 9H), 0.22 (s, 3H), 0.20 (s, 3H). ¹³C NMR (100 MHz, CDCl₃) δ: 169.6, 162.6, 148.8, 139.0, 136.4, 130.3, 128.1, 113.5, 66.1, 52.4, 46.8, 40.6, 30.0, 25.9, 21.6, 18.5, -3.4, -3.5. HRMS (ESI⁺): calcd for C₂₂H₃₃N₂O₄Si [M+H]⁺ 417.2210, found 417.2201.



Methyl 6-(*tert*-Butyldimethylsilyloxy)-8-(4-chlorophenyl)-3-oxo-2,3,7,8-tetrahydro-1H-pyrazolo[1,2-*a*]pyridazine-5-carboxylate (62c): 80% yield, ¹H NMR (400 MHz, CDCl₃) δ: 7.41 (d, *J* = 8.5 Hz, 2H), 7.30 (d, *J* = 8.5 Hz, 2H), 3.99-3.82 (m, 4H), 3.41 (dt, *J* = 11.5, 9.0 Hz 1H), 2.95-2.85 (m, 1H), 2.73-2.35 (m, 4H), 0.95 (s, 9H), 0.22 (s, 3H), 0.20 (s, 3H). ¹³C NMR (100 MHz, CDCl₃) δ: 169.0, 162.3, 147.6, 138.1, 135.0, 130.0, 129.4, 113.8, 65.9, 52.4, 47.0, 40.4, 30.0, 25.9, 18.5, -3.4, -3.5. HRMS (ESI⁺): calcd for C₂₁H₃₀ClN₂O₄Si [M+H]⁺ 437.1663, found 437.1670.

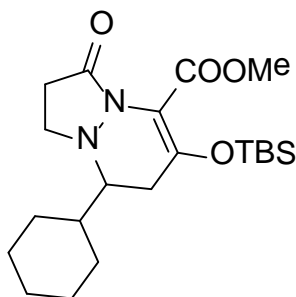


Methyl 6-(*tert*-Butyldimethylsilyloxy)-8-(2-methoxyphenyl)-3-oxo-2,3,7,8-tetrahydro-1H-pyrazolo[1,2-a]pyridazine-5-carboxylate (62d): 86% yield, ^1H NMR (400 MHz, CDCl_3) δ : 7.39 (dd, $J = 7.5, 1.5$ Hz, 1H), 7.33 (ddd, $J = 8.3, 7.5, 1.5$ Hz, 1H), 7.05 (td, $J = 7.5, 0.8$ Hz, 1H), 6.94 (dd, $J = 8.3, 0.8$ Hz, 1H), 4.59-4.50 (m, 1H), 3.86 (s, 3H), 3.84 (s, 3H), 3.45 (dt, $J = 11.7, 8.8$ Hz, 1H), 3.10-2.87 (m, 1H), 2.78-2.30 (m, 4H), 0.95 (s, 9H), 0.22 (s, 3H), 0.20 (s, 3H). ^{13}C NMR (100 MHz, CDCl_3) δ : 170.2, 162.4, 157.4, 149.5, 129.7, 128.3, 127.5, 121.9, 113.5, 111.1, 55.9, 52.3, 46.6, 39.0, 30.2, 25.9, 25.8, 25.6, 18.6, -3.4, -3.5. HRMS (ESI+): calcd for $\text{C}_{22}\text{H}_{33}\text{N}_2\text{O}_5\text{Si}$ $[\text{M}+\text{H}]^+$ 433.2159, found 433.2170.

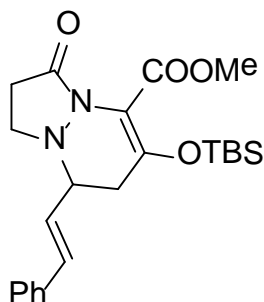


Methyl 6-(*tert*-Butyldimethylsilyloxy)-8-(4-methoxyphenyl)-3-oxo-2,3,7,8-tetrahydro-1H-pyrazolo[1,2-a]pyridazine-5-carboxylate (62e): 78% yield, ^1H NMR (400 MHz, CDCl_3) δ : 7.27 (d, $J = 8.7$ Hz, 2H), 6.95 (d, $J = 8.7$ Hz, 2H), 3.97-3.69 (m, 7H), 3.36 (dt, $J = 11.5, 8.6$ Hz, 1H), 2.99-2.90 (m, 1H), 2.74-2.21 (m, 4H),

0.95 (s, 9H), 0.22 (s, 3H), 0.20 (s, 3H). ^{13}C NMR (100 MHz, CDCl_3) δ : 169.4, 162.5, 160.2, 148.4, 131.5, 129.3, 114.9, 113.7, 65.9, 55.7, 52.4, 46.7, 40.4, 30.0, 25.9, 18.6, -3.4, -3.5. HRMS (ESI⁺): calcd for $\text{C}_{22}\text{H}_{33}\text{N}_2\text{O}_5\text{Si}$ $[\text{M}+\text{H}]^+$ 433.2159, found 433.2179.

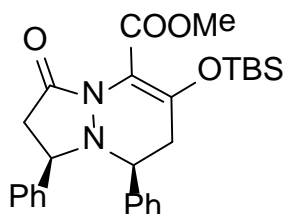


Methyl 6-(*tert*-Butyldimethylsilyl)oxy-8-cyclohexyl-3-oxo-2,3,7,8-tetrahydro-1H-pyrazolo[1,2-a]pyridazine-5-carboxylate (62f): 77% yield, ^1H NMR (400 MHz, CDCl_3) δ : 3.79 (s, 3H), 3.60 (ddd, $J = 10.5, 8.7, 6.6$ Hz, 1H), 3.06 (dt, $J = 10.5, 8.7$ Hz, 1H), 2.81-2.73 (m, 1H), 2.64-2.57 (m, 2H), 2.39 (dd, $J = 17.4, 9.8$ Hz, 1H), 2.13 (dd, $J = 17.4, 4.8$ Hz, 1H), 1.90-1.67 (m, 5H), 1.54 (d, $J = 12.2$ Hz, 1H), 1.36-0.98 (m, 6H), 0.94 (s, 9H), 0.22 (s, 3H), 0.19 (s, 3H). ^{13}C NMR (100 MHz, CDCl_3) δ : 166.9, 162.5, 146.5, 113.4, 65.6, 52.3, 47.4, 39.2, 31.5, 30.9, 30.7, 30.1, 27.5, 27.5, 27.0, 26.9, 26.5, 26.0, 25.9, 25.0, 18.5, -3.3, -3.6. HRMS (ESI⁺): calcd for $\text{C}_{21}\text{H}_{37}\text{N}_2\text{O}_4\text{Si}$ $[\text{M}+\text{H}]^+$ 409.2523, found 409.2529.



Methyl (*E*)-6-(*tert*-Butyldimethylsilyl)oxy-3-oxo-8-styryl-2,3,7,8-tetrahydro-1H-pyrazolo[1,2-a]pyridazine-5-carboxylate (62g): 84% yield, ^1H

NMR (400 MHz, CDCl₃) δ : 7.45-7.28 (m, 5H), 6.67 (d, $J = 15.9$ Hz, 1H), 6.03 (dd, $J = 15.9, 8.9$ Hz, 1H), 3.81 (s, 3H), 3.64-3.46 (m, 2H), 3.46-3.26 (m, 1H), 2.84-2.26 (m, 4H), 0.94 (s, 9H), 0.22 (s, 3H), 0.20 (s, 3H). ¹³C NMR (100 MHz, CDCl₃) δ : 169.3, 162.3, 147.6, 136.0, 135.3, 129.2, 128.9, 127.0, 113.6, 64.9, 52.4, 46.6, 38.0, 30.1, 25.9, 18.6, -3.4, -3.5. HRMS (ESI⁺): calcd for C₂₃H₃₃N₂O₄Si [M+H]⁺ 429.2210, found 429.2233.



Methyl (1RS,8SR)-6-(tert-Butyldimethylsilyloxy)-3-oxo-1,8-diphenyl-2,3,7,8-tetrahydro-1H-pyrazolo[1,2-a]pyridazine-5-carboxylate (62h): 72% yield; ¹H NMR (CDCl₃, 400 MHz) δ : 7.32-7.17 (m, 10H), 4.20 (dd, $J = 12.0, 4.0$ Hz, 1H), 4.11 (dd, $J = 8.0, 4.0$ Hz, 1H), 3.83 (s, 3H), 3.20 (dd, $J = 16.0, 8.0$ Hz, 1H), 2.68-2.58 (m, 3H), 0.95 (s, 9H), 0.24 (s, 3H), 0.21 (s, 3H); ¹³C NMR (CDCl₃, 100 MHz) δ : 168.6, 161.7, 150.4, 142.4, 139.1, 129.0, 128.7, 128.5, 127.8, 127.3, 126.4, 112.8, 67.5, 59.6, 51.9, 40.9, 37.5, 25.5, 18.2, -3.73, -3.76; HRMS (ESI⁺): C₂₇H₃₅N₂O₄Si [M+H]⁺ 479.2366, found 479.2309.

NMR graphs and HPLC chromatograms can be obtained from the supporting information of the paper published in the *Journal of the American Chemical Society*: Xu, X.; Qian, Y.; Zavalij, P. Y.; Doyle, M. P. *J. Am. Chem. Soc.* **2013**, *135*, 1244-1247.

V. References

- (1) Zhang, Y.; Wang, J. *Chem. Comm.* **2009**, 5350.

- (2) Bug, T.; Hartnagel, M.; Schlierf, C.; Mayr, H. *Chem.–Eur. J.*, **2003**, *9*, 4068.
- (3) Li, W.; Liu, X.; Hao, X.; Hu, X.; Chu, Y.; Cao, W.; Qin, S.; Hu, C.; Lin, L.; Feng, X. *J. Am. Chem. Soc.* **2011**, *133*, 15268.
- (4) Liu, Y.; Bakshi, K.; Zavalij, P.; Doyle, M. P. *Org. Lett.* **2010**, *12*, 4304.
- (5) Doyle, M. P.; McKervey, M. A.; Ye, T., *Modern Catalytic Methods for Organic Synthesis with Diazo Compounds*, Wiley, New York, **1998**.
- (6) Jiang, N.; Wang, J. *Tetrahedron Lett.* **2002**, *43*, 1285.
- (7) Karady, S.; Amato, J. S.; Reamer, R. A.; Weinstock, L. M. *J. Am. Chem. Soc.* **1981**, *103*, 6765.
- (8) Calter, M. A.; Sugathapala, P. M.; Zhu, C. *Tetrahedron Lett.* **1997**, *38*, 3837.
- (9) Calter, M. A.; Sugathapala, P. M. *Tetrahedron Lett.* **1998**, *39*, 8813.
- (10) Calter, M. A.; C. Zhu *J. Org. Chem.* **1999**, *64*, 1415.
- (11) Doyle, M. P.; Kundu, K.; Russell, A. E. *Org. Lett.* **2005**, *7*, 5171.
- (12) Deng, G.; Tian, X.; Wang, J. *Tetrahedron Lett.* **2003**, *44*, 587.
- (13) Deng, G.; Tian, X.; Qu, Z.; Wang, J. *Angew. Chem., Int. Ed.*, **2002**, *41*, 2773.
- (14) Balsells, J.; Davis, T. J.; Carroll, P.; Walsh, P. J. *J. Am. Chem. Soc.* **2002**, *124*, 10336.
- (15) Katady, S.; Amato, J. S.; Reamer, R. A.; Weinstock, L. M. *Tetrahedron Lett.* **1996**, *46*, 8277.

- (16) Jaber, D. M.; Burgin, R. N.; Hepler, M.; Zavalij, P.; Doyle, M. P. *Chem. Comm.* **2011**, *47*, 7623.
- (17) Kundu, K.; Doyle, M. P. *Tetrahedron: Asymmetry* **2006**, *17*, 574.
- (18) Liu, Y.; Zhang, Y.; Jee, N.; Doyle, M. P. *Org. Lett.* **2008**, *10*, 1605.
- (19) Qian, Y.; Xu, X.; Wang, X.; Zavalij, P. J.; Hu, W.; Doyle, M. P. *Angew. Chem., Int. Ed.*, **2012**, *51*, 5900.
- (20) Truong, P.; Shanahan, C. S.; Doyle, M. P. *Org. Lett.* **2012**, *14*, 3608.
- (21) Xu, X.; Hu, W. H.; Doyle, M. P. *Angew. Chem., Int. Ed.*, **2011**, *50*, 6392.
- (22) Xu, X.; Hu, W.-H.; Zavalij, P. Y.; Doyle, M. P. *Angew. Chem., Int. Ed.*, **2011**, *50*, 11152.
- (23) Xu, X.; Ratnikov, M. O.; Zavalij, P. Y.; Doyle, M. P. *Org. Lett.* **2011**, *13*, 6122.
- (24) Nickon, A. *Acc. Chem. Res* **1993**, *26*, 84.
- (25) Liu, M. T. H. *Acc. Chem. Res* **1994**, *27*, 287.
- (26) Farlow, R. A.; Thamattoor, D. M. *J. Org. Chem.* **2002**, *67*, 3257.
- (27) Okuyama, T. *Acc. Chem. Res* **2002**, *35*, 12.
- (28) Sromek, A. W.; Kel'in, A. V.; Gevorgyan, V. *Angew. Chem., Int. Ed.*, **2004**, *43*, 2280.
- (29) Kirsch, S. F.; Binder, J. T.; Liebert, C.; Menz, H. *Angew. Chem., Int. Ed.*, **2006**, *45*, 5878.
- (30) Dudnik, A. S.; Gevorgyan, V. *Angew. Chem., Int. Ed.*, **2007**, *46*, 5195.
- (31) Dudnik, A. S.; Sromek, A. W.; Rubina, M.; Kim, J. T.; Kel'in, A. V.; Gevorgyan, V. *J. Am. Chem. Soc.* **2008**, *130*, 1440.

- (32) Dudnik, A. S.; Xia, Y.; Li, Y.; Gevorgyan, V. *J. Am. Chem. Soc.* **2010**, *132*, 7645.
- (33) Snape, T. J. *Chem. Soc. Rev.* **2007**, *36*, 1823.
- (34) Wang, B.; Tu, Y. *Acc. Chem. Res.* **2011**, *44*, 1207.
- (35) Song, Z.; Fan, C.; Tu, Y. *Chem. Rev.* **2011**, *111*, 7523.
- (36) Trost, B. M.; Yasukata, T. *J. Am. Chem. Soc.* **2001**, *123*, 7162.
- (37) Langer, P.; Bose, G. *Angew. Chem., Int. Ed.*, **2003**, *42*, 4033.
- (38) Trost, B. M.; Xie, J. *J. Am. Chem. Soc.* **2008**, *130*, 6231.
- (39) Leboeuf, D.; Huang, J.; Gandon, V.; Frontier, A. J. *Angew. Chem., Int. Ed.*, **2011**, *50*, 10981.
- (40) Leboeuf, D.; Gandon, V.; Ciesielski, J.; Frontier, A. J. *J. Am. Chem. Soc.* **2012**, *134*, 6296.
- (41) House, H. O.; Grubbs, E. J.; Gannon, W. F. *J. Am. Chem. Soc.* **1960**, *82*, 4099.
- (42) Namyslo, J. C.; Kaufmann, D. E. *Chem. Rev.* **2003**, *103*, 1485.
- (43) Leemans, E.; D., M.; Kimpe, N. D. *Chem. Rev.* **2011**, *111*, 3268.
- (44) Hashimoto, T.; Naganawa, Y.; Maruoka, K. *J. Am. Chem. Soc.* **2011**, *133*, 8834.
- (45) Li, W.; Liu, X.; Hao, X.; Cai, Y.; Lin, L.; Feng, X. *Angew. Chem., Int. Ed.*, **2012**, *51*, 8644.
- (46) Marion, N.; Nolan, S. P. *Angew. Chem., Int. Ed.*, **2007**, *46*, 2750.
- (47) Hashmi, A. S. K. *Angew. Chem., Int. Ed.*, **2008**, *47*, 6754.
- (48) Li, Z.; Brouwer, C.; He, C. *Chem. Rev.* **2008**, *108*, 3239.

- (49) Arcadi, A. *Chem. Rev.* **2008**, *108*, 3266.
- (50) Gorin, D. J.; Sherry, B. D.; Toste, F. D. *Chem. Rev.* **2008**, *108*, 3351.
- (51) Rudolph, M.; Hashmi, A. S. K. *Chem. Comm.* **2011**, *47*, 6536.
- (52) Lu, B.; Dai, L.; Shi, M. *Chem. Soc. Rev* **2012**, *41*, 3318.
- (53) Hashmi, A. S. K. *Angew. Chem., Int. Ed.*, **2012**, *49*, 5232.
- (54) Doyle, M. P.; McKervey, M. A.; Ye, T. **1998**.
- (55) Ye, T.; McKervey, M. A. *Chem. Rev.* **1994**, *94*, 1901.
- (56) Shi, W.; Jiang, N.; Zhang, S.; Wu, W.; Du, D.; Wang, J. *Org. Lett.* **2003**, *5*, 2243.
- (57) Shi, W.; Xiao, F.; Wang, J. *J. Org. Chem.* **2005**, *70*, 4318.
- (58) Vitale, M.; Lecourt, T.; Sheldon, C. G.; Aggarwal, V. K. *J. Am. Chem. Soc.* **2006**, *128*, 2524.
- (59) Shintani, R.; Fu, G. C. *J. Am. Chem. Soc.* **2003**, *125*, 10778.
- (60) Suárez, A.; Downey, C. W.; Fu, G. C. *J. Am. Chem. Soc.* **2005**, *127*, 11244.
- (61) Shintani, R.; Hayashi, T. *J. Am. Chem. Soc.* **2006**, *128*, 6330.
- (62) Suga, H.; Funyu, A.; Kakehi, A. *Org. Lett.* **2007**, *9*, 97.
- (63) Shintani, R.; Murakami, M.; Hayashi, T. *J. Am. Chem. Soc.* **2007**, *129*, 12356.
- (64) Chan, A.; Scheidt, K. A. *J. Am. Chem. Soc.* **2007**, *129*, 5334.
- (65) Chen, W.; Du, W.; Duan, Y.; Wu, Y.; Yang, S.; Chen, Y. *Angew. Chem., Int. Ed.*, **2007**, *46*, 7667.

- (66) Sibi, M. P.; Rane, D.; Stanley, L. M.; Soeta, T. *Org. Lett.* **2008**, *10*, 2971.
- (67) Shapiro, N. D.; Shi, Y.; Toste, F. D. *J. Am. Chem. Soc.* **2009**, *131*, 11654.
- (68) Perreault, C.; Goudreau, S. R.; Zimmer, L. E.; Charette, A. B. *Org. Lett.* **2008**, *10*, 689.
- (69) Hashimoto, T.; Maeda, Y.; Omote, M.; Nakatsu, H.; Maruoka, K. *J. Am. Chem. Soc.* **2010**, *132*, 4076.
- (70) Varvounis, G.; Fiamegos, Y.; Pilidis, G. *Adv. Heterocycl. Chem.* **2001**, *80*, 75.
- (71) Eicher, T.; Hauptmann, S. *The Chemistry of Heterocycles, 2nd ed.*; Wiley-VCH: Weinheim **2003**.
- (72) Konaklieva, M. I.; Plotkin, B. J. *Curr. Med. Chem. Anti-Infect. Agents* **2003**, *2*, 287.